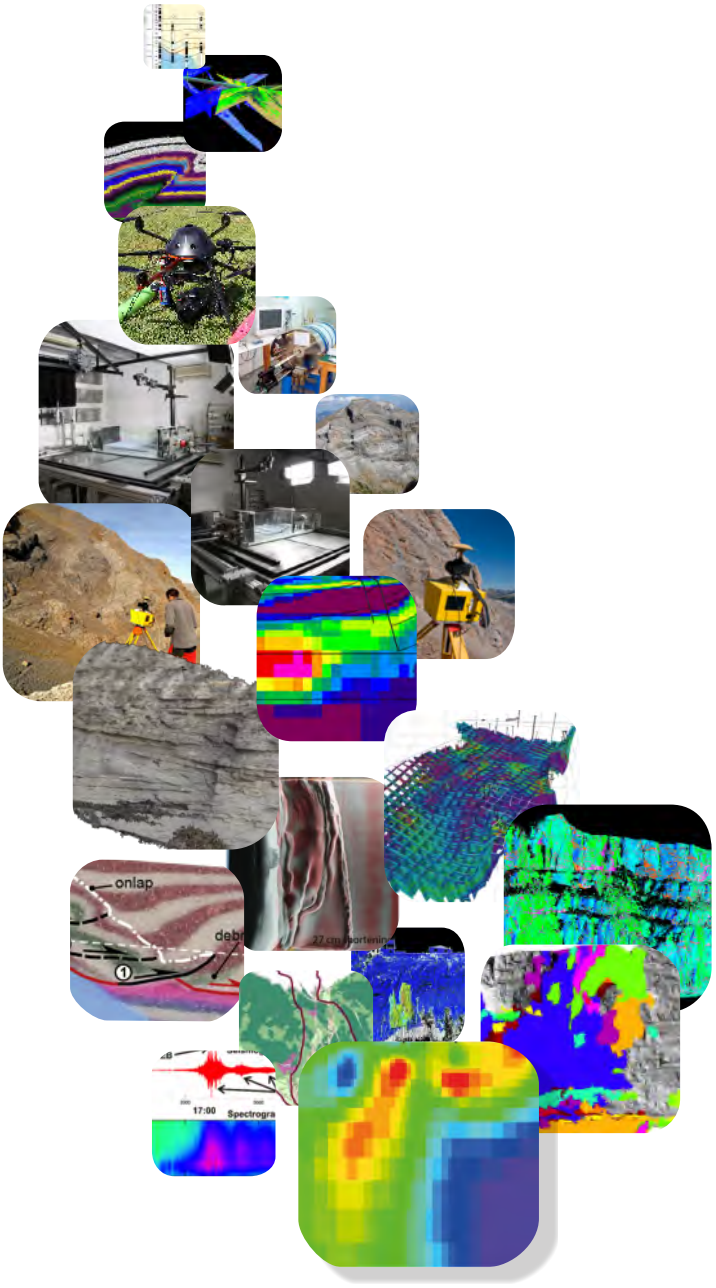

geomodels

institut de recerca

MEMÒRIA D'ACTIVITATS 2016

Barcelona, Gener del 2017

UNIVERSITAT DE BARCELONA

B:KC Barcelona Knowledge Campus

0 Índex

1 INTRODUCCIÓ

Seguint les línies de recerca principals definides dins de l'Institut de Recerca Geomodels, la recerca duta a terme desde finals del 2015 fins a finals del 2016, es pot agrupar segons la relació següent:

A. Adquisició de dades i Modelització geològica 3D
B. Laboratori de modelització analògica
C. Modelització numèrica de cossos i processos geològics
D. Models d'alta resolució i Sensors Remots
E. Dinàmica i caracterització de moviments de vessants
F. Estudi i incorporació de dades geofísiques
G. Tectònica Activa

En general, s'ha realitzat un avanç positiu en totes les línies d'investigació i la activitat segueix, al dia, el pla descrit per cadascuna d'elles.
Tot i que en totes les línies d'investigació hi ha hagut un avenç, poden destacar-se els següents:

- ✓ Seguim amb el desenvolupament de les diferents eines creades per extreure informació geològica de models del terreny d'alta resolució, ja sigui adquirits mitjançant Laser Scaner (LIDAR), ja sigui mitjançant altres eines més assequibles com poden ser fotografies a partir de càmeres convencionals o d'ús domèstic. Tenint en ment la transferència del coneixement entre Universitat-Empresa, l'any vinent s'iniciarà un Doctorat Industrial amb la realització d'una tesi que permetrà seguir desenvolupant les eines i, el que és més important, tendir a una aplicació directe de les eines desenvolupades per a la empresa privada. A més a més, també s'estan redactant diferents articles i contribucions a congressos per a seguir mostrant la feina feta i la seva possible aplicació.

- ✓ El que fa referència a la modelització numèrica, tant la part sedimentològica com el programa que combina processos tectono-sedimentaris, segueix avançant incorporant noves funcionalitats i aplicant les noves eines a exemples concrets que ens ha permès obtenir resultats molt interessants i engrescadors. En aquest sentit, ha sorgit dues publicacions, s'han finalitzat dues tesis doctorals i s'estàn aplicant els codis a nous exemples.

- ✓ Es prossegueix amb els diferents projectes relacionats amb la construcció de models 3D, ja sigui per obtenir models estructurals deterministes, com per a ser utilitzats com a base per a posteriors càlculs, com pot ser la migració de fluids. Cal destacar els projectes engegats a Iran i a la Xina.

- ✓ En relació al Laboratori de Modelització Analògica, l'activitat que s'hi desenvolupa segueix creixent, fet que queda palès en la ocupació del laboratori durant bona part de l'any per a realitzar els diferents models analògics (tant per projectes d'investigació ,

així com per diferents treballs de recerca a nivell de màster que involucren l'ús de la infraestructura). Enguany la segona taula de modelització ja està en funcionament i ja s'hi han realitzat diferents models analògics, de caràcter senzill, per tal de testejar el seu funcionament.

La activitat investigadora del grup durant el període **dec. 2015 - dec. 2016** s'ha traduit en **113** contribucions a congressos (72 de caràcter internacional) i **99 publicacions** segons la relació següent:

34 Publicacions en llibres; derivades de congressos nacionals i internacionals; o en revistes **no** SCI.

65 publicacions en revistes **SCI**, de les que:

6 en revisió o acceptades per publicar

5 enviades

54 publicades

Pel que fa a les Tesis Doctorals, durant aquesta anualitat, s'han defensat **12 tesis doctorals**, la majoria amb qualificacions d' Excel·lent Cum Laude.

Pel que fa a la part econòmica, en resum, l**es fonts de finançament principal de l'Institut de recerca provenen bàsicament de projectes**. En total són **43 projectes actius** en la present anualitat, que provenen de 16 projectes finançats per fons públics i 27 de privats. D'aquests 43 projectes, n'hi ha **35 liderats per membres de l'Institut**, i 8 on hi participen membres de l'Institut.

L'aportació econòmica aproximada d'aquests 35 projectes liderats per membres de l'Institut **per a l'anualitat 2016 ha estat d'uns 1,9 M d'€.**

Per finalitzar, destacar també que l'Institut de Recerca Geomodels, continua amb els acords de col·laboració signats amb diferents companyies de software d'interpretació i modelat 3D geològic comercial dins dels quals es cedeix gratuïtament o a un cost molt reduït programari valorat en més de 2 milions d'euros, i que s'utilitza tant en investigació com en la docència del Grau de Geologia i en les classes de màster.

RESUM ACTIVITAT INVESTIGADORA

Summary of the scientific activity

2

geomodels

institut de recerca

A Adquisició de dades i Modelització geològica 3D

Data acquisition and 3D reconstruction and modelling

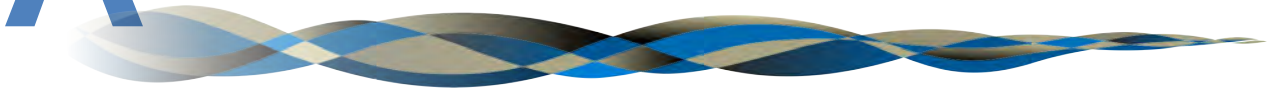

geomodels
institut de recerca

Salt tectonics modelling at Kuqa foreland fold and thrust belt, Tarim Oilfield

[1]Esther Izquierdo, [1]Oriol Pla, [1]Anna Carmona, [2]Mark Rowan, [1]Josep Anton Muñoz, [1]Eduard Roca

[1]Geomodels Research Institute, Group of Geodynamics and Basin Analysis. Departament de Geodinàmica i Geofísica, Facultat de Geologia, Universitat de Barcelona, Spain.

[2]Mark G. Rowan Consulting, Inc., 850 8th St. Boulder, CO 80302, USA

Introduction

This project starts at February 2015. The introduction and objectives were defined in the previous year report.

Work done

Regional cross sections

- Interpretation at depth from seismic lines (Fig. 1).
- Incorporation of surface data.
- Sequential restoration of the cross section.

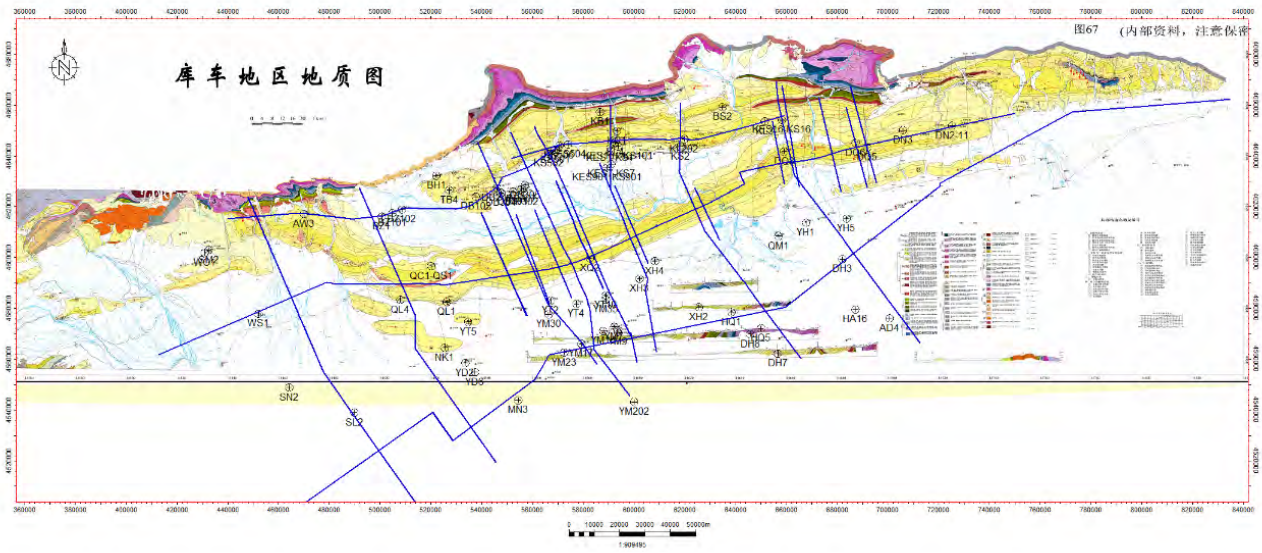

Fig. 1: Geological map showing the location of regional and short cross sections.

Short cross sections

- Interpretation at depth from seismic lines (Fig. 1).

Analogue models

2D configurations:

MODEL NAME	Density lower décollement (g/cm^3)	Visosity lower décollement (Pa·s)	Syn-tectonic sedimentary rate (mm over rotation axis)
Model A	0.97	$1.18 \cdot 10^4$	2mm
Model B	1.38	$2.83 \cdot 10^4$	2mm
Model C	1.55	$3.35 \cdot 10^4$	2mm
Model D	1.38	$2.83 \cdot 10^4$	1mm

Table 1: Table showing set-up 2D configurations.

3D configurations:

MODEL NAME	Syn-tectonic sedimentary rate (mm over rotation axis)
Model E	2mm
Model F	3mm
Model G	1mm
Model H	Without syn-tectonic sedimentation

Table 2: Table showing set-up 3D configurations.

Numerical models

- Models with wedge geometry and one interlayered weak décollement (Fig. 2).

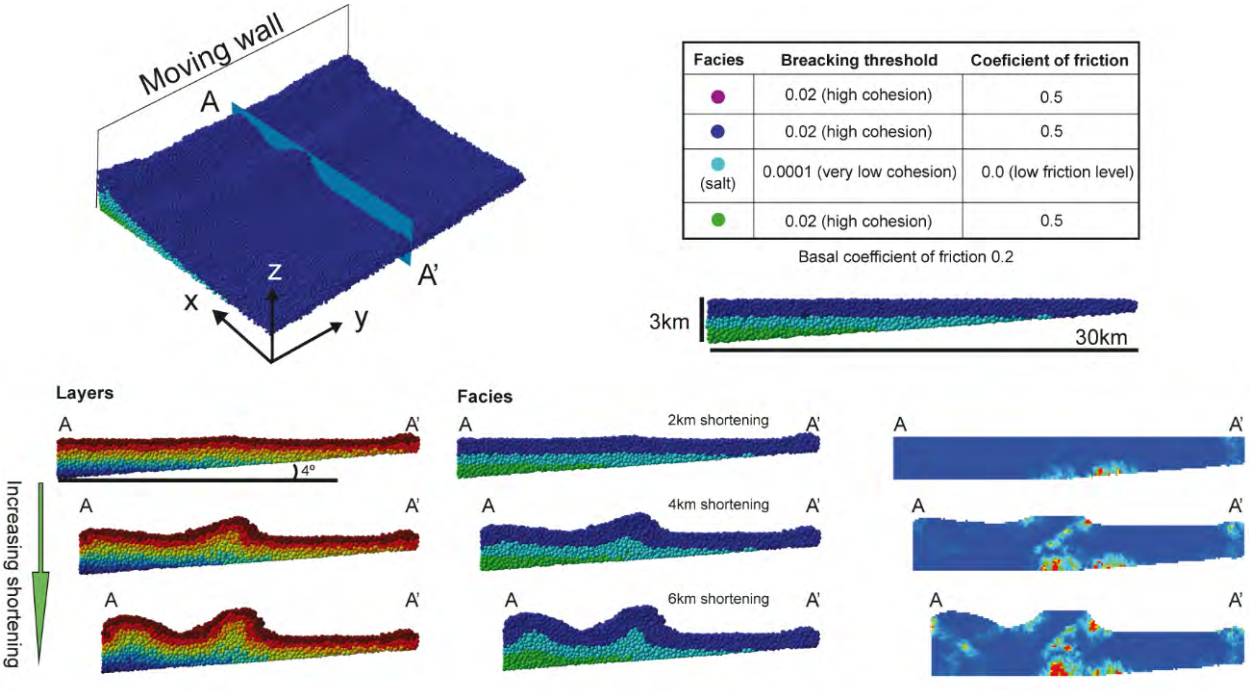

Fig. 2: Same sections of layers, facies, and maximum strain at diferent shortening, and the properties used.

- Models with horizontal layering, one interlayered weak décollement that ends laterally (Fig. 3 and 4).

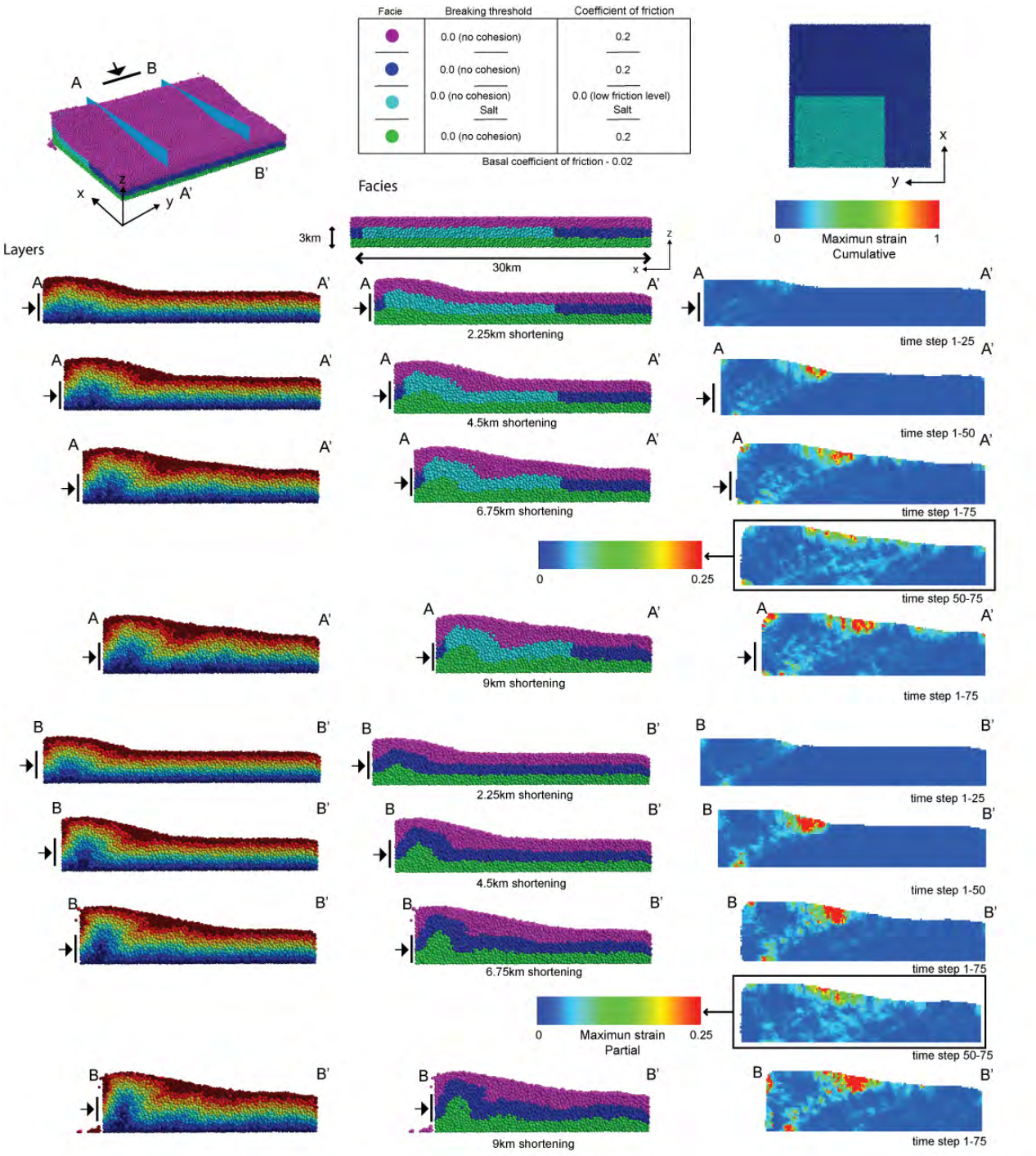

Fig. 3: Same sections of layers, facies, and maximum strain at diferent shortening, and the properties used.

Conclusions

Regional cross sections

dpm-11:

- The Lower Jurassic behaved as a main detachment controlling the development of an imbricate system of foreland directed thrusts. Local thrust flats are recognized in the Cretaceous sequence (Fig. 4).

- This thin-skinned thrust system is cut and tilted by two main basement faults.

- The basement fault beneath the Tuzimaza produced its uplift (similarly to the analogue models) and the formation of a passive roof back-thrust in its footwall.

- The Kumugeliemu anticline is cored by a fault-bend anticline deforming Mesozoic units. The thrust branches to the Tuzimaza thrust.

- The Kumugeliemu Group is the main décollement although the Jidike Fm also behaved as a detachment level in the Qiulitage and the Kelasu structural belt (passive-roof back-thrust beneath the Tuzimaza).

- The Qiulitage developed in the foreland pinch-out of the Kumugeliemu Group whose position is probably controlled by the early reactivation of steeply dipping basement structures.

- The total shortening in the cross section is about 29 km. Most of the shortening took place coevally to the sedimentation of the Kuqa and Kangcun Fms, although initial shortening (pre-dating the Kangcun Fm) was accommodated in the southern Qiulitage anticline and the Kumugeliemu anticline-Tuzimaza structure (and the basement structure related to it, the Kuqa anticline).

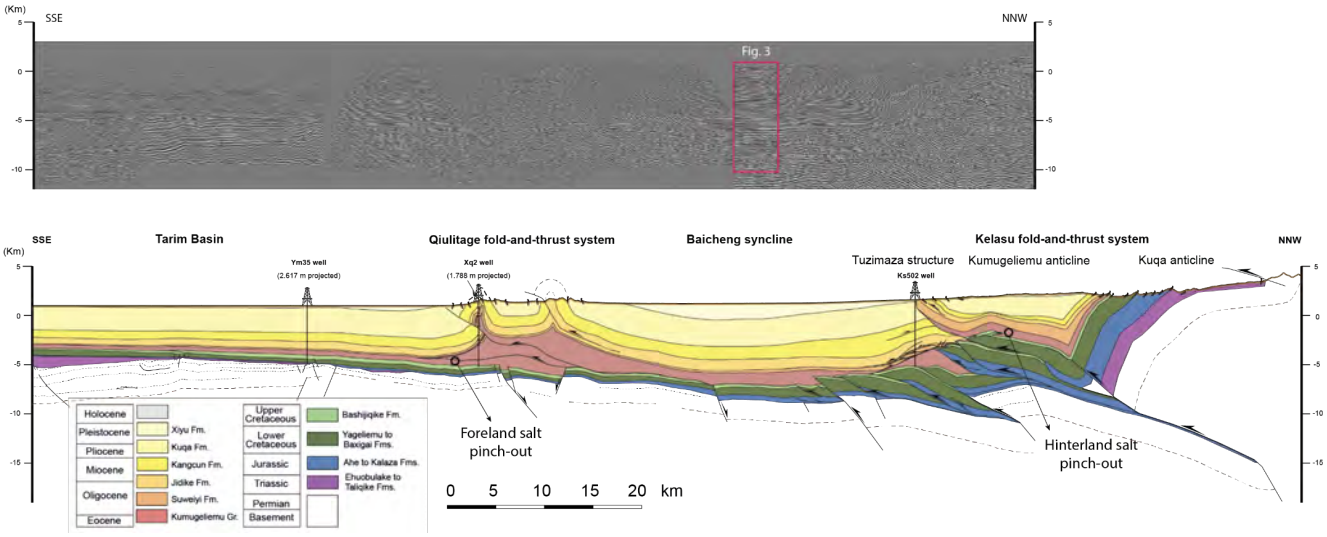

Fig. 4: Regional cross section depm-11.

dpm-05:

- The structure of the Mesozoic units is mainly controlled by basement faults (minor influence of the Mesozoic coal layers).

- Shortening in the Paleozoic basement and the Mesozoic units is transferred to three main structures in the Cenozoic cover: the Quele thrust and two anticlines to the South.

- To the South of the Qiulitage, a south-vergent basement structure is observed. It was reactivated before sedimentation of the Upper Cretaceous (the Bashijiqike Fm is unconformably overlying Mesozoic units) and also during the Cenozoic compression.

- Development of salt welds related to basement deformation produced the migration of supra-salt deformation from the southern pinch-out of the Kumugeliemu evaporites towards the North in a break-back sequence.

- The total shortening in the cross section is about 33 km. Most of the shortening took place coevally to the sedimentation of the Kuqa Fm, although early shortening was accommodated in the southern pinch-out of the Kumugeliemu evaporites and the northernmost portion of the cross section (Kuqa anticline).

dpm-16:

- The Upper Triassic behaved as a main décollement controlling the development of an imbricate system of foreland directed thrusts, although backthrusts also formed in the northern portion of the cross section.

- The Kumugeliemu Group is only effective as detachment level in the Qiulitage and very locally in the Bashijiqike anticline.

- Presence of superposed detachment layers favors the development of fish-tail structures as observed in the core of the Quilitage structure.

- Basement faults inherited from Mesozoic times reactivated as thrusts. They control the position of the Qiulitage frontal structure, which is located above one of these reactivated basement faults.

- The total shortening in the cross section is about 24 km. Most of the shortening took place coevally to the sedimentation of the Kuqa and Kangcun Fm, although early shortening was accommodated in the northern part of the cross section.

Short cross sections

Central part of the Qiulitage structure:

- The position is controlled by the southern pinch-out of the Kumugeliemu evaporites.

- It is formed by two tight anticlines separated by a broader syncline. The **northern anticline** is South-vergent and its hinge zone is cut by a North-

dipping thrust that is detached in the Jidike Fm. The **southern anticline** is South-vergent and its hinge-zone is also affected by a thrust: a North-dipping thrust that corresponds to a tilted, originally South-dipping back-thrust. Both anticlines and the central syncline are southwards transported and uplifted by a South-directed thrust detached in the Kumugeliemu evaporites.

- Beneath the Kumugeliemu Group, the Mesozoic sequence is deformed by steeply dipping normal and reverse faults producing block rotation. The reactivation of these structures during early Cenozoic times could control the sedimentation of Eocene salt units.

Eastern part of the Qiulitage structure:

- The position is controlled by sub-salt structures.

- Mesozoic beneath the Qiulitage is deformed by a fault-related anticline, characterized by an intermediately South-dipping forelimb. The main sub-salt thrust is connected to a passive back-thrust that is detached in the Kumugeliemu Group (forming a fish-tail structure).

Angalogue models

2D configuration:

Influence of the lower décollement properties.

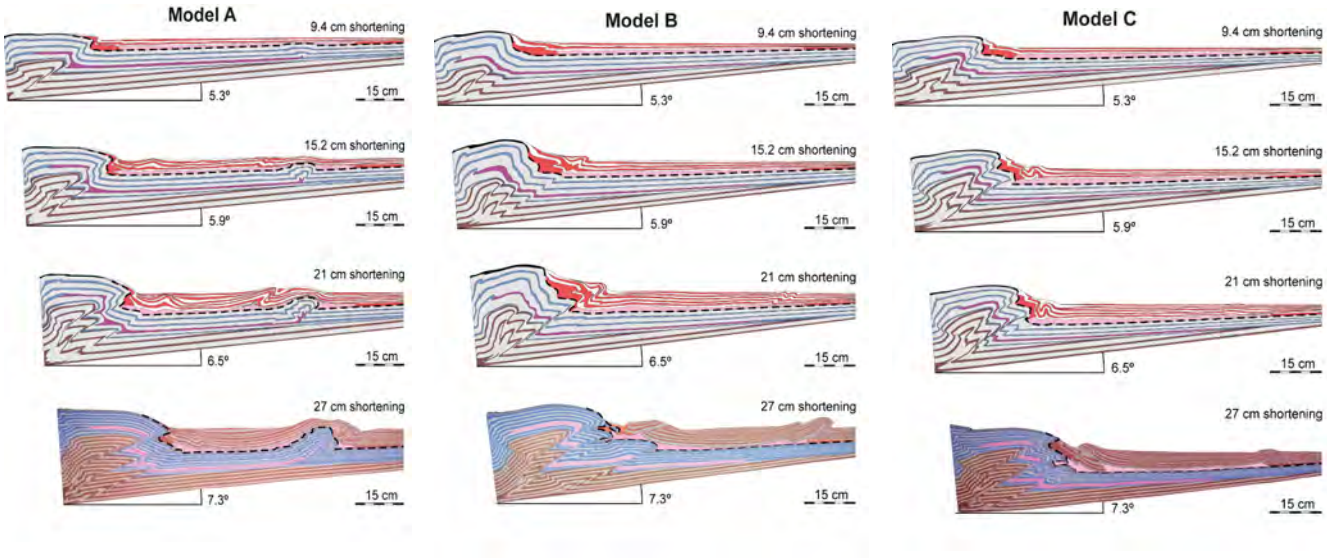

Fig. 5: Same sections at diferent shortening steps showing the evolution.

- The main differences were observed in model A → after formation of forethrust II, deformation migrated to the foreland pinch-out of the lower décollement. The development of this structure partly inhibited the migration of the deformation towards the upper décollement pinch-out.
- In models B and C, deformation migrated towards the foreland pinch-out of the lower décollement after 14 and 19 cm of shortening, respectively.

- The lower décollement showed a lower effectiveness as a detachment layer than in model A. Nevertheless, the presence of this weak layer interbedded in the pre-tectonic sequence has an influence on the building of the thick-skinned domain. It favored the development of thrust splays in model C whereas minor thrusts and back-thrusts detached in this weak layer are found in both models B and C.
- To reduce the syn-tectonic sedimentary rate had an important influence on the geometry of the thin-skinned system. On the one hand, the wavelength of the structures detached over the upper silicone plate was smaller since they affected a thinner sedimentary cover. On the other hand, the lower syn-tectonic sedimentary thickness facilitated the migration of shortening towards the foreland pinch-out of the lower décollement and a pop-up developed at this part of the model during the last shortening stages. Higher sedimentary rates (model B) inhibited the development of this structure.

3D configuration:

Influence of the syn-tectonic rate.

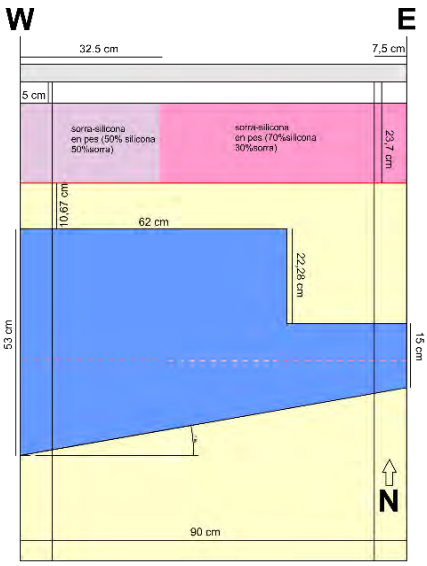

Fig. 6: Top view of the set-up.

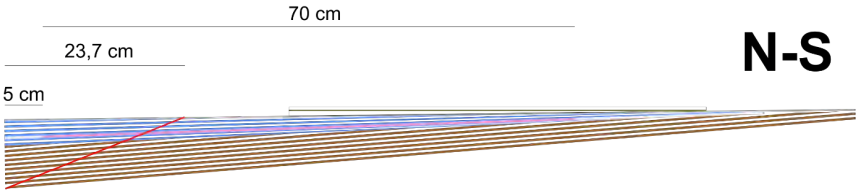

Fig. 7: Section of the lateral view 1 (westernmost section).

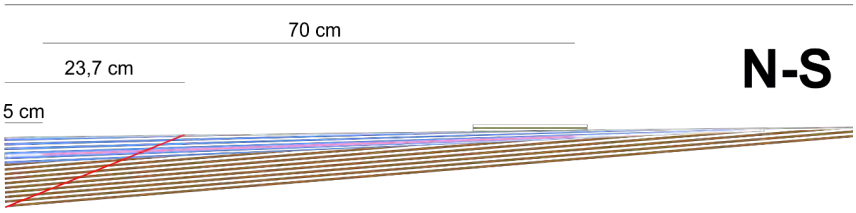

Fig. 8: Section of the lateral view 2 (easternmost section).

Fig. 9: Top views of models G, E, and F at the final stage of deformation.

- There is a relay between thin-skinned structures detached over the lower and the upper décollement foreland pinch-outs.
- The frontal structure is oblique to the shortening direction
- Back-thrusting in the thick-skinned domain is more important towards the lateral view 2 (Fig. 8).
- In the three models, the frontal structure is mainly controlled by (1) the foreland pinch-out of the lower décollement towards lateral 2 and (2) the foreland pinch-out of the upper décollement towards lateral 1 (Fig. 7).
- The increase in the syn-tectonic sedimentary rate delays the propagation of the deformation towards the foreland pinch-out of the upper décollement (Fig. 9).

Numerical models

- The lateral termination of a weak intermediate layer generates lateral variations in the geometry of a fold-and-thrust system.
- When a weak layer is interbedded in the basin infill, deformation is first localized in its hinterland pinch-out. Increasing shortening is accommodated by an anticline close to the moving-wall. On the contrary, when the stratigraphic sequence is frictional and homogeneous, a pop-up close to the moving-wall developed first and then deformation propagates foreland-wards in a piggy-back thrust sequence.
- During the last shortening stages, deformation was localized at the foreland pinch-out of the intermediate frictionless layer. .
- Similar geometries and strain distributions were obtained along the whole model, independently of the interbedded weak layer.

Future work

1. Interpretation of 3D analogue models.
2. Depth conversion of short lines (Petrel).
3. Cross section construction of short lines in Move integrating both surface data and depth data (seismic interpretation and wells).
4. Cross section balancing of short lines.
5. Design numercial models with syn-tectonic sedimentation.

Potential salt related hydrocarbon traps in the southern Zagros Belt and Persian Gulf (Onshore-Offshore) Block-2

[1]Mireia Butillé, [1]Núria Carrera, [1]Joana Mencos, [1]Marco Snidero, [2]Josep Giner, [1]Josep Anton Muñoz, [1]Francesc Sàbat.

[1] Dept. Geodinàmica i Geofísica
[2] Dept. Geoquímica, Petrologia I Prospecció Geològica

Introduction and Objectives

The Fars province of the southern Zagros Fold and thrust belt is very well known among the geological community by the occurrence of spectacular diapirs (Figure 1). Apart from the beauty of these structures and their academic interest, their knowledge is fundamental for the proper understanding of the Petroleum Systems and the location of the main plays related with the significant hydrocarbon reserves stored in the area.

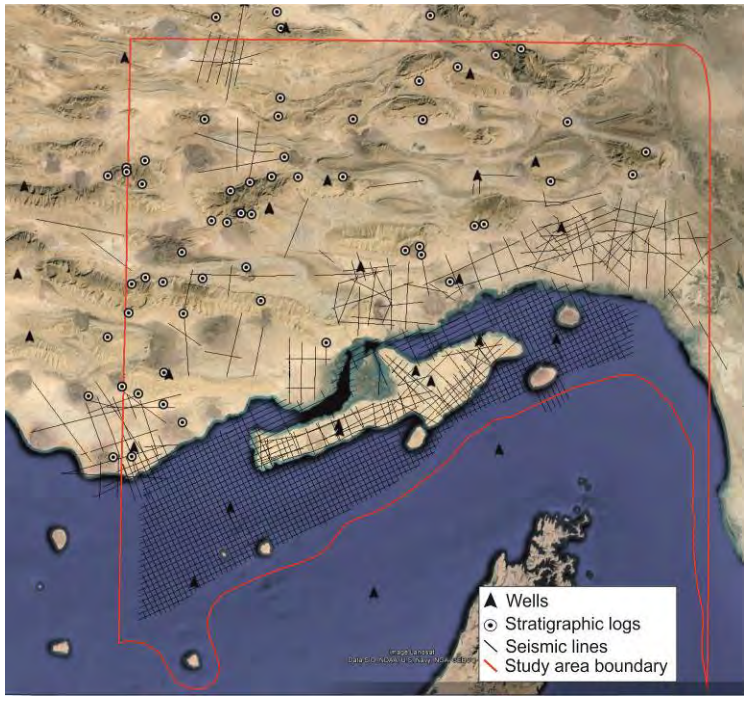

Figure 1. Location of study area at the eastern termination of the Zagros Fold and thrust belt and Persian Gulf (Hormozgan province, S Iran). Data used in the study are also located in the map.

The salt structures of this area involve the Upper Precambrian-Cambrian Hormuz salt and range from salt domes and salt pillows, to salt walls and diapirs with different shapes. Salt movement started since Paleozoic times (Permian) and continued until Present. The presence of the Hormuz salt has also controlled the structural style and evolution of the Neogene contractional structures of the Zagros fold and thrust belt. Detachment folds cored by the Hormuz salt are the predominant structures. It is accepted that salt structures developed before the contractional deformation events that shaped the Zagros since the Late Cretaceous. The main Neogene contractional event would have reactivated the existing salt structures, but also the older events. In Fars the presence of multiple pre-existing diapirs complicates the fold geometry and highlights the great difficulty in extrapolating geometry at depth when subsurface data are lacking.

Despite the main geological and structural evolution of the Southern Zagros fold and thrust belt is relatively well known, and despite salt structures in the Fars area have been widely studied, the detailed time of salt movement and subsequent episodes of growth of salt structures are not well constrained, as well as their relationships with the sedimentary and structural evolution of the area. In addition, new concepts on salt tectonics have been recently raised and new paradigms developed, such as the conditions under which the salt is able to move and pierce the sedimentary overburden.

The aim of the proposed study is to identify the exploration targets related to the salt structures in the Southern Zagros fold and thrust belt, both onshore and offshore (block 2, see Figure 1). In continuation with the results reached in the previous phase of the project, a consistent work program combining both offshore and onshore data in the Fars area has been conducted in order to define and characterize the different salt structures, their relationship with the geodynamic context and the different types of related hydrocarbon traps. Work has focused on the integration of onshore and offshore data, defitinion of depositional sequences and characterization of their boundaries (trough the confection of stratigraphic correlations and paleogeographic maps at selected stratigraphic intervals), the detailed study of selected salt structures (in terms of geometric definition, kinematic evolution, and salt-related geometries) and the elaboration of regional cross sections and a 3D model that condense all the observations made. Furthermore, the structural evolution of the area, the potential source rocks, and the timing of hydrocarbon generation and migration are evaluated.

Work done

- Field trip to the eastern part of the study area (Block 2), near the city of Bandar-Abas.
- Well log QC and improving.
- Interpretation of the whole available seismic data (both offshore and onshore seismic lines) using Petrel software (Figure 2).
- Time to depth conversion of horizon interpretations using and ad-hoc 3D velocity cube.
- Well log data analysis and construction of stratigraphic panels from well correlations and available stratigraphic field logs (Figure 3).
- Digital geological mapping of selected key structures in a 3D environment. Ortophotographs and satellite images have been draped on top of 30m Digital elevation models (DEM) as a base for the digital mapping (Move software) (Figure 4).
- Detailed studies in key outcrops using high resolution digital elevation models obtained from panoramic pictures taken from a helicopter during the first and second field trip (Agisoft software).
- Geological cross-section reconstruction of two regional transect across the eastern part of the study area (Move software) (Figure 5).
- 3D modelling of seven selected regional surfaces using a geological-constrained 3D reconstruction methodology (Figure 6).
- Paleogeographic reconstructions of depositional sequences at selected times (Figure 7).
- Analysis of the petroleoum systems.

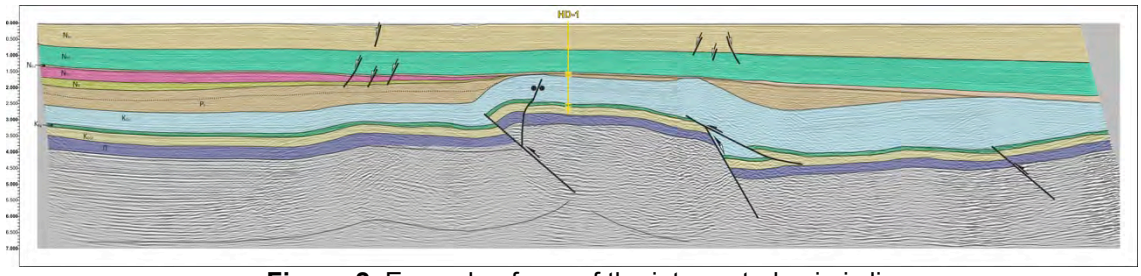

Figure 2. Example of one of the interpreted seimic lines

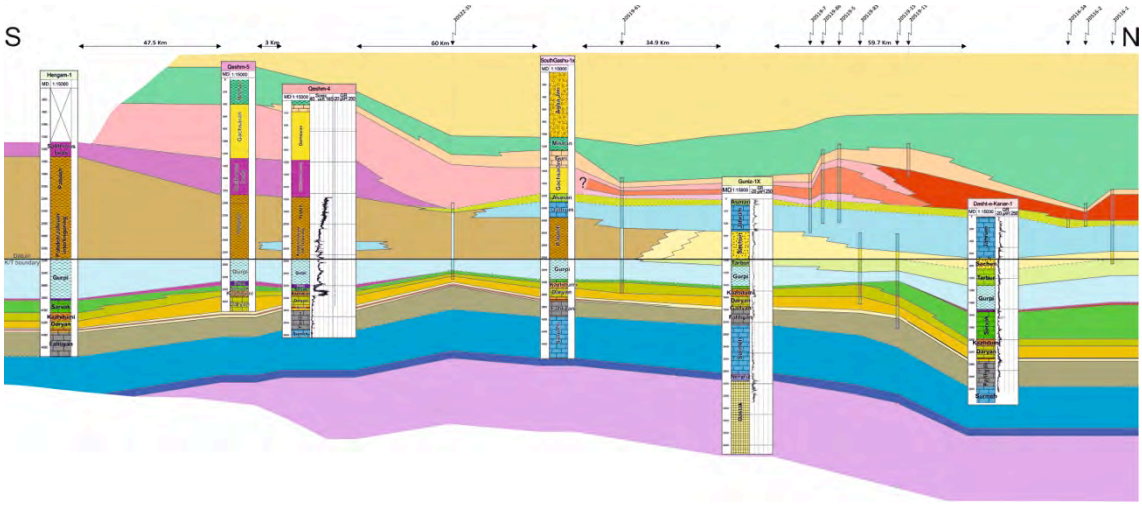

Figure 3. Correlation of the provided stratigraphic logs (both wells and field logs).

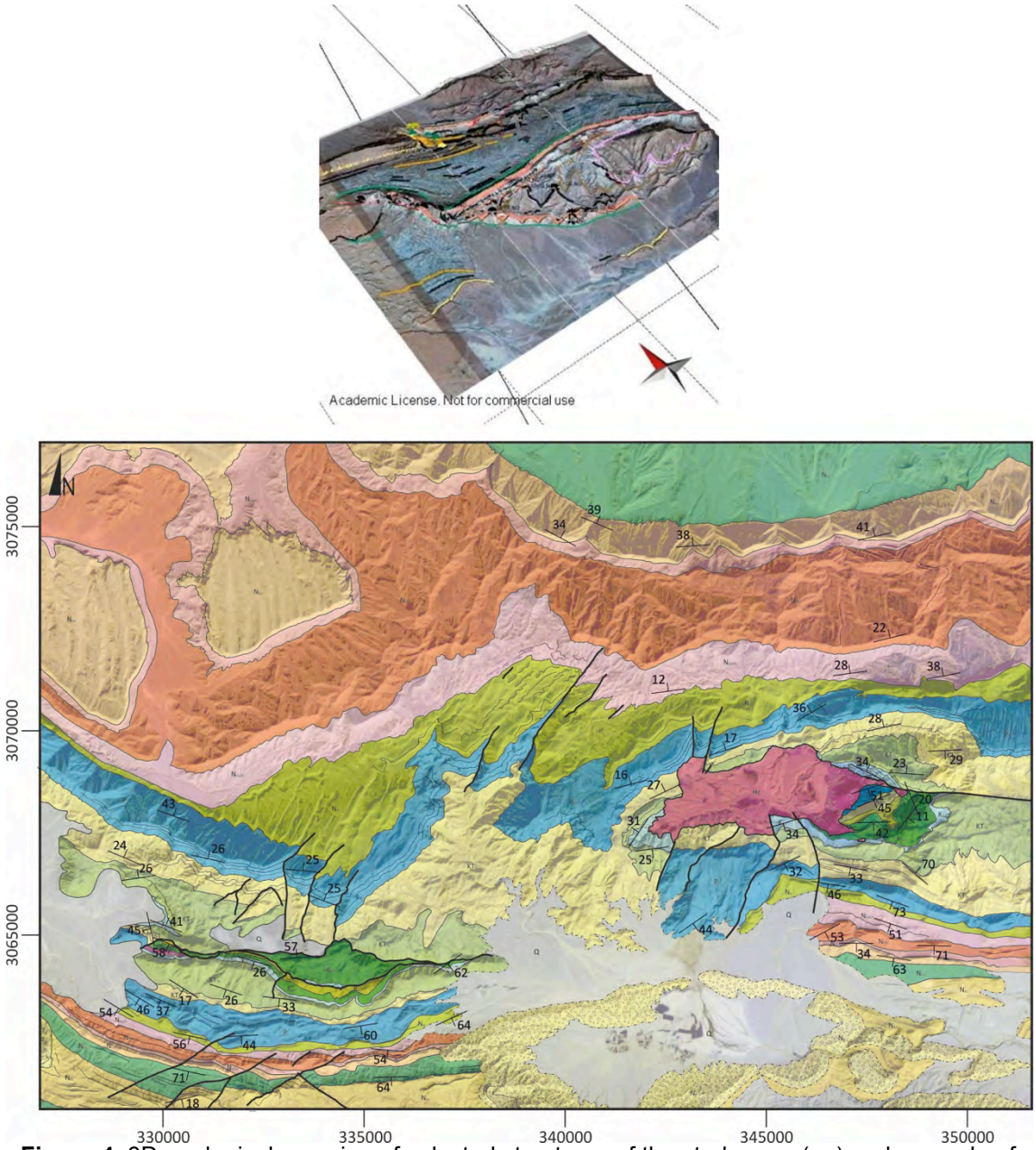

Figure 4. 3D geological mapping of selected structures of the study area (up) and example of the resultant geological map (down).

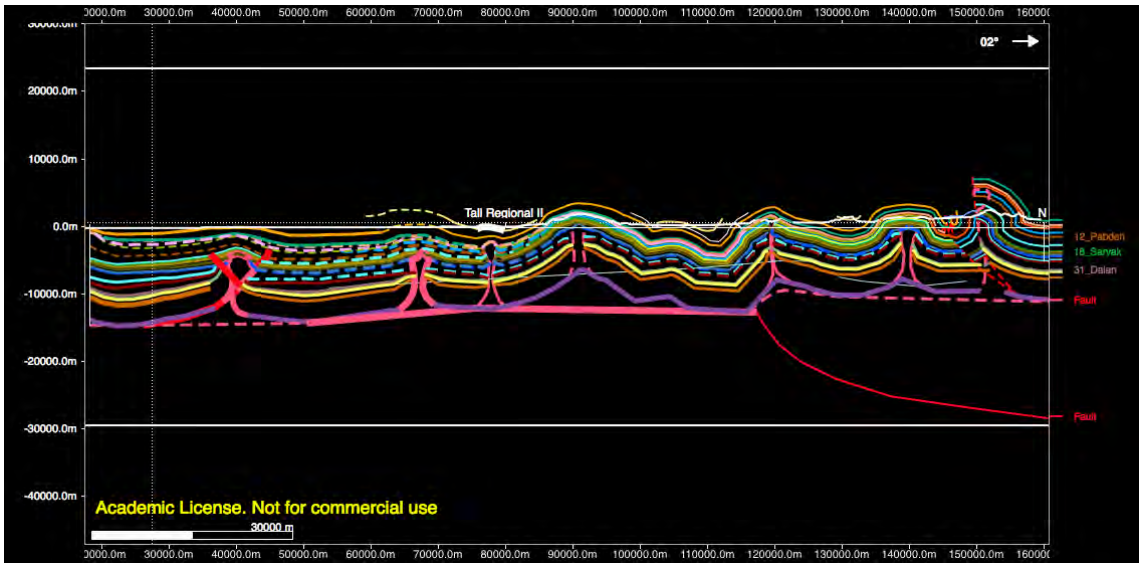

Figure 5. Regional Cross-section at the eastern portion of the study area.

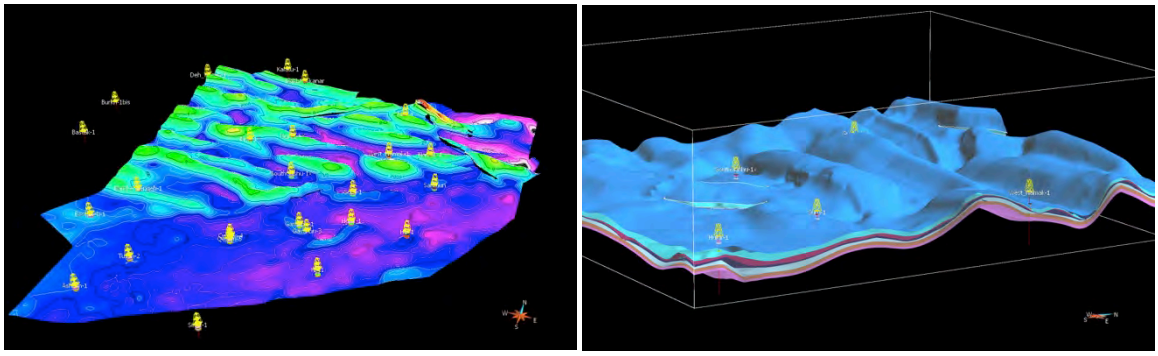

Figure 6. 3D view of the 3D reconstruction performed

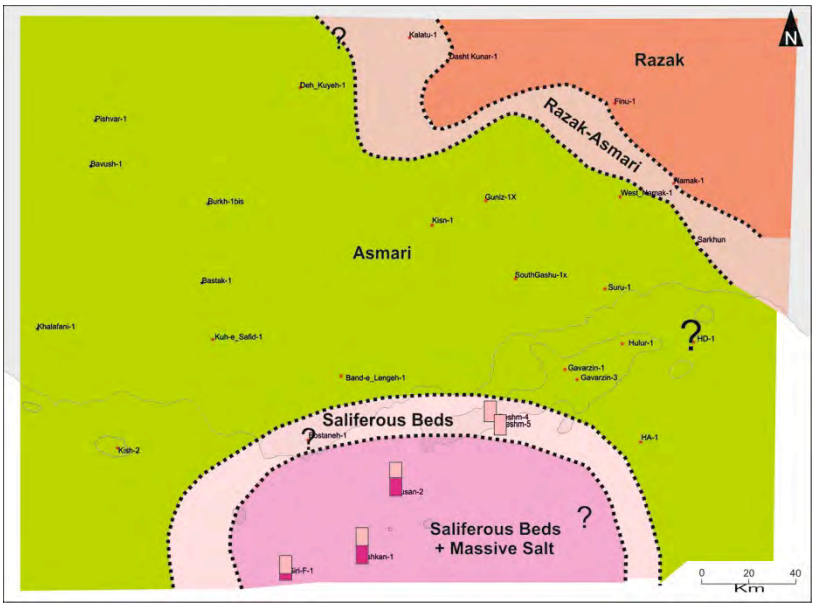

Figure 7. Paleogeographic map of the Miocene depositional sequence, constructed from well data, surface data and structural maps.

Conclusions

- Field work evidences salt tectonics was active during Mesozoic times. As an example, in the Darmadan Anticline characteristic geometries related to the growth of salt diapirs have been observed within the Sarvak Formation (Middle Cretaceous). In other structures, these geometries are present also in younger units, thus implying a continuous salt activity from Middle Cretaceous until now.
- Several structural trends have been identified as related to different tectonic events and ages, which control the position, geometry and timing of the structures and associated facies belts: Neotethys opening and subsequent closure, Oman orogeny, Zagros orogeny, and Makran prism development.
- Geometry and distribution of Hormuz sediments and presence of Hormuz salt walls played an important role in the geometry and distribution of later structures.
- Existence of a Cenozoic mobile layer (Fars salt) interacted with Hormuz salt forming characteristic salt structures in the Persian Gulf (Abumusa and Tomb circular structures). Fars salt basin morphology and configuration have been characterized.
- Distribution of potential plays and migration pathways have been evaluated in Permian units, as well as in Upper Cretatecous - Lower Tertiary and Miocene units.

This project is a joint study between the Geomodels Institut and the National Iranian Oil Company. The project finalizes end of 2016.

Impact of basin structure and evaporite distribution on salt tectonics in the Gulf of Cadiz, Southwest Iberian margin

Adrià Ramos[1], Oscar Fernández[2], Pedro Terrinha[3], Josep Anton Muñoz[1]
[1]Institut de Recerca Geomodels, Departament de Dinàmica de la Terra i de l'Oceà, Universitat de Barcelona, Barcelona, Spain
[2]Repsol Exploración, Dirección de Geociencias, Madrid, Spain
[3]*Instituto Português do Mar e da Atmosfera*, Divisão de Geologia e Georecursos Marinhos, Lisboa, Portugal

Introduction

The Gulf of Cadiz is located in the SW Iberian margin (Fig. 1) and was configured as a passive margin during the Mesozoic, with evaporites being deposited during the early phases of rifting in the earliest Jurassic. This margin underwent compression during Cenozoic and it is partially inverted at present-day (Ramos et al., submitted).

The Mesozoic evaporitic basins of the northern part of the Gulf of Cadiz contain many of the elements observed in salt-related deformation in passive margins worldwide, such as salt diapirs, sat tongues, salt expulsion rollovers, salt-withdrawal mini-basins, among others. Despite a relatively complex evolution, including various extensional pulses (stretching, thinning and hyper-extension processes; (Ramos et al., submitted), dip-slip extension in the Algarve Basin (e.g., onshore Algibre Fault; Ramos et al., 2016), transtensional deformation between Africa and Iberia in the Mesozoic, to compression in the Cenozoic (inversion of the margin; Ramos et al., submitted tectonics) associated to frontal collision and roll-back of the west Mediterranean oceanic slab, the medium dimension of the basin and the dense MCS data availability make it a good candidate to study the different factors that govern the evolution of an evaporite basin in a passive margin.

The interest in salt tectonics in the Gulf of Cadiz has increased in recent years in part due to the reevaluation of the petroleum systems of the Algarve Basin. Initially, in the onshore, a series of salt structures such as diapirs and salt walls were described by (Afonso, 1983; Manuppella, 1992; Terrinha, 1998; Terrinha et al., 1990). The availability of seismic and gravity data led to the identification of various types of salt structures in the offshore portion of the SW Iberian margin (e.g., Fernández-Puga et al., 2007; Lopes et al., 2006; Maestro et al., 2003; Matias, 2007; Terrinha, 1998). One of the most interesting elements of the margin is the presence of an allochthonous salt nappe in the center of the northern Gulf of Cadiz, the so-called Esperança Salt (Matias, 2007; Matias et al., 2011; Terrinha, 1998). Most recently, Ramos et al. (2016) discussed the influence of the interaction of basement and salt structures on extension and contraction in the onshore part of the basin.

Based on a 2D seismic regional survey, Matias et al. (2011) presented a description of salt-related structures, their distribution and the implications on petroleum systems, focused on the western Gulf of Cadiz, including the existence of an allochthonous salt nappe in the center of the northern Gulf of Cadiz, the so-called Esperança Salt (Matias, 2007; Matias et al., 2011; Terrinha, 1998). In this paper we present a more detailed description of salt-related structures based on 2D and 3D MCS comprising the entire northern part of the Gulf of Cadiz. This study reveals significant variability in the structural styles throughout the basin. The aim of this paper is to tie the origin of this variability to the structural evolution of the margin and to the initial configuration of the evaporitic basin.

Work done

Integration of field mapping, well data and seismic interpretation has made it possible to map the salt structures of the Gulf of Cadiz (Fig. 1). The basin is characterized by a variety of types of salt structures, of which diapirs, salt walls and allochthonous salt bodies are the most relevant. This section describes these different features, their origin and evolution, and their distribution.

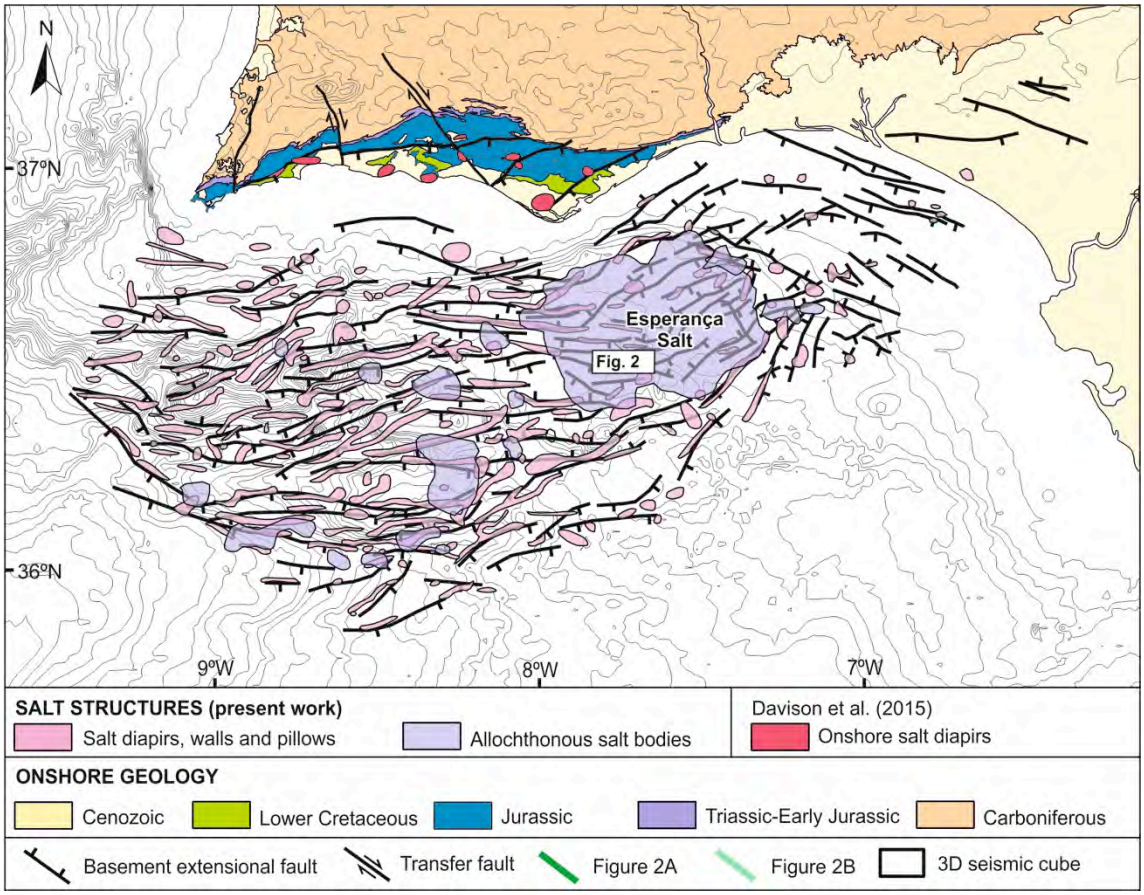

Figure 1. Map of salt structures and the extensional fault system of the basement in the Gulf of Cadiz Basin on the SW Iberian margin. Salt structures mapped in this paper are depicted by pink polygons, their area defined by the cutoff of the top of the Lower Jurassic. Allochthonous units are shown by lilac polygons, mapped according to their greatest lateral extent. Onshore diapirs are taken from Davison (2015). Notice the control of the basement structure on geometry, orientation and location of salt structures through the margin, from onshore to offshore.

Perhaps the most striking feature of the Hettangian evaporite basin of the Gulf of Cadiz is the Esperança Salt Nappe (Matias, 2007; Matias et al., 2011; Terrinha, 1998; Fig. 2). This is the largest allochthonous salt body of the margin and is located in the transition between the western Gulf of Cadiz, dominated by salt walls, diapirs and minor allochthonous bodies, and the eastern part of the basin dominated by isolated diapirs (Fig. 1). It extends over an area of approximately 1800 km^2, from the offshore Portugal-Spain border, in the east, to south of Faro in the west. To the north it is limited by the present-day shelf-brake, while to the south it is limited by the Guadalquivir Bank.

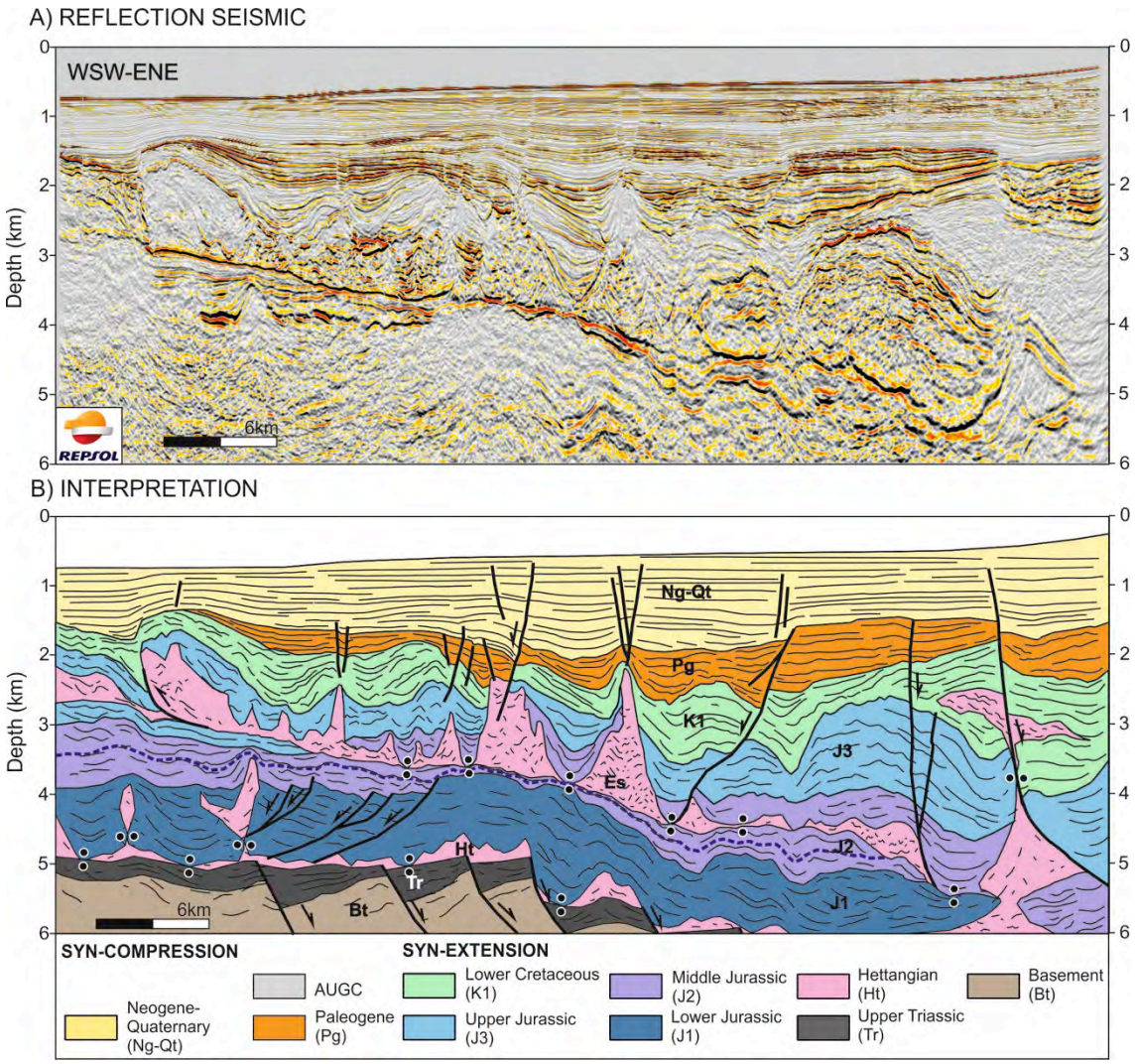

Figure 2. A) Seismic section in depth across the Esperança Salt. B) Interpretation of the seismic section. The section shows how the base of the Esperança Salt truncates progressively younger sediments towards the west. It also illustrates the contrast between the strong control of halokinetics on sediments above the allochthonous Esperança Salt, and the limited amount of salt-related deformation observed below the Esperança Salt. Es: Esperança Salt. Data courtesy of Repsol.

Conclusions

The Mesozoic basement structure of the Gulf of Cadiz controlled the distribution of facies and thickness of the Hettangian evaporite unit. These factors in turn played a critical role in controlling the distribution of the salt tectonic styles and the evolution of individual salt structures though time. Salt structures in the Gulf of Cadiz started to develop in the Early Jurassic and ceased in later stages of Early Cretaceous, being mostly fossilized by Late Cretaceous to Paleogene times. In the western Gulf of Cadiz passive downbuilding has continued to Neogene times, whereas in the central and eastern Gulf of Cadiz Neogene activity of salt structures has been limited to shortening related to Cenozoic inversion.

The facies distribution of the evaporite basin follows a bull-eye pattern, with the most proximal facies towards the north and north-east. In the center of the basin, where the

facies are dominated by the halite and the thickness of the initial evaporite unit was greatest, salt tectonics are most intense.

Within the domain of intense salt tectonics in the central and eastern Gulf of Cadiz, the Esperança Salt is a large salt canopy emplaced from Middle Jurassic to Early Cretaceous times within Mesozoic strata. It is sourced by a L-shape linear feeder along its northern margin. Above the allochthonous salt, deformation of the overburden is accommodated through extensional faults to the north and compressional faults to the south.

Future work

The characterization of salt tectonics, and also the previously presented results about the onshore structure, the compression tectonics and the crustal structure of the margin, can be usefull to predict depositional enironments through the margin. This will allow us to obtain paleogeographic maps for each phase of Mesozoic evolution of the SW Iberian margin.

Salt wall terminations controlled by merged counterregional structures)

[1]Frederic Oriol Escosa Bernal, [2]Mark Rowan, [3]Katherine A. Giles, [3]Kyle Deatrick

[1] GEOMODELS Research Institute, Group of Geodynamics and Basin Analysis. Departament de Geodinàmica i Geofísica, Facultat de Geologia, Universitat de Barcelona, Spain.
[2] Institute of Tectonic Studies. The University of Texas at El Paso
[3] Rowan Consulting Inc.

Introduction and objetives

In recent years, there has been an increasing interest to decipher the geometry of salt walls terminations and the adjacent strata architecture for their potential as hydrocarbon traps. As a result of this, the knowledge of the geometry and evolution of salt bodies has greatly advanced in the last 30 years, primarily because the improving of seismic data acquisition and processing (e.g. Ratcliff 1993), analogue modelling (e.g. Vendeville & Jackson 1992; Ferrer et al. 2016), structural restoration (e.g. Hossak 1995; Rowan & Ratliff 2012) and field studies (Giles & Lawton 2002; Rowan et al. 2003; Lawton & Buck 2006; Lawton et al. 2015).

Despite of the improvement of the before outlined techniques, there are few examples where seismic data show a good resolution of the salt-sediment interface and most of them are located offshore rather than on the continent (Swanston et al. 2011; Giles & Rowan 2012; Hearon et al. 2014; Jackson et al. 2014). Usually, bad resolution of the acquired seismic data is promoted by a complex architecture of the diapirs, aggravated by the existence of evaporite rocks in contact with up to vertical old basinal beds and hence the abrupt lateral variation of the rheological properties of the involved rocks. Is well known that in oil exploration, the existence of vertical strata in salt related reservoirs can carry some misunderstanding aspects that can cost a huge amount of money spent in failed drilling projects. Hence, understanding the salt wall termination architecture is critical for a successful petroleum exploration of three-way truncation traps against salt (Rowan et al. 2016).

Because of all this, recently, there has been renewed interest in detailed field work on exposed analogue salt related structures located in a variety of geological contexts (Trudgill 2011; Alsop et al. 2015; Lawton et al. 2015). Detailed field work has become a fundamental technique providing new insights into the geometrical architecture of the outcropping salt bodies and surrounding rocks where seismic data is not able to image. Nevertheless, very little is known about salt wall terminations and their implications for the along strike architecture of the adjacent strata.

Elongated diapirs (or salt walls) may result from subsalt thick-skinned extension. Differential overburden pressure trigger salt flow towards the footwall of the main subsalt fault promoting salt inflation during the first stages and reactive to passive diapirs in the more evolved stages. Moreover, the termination of a salt wall may be related to a decreasing offset of the subsalt fault (tip of the fault), the presence of a relay ramp or by the existence of suprasalt counterregional faults merging into the margin of diapirs (Schuster 1995; Trudgill & Rowan 2004; Rowan & Inman 2005). Coeval to that, next to passive salt walls, drape folding promotes steep attitudes of the thinned adjacent minibasin strata creating zones of significant structural relief. In these

areas, old basinal strata may become near vertical or even overturned creating great structural reliefs named “megaflaps”. These structures, worldwide recognized (e.g. Schachl 1987; Baldschuhn et al. 2001; Stovba & Stephenson 2003; Brun & Fort 2004; Graham et al. 2012; Rowan & Ratliff, 2012; Ringenbach et al. 2013; Harrison & Jackson 2014; Deatrick et al. 2015; Hearon et al. 2015; Parravano et al. 2015) are formally defined by Rowan et al. (2016) as “thinned stratal panels that extend far up the sides of steep diapirs or their equivalent welds. Their vertical relief is generally greater than 2 km and may be more than 7 km, and bedding attitudes range from near vertical to completely overturned beneath allochtonous salt”.

Based on fieldwork, this work offers a new model for understanding the salt wall terminations and its relationship with the adjacent strata architecture. We localize our research in the Colorado portion of the Paradox Basin (western USA) characterized by outstanding salt-related outcrops. Therefore, the main aim of this paper is threefold: 1) to characterize the structure and kinematic evolution of the southeastern termination of the Gypsum valley salt wall to depict the control exceeded by the merged counterregional fault; 2) stablish a relationship with other salt walls located in the Paradox Basin and finally 3) to use this field analogue for and updated interpretation of the primary counterregional systems located in the northern Gulf of Mexico.

Work done

In order to address the goals outlined for this study, both subsurface and field data were incorporated into this analysis. Subsurface data include one regional 2D depth converted seismic profile across the southern end of the Gypsum Valley salt wall and more than 170 wells with public but incomplete logs (see well location in Fig. 1).

Field data include more than 1000 stations (1064) with structural and stratigraphic data obtained from fieldwork and digital outcrop analysis based on the method developed by Fernández (2005). Post-fieldwork has been carried out in Move 2016® integrating surface and subsurface data in order to construct the geological map as well as the cross-sections along the southeastern termination of the Gypsum Valley salt-wall.

Therefore, we have constructed a detailed geological map (Fig. 1) and six cross-sections along the southern end of the Gypsum Valley salt wall (Fig. 2) supported by 2D depth converted seismic data. Finally, the conclusions of this research should be useful both to researchers and to industry geoscientists whose research is focused in salt related reservoirs in counterregional salt systems located worldwide.

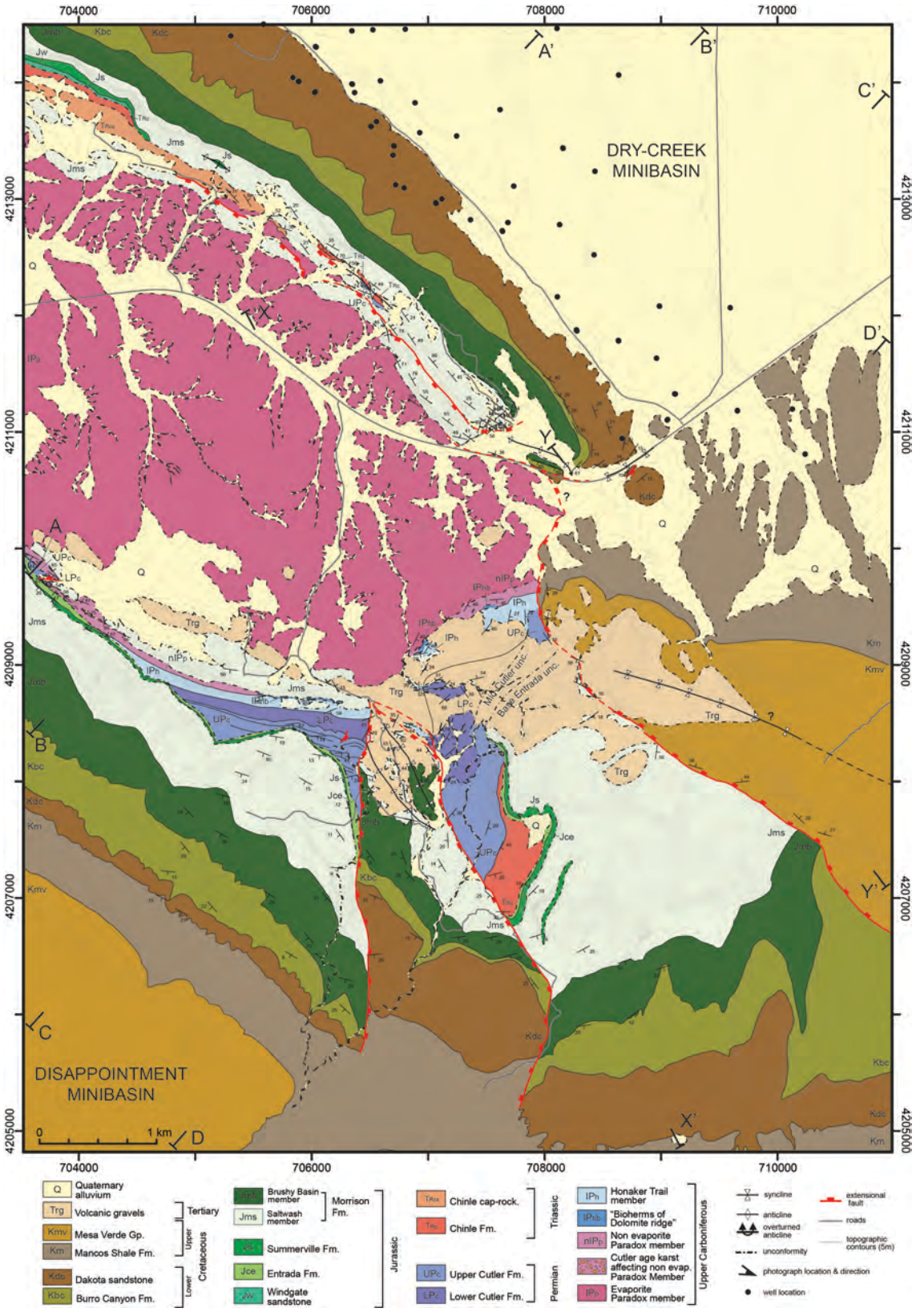

Figure 1. Detailed geological map of the southern termination of the Gypsum Valley salt wall (see location in Fig. 1 B). Lines of cross sections of Figure 7, well location and trace of the seismic profile shown in Figure 1 D and its restoration in Figure 8 is indicated.

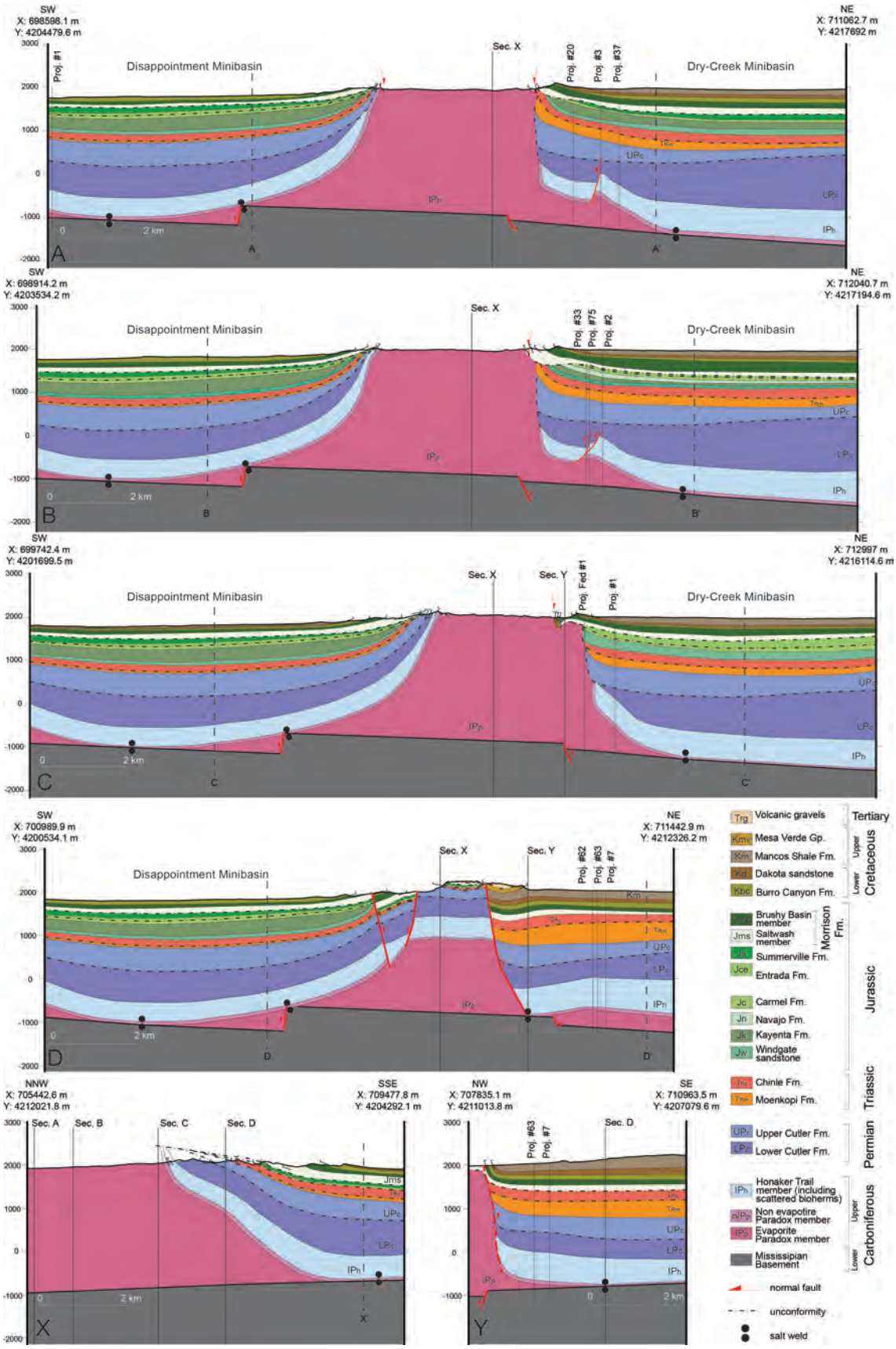

Figure 2. Geological cross-sections located along the southern termination of the Gypsum Valley salt wall (see location in Fig. 2). Note A-A', B-B', C-C', D-D' and X' indicating the limits of the geological map shown in Figure 2.

Conclusions

The Paradox Basin contains outstanding salt-related outcrops providing a great opportunity to study the 3D architecture of salt wall terminations. From the raised model and its application on offshore analogues, we have demonstrated that:

1. Thick-skinned deformation led by subsalt faults controlled the position and development of elongated salt walls along the Paradox Basin. Moreover, the presence of merged suprasalt counterregional structures may control the development of the salt wall terminations.

2. The architecture of the salt wall termination may control the differential subsidence immediately adjacent to the diapir. This termination may be abrupt (e.g. Gypsum Valley, Castle Valley or Fisher Valley salt walls) or gradual (e.g. Moab Valley or Lisbon Valley salt walls). Abrupt terminations, characterized by merged early-diapiric counterregional faults (e.g. Gypsum Valley or Fisher Valley salt walls) or their equivalent counterregional welds (e.g. Castle Valley salt wall) promote asymmetric salt wall architectures. Conversely, gradual terminations, characterized by having either early-diapiric extensional faults (e.g. Lisbon Valley salt wall) or late extensional faults post-dating diapirism (e.g. Moab Valley salt wall) promote symmetric architectures.

3. The analysis of architectural patterns of salt wall terminations arises similarities and differences in counterregional systems located in northern Gulf of Mexico and the abrupt salt wall terminations in the Paradox Basin. Although the structural geometry is similar, both locations differ in the relative timing of the counterregional faulting and the existence of an extruded secondary level of allochthonous salt. In any case, differential subsidence is still high immediately adjacent to the diapirs taken up by slip on counterregional faults that curve away from the diapirs following the margins of the minibasins.

4. The structural style of the upthrown sides of the merged counterregional structures located in northern Gulf of Mexico and Paradox Basin is dominated by monoclinal folding. Hence, the structural traps tend to be three-way closures against counterregional faults or their equivalent secondary welds. The presence of radial faults located in the upthrown side of the counterregional structures breaking the megaflap panel can modify the general trap geometry and hence enhancing the trap capacity of the petroleum system.

Thin- vs. thick-skinned deformation in an inverted salt-bearing passive margin (the Eastern Prebetic)

[1]Frederic Oriol Escosa Bernal, [1]Eduard Roca, [1]Oriol Ferrer

[1] GEOMODELS Research Institute, Group of Geodynamics and Basin Analysis. Departament de Geodinàmica i Geofísica, Facultat de Geologia, Universitat de Barcelona, Spain.

Introduction and objetives.

In general, alpine Mediterranean chains could be affected by a multiphase deformation history including extension and later contraction. Moreover, the presence of pre-rift salt in some of these chains strongly influenced their structural style decoupling thick- and thin-skinned deformation. During extension, pre-rift salt usually decouples deformation of sub- and suprasalt strata (Warren, 2006; Ferrer et al., 2012; Rowan, 2014). In this scenario, the offset between subsalt faults, commonly trigger salt flow developing drape folding in the overburden. The factors that control the structural style of extensional systems with a salt detachment layer are: 1) the thickness of the overburden, 2) the slip rate of the extensional fault, 3) the sedimentation rate of the syn-extensional units, 4) the thickness of the evaporite layer and 5) the physical properties and rheology of the viscous layer (Jackson et al., 1994, Jackson and Vendeville, 1994; Withjack et al., 1995; Withjack and Callaway, 2000). Hence, the location of the subsalt faults controls the development of salt structures. Whereas salt inflation, salt rollers and diapirism occurs above the footwalls of subsalt faults, syncline basins generally welded after salt depletion can develop in their hangingwalls.

According to Péron-Pinvidic and Manatschal (2009) when the stretching increases, rift basins without evaporites evolve throughout several phases (thinning and exhumation). The last phase is the seafloor spreading generating oceanic crust and the development of passive margins. Nevertheless, the architecture of these passive margins will be “atypical” when they include post-rift evaporites (e.g. South-Atlantic passive margin). Here, the deformation is accommodated by a linked thin-skinned system with upslope extension and downslope contraction above a salt detachment (Fort et al., 2004a, 2004b; Rowan et al., 2004; Rowan and Vendeville, 2006). In contrast in passive margins with pre-rift salt, the increasing of deformation supposes the evolution from initially decoupled to coupled extensional systems with the subsequent upward propagation of sub-salt faults into the overburden (thick-skinned deformation), and the development of reactive diapirs and synclinal basins (Dooley et al., 2005; Ferrer et al., 2012; Rowan, 2014).

Some of these margins, with pre-rift salt, can be later inverted as occurred in Alpine Chains (Callot et al., 2007; Dooley et al., 2009; Lemoine et al., 1981; Muñoz, 1992; Muñoz et al., 1994; Muñoz, 2002; Roca et al., 2006; Teixell, 1996; Vendeville and Nilsen, 1995). In this case, the inherited extensional structure as well as the continuity and thickness of the evaporite unit dramatically constrain subsequent inversion (Ferrer et al., 2016; Roma et al., submitted). At the beginning of inversion, the main extensional faults are initially inverted producing the uplift of the extensional basin that subsequently can be incorporated into a fold-and-thrust belt as occurred into the Pyrenean Rift System (Roca et al., 2011; Ferrer et al., 2016). In this scenario, salt acts as an efficient contractional décollement allowing the squeezing of salt bodies and favoring the development of salt welds, shortcuts and back-thrust faults triggered by buttressing (Rowan and Vendeville, 2006; Ferrer et al., 2012). The structure of these

margins can be even more complex if, like occurs in the Eastern Iberia margin (Coastal Catalan ranges and Betics), where there is a later extension overprinting the previous contractional structure.

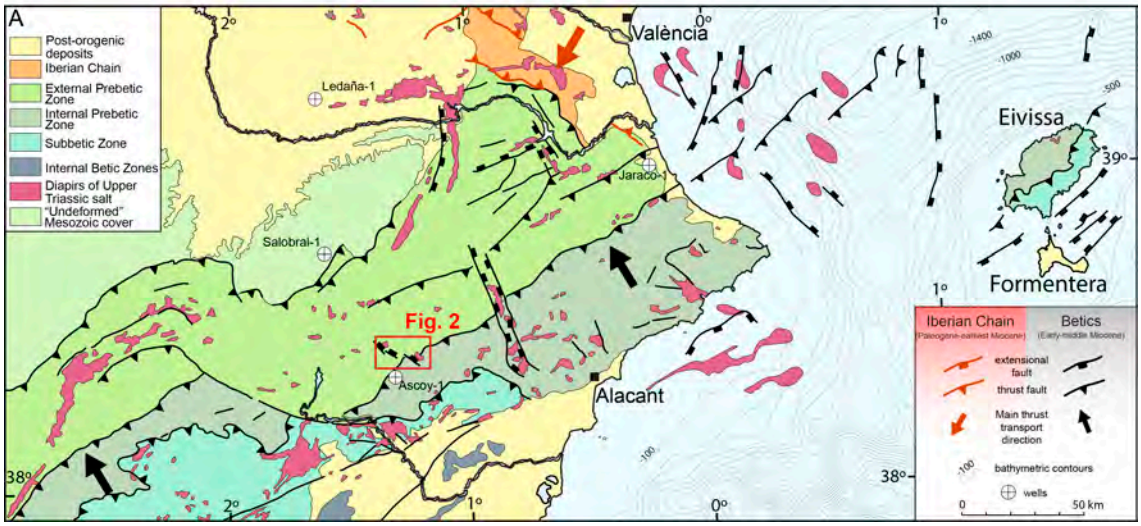

Figure 1. Tectonic map of the Eastern Prebetic, Eivissa and Formentera islands. Red square points out the study area location depicted in Fig. 2.

Using field and geophysical data, this article illustrates how the presence of a pre-rift evaporite unit (Upper Triassic in age) controlled the polyphasic deformation of the Prebetic of Jumilla (Eastern Prebetic, SE Iberia) (Fig. 1). New geodynamic constrains are proposed in order to explain the Mesozoic extension (South Iberian margin), the subsequent inversion (Betic Orogeny) and the later extension during the Upper Miocene.

Therefore, the aim of this research is twofold: 1) to characterize the structure and kinematic evolution of the area, and 2) to depict the interaction between thin- and thick-skinned deformation in a salt province affected by several deformation stages.

Work done

In order to achieve these objectives, we have carried out a detailed geological map (Fig. 2) and three regional (Fig. 3 and 4) cross-sections of the study area supported by 2D depth converted seismic data (Fig. 5). The polyphasic deformation that affected this area has been illustrated by the restoration of a regional cross-section (Fig. 6).

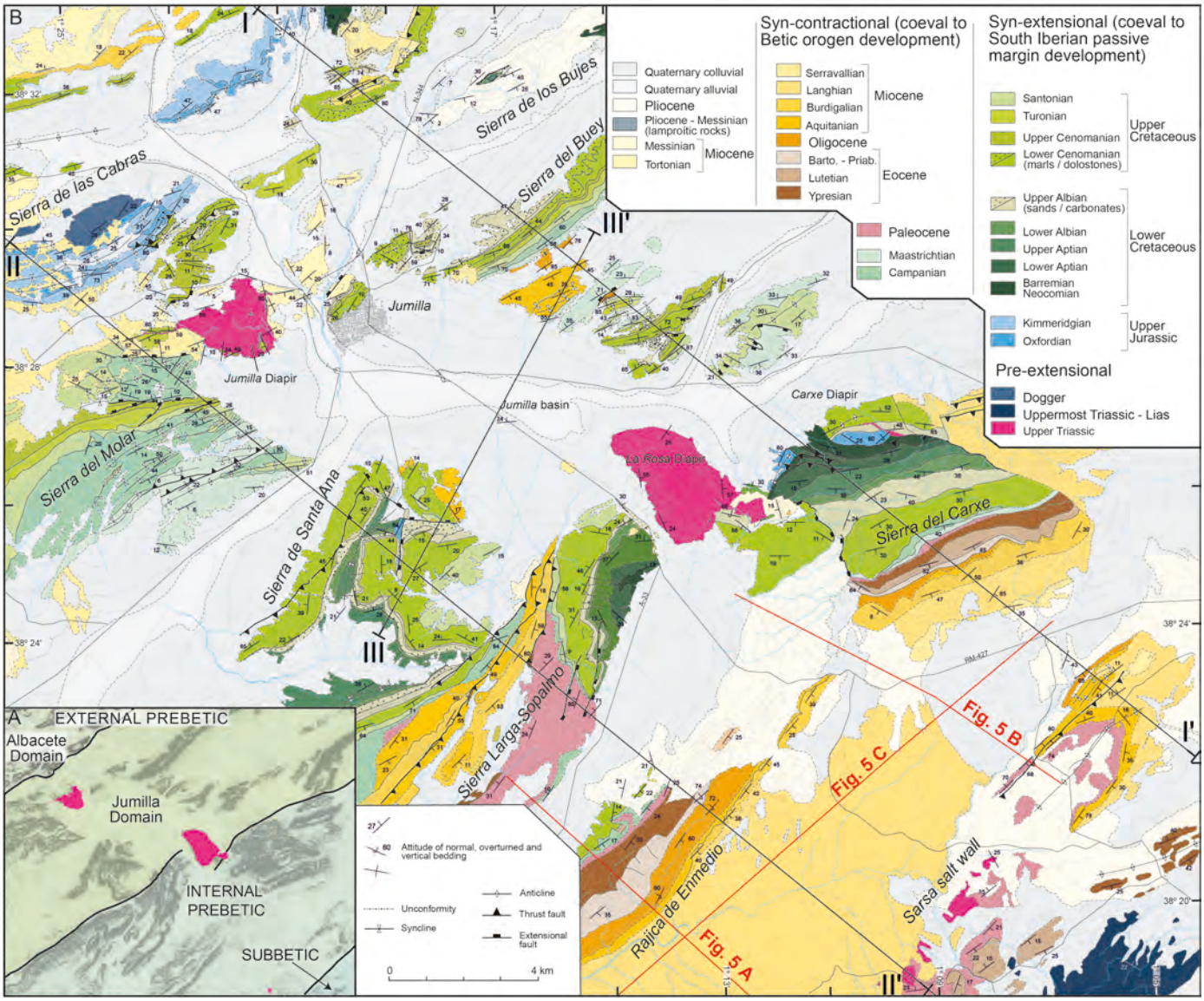

Figure 2. A) Structural sketch showing the location of the thick-skinned fault systems and passive diapirs. B) Detailed geological map of the Prebetic of Jumilla. Note the location of three regional cross-sections and the provided depth converted seismic lines in Fig. 4.

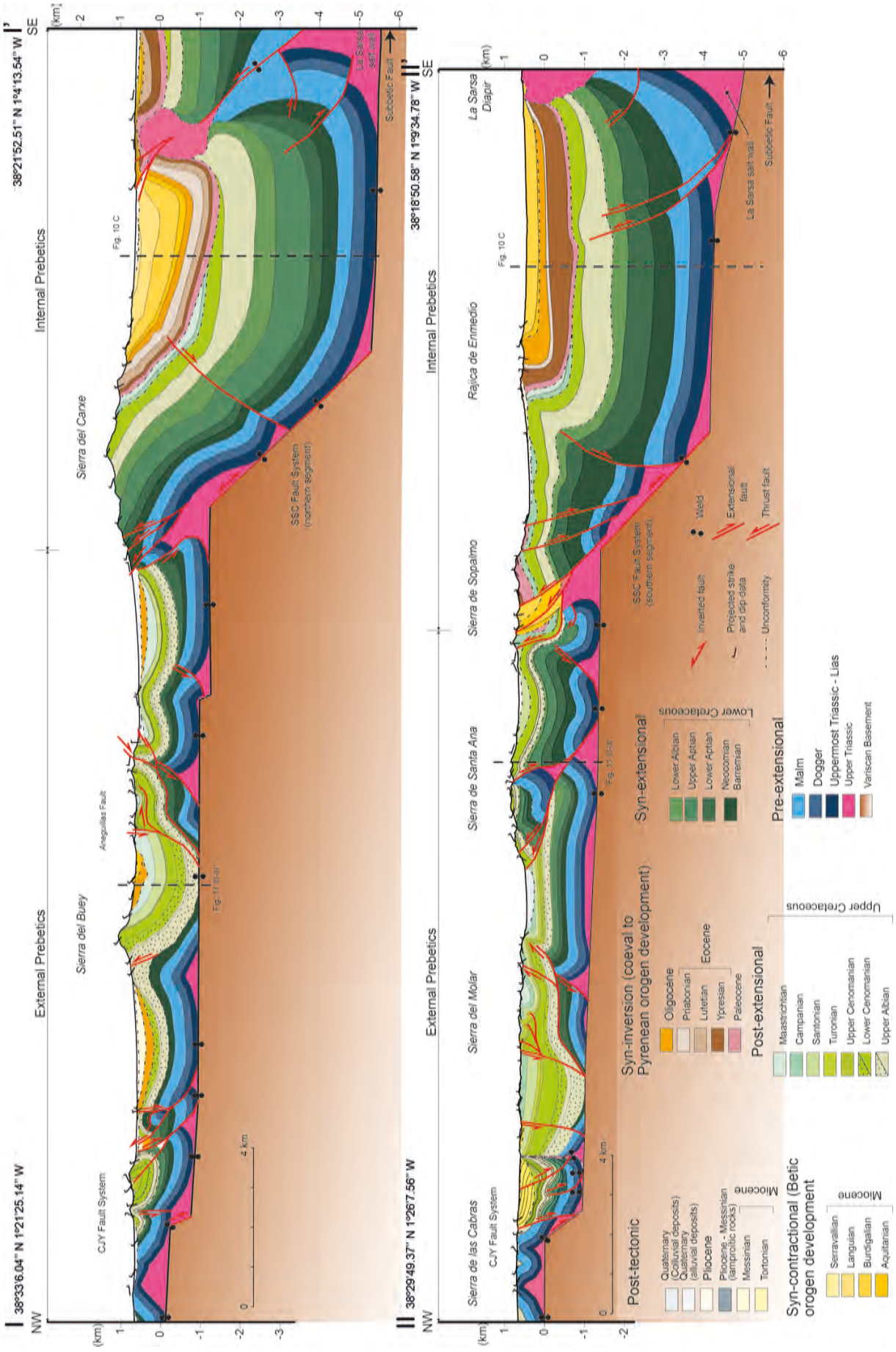

Figure 3. Regional cross-sections throughout the Prebetic of Jumilla. (I-I') Eastern cross-section. (II-II') Western cross-section. See location of respective cross-section in Fig. 1 B.

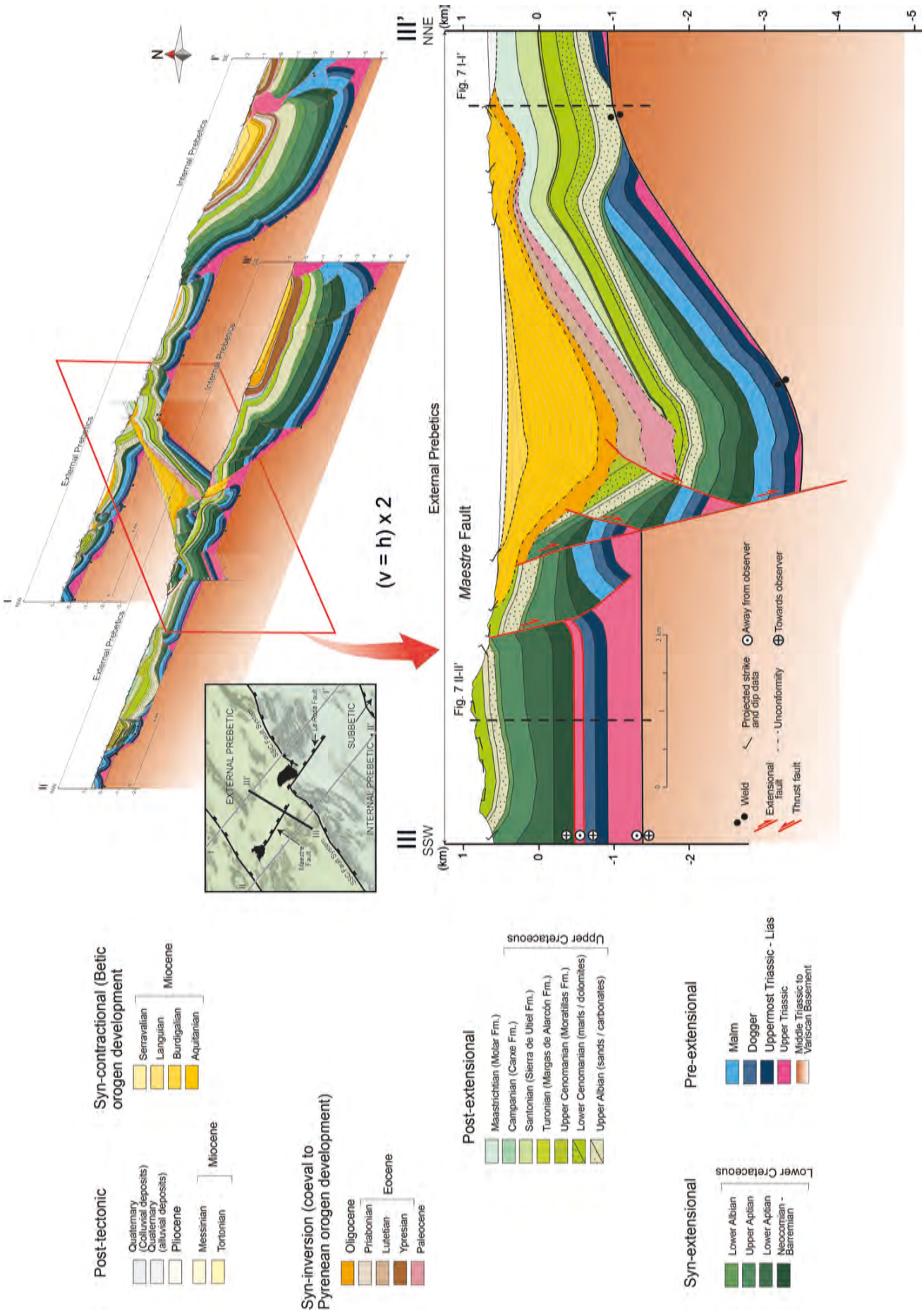

Figure 4. Regional cross-section parallel to the Betic structures (see location in Fig. 1 B)

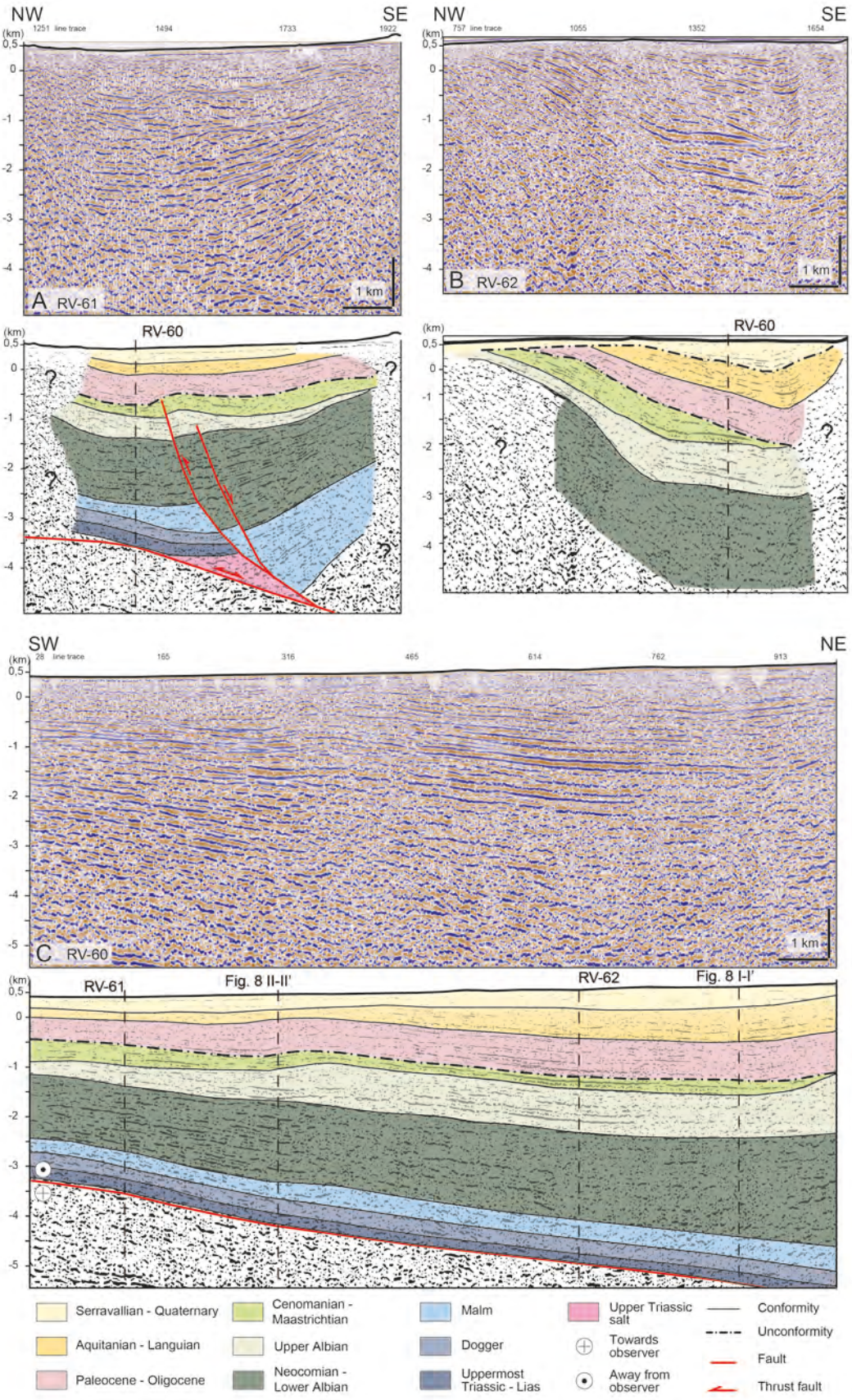

Figure 5. 2D depth converted seismic profiles with their respective interpretation. A) RV-61. B) RV-62. C) RV-60. See location in Fig. 1 B

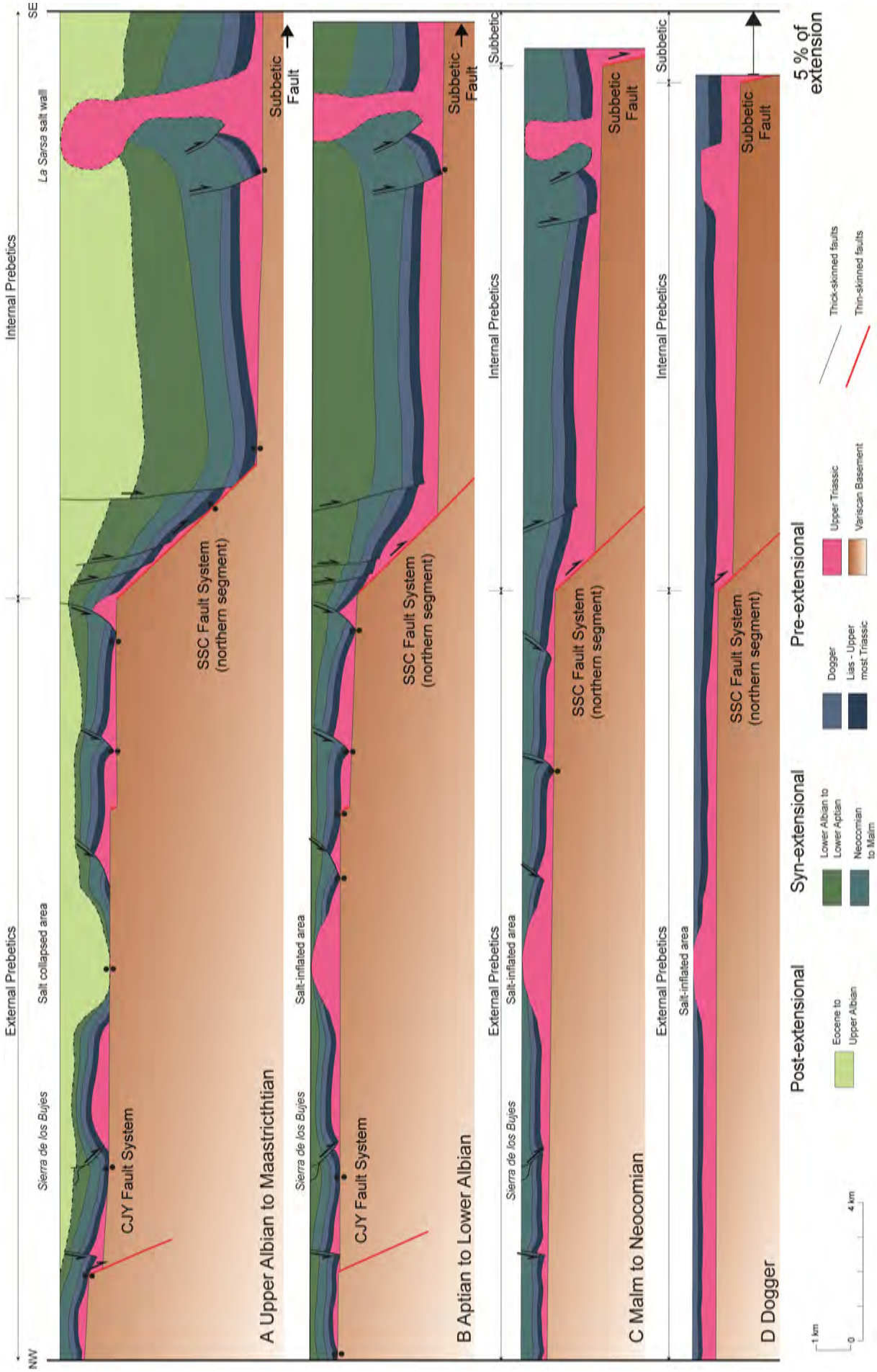

Figure 6. Qualitative sequential restoration of the I-I' regional cross-section

Conclusions

This study depicts the role played by a pre-rift salt layer (Upper Triassic evaporites) on the decoupling of sub- and suprasalt units in an area affected by a polyphasic deformation. The structural and sedimentary analysis of field and subsurface data of the Prebetic of Jumilla unravels the following points:

1. Subsalt faults with orthogonal orientations controlled the basement geometry during the development of the South Iberian margin. Moreover, the major NE-SW subsalt fault systems promoted the development of two differentiated domains (Internal and External Prebetic).

2. The structure of the suprasalt layers was controlled by the degree of decoupling and in general mimicking the subsalt geometry.

3. The thickness and continuity of the evaporite layer as well as the inherited extensional structure constrained subsequent Betic inversion. The location and geometrical characteristics of the Betic fold-and-thrusts were controlled by the inversion of the preexisting thick- and thin-skinned Mesozoic extensional fault systems. Therefore, salt as the weakest rheological material allowed diapir squeezing favoring the development of secondary salt welds.

4. The subparallel orientation between the NNW-SSE thick-skinned structures respect the main Betic compressional stresses as well as the local depletion of the evaporite layer strongly controlled the presence of non-deformed zones where extension continued prevailing during the Betic orogeny and the post-orogenic stage.

Geological characterization of the south Pyrenean front

[1]Oriol Pla, [1]Eduard Roca, [1]Òscar Gratacós, [1]Oriol Ferrer [1]Josep Anton Muñoz

[1]Geomodels Research Institute. Departament de Dinàmica de la Terra i de l'Oceà, Facultat de Ciències de la Terra, Universitat de Barcelona, Spain.

Introduction

This research is included in my PhD. It was started on 2014. The introduction and objectives were described in the two previous reports.

Work done

1. We have done more than four thousand field data sites in order to construct a detailed geological map of the study area (Fig. 1).

2. We have interpreted the main reflectors in the available seismic profiles (Fig. 2).

3. We have constructed a cross section using field data, sisimic data, and well data (Fig. 2).

Results

From the carried out mapping as well as seismic data and well data is verified that Cardona salt (Cardona Fm) and Yesos de Barbastro (Barbastro Fm) are the main syn-orogenic levels. These levels define the basal detachment of the triangular zone that shows a flat-ramp geometry. The flats are developed in the evaporitic levels and the ramps coincides with its southern pinch-outs. The ramps locations at depth matches with the orientation variation of the folds and thrusts at surface (Fig. 2A and B).

La Sentiu-Almenara anticline is the forntal structure. This structure is defined by a smooth anticline and its geometry shows a fault propagation fold. The southern pinch-out of the Barbastro Fm trigger a ramp that conectres the top of the Barbastro Fm with the top of Talavera Fm. This ramp links with a short flat and ends with the frontal backthrust system showing a fish tale structure (Fig. 2B).

The Sanaüja anticline is a complex structure, roughly consists in two anticlines and one syncline. The geometry of these folds is partially controlled by thrusts and backthrusts cutting the frontal south-pyrinean thrust (CFSP) (Fig 2B). The intense deformation of the gypsum in the core of both anticlines constrasts with the ordered structure of the gypsum in the syncline and in detritic sequence in the southern limb of the Sanaüja anticline. In the core of the anticlines and at depth has been interpreted the existence of sal acumulations (Cardona Fm).

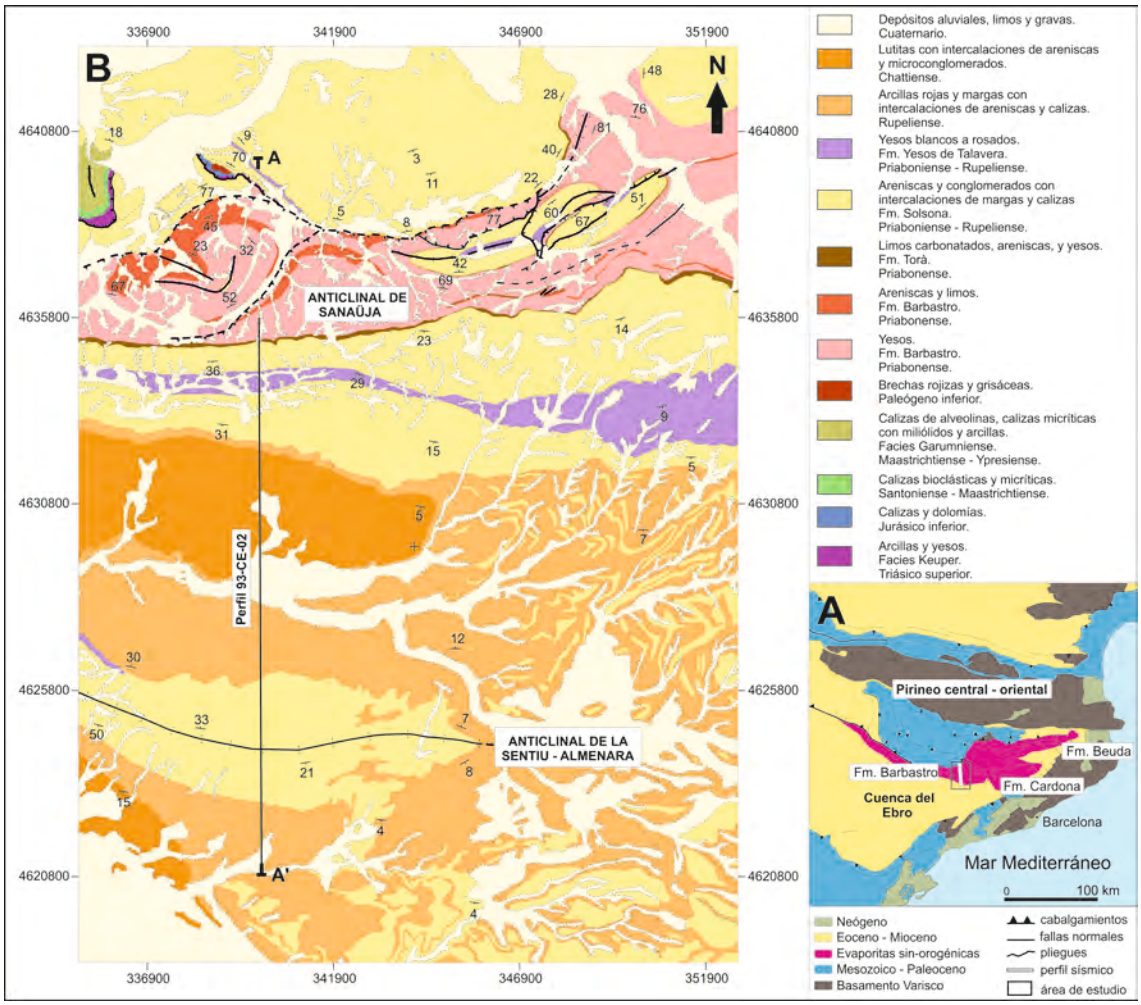

Figure 1. *(A) Map showing the location of the Central – Eastern Pyrenees and the syn-orogenic evaporitic formations. Modified from Sans (2003). (B) Geological Map of the study area showing the location of the A – A' cross section and the 93-CE-02 seismic profile.*

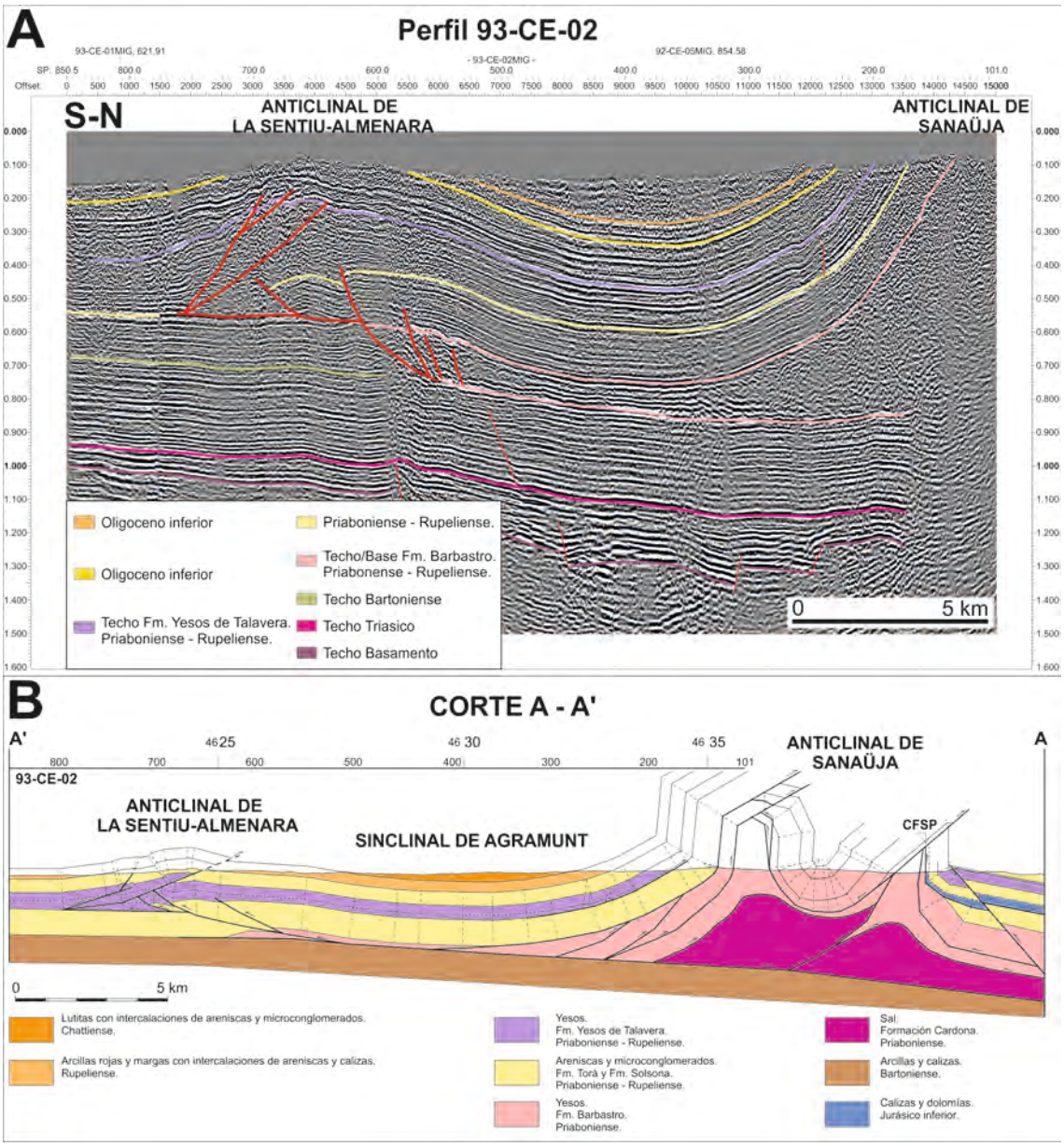

***Figure 2**. (A) 93-CE-02 N-trending seismic profile showing the main features of the La Sentiu – Almenara anticline and its relationship with the distribution of the evaporitic levels of Yesos de Barbastro Fm. and Barbastro Fm. (B) A-A' N-trending cross section. The Southern part of the cross section coincides with the 93-CE-02 seismic profile*

Conclusions

The structure of the La Sentiu-Almenara and the Sanaüja anticlines is controlled by the posicion of the ramps of the basal detachment. It is also controlled by the termination of the evaporitic facies.

La Sentiu-Almenara and Sanaüja anticlines show a diferent geometry and internal structure. La Sentiu-Almenara anticline is a fault propagation fold. Its upper ramp defines a thrust wedge typical of a frontal triangular zone.

Sanaüja anticline is a detachment fold. It has a complex internal structure result of an interference between folds-and-thrusts and an intense deformation of the gypsum. This anticline overlaps previous folds and thrusts dipping to the north and to the south. Furthemore during the fold growth were formed backthrusts and detachments between gypsum and the detritic cover, and also between gypsum and salt accumulations in depth.

The main observed structures deform the outcropping sequence, therefore its age is post-Oligocene.

Future work

6. Complete a detailed geological map of the study area.
7. Complete the interpretation of available seismic profiles.
8. Construct three cross sections trough the study area.
9. Construction of a 3D structural model.

Basement-involved reactivation in fold and thrust belts: the Alpine-Carpathian Junction (Austria)

[1]Granado, P., [2]Thöny, W., [1]Carrera, N., [2]Grazter, O., [2]Strauss, P. [1]Muñoz, J.A.

[1]Institut de Recerca Geomodels, Dept. de Dinàmica de la Terra i de l'Oceà, Universitat de Barcelona, Barcelona, Spain

[2]OMV Exploration and Production GmbH, Trabenstraße 6-8.1020, Vienna, Austria.

The Late Eocene to Early Miocene Alpine-Carpathian fold-and-thrust belt (FTB) lies in the transition between the Eastern Alps and the Western Carpathians, southeast of the Bohemian crystalline massif. Our study shows the involvement of crystalline basement from the former European Jurassic continental margin in two distinct events: a first extensional event coeval with Egerian to Karpatian thin-skinned thrusting reactivated the rift basement fault array and resulted from the large degree of lower plate bending promoted by high lateral gradients of lithospheric strength and slab pull forces. Slab-break off during the final stages of collision in Karpatian to Badenian times promoted large wavelength uplift and an excessive topographic load. The orogenic wedge reacted by the reactivation of the deep detachment in the lower plate promoting the positive inversion of the basement fault array beneath and ahead the thin-skinned thrust front, the extensional collapse of the hinterland summits leading to the opening of the Vienna and ultimately, the broadening of the orogenic prowedge to reduce the topographic load. Although this work specifically deals with the involvement of the basement in the Alpine-Carpathian Junction, the main conclusions are of general interests to the understanding of orogenic systems (Fig.1). This work has been published recently in the *Geological Magazine* journal.

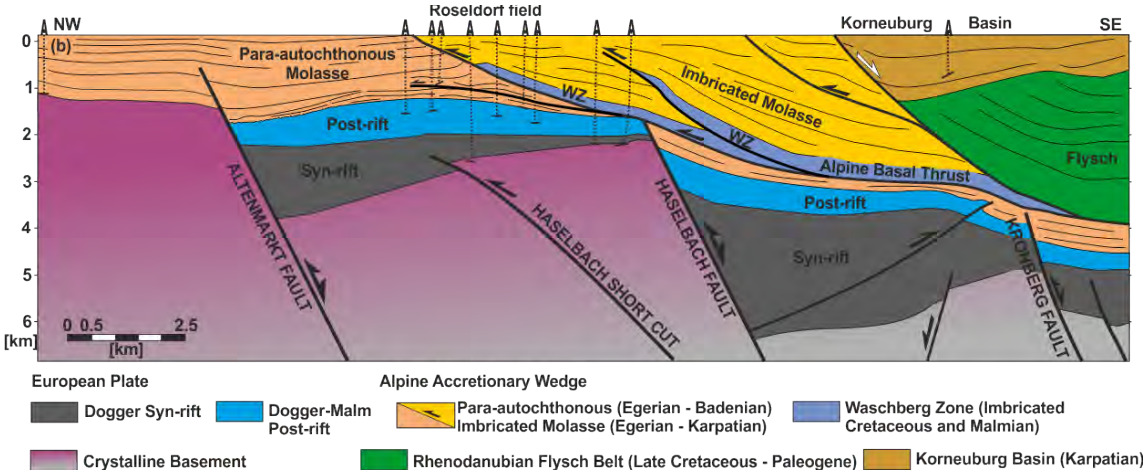

Figure 1. NW-SE striking cross section along the Alpine-Carpathian Junction illustrating the main tectonic units and structure in the basement, fold-and-thrust belt and overlying middle to late Miocene successor basin

Geodynamical framework and hydrocarbon plays of a salt giant: the North Western Mediterranean Basin.

[1]Granado, P., [2]Urgeles, R., [1]Sabat, F., [3]Albert-Villanueva, E., [1]Roca, E., [1]Muñoz, J.A., [4]Mazzucca, N., [5]Gambini, R.

[1]Institut de Recerca Geomodels, Dept. de Dinàmica de la Terra i de l'Oceà, Universitat de Barcelona, Barcelona, Spain.
[2] Dept. de Geociències Marines, Institut de Ciències del Mar (CSIC), Pg. Marítim de la Barceloneta, 37-49, 08003 Barcelona, Spain.
[3]Dept. de Geoquímica, Petrologia i Prospecció Geològica, Universitat de Barcelona.
[4]Enel S.p.A., viale Regina Margherita 137, 00198 Rome, Italy
[5]Enel Trade S.p.A. via Arno 42, 00198 Rome Italy

The North Western Mediterranean Basin developed during the Oligocene-Miocene rifting of the Eastern Iberian-European magma-poor continental margin. The margin developed as a result of back-arc extension associated with the roll-back of the retreating Calabrian-Tethys subduction zone. Reinterpretation of 2D regional seismic reflection data suggests that rifting took place by hyperextension of the Iberian-European lithosphere. This process led to the seaward arrangement of distinct crustal domains, namely proximal, necking and distal. The late post-rift Messinian Salinity Crisis (MSC) gave place to significant margin erosion and canyon incision whose lowstand sedimentary by-products were largely deposited prior to the Messinian evaporitic sequences. Mesozoic-Cenozoic and Messinian to recent salt tectonics events have been recognized. A regional hydrocarbon play concept is here proposed for shelf to deep waters settings, including pre-salt, Messinian and post-salt plays (fig.1). This work has been published recently in the *Petroleoum Geoscience* journal.

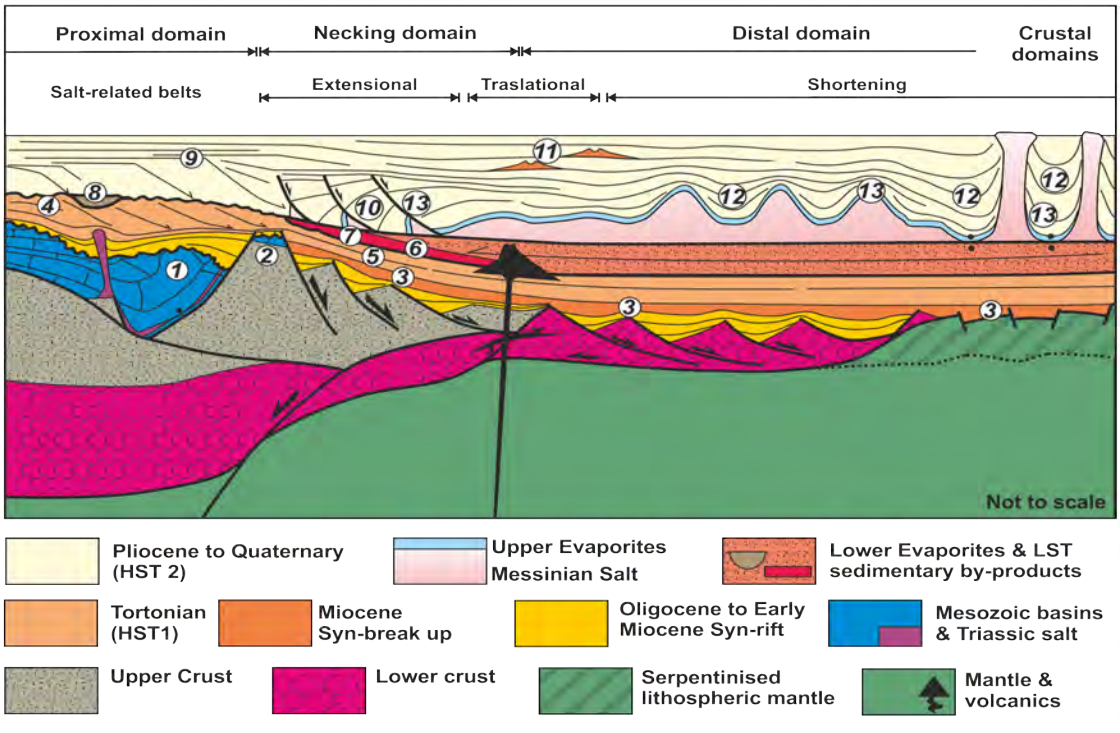

Figure 1. Conceptual lithospheric section illustrating the main play types defined in this study.

Syn-thrusting, near-surface flexural-slipping and stress deflection along folded sedimentary layers of the Sant Corneli-Bóixols Anticline (Pyrenees, Spain)

[1]Tavani, S., [2]Granado, P., [2]Arbués, P., [2]Muñoz, J.A.

[1]DISTAR, Dipartimento di Scienze della Terra, dell'Ambiente e delle Risorse, Universita Federico II,
Napoli, Italy
[2]Institut de Recerca Geomodels, Dept. de Dinàmica de la Terra i de l'Oceà, Universitat de Barcelona, Barcelona, Spain.

In the Spanish Pyrenees the Sant Corneli-Bóixols thrust-related anticline displays an outstandingly preserved growth strata sequence. These strata lie on top of a major unconformity exposed at the anticline's forelimb that divides and decouples a lower pre-folding unit from an upper syn-folding one. The former consists of steeply-dipping to overturned strata with widespread bedding-parallel shears indicative of folding by flexural-slip, whereas the syn-folding strata above define a 200-m amplitude S-shaped fold. In the inner and outer sectors of the forelimb, both pre- and syn-folding strata are near-vertical to overturned and the unconformity angle ranges from 10° to 30º. In the central portion of the forelimb, syn-folding layers are shallowly-dipping, whereas the angular unconformity is about 90° and the unconformity surface displays strong S-C shear structures, which provide a top-to-the foreland shear sense. This sheared unconformity is offset by steeply-dipping faults which are at low angles to the underlying layers of the pre-folding unit. Strong shearing along the unconformity surface also occurred in the inner sector of the forelimb with S-C structures providing an opposite, top-to-the hinterland, shear sense. Cross-cutting relationships and shear senses along the pre-folding bedding surfaces and the unconformity indicate that regardless of its orientation, layering in the pre- and syn-folding sequences of the Sant Corneli-Bóixols anticline was continuously sheared (figure 1). This shearing promoted an intense stress deflection, with the maximum component of the stress tensor keeping at low angles to beds during most of the folding process.

This work is in under review in the *Journal of Geophysical Research – Solid Earth.*

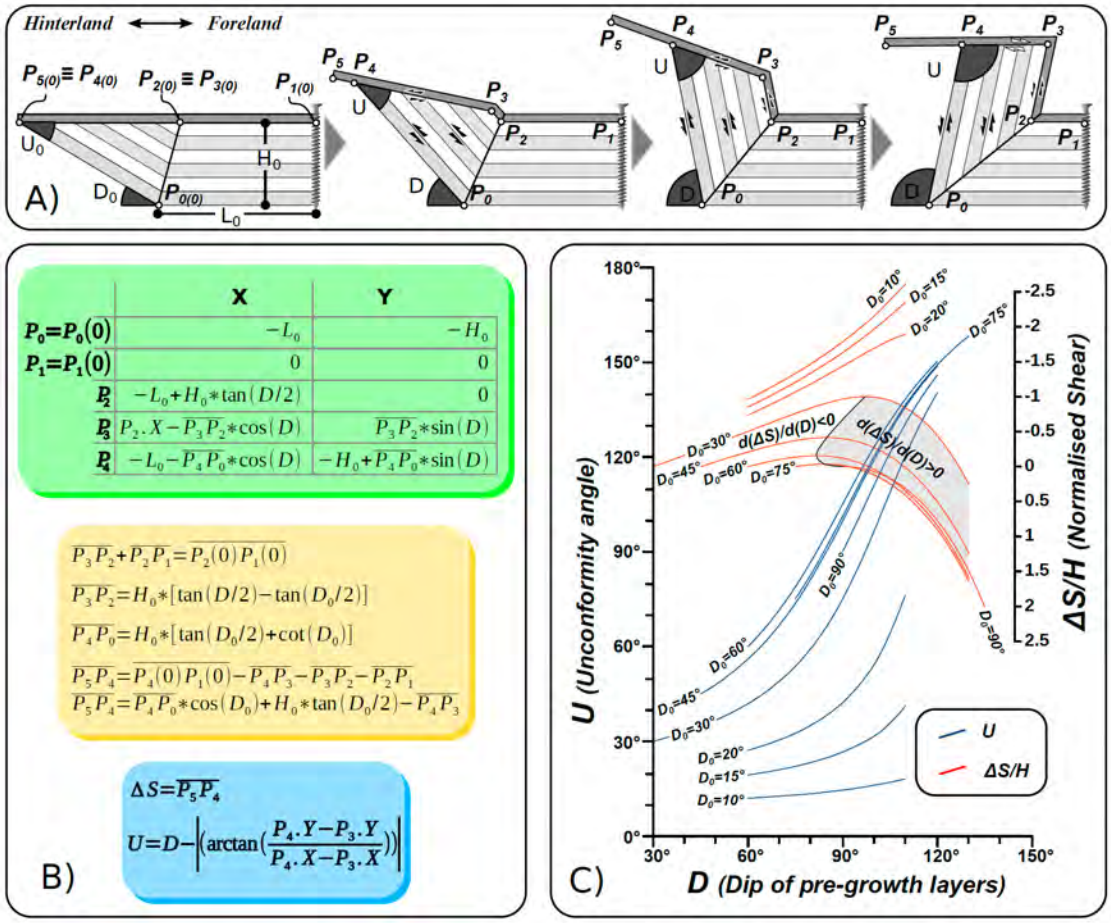

	X	Y
$P_0=P_0(0)$	$-L_0$	$-H_0$
$P_1=P_1(0)$	0	0
P_2	$-L_0+H_0*\tan(D/2)$	0
P_3	$P_2.X-\overline{P_3P_2}*\cos(D)$	$\overline{P_3P_2}*\sin(D)$
P_4	$-L_0-\overline{P_4P_0}*\cos(D)$	$-H_0+\overline{P_4P_0}*\sin(D)$

$$\overline{P_3P_2}+\overline{P_2P_1}=\overline{P_2(0)P_1(0)}$$
$$\overline{P_3P_2}=H_0*[\tan(D/2)-\tan(D_0/2)]$$
$$\overline{P_4P_0}=H_0*[\tan(D_0/2)+\cot(D_0)]$$
$$\overline{P_5P_4}=\overline{P_4(0)P_1(0)}-\overline{P_4P_3}-\overline{P_3P_2}-\overline{P_2P_1}$$
$$\overline{P_5P_4}=\overline{P_4P_0}*\cos(D_0)+H_0*\tan(D_0/2)-\overline{P_4P_3}$$

$$\Delta S=\overline{P_5P_4}$$
$$U=D-\left|\left(\arctan\left(\frac{P_4.Y-P_3.Y}{P_4.X-P_3.X}\right)\right)\right|$$

Figure 1. (A) Evolving angular relationships between unconformable sequences during flexural-folding in the inner limb of a syncline, with shear senses along pre-unconformity layers and along the unconformity indicated. The position of six key-points undergoing folding is illustrated, as well as the dip of pre-unconformity layers (*D*) and of the unconformity angle (*U).* (B) X and Y coordinates of the six points of figure 6a, with length of segments, and derived amount of shear along the unconformity (DS) and unconformity angle (U). (C) Graphical solution of equations in figure 6b. Blue lines relate the unconformity angle (*U*) to the dip of pre growth strata (*D*) for different initial unconformity angle (U_0). Red lines relates the normalised shear along the unconformity in the inner portion (i.e. DS = P_4P_5 segment divided *H*) to *D*, for different initial unconformity angle (U_0). Notice that the Y axis for red lines is on the right and that positive and negative values are flipped. The lines indicate the cumulative shear along the unconformity, while the grey area bordered by the black line, indicate the area where the incremental shear is negative.

Reactivation of a syn-growth unconformity duing flexural-slip folding (Bóixols Anticline, Pyrenees, Spain)

[1]Tavani, S., [2]Granado, P., [2]Arbués, P., [2]Muñoz, J.A.

[1]DISTAR, Dipartimento di Scienze della Terra, dell'Ambiente e delle Risorse, Universita Federico II, Napoli, Italy
[2]Institut de Recerca Geomodels, Dept. de Dinàmica de la Terra i de l'Oceà, Universitat de Barcelona, Barcelona, Spain.

The contractive growth strata of the Bóixols anticline (Spanish Pyrenees) include a major Upper Cretaceous synkinematic unconformity outstandingly exposed at the anticline forelimb. The unconformity divides and decouples the growth-sequence in two units of contrasting geometry. In the outer sector of the forelimb, the unconformity preserves its stratigraphic attitude, showing an angle of less than 20º and separating near-vertical to south-dipping upper and lower unit syn-kinematic strata. In the central portion of the forelimb, the multilayered lower unit acquires a near-vertical attitude, whereas layers of the upper unit become shallow-dipping. The angular unconformity there is about 90_ and the unconformity is affected by meso-faults and S-C structures providing a top to the foreland shear sense. Such a shear zone is offset by high-angle reverse faults propagating from the underlying layer-parallel faults of the lower syn kinematic unit. In the inner sector of the forelimb, strata of the lower and upper units are overturned and near-vertical, respectively. Still, the unconformable contact represents a shear zone, indicating a top to the crest shear sense. Shear senses along with relative timing and cross-sectional distribution of deformation structures, indicate flexuralslip folding in the growth sequence. Layer-parallel anisotropies oblique to each other were active at the same time and only during the later stage of folding, when layers of the lower unit were becoming orthogonal to those of the upper package, the flexural-slip mechanism arrested in the upper package. These observations point out that, regardless of its orientation, layering in the growth sequence of the Bóixols anticline promoted stress channeling, with the maximum stress keeping about parallel to beds almost for the entire folding process.

This work was presented as an oral contribution in Vienna's EGU General Assembly 2016. It can be referenced as Geophysical Research Abstracts Vol. 18, EGU2016-2096, 2016.

A Pyrenean mid-Cretaceous extensional fault system in the Briançonnais Domain of the Alps: implication for the Eastern termination of the segmented Bay of Biscay-Pyrenean rift system.

[1]Tavani, S., [2]Bertok, C., [1]Corradetti, A., [3]Granado, P., [4]Vigna, B.

[1]DISTAR, Dipartimento di Scienze della Terra, dell'Ambiente e delle Risorse, Universita Federico II,Napoli, Italy.
[2]Dipartamento di Scienze della Terra, Università degli Studi di Torino, Torino, Italy
[3]Institut de Recerca Geomodels, Dept. de Dinàmica de la Terra i de l'Oceà, Universitat de Barcelona, Barcelona, Spain.
[4]Dipartamento di Ingegneria dell'Ambiente, del Territorio e delle Infrastucture, Politecnico di Torino, Italy.

In the Briançonnais domain of the Ligurian Alps, Digital Elevation Model, orthophotos, and geological maps have been integrated with field observations and subsurface data from the karst network, in order to reconstruct the 3D structure of a crustal-scale mid-Cretaceous extensional fault system. This is made by a major E-W striking fault that has in its northern block a set of E-dipping transverse extensional faults. The master fault has been reactivated as a strike-slip structure during the alpine deformation and its original geometry, including fault dip and cutoff angles, is no longer recognisable. Conversely, the E-dipping faults and the fault-bounded blocks almost completely preserve their Cretaceous geometry. The alpine deformation has poorly modified these transverse faults, which affect a Mesozoic sedimentary sequence and the underlying Paleozoic basement with extensional displacements in the order of many hundreds of meters. Removing the about 120° counter-clockwise vertical axis rotation associated with the alpine orogeny, leads the E-dipping fault to become about SSW-dipping, while the master fault becomes almost parallel to a suite of NNE-SSW to NE-SW striking transfer faults that connect the eastern portion of the Pyrenean mountain range to the north-verging thrust system of the Provence region, in the foreland of the western Alps. These faults, which have been inherited from the extensional stage associated with the opening of the Alpine Tethys, were delimiting to the east the Pyrenean rift system during the mid-Cretaceous separation of Iberia from Eurasia. We propose that the mid-Cretaceous extensional fault system described here represented part of such a NNE-SSW striking transfer zone, likely ensuring the connection between the Pyrenean arm of the Bay of Biscay - Pyrenean rift system and a further eastern, intra-plate, arm.

This work was presented as an oral contribution in the 88º Congresso della Società Geologica Italiana, Napoli, Italia.

Inversion Tectonics in the Höflein Area (Austria)

[1]Granado, P., [1]Muñoz, J.A.

[1]Institut de Recerca Geomodels, Dept. de Dinàmica de la Terra i de l'Oceà, Universitat de Barcelona, Barcelona, Spain

Introduction.

This introduction summarises the 2 years technology project "Inversion Tectonics in the Höflein Area" carried out by the Institut de Recerca Geomodels (Universitat de Barcelona, UB) in close cooperation with OMV Exploration and Production GmbH (Austria) within the project FBG-307451.The main objective of the research was the validation of recent structural interpretations of the Höflein field which are indicative of positive tectonic inversion of the Jurassic rift basin. These new structural interpretations imply the presence of additional inversion-related structures in the sub-thrust region. Re-appraisal of the full Jurassic rift system at Donau Nord using inversion tectonics concepts was also carried out. This approach was also brought into the regional Alpine-Carpathian-Pannonian tectonic context.

Structural validation of sub-thrust structures has been carried out by the re-interpretation of the full extent of the Donau Nord 3D depth-migrated seismic merge ~500 km^2). The new exploration concept has also been validated by the re-interpretation of regional time-migrated 2D seismic profiles coupled with several tens of exploration and production wells, subsequent structural modelling, balanced cross-section construction, and structural restorations (Fig.1).

To further validate the structural model presented here, 2D and 3D sandbox analogue models were run based on the seismic interpretations carried out for the Höflein area. Sandbox analogue models have provided insights into the development of structural traps related with the inversion of geometrically complex extensional fault systems. The interpretation of the sandbox analogue mdelling results has been aided by the use of white-light topography scans and image-based voxel reconstrutions.

Comprehensive understanding of world-class outcrop analogues of inversion structures from the Spanish and French Pyrenees have also provided key insights into the impacts of inversions tectonics in hydrocarbon systems. Discussions during the fieldtrips added a fundamental value for the re-appraisal of the Donau Nord area.

Gas reserves estimations were carried out for a series of sub-thrust leads using a MIN, Most Likely and MAX which include the Höflein Fault Hanging-wall (Wiedling, Leopolds, Höflein Sud leads), the Höflein Footwall Imbricates lead, the Stockerau Anticline lead, the Roseldorf Ridge lead and the Herzogbirbaum lead on the Altenmarkt Fault hanging-wall.

Conclusions

The inversion tectonics exploration concept was proven. Prospective structures related with inversion tectonics in the Donau Nord sub-trust have been defined, and their potential gas accumulations, calculated. The identified inversion structures are located in the updip migration path and/or directly above the deepest syn-rift kitchen areas at Haselbach half-graben. The presence of Jurassic primary and secondary reservoir targets (i.e., Höflein Fm and Altenmarkt Gp., respectively) is proven by nearby well

data and seismic facies. Vertical sealing could be provided by the unconformable Egger to Eggerian successions and the Malmian Mikulov Fm and Carbonate Banks Fm. Lateral sealing could also have been favoured by faults, as in the Höflein field. Migration and entrapment in the area are known to have occurred, so the main concern for exploration success is the existence of traps and their integrity.

Additional prospective structures along the NW boundary of the Lower Austria Basin may be present. 3D structural reconstructions from seismic interpretations suggest a sub-thrust anticline at Stockerau similar in size to the Höflein field. The authors are aware of the current economic shortage in relation with low oil prices, but in order to fully constrain the existence of these potentially large hydrocarbon accumulations, additional 3D coverage is needed. The preferred area for new 3D seismic acquisition would be along the NW boundary of the Lower Austria Mesozoic Basin, linking with the poorly covered Höflein area. This new 3D seismic survey should overlap with the Höflein area, as the full potential of inversion structures cannot be properly assessed with the existing seismic and well data. As to the Höflein-Aderklaa area, significant prospectivity is also still present. Structural modelling and results from Höflein 5b, Wiedling and Aderklaa UT wells, in addition to evidences from geological maps of Lower Austria, sandbox analogue models, and field analogues of inversion structures indicate that Jurassic reservoirs are present on the Höflein fault hanging-wall and that the structural traps associated with Wiedling and Höflein Sud could have been charged from the Aderklaa area or the same Höflein hanging-wall syn-rift section.

Based on our re-appraisal, the Lower Austria Mesozoic Basin can be considered as a locally inverted rift basin. These systems tend to show a high degree of reserves concentration in the largest field. This can be explained either as inversion resulted in the formation of one major structure that constituted a migration focus, accessing the majority of the basin's kitchen area. We wonder if this would be the case for the Höflein field, but additional 3D coverage at Stockerau and the NW boundary of the Lower Austria Mesozoic Basin is needed to fully constrain the potential. Such new survey may shed light not just into new structural traps in the para-autochthonous, but also into syn-rift stratigraphic traps within the Gresten Gp. delta system.

As main goals, it is worth highliginthg the following:

- Project advances and results have been presented and discussed in several workshops held in Vienna HO and Barcelona with OMV staff, and have been also presented at AAPG congresses in Barcelona, Lisbon and Melbourne during 2014 and 2105. The main results from an Alpine-Carpathian-Pannonian geodynamical perspective have been published on the indexed journal *Geological Magazine* (IF:1.863)
- An additional publication on sandbox analogue modelling of inversion tectonics is in press on the journal *Tectonophysics* (IF: 2.650)
- Our work has been positively regarded by OMV Exploration and Production GmbH. A relationship of trust has been established between the Institute de Recerca Geomodels and this company, as proven by the fact that additional research projects and scientific collaborations are to be carried out from 2017 onwards (in the process of signing at the moment).
- The company has provided Geomodels with a large high-quality database of subsurface data, including: 3D time- and depth-coverted seismic surveys, 2D time migrated profiles, and a wealth of well and log data. These resources are available for additional research and can be used for teaching purposes.

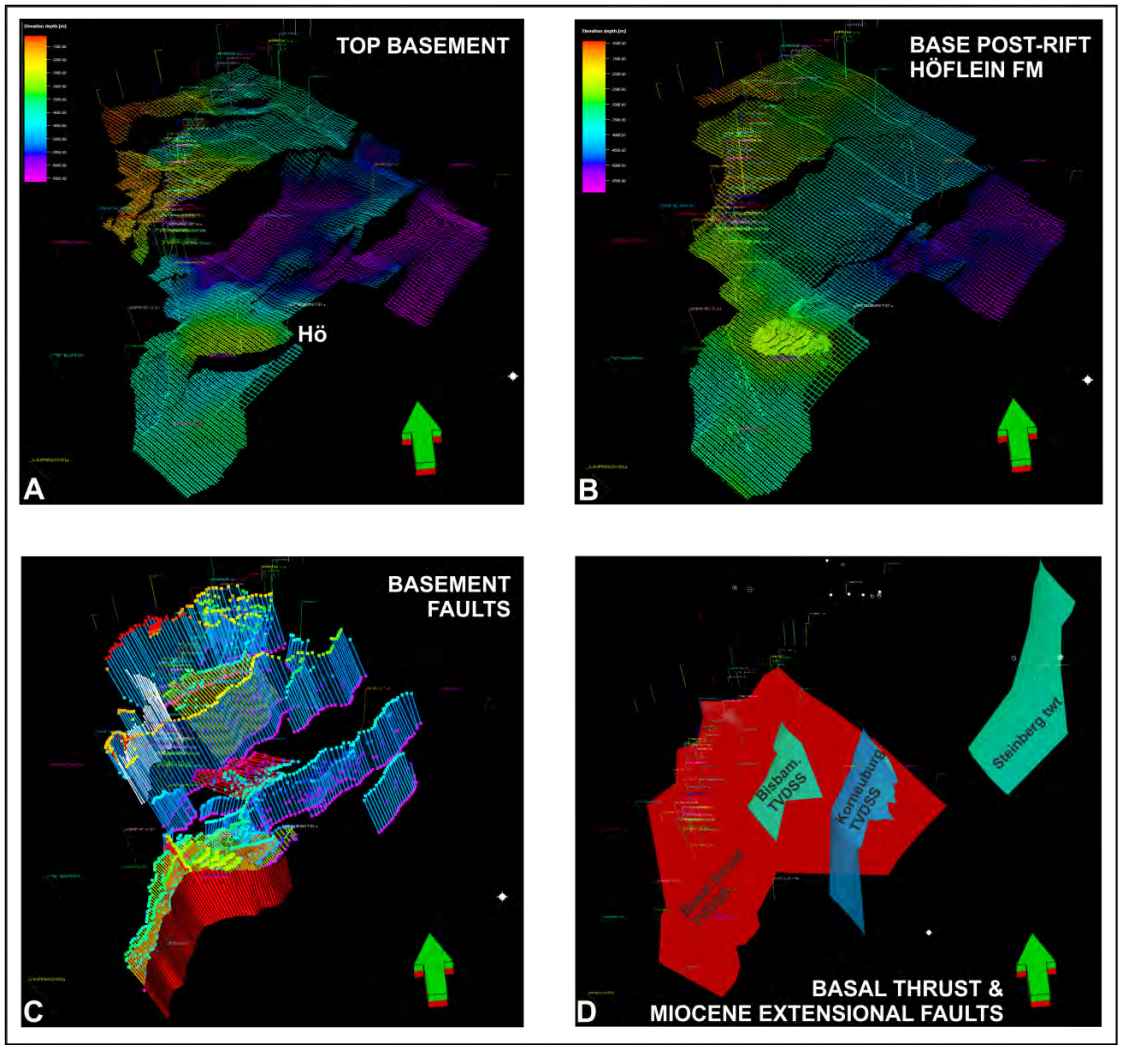

Figure 1. Horizons and faults interpretations from Donau Nord 3D survey and Vienna's VBSM_PSTM_noAGC (time-migrated) survey carried out in Petrel. A) Top Basement. B) Höflein Fm. C) Para-Autochthonous faults, including Jurassic Rift Faults, and Inversion Related Faults. D) Alpine Basal Thrust (red), Bisbanberg (green) and Korneuburg (blue) Faults and the Steinberg Fault (green, in twt). Hö: Höflein Fault and Höflein Field shown for reference.

Future work

Future work includes the construction of a regional cross section, and numerical modelling on the influence of deep-seated lithospheric procees on surficial ones.

During this year, research collaboration has been maintained with:

- OMV Exploration and Production GmbH, Trabenstraße 6-8.1020, Vienna, Austria. Collaboration has been maintained in the following topics:

  Understanding the processes goberning the inversion of extensional basins and their impact on exploration in mature hydrocarbon basins by means of integrating subsurface data, outcrop analogues and sandbox modeling.

  Calculation of yet-to-find hydrocarbon resources in deep-seated, poorly-imaged sub-thrust settings.

  Structural modelling of the deep-seated gas fields beneath the Vienna Basin from outcrop analogues in the Northern Calcareous Alps (to be potentially followed by a 2 yrs. research project).

- Dipartimento di Scienze della Terra, de'll Ambiente e delle Risorse, Universitaà Federico II, Napoli. Collaboration has been maintained with this research group in the following topics:

  Characterization of naturally fractured carbonate reservoirs.

  Structural characterization of reservoirs associated with salt tectonics in compressional tectonic settings.

  Development of structural models of midly-inverted extensional forced fold systems in salt basins applied to resource exploration.

  Paleogeographic studies in the Briançonnais Domain of the Alps and implications for the correlation of the Bay of Biscay-Pyrenean Rift system and Western Alps.

- REPSOL CTR. Characterization of naturally fractured reservoirs by means of Virtual Geological Models using LiDAR and Photogrammetric techniques.

An integrated approach to define new stratigraphic plays in the mature oil Middle Magdalena Valley Basin (Colombia)

[1]Cabello, P., [2]López, C., [2]Dussán, M. I., [2]Gamba, N., [2]Torres, E., [2]Ballesteros, C., [2]Cantisano, M. T., [2]Marfisi, N., [1]Calvo, C., [3]Vázquez, Y., [1]Ramos, E.

[1]Dept. Dinàmica de la Terra i de l'Oceà, Institut de Recerca Geomodels. Facultat de Geologia, Universitat de Barcelona, c/Martí i Franquès s/n, 08028, Barcelona. pcabello@ub.edu
[2]Ecopetrol S.A., Carrera 7 No 32-13 Ed. San Martín, Piso 7, Bogotá, Colombia
[3]Escuela de Ciencias Geológicas e Ingeniería, Yachay Tech University, Hacienda San José s/n y Proyecto Yachay, San Miguel de Urcuquí, Ecuador

Abstract

The Colombian Middle Magdalena Valley Basin has produced oil for over a century, mostly from reservoirs forming part of the Tertiary fluvial formations of Lisama, La Paz, Esmeraldas, Mugrosa and Colorado. Since the structural traps are plays already proved in this mature basin, new opportunities for finding the remaining reserves are expected to be associated with stratigraphic traps (Figure 1).

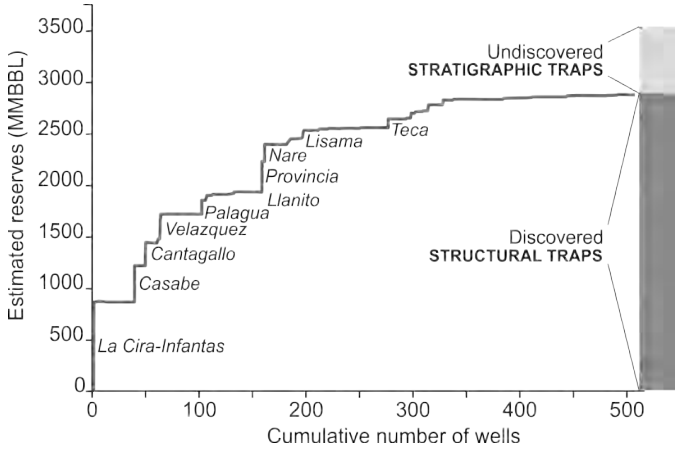

Figure 1. Creaming curve of the Middle Magdalena Valley Basin. The proved reserves (i.e. about 3000 MMBBL), located in structural traps, do not reach the total estimated reserves, which are expected to be related to undiscovered stratigraphic traps.

In this project we developed an approach that has proved useful in redirecting the exploratory activities in the Middle Magdalena Valley Basin. The method is based on the construction of a 3D exploration scale geocellular facies model of the productive units in the whole basin. The approach compiles and integrates both subsurface and outcrop geological data. It is based on a sedimentological study of the Tertiary fluvial productive units, and on the subsequent construction of a 3D facies model. Paleogeographical reconstructions based on facies proportion maps, fault activity, paleocurrent data and conceptual depositional facies models were used to derive statistical parameters involved in the stochastic facies modeling process. The model, which is the first one constructed for the whole Middle Magdalena Valley Basin, depicts the complete structure of the basin in three dimensions, including the major faults and the horizons bounding the oil producing fluvial units, along with the gross distribution of reservoir-like and seal-like rocks (Figure 2). It was used to search for new areas of interest associated with potential stratigraphic traps, and constitutes a starting point from which to develop new studies and exploratory efforts.

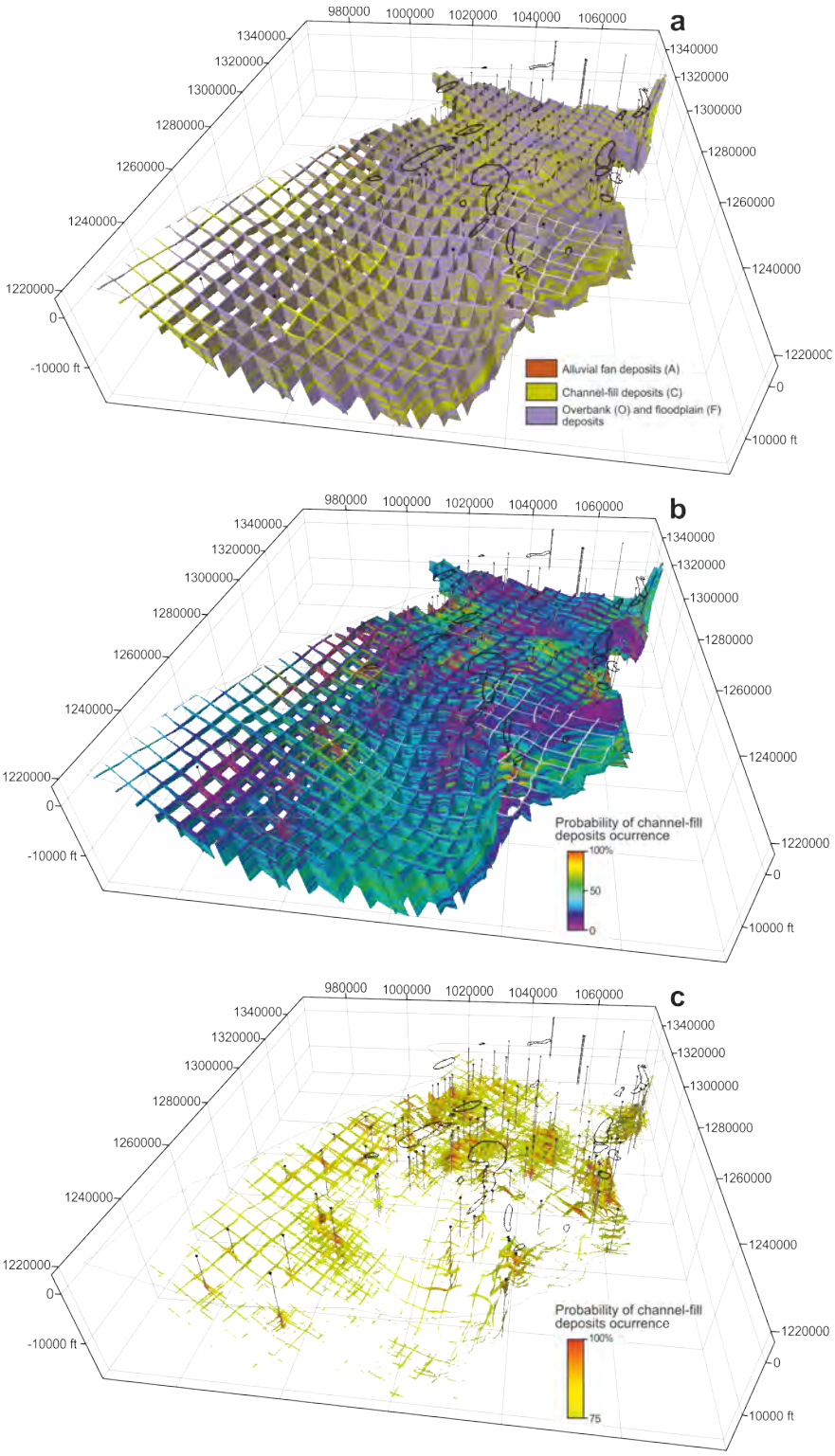

Figure 2. Figure 21. a) Facies association 3D model of the Middle Magdalena Valley Basin, reproducing the distribution of channel-fill deposits, floodplain and overbank deposits, and alluvial fan deposits. b) 3D parameter showing the probability of occurrence of channel-fill sandstone bodies resulting from averaging the twenty realizations of the 3D facies model. c) Probability parameter shown in b filtered for probabilities above 75%. Coordinates are in Universal Transverse Mercator (UTM) system, Colombia Bogota Zone. Vertical scale is indicated in feet and exaggeration is 4x.

Depositional and Architectural Evolution of a Turbidite Channel System from Outcrop and Behind-the outcrop Data: the Solitary Channel Complex (Miocene, Tabernas Basin, SE Spain)

[1]Marco De Matteis, [1,2]Pau Arbués, [1,2]Patricia Cabello, [1,2]Pablo Granado, [1,2]Miguel López-Blanco, [3]Vitor Abreu, [4]Timothy Demko, [1,2]Mariano Marzo, [1,2]Josep Anton Muñoz, [1,2]Zaín Belaustegui.

[1]Departament de Dinàmica de la Terra i de l'Oceà. Universitat de Barcelona.
[2]Insititut de Recerca Geomodels, Universitat de Barcelona.
[3] *Abreu Consulting and Training, Houston, TX, United States.*
[4] Exxon-Mobil Upstream Research Company, Houston, TX, United States.

Introduction and main objetives

Research in the Solitary Channel (SC) was initiated in 2014. It aimed at contributing to the study of deepwater outcrop analogs from the broad perspective of integrating conventional outcrop datasets with behind-the-outcrop data, and leading to both static and dynamic models. The datasets and models could render numerous, effective, and quantifiable ways of comparison to their real reservoir counterparts and be used in training and research.

2014 reached the integration of conventional and behind-the-outcrop data and gave sedimentologic and architectural interpretations (Fig. 1a). The continuation of the research troughout 2015, was oriented towards static 3D facies models from the SC. More particularlly of the stratigraphic slice between the SC basal boundary and the top surface of a local key bed named Orange Bed. This portion of the sedimentry volume is well exposed over all the study area giving a really good approximation of the 3D architectural geometry and facies relationships. The 3D facies modelling was aimed at:

1) Test the existing architectural interpretations
2) Explore new implements in comercial facies modeling algorithms
3) Produce geocellular facies models to be the grounds for subsequent petrophysics models and dynamic (flow) models and synthetic seismic models.

Results of previous project phases were already reported. These resolve lithologic facies and architecture by means of: conventional outcrop dataset (Fig. 1A), interpreted Digital Outcrop models, digital hierarchical surface framework (Fig. 1B), and hierarchical geocellular facies models built in by use of reservoir specialized software packages (Figs. 1C and 1D). The main conclusions of this phase relate to facies modeling methods.

Further work was carried throughout 2016, aimed at integrating more information in order to:

1) Explore the potential of Computerized Axial Tomography (CTScan) as a tool leading to a refined understanding of sedimentary structures, and therefore transport-sedimentation processes and subsequent sediment disturbation by organic activity.
2) Contribute additional criteria to the architectural subdivision scheme and paleodepositional setting by means of a detailed ichnological study.

Work done

In order to evaluate the potential of the CTScanning technique, a 30 cm long core sample from well SC-DD-01 (from the SCC) was taken to the Corelab device (XRE CoreTom) installed in the scientific campus at UB. The sample was scanned using a setup which yielded a 85 microns resolution. The obtained images were loaded on a specialized software allowing for multiple visualization operations and image processing capacities (Fig. 2). Preliminary analysis indicates that the dataset is suitable for discriminating all the sedimentary structures visible on core surface, with value gained by adding a third dimension. Implements are:

- Ripple cross lamination could be classified in terms of ripple indices and crest sinuosity
- Parallel lamination exhibiting compositional changes both lateral and vertically, could be identified.
- Grain orientation could be measured for the sediment grain sizes larger than coarse grained sand.
- Large trace fossils could be described in terms of 3D geometry, details on shape, and infill.

The ichnological study was based exclusively in the entire core material (visual inspection of the core surface) and combined with the exisiting lithological descriptions. Outcrop has not been studied yet. The results are five ichnofabrics (Fig. 3), reflecting a variety of depositional settings. Orderly, the *Glossifungites* ichnofabric is characteristic of omission/erosion surfaces and correlates for most cases to previously interpreted main erosional architectural boundaries; whereas the *Nereites* ichnofabric indicates the lowest energy depositional environments, still receiving significant amount of nutrients in a lobe fringe setting. The Nereites ichnofabric is exclusive of the mudstone-rich units below the SCC, which contrasts with the diversity in the SCC and can be used as an additional criterion for a significant discontinuity at the base of SCC.

Conclusions

CTScanning revealed as a technique providing addtional sedimentologic information from the core data. From quantification, the dataset on sedimentary structures will be ready to considerations on the parameters of the parent flows.

The ichnological study resulted in five ichnofabrics which can be used as an additional criterion to stratigraphic subdivision.

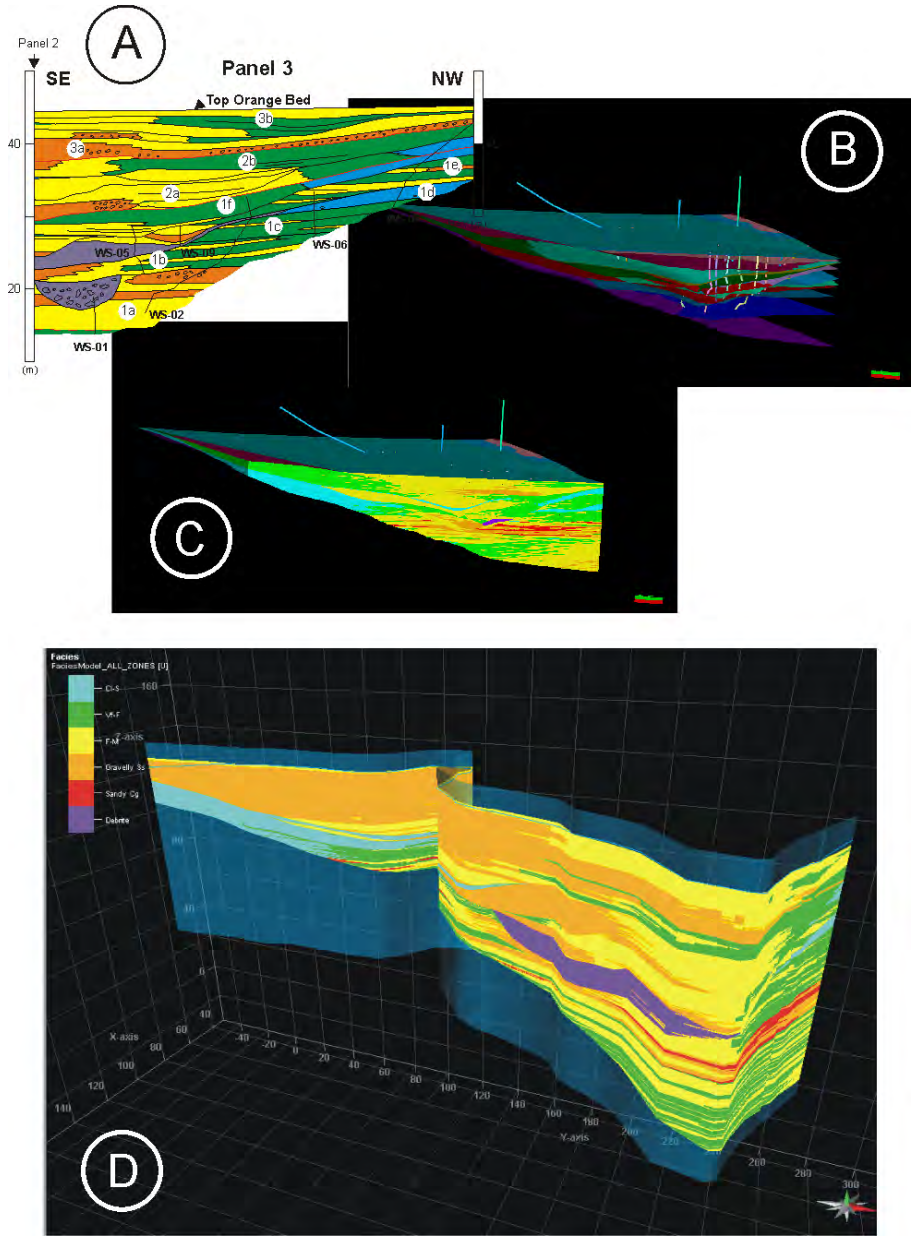

Figure 1. A) conventional outcrop dataset represented as correlation pannel. B) Surface framework reconstructing the 3D architecture; C) Geocellular 3D Facies model; D) Sections of the geocellular model made available for comparison to the outcrop dataset.

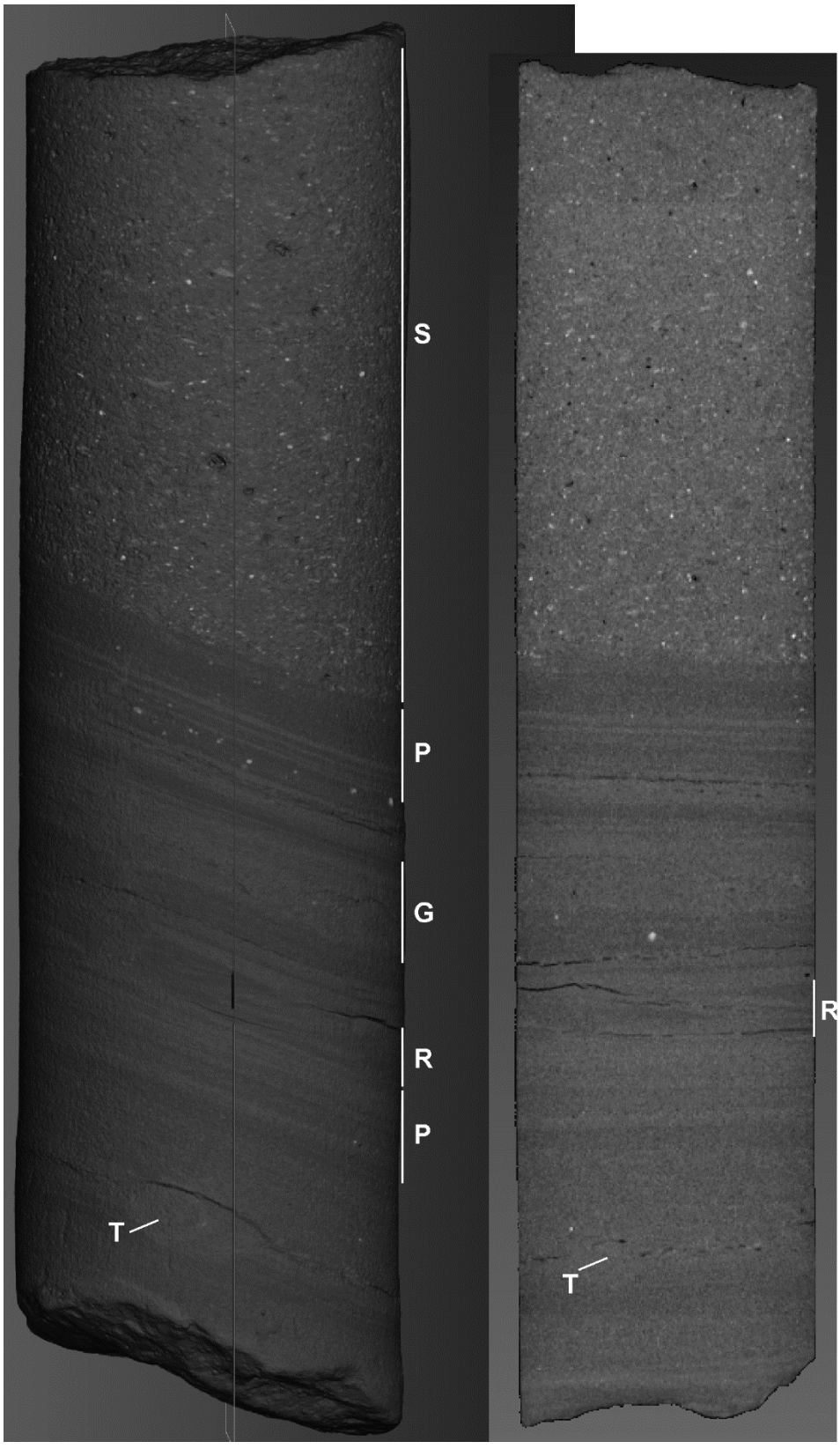

Figure 2: Results from the CTScan experiment using the XRE Multitom Core Xray CT System at UB. The core 63.5 mm wide (seen as whole core on the left and strike axial section on the right, stratigraphic top is upwards) Accuracy was set at 85 microns, which suffices for the identification and quantification of physical and biogenic sedimentary structures as well as for insights on grain shape and orientation. T: Trace fossil, P: parallel lamination, R: Ripples; G: graded unit, S: structureless interval.

OPHIOMORPHA ICHNOFABRIC

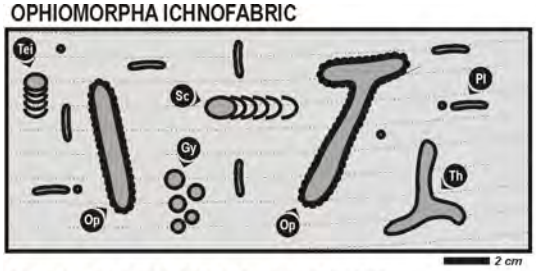

PLANOLITES-PALEOPHYCUS ICHNOFABRIC

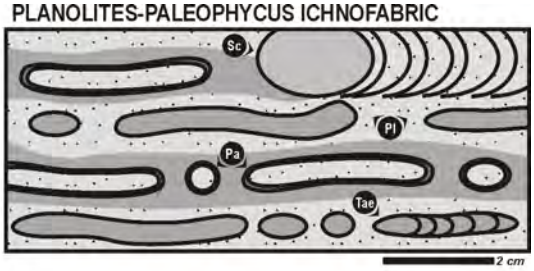

NEREITES-PHYCOSIPHON-ZOOPHYCOS-CHONDRITES ICHNOFABRIC

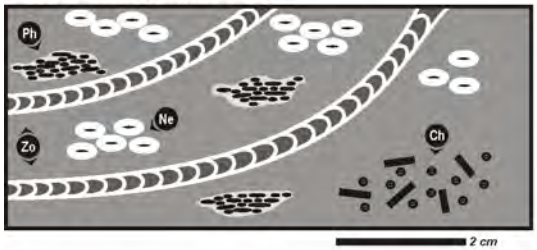

NEREITES ICHNOFABRIC

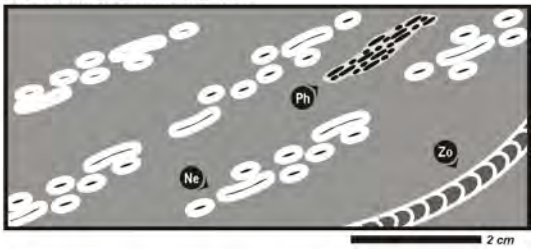

GLOSSIFUNGITES (OMISSION SURFACE)

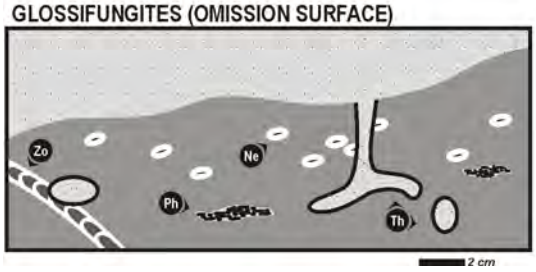

Ne *Nereites*	Pl *Planolites*
Ch *Chondrites*	Sc *Scolicia*
Gy *Gyrolithes*	Tae *Taenidium*
Op *Ophiomorpha*	Tei *Teichichnus*
Pa *Palaeophycus*	Th *Thalassinoides*
Ph *Phycosiphon*	Zo *Zoophycos*

Salt Tectonics in the Prebetic of Pinoso (SE Spain)

E. Górriz, F. Escosa & E. Roca

GEOMODELS Research Institute, Departament of Dynamics of the Earth and the Ocean, University of Barcelona. C/Martí Franquès s/n, 08028 Barcelona (Spain).

Abstract

During the 2016, a structural and geological characterization of the Pinoso Diapir and adjacent areas, located at the Prebetic Zone of Pinoso (SE Spain), have been carried out.

The Prebetic Zone of Pinoso is located within the external part of Betic Range and it is a good example of the development of the salt-bearing passive margin and its posterior inversion. It is constituted by Mesozoic to Middle Neogene materials detached from the Paleozoic basement by the Triassic evaporites and mudstones. The Pinoso Diapir is located at northwest of La Taja Chain, in the junction between the Internal Prebetic and the Subbetic Zones (Figure 1). This area represents the outer part of the foreland fold-and-thrust belt in the Betic Cordillera.

The results obtained until now indicate that the Pinoso Diapir has a recent activity, because in the affection area of the diapir have been observed Quaternary materials strongly influenced by the Keuper facies, which characterize this saline structure. Furthermore, other drive salt structures have also been observed in nearby areas, such as the squeezed diapir or possible feeder at the south of Xinorlet, or the remains of a possible salt sheet in El Tossal Mountain (Figure 1).

Future work

Future work will be mostly focused on making a detailed cartography from El Carche Chain to Elda Salt Sheet and carring out several cross-sections to infer the regional structure of this part of Prebetic Zone.

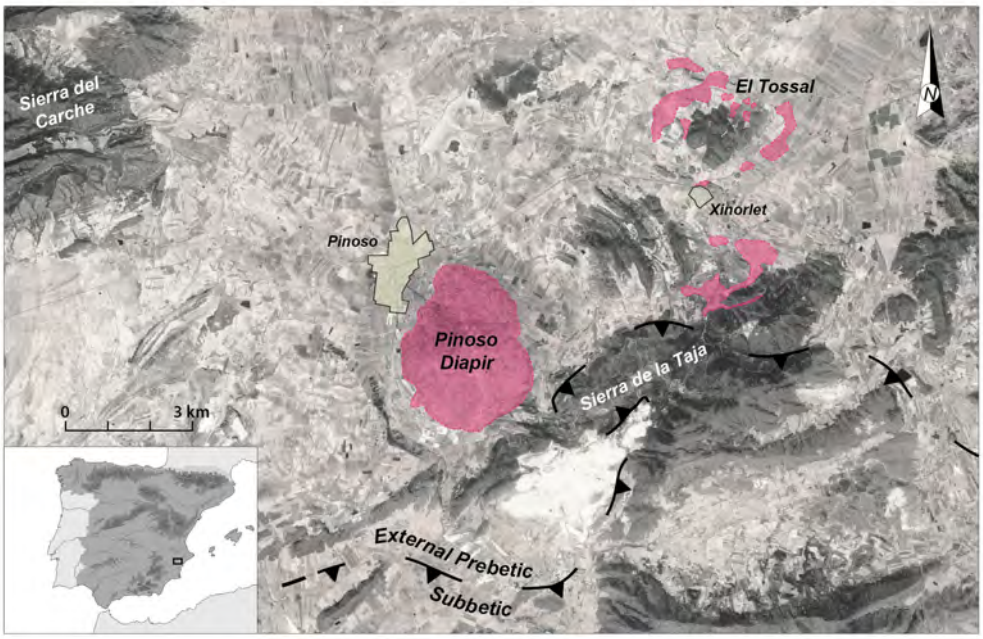

Figure 1. Location of the study area within the Prebetic Zone (SE Spain). The keuper facies identified on the field are shown with pink color.

Magnetostratigraphic dating of the Uncastillo Fm. (External Sierras, Southern Pyrenees)

[1] Oliva, B., [2,3] Beamud, E., [3]Garcés, M., [4]Soto, R., [5] Arenas, C., Pueyo, [4]E.L.

[1] Dpto. Geología y Geoquímica. Universidad Autónoma de Madrid
[2] Laboratori de Paleomagnetisme CCiTUB-CSIC, Institut de Ciències de la Terra "Jaume Almera", C/ Solé i Sabarís s/n, 08028 Barcelona
[3] GEOMODELS Research Institute, Geodynamics and Basin Analysis Research Group, Dept of Earth and Ocean Dynamics, University of Barcelona
[4]IGME - Instituto Geológico y Minero de España. Unidad de Zaragoza
[5] Dept. de Ciencias de la Tierra. Universidad de Zaragoza.

Introduction.

The Uncastillo Fm crops out along the southern boundary of the External Sierras, which represents the southernmost limit of the Pyrenean Range (Figure 1). Three tectosedimentary units related to tectonic pulses have been previously differentiated in this formation. The sedimentary evolution of the Uncastillo Fm is mainly related to the tightening of the WNW-ESE Santo Domingo anticline in the External Sierras during Chattian-Aquitanian times and records the younger tectonic movement of the south Pyrenean sole thrust. The Uncastillo Fm represents the change to overall southward-flowing alluvial and fluvial systems from overall west-northwest-flowing fluvial systems (Campodarbe Fm). Recent magnetostratigraphic results from the underlying Campodarbe Fm shift to younger ages (from chron 10r to 7r) the top of the Campodarbe Fm in the proximal area of the fluvial system (Luesia fan) (Oliva-Urcia, *et al.*, 2016). In order to check that reassignment and refine the age of the Uncastillo Fm, a new magnetostratigraphic study has been conducted in laterally equivalent deposits that represent middle-distal areas located to the east of the Luesia fan. These deposits consist of mudstones with interbedded sandstones. These finer grain size sediments allow for a magnetostratigraphic sampling in the Fuencalderas section of ~1300 m, which complete the chronostratigraphic frame of the last tectonic pulses of the Pyrenean Range.

Work done

The Uncastillo Fm. has been sampled along the trail between Fuencalderas and San Miguel de Liso (Fuencalderas section). 205 sites from mudstones and fine-grained sandstones were obtained along ~1300 m. Each site is composed by two *in-situ* oriented samples.
The laboratory measurements have consisted in stepwise thermal demagnetization up to 680 ºC and subsequent measurement of the natural remanent magnetization (NRM) with a superconducting rock magnetometer at the Paleomagnetic Laboratory CCiTUB-ICTJA CSIC. After visual inspection of the demagnetization diagrams (Figure 2) the characteristic component was calculated for each sample in order to compute the virtual paleopole latitude at the site level and build the local magnetostratigraphy.

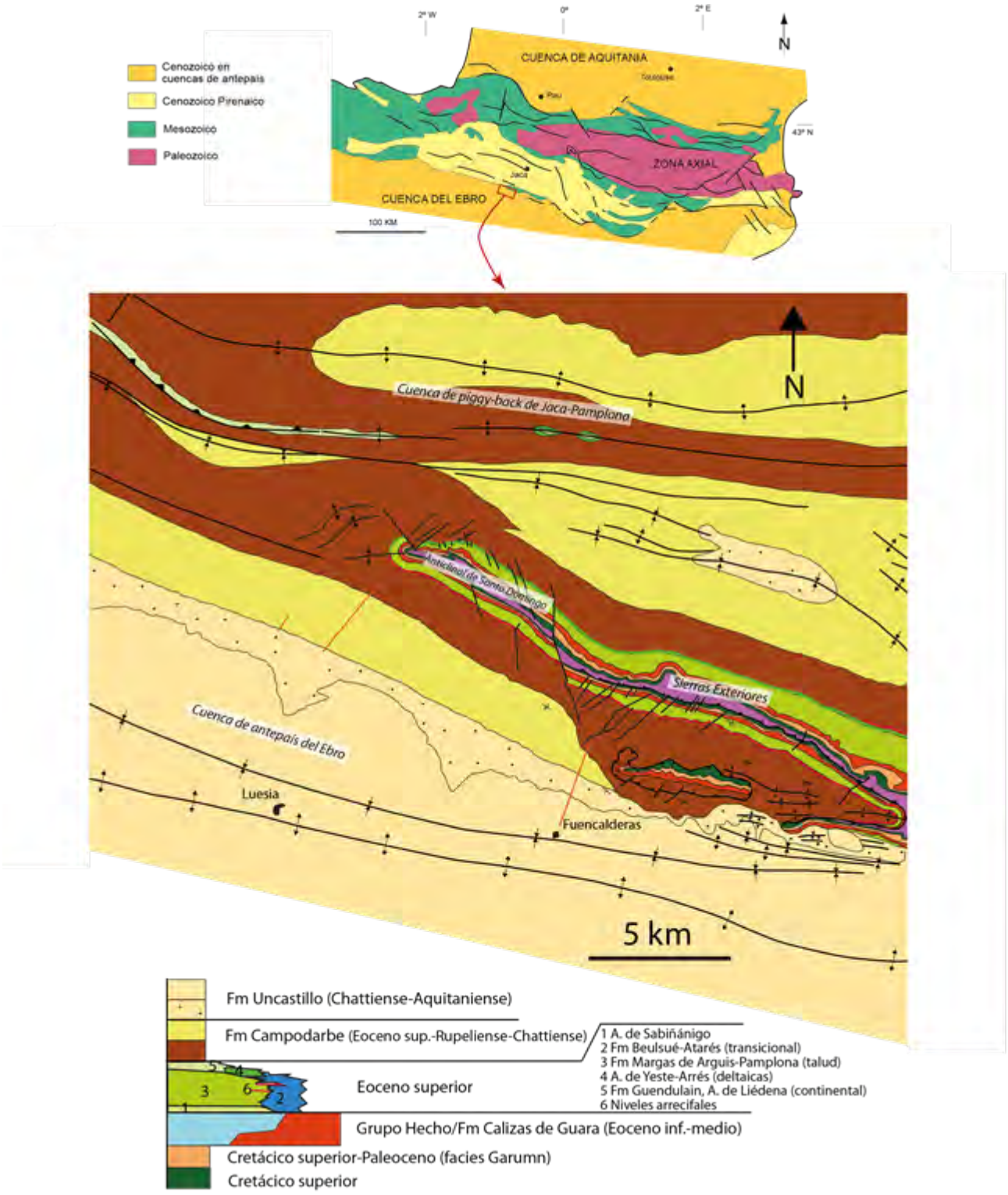

Figure 1. Geological map with the location of the magnetostratigraphic sections of Luesia (to the west) and Fuencalderas (to the east). (Modified from Puigdefàbregas 1975).

Results

The Fuencalderas local magnetostratigraphy has been correlated to the Geomagnetic Polarity Time Scale (GPTS) (Figure 3). From this correlation, it can be observed that the limit between the Campodarbe and Uncastillo Fms. is set at the C7r (~ 24.5 Ma)

consistent with previous results in the nearby Luesia section (Oliva-Urcia et al, 2015) and remarkably younger than established in previous works (Hogan and Burbank, 1996). The Uncastillo Fm. would have been deposited in about 3 Myr (from 24.5 to 21.5 Ma). It is worth pointing out that, despite it doesn't change the overall age of the section, an alternative correlation for magnetozone N3 exists considering the existence of a cryptochron within C6Cr as reported in other studies (Channell et al., 2003; Valero et al., 2014). The proposed correlations allow the calculation of the sedimentation rate for these sediments (Figure 4). Sedimentation rates show an overall decreasing trend from ~44 cm/kyr to ~ 27 cm/kyr. It can be observed that the alternative correlation in red, yields a smoother trend in sedimentation rates.

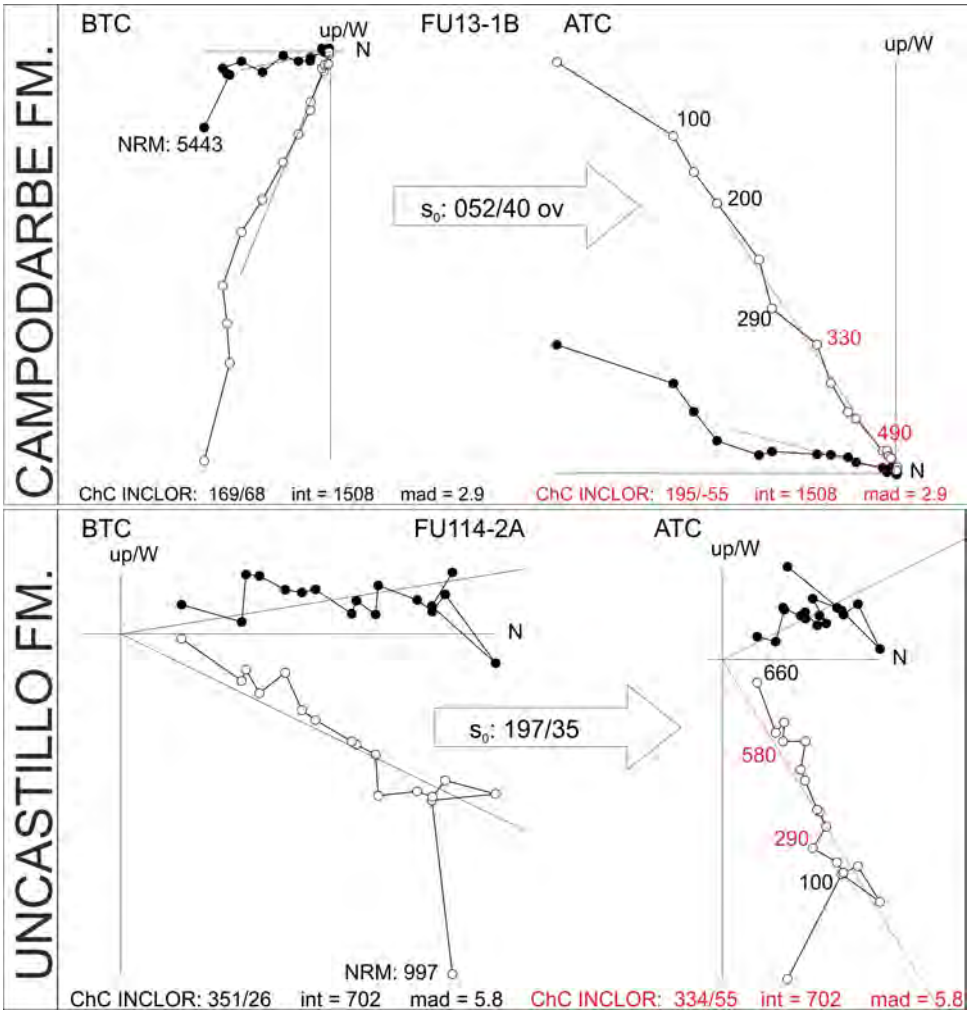

Figure 2. Demagnetization diagrams of Campodarbe and Uncastillo Fms. representative samples. NRM values in $1 \cdot 10^{-6}$ A/m, temperatura steps in ºC. The selected inteval used to calculate the characteristic component (ChC) is represented in red. BTC: before tectonic correction; ATC: after tectonic correction.

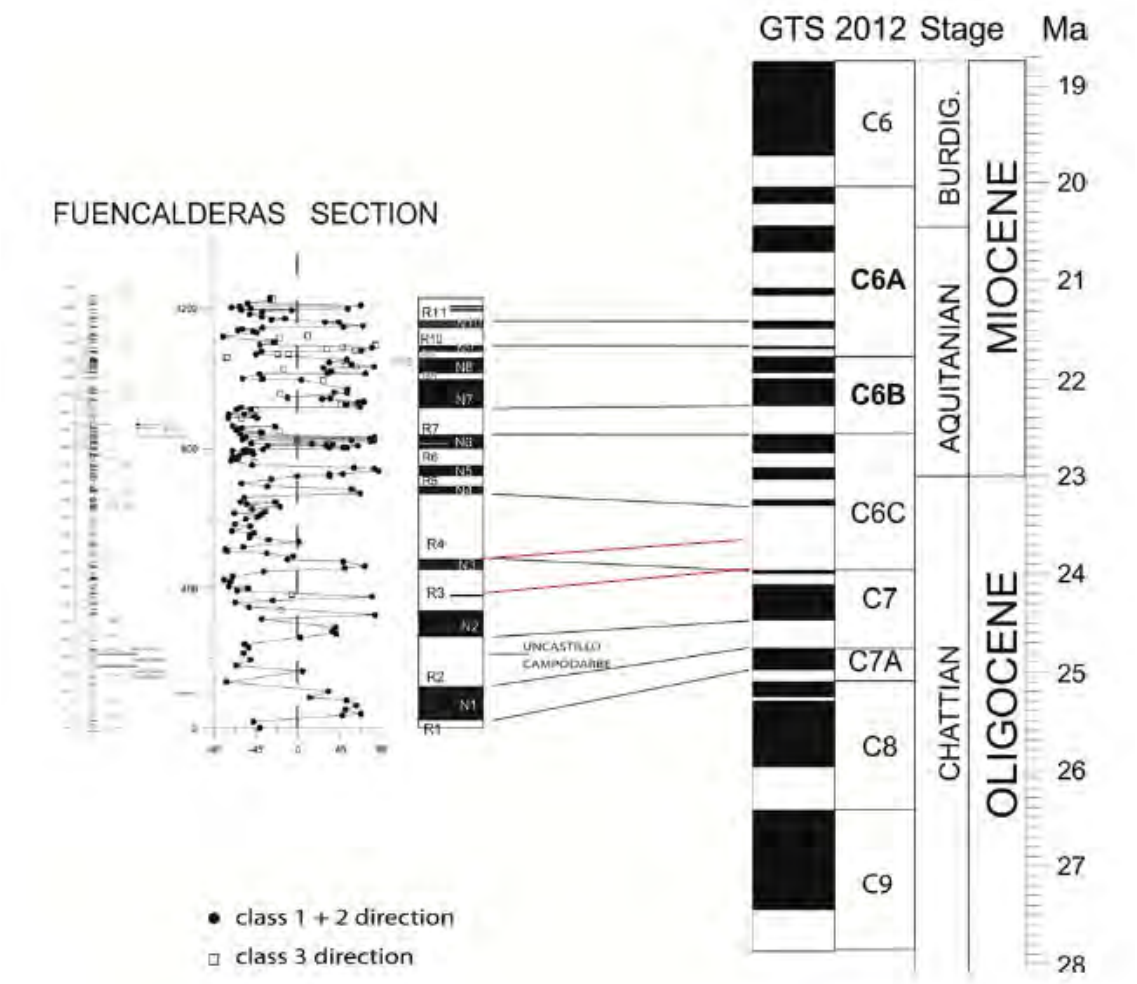

Figure 3. Correlation of the Fuencalderas section to the GPTS (Gradstein and Ogg, 2012).Red line represents an alternative correlation considering the existence of a cryptochron within C6Cr

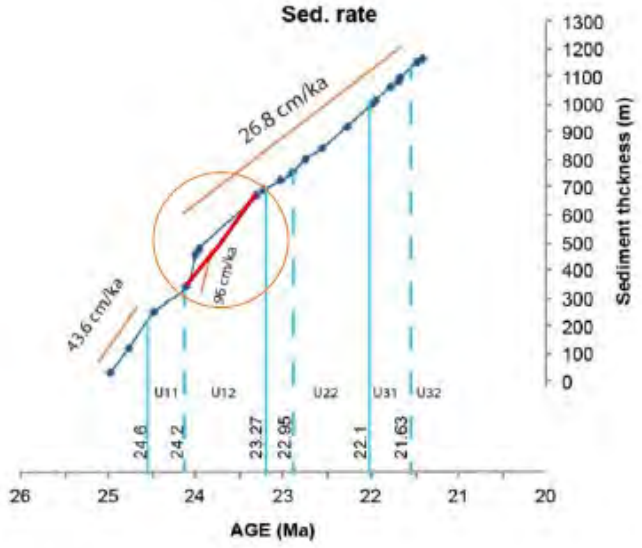

Figure 4. Sedimentation rates obtained from the proposed correlation. Encircled red line represents the resultant sedimentation rate from the alternative correlation (N3 correlated to a cryptochron within C6Cr)

Conclusions

- The limit of Campodarbe and Uncastillo Fms. is set at C7r (~ 24.5 Ma), about 5 Myr younger than previously established (Hogan and Burbank, 1996) and consistent with the results of Oliva-Urcia et al., (2016) in the Luesia section.
- The Campodarbe and Uncastillo Fms. boundary is fairly isochronous between the Luesia and the Fuencalderas sections.
- The age of the Uncastillo Fm. is set between 24.5 and 21.5 Ma.

This work has been carried out in cooperation with:
- Universidad Autónoma de Madrid
- IGME

In the frame of the Project SEROS - CGL 2014-55900-PL

Future work

Publish these results in SCI journals.

Kinematics of the Mediano Anticline (Ainsa Basin)

[1] Muñoz, J.A., [1,2] Beamud, E., [3]Pueyo, E.L., [1,2]Valero, L., [1]Martínez-Granado, P.

[1] GEOMODELS Research Institute, Geodynamics and Basin Analysis Research Group, Dept of Earth and Ocean Dynamics, University of Barcelona
[2] Laboratori de Paleomagnetisme CCiTUB-CSIC, Institut de Ciències de la Terra "Jaume Almera", C/ Solé i Sabarís s/n, 08028 Barcelona
[3]IGME - Instituto Geológico y Minero de España. Unidad de Zaragoza

Introduction

The Mediano anticline belongs to the Sobrarbe fold system (Fernández-Bellon, 2004; Fernández et al., 2012), which is a system of kilometer-scale N-S trending folds (Mediano, Olsón, Añisclo and Boltaña anticlines) in the footwall of the Cotiella and Peña Montañesa-Montsec thrust sheets. These folds are detachment to fault-propagation folds, which detached into the Triassic evaporites and deform the Upper Cretaceous-Paleogene stratigraphic succession of the Gavarnie thrust sheet (Figure 1). They have been described by many authors due to their high obliquity with respect the main E-W to ESE-WNW Pyrenean structural trend and have been the subject of numerous paleomagnetic studies aimed to explain the origin of this obliquity.

The Mediano anticline is a 20 km long detachment fold cored by Triassic evaporites. In its southern sector it displays eastward vergence (Figure 1) and a northward plunge of about 10º. To the north, the Mediano anticline changes to a NW-SE trend before terminating below the turbidites of the Ainsa basin. Previous paleomagnetic studies in Ilerdian to upper Lutetian sediments of the Mediano anticline by Dinarès-Turell (1992), Bentham (1992) and Muñoz et al., (2013) carried out over a relatively small area within which there are no major faults, identified vertical axis rotations (VAR) between 58º and 80º in sediments of Ilerdian, Cuisian and lower Lutetian age. The magnitude of rotation decreases progressively through Lutetian times to reach minimum values of VAR during the upper Lutetian to Bartonian (15º to 35º) (Figure 1). Despite the abundance of paleomagnetic data, a better VAR/age control is needed to precisely establish the onset of rotation linked to the growth of the Mediano anticline and refine its kinematic history.

Work done

20 new paleomagnetic sites were sampled in order to better constrain the kinematics of the Mediano anticline (Figure 2). Each site is composed by 10 samples oriented *in situ*. Sites MD1 to MD7 were drilled in the western limb of the southern portion of the Mediano anticline, close to the Mediano dam. Sites MD8 to MD20 were distributed along a north-south transect in order to paleomagnetically constrain the change in trend of the Mediano anticline from N-S to NW-SE. Most of these sites were drilled in its eastern limb, except MD18 to MD20 which were obtained in its western limb, close to the Labuerda village (Figure 2). The samples have been prepared in the Paleomagnetic Laboratory (CCiTUB-ICTJA CSIC) and are waiting to be analyzed during 2017.

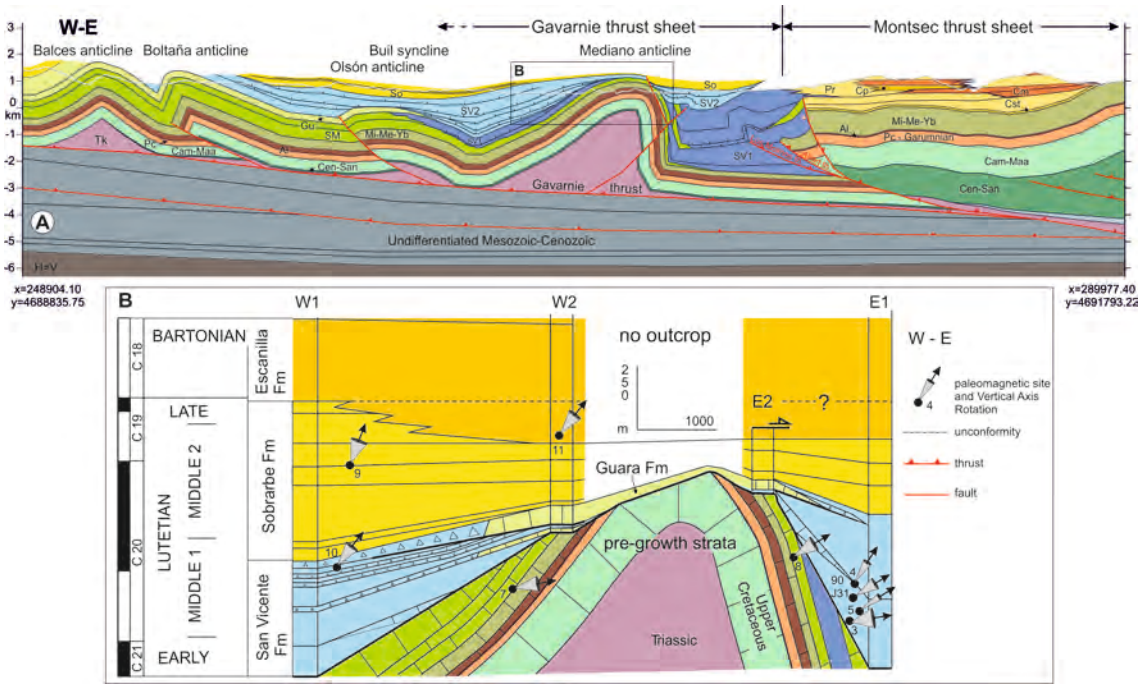

Figure 1. A. Cross-section of the southern part of the Ainsa Oblique Zone. B. Enlargement of the Mediano anticline and location of the paleomagnetic sites with respect to the syn-folding growth sequence. W1, W2, E1 and E2 correspond to four stratigraphic columns constructed across the growth sequence, two of them in the west limb and two of them in the east limb of the anticline. (Muñoz, et al., 2013)

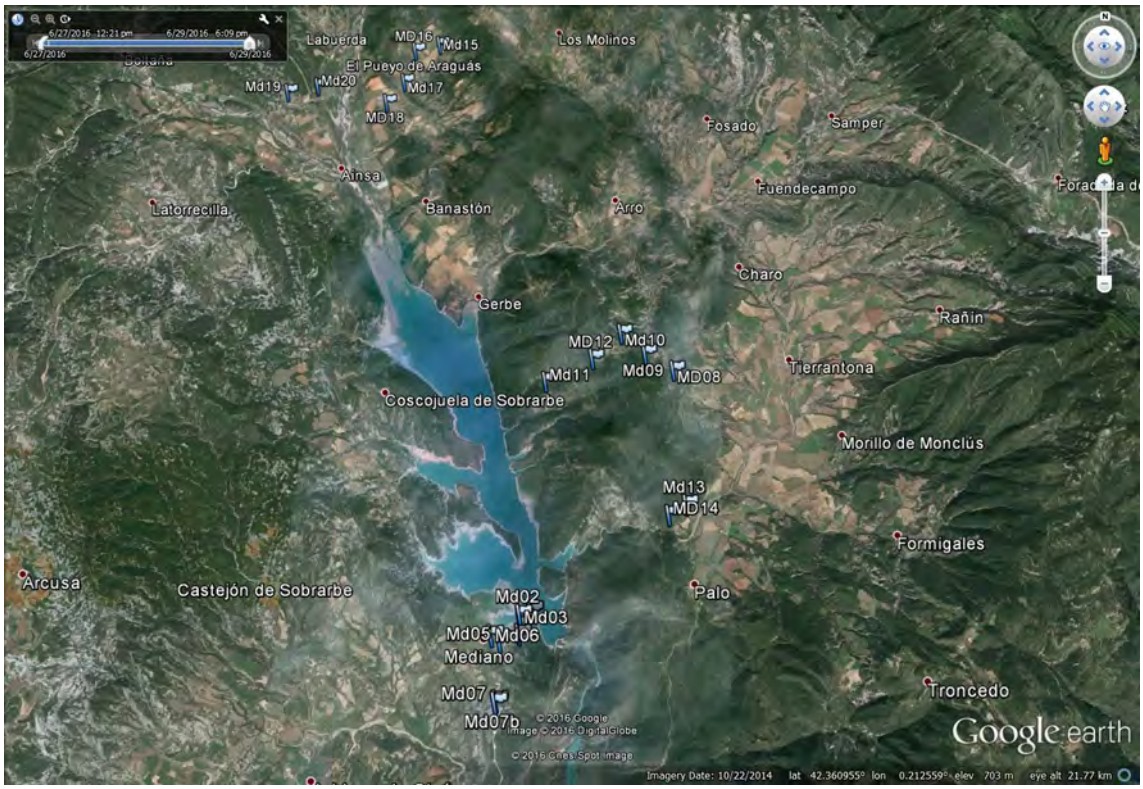

Figure 2. Google Earth image of the study area with the location of the new paleomagnetic sites (MD1 to MD20)

This work is being carried out in cooperation with:

- IGME

In the frame of the Project SALTECRES CGL2014-54118-C2-1-R

Future work

Laboratory analyses: stepwise thermal demagnetization of the Natural Remanent Magnetization and calculation of the characteristic components and associated VAR. These results will be integrated with the magnetostratigraphic sections (Labuerda and Bco. Forcaz) (Figure 3) carried out by other components of the Geomodels group in the frame of the Project SEROS - CGL 2014-55900-PL in cooperation with the University of Geneve (Switzerland).

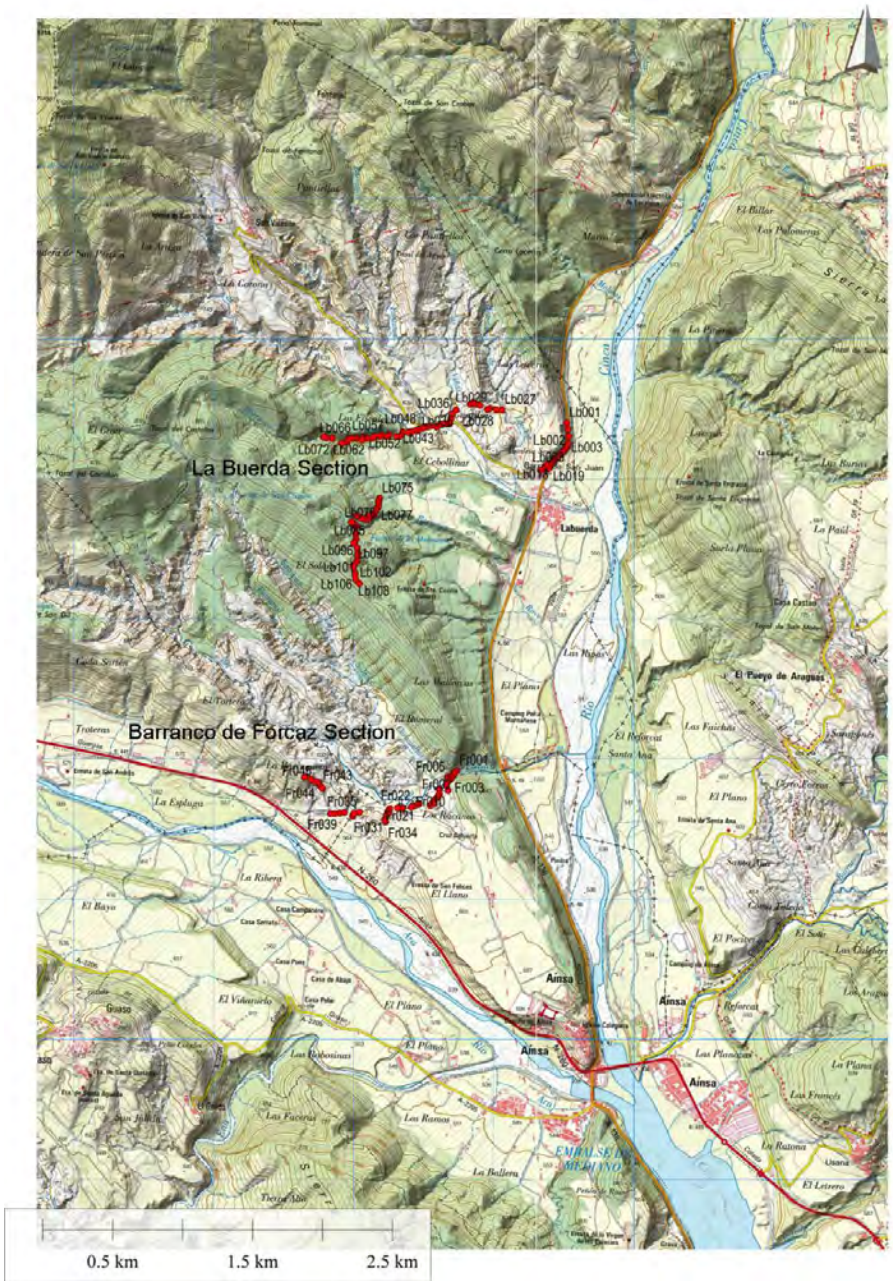

Figure 3. Sampling of the Hecho Gp. turbidites in the Ainsa Basin along the Labuerda and Barranco de Forcaz sections.

Paleomagnetic constraints to the kinematics of contractive detachment folds: Artesa de Segre and Cardona fold systems

[1,2] Beamud, E., [1] Gratacós, O., [1,2]Valero, L., [1] Roca, E., [3] Soto, R.

[1] GEOMODELS Research Institute, Geodynamics and Basin Analysis Research Group, Dept of Earth and Ocean Dynamics, University of Barcelona
[2] Laboratori de Paleomagnetisme CCiTUB-CSIC, Institut de Ciències de la Terra "Jaume Almera", C/ Solé i Sabarís s/n, 08028 Barcelona
[3]IGME - Instituto Geológico y Minero de España. Unidad de Zaragoza

Introduction

Upper Eocene-Oligocene alluvial and lacustrine sediments of the eastern Ebro foreland basin are deformed in a set of NE-SW trending folds (red squares in Figure 1) detached on top of the Upper Eocene Cardona evaporites. The trend of these folds is highly oblique with the main E-W Pyrenean trend. To the north, in the Oliana anticline, 20 º of counterclockwise vertical axis rotation occurred during Late Eocene-Oligocene times (Sussman et al., 2004) (Figure 1). This rotation has been interpreted as the result of continued motion of the Oliana anticline along the Upper Eocene Cardona evaporites and emplacement of thrusts in the north (Sussman et al., 2004).

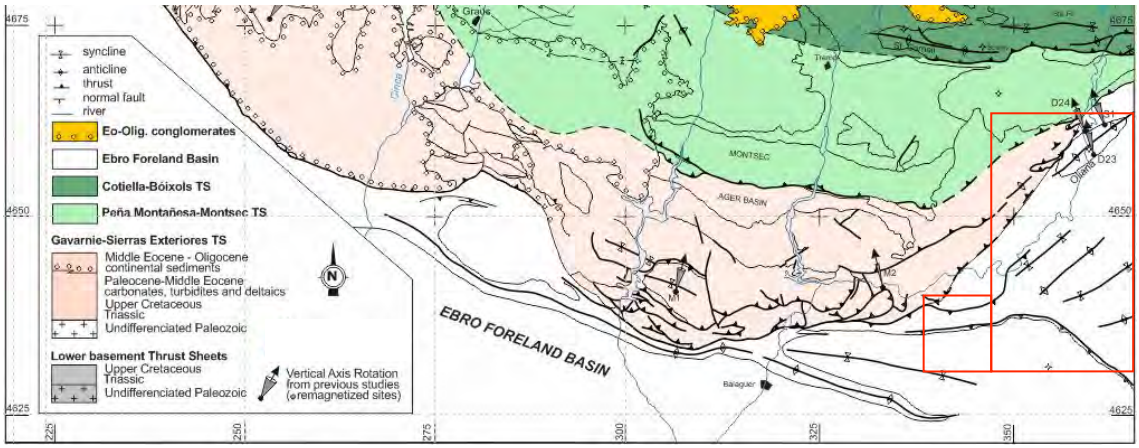

Figure 1. Geological map of the South-Central Pyrenees (modified from Beamud, 2013) with indication of the study area (red squares) and the vertical axis rotations derived from previous works (grey arrows). D: Dinarès-Turell (1992), S: Sussman et al., (2004) and M: Meigs (1995).

A paleomagnetic study is being conducted in the area located between the villages of Artesa de Segre and Cardona (red squares in Figure 1) to assess the extension of the vertical axis rotation area related to the emplacement of the Serres Marginals thrust sheet and to unravel the origin and kinematic evolution of these contractive detachment folds.

Work done

45 paleomagnetic sites were sampled in the study area. Sites 1 to 12 and 40 to 51 were drilled in both limbs of the oblique folds in a roughly W-E transect (from Vilanova de l'Aguda anticline to Torà and Pinós folds) (Figure 2). Additionally, sites 13 to 31 were sampled along a N-S transect around Artesa de Segre to combine anisotropy of magnetic susceptibility (AMS) with structural data on a cross-section. 10-12 samples per site were obtained with an electrical cordless drill cooled by water and were

oriented *in situ* with a magnetic compass fixed to an orienting device. Sampling focused on red mudstones and fine grained sandstones and light grey mudstones from Upper Eocene – Oligocene alluvial and lacustrine sediments.

Figure 2. Google Earth image with superimposed geological map (IGC M250M, 2015) of the study area with location of the paleomagnetic sites (AS1 to AS51)

Samples are being analyzed in the Paleomagnetic Laboratory (CCiTUB-ICTJA CSIC). So far 12 sites have been demagnetized and AMS have been measured on 30 sites. Laboratory treatment has consisted in stepwise thermal demagnetization up to 670 ºC and measurement of the Natural Remanent Magnetization (NRM) of 12 sites and measurement of AMS of 30 sites.

Preliminary results

Preliminary results suggest a counterclockwise vertical axis rotation (VAR) of ~ 20 º in sites AS3 and AS4 and negligible to non rotation in the other sites (Figure 3). Regarding AMS, K_{max} tends to be parallel to the fold axis (NE-SW) in the Vilanova de l'Aguda anticline and show a Pyrenean E-W direction in sites far from this structure (Figure 4).

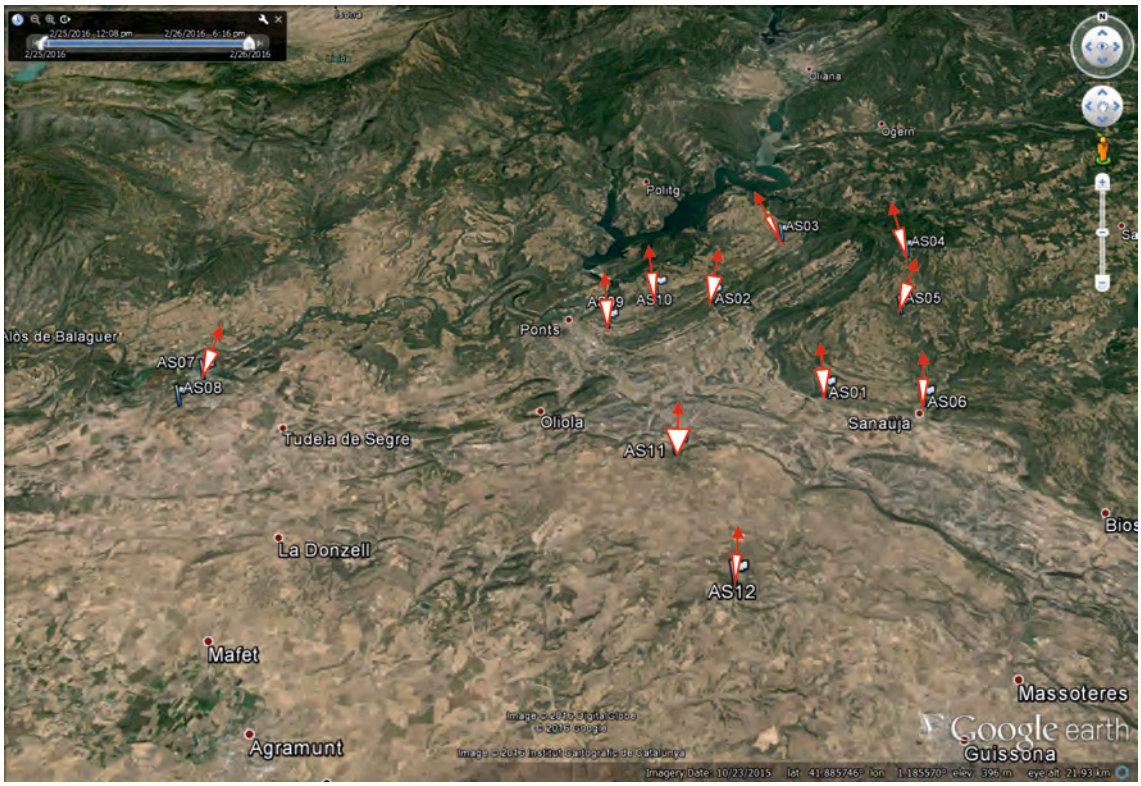

Figure 3. Google Earth image with preliminary results of VAR around Vilanova de l'Aguda anticline. It can be observed a significant counterclockwise VAR of ~ 20 º in sites AS3 and AS4

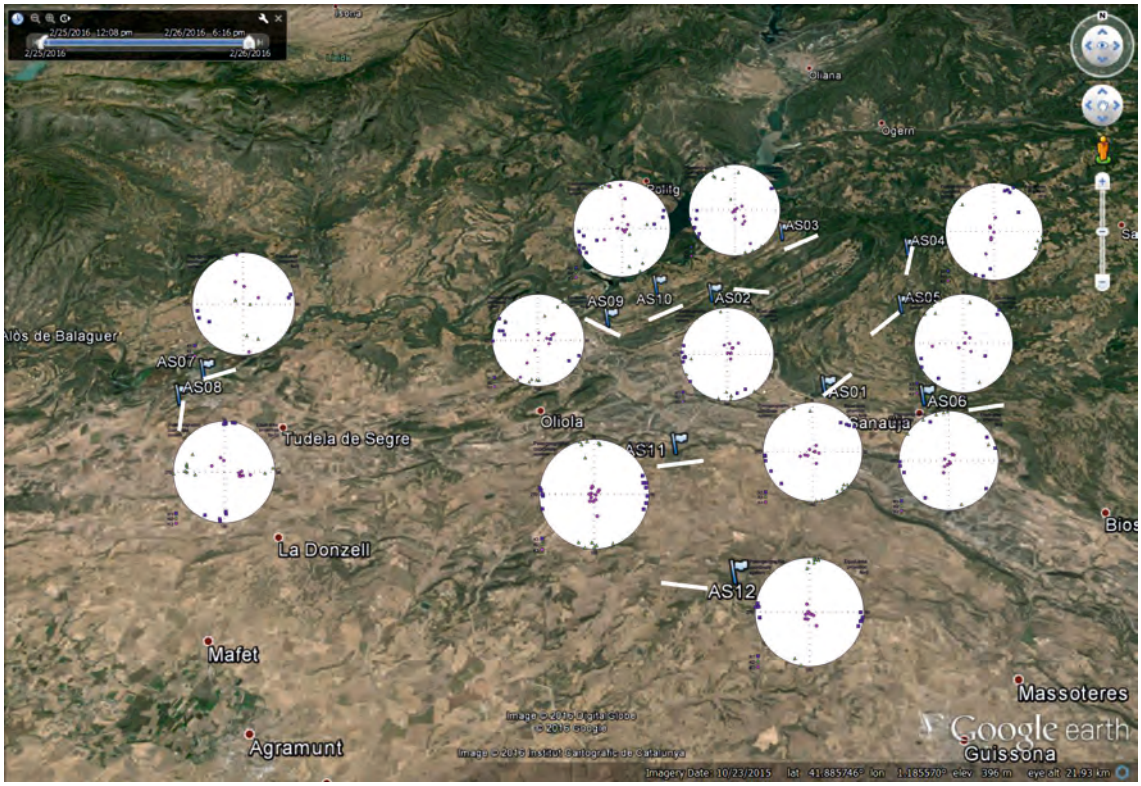

Figure 4. Google Earth image with preliminary results of AMS. White line represent the orientation of k_{max}

This work is being carried out in cooperation with:

- IGME

In the frame of the Project SALTECRES CGL2014-54118-C2-1-R

Future work

Sampling of new paleomagnetic sites near Cardona

Laboratory analyses: AMS measurements, stepwise thermal demagnetization and measurement of the Natural Remanent Magnetization and calculation of the characteristic components and associated VAR.

Integration of these results with structural data and cross-sections

Paleomagnetic data in Aptian-Albian syn-diapiric rocks (Basque-Cantabrian basin, N Iberia).

[1,2] Beamud, E., [3] Soto, R., [1] Roca, E., [1] Carola, E., [4] Almar, Y., [1] Escosa, F.

[1] GEOMODELS Research Institute, Geodynamics and Basin Analysis Research Group, Dept of Earth and Ocean Dynamics, University of Barcelona
[2] Laboratori de Paleomagnetisme CCiTUB-CSIC, Institut de Ciències de la Terra "Jaume Almera", C/ Solé i Sabarís s/n, 08028 Barcelona
[3] IGME - Instituto Geológico y Minero de España. Unidad de Zaragoza
[4] ICT "Jaume Almera", CSIC, Solé i Sabarís, s/n, 08028 Barcelona.

Abstract

In order to obtain a kinematic model linking the diapir formation and the geometry of the syn-diapir sediments, a paleomagnetic study has been conducted in selected syn-diapiric sequences of the Basque-Cantabrian Basin (Figure 1). The studied diapirs (Bakio, Bermeo, Guernika and Mungia) developed during the Early Cretaceous in relation to the North Iberian extensional margin which was subsequently reactivated during the Pyrenean contractional deformation (Late Cretaceous-Miocene). They are cored by Triassic red clays, evaporates and ophites and they are flanked by synkinematic Albian shelf and slope carbonates and Upper Albian to Cenomanian siliciclastics. The paleomagnetic study has focused on the synkinematic overburden to detect and quantify vertical axis rotations related to the growth of the diapirs. 29 paleomagnetic sites have been analyzed. After obtaining the site mean directions it can be concluded that sites around the Bakio diapir are remagnetized, hindering its kinematics to be deduced (Figure 2). The age of this remagnetization is difficult to assess, it could be either an earlier Albian-Maastrichtian remagnetization or a remagnetization linked to the Pyrenean compression. Fold tests for the Bermeo and Guernika diapirs are less conclusive and the obtained mean paleomagnetic directions can be integrated in the regional framework (Figure 3). The general trend show that west of Gernika paleomagnetic sites show counterclockwise vertical axis rotations (VAR), whereas east of Gernika paleomagnetic sites show clockwise VAR.

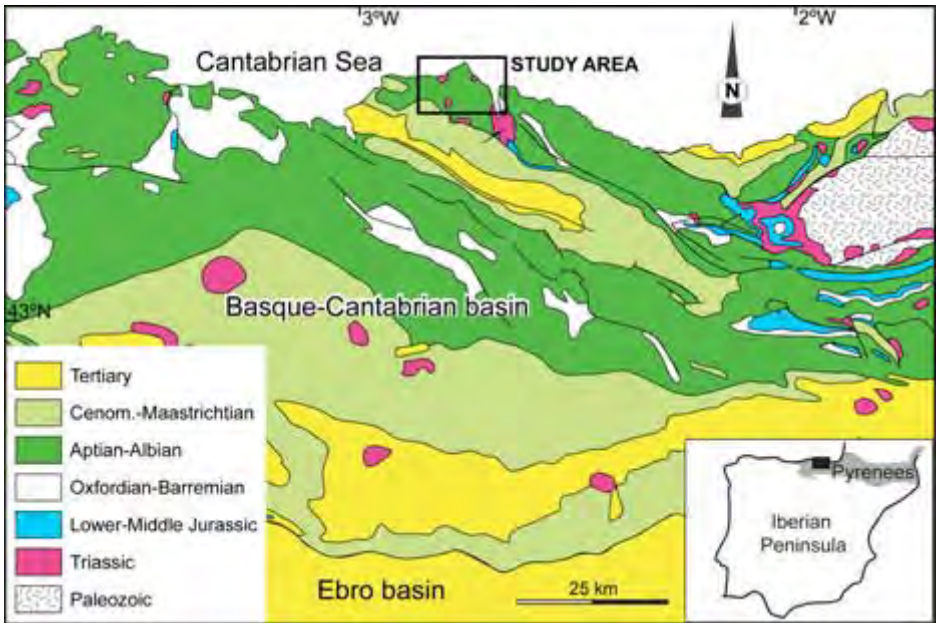

Figure 1. Location and geological map of the study area.

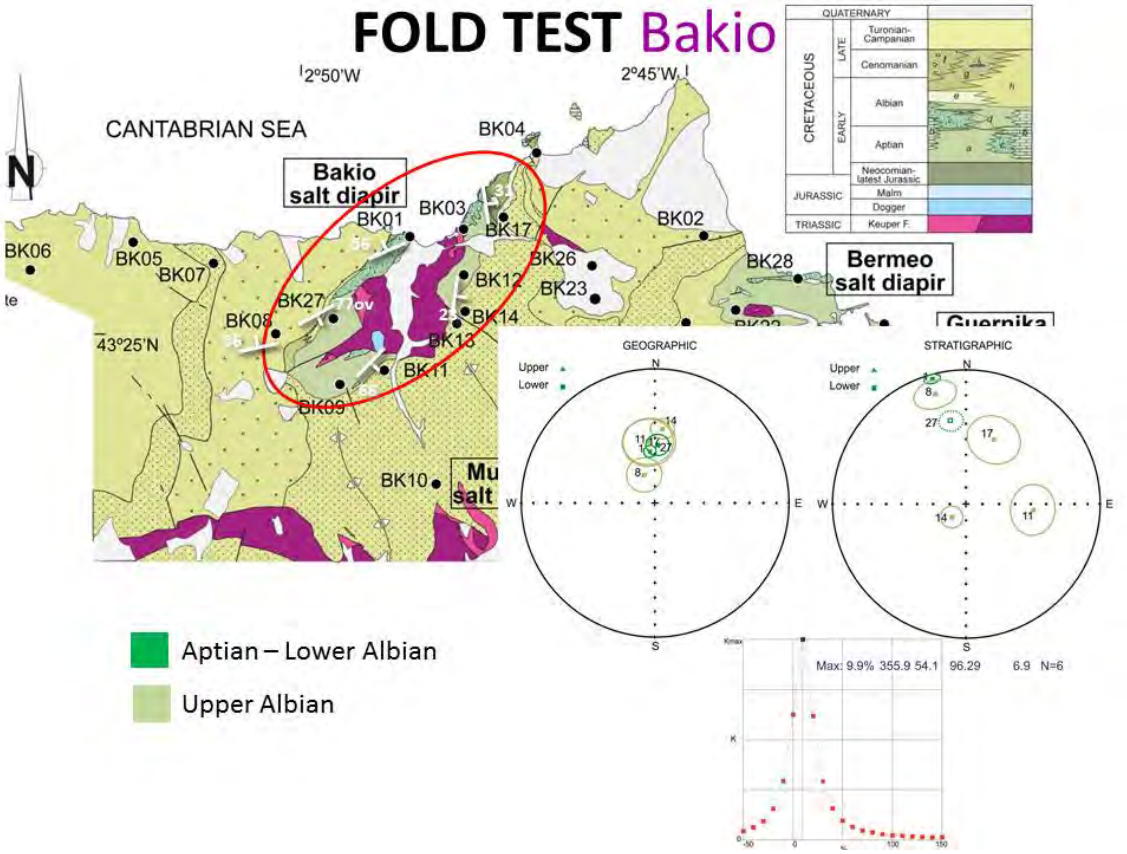

Figure 2. Study area with location of the paleomagnetic sites. Modified from the Basque Country Geological Map 1:25.000 (EVE) and fold test for the Bakio diapir sites. It can be observed that a negative fold test is obtained (better grouping of the paleomagnetic directions in geographic coordinates, at only 9% of unfolding).

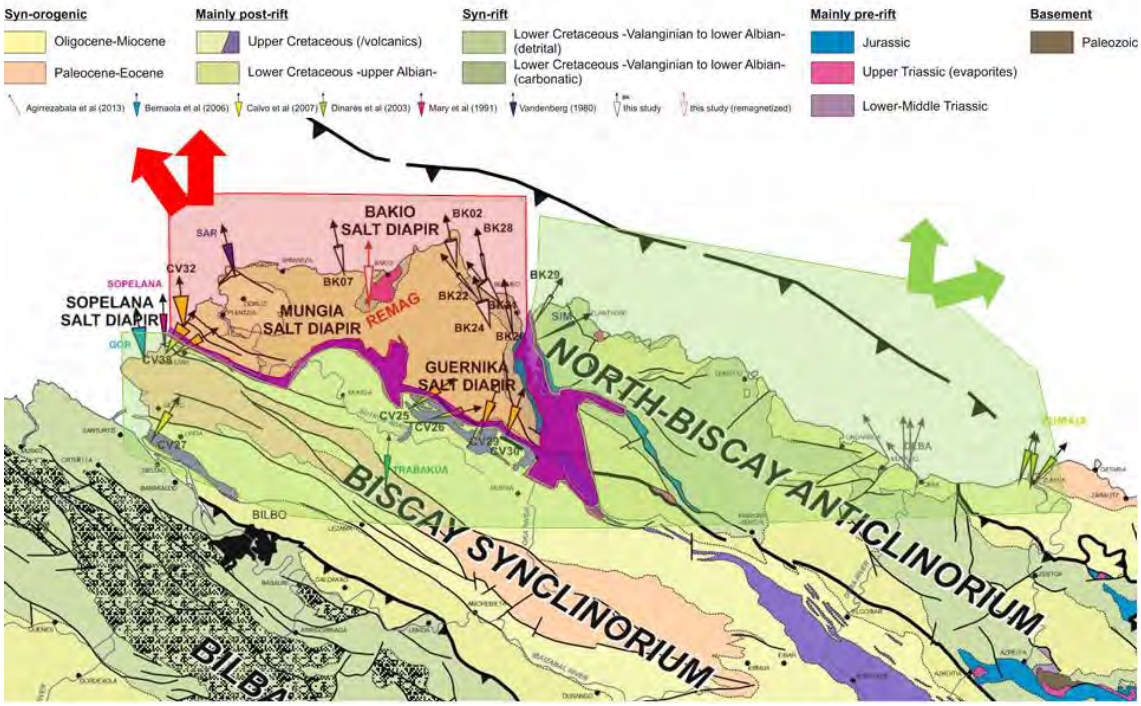

Figure 3. Integration of the paleomagnetic results with previous paleomagnetic studies in the Basque-Cantabrian Basin.

Sediment Routing Systems: Stratigraphic Analysis and Models

[1]Miguel Garcés, [1]Miguel López-Blanco, [1]Andreu Vinyoles, [1]Pau Arbués, [1]Patricia Cabello, [1]Luís Valero, [1,2]Elisabeth Beamud, [3]Belen Oliva

[1]Grup de Geodinàmica i Anàlisi de Conques, Dept de Dinàmica de La Terra i l'Oceà,Universitat de Barcelona
[2]Laboratori de Paleomagnetisme CCiTUB-CSIC, Institut de Ciències de la Terra Jaume Almera
[3]Dept. Geologia y Geoquímica, Universidad Autónoma de Madrid

Introduction.

Foreland systems are among the regions on Earth where the interplay between deep and surface processes is best exemplified. Mountain building, erosion and sediment transfer are intimately coupled to keep the mass balance during the growth of the orogenic wedge. Understanding causes and feedbacks which operate in foreland systems requires that the sedimentary record is placed in a precise chronostratigraphic frame. High-resolution basinscale correlations are essential to reconstruct the basin evolution and to have a reliable picture of the paleogeographic scenario through time. Progress in this fundamental knowledge has its application in the exploration of natural resources and the modeling of geological reservoirs by providing realistic boundary conditions as input parameters in forward numerical modeling.

The general objectives of this project are connected with the analysis of basin stratigraphic architecture and the characterization of sedimentary bodies in a broad range of scales. First, we aim at completing the chronostratigraphic framework at basin scale and, with this, to contribute the evolution of sediment transfer systems and its relation with subsidence. High-resolution chronostratigraphic tools such as magnetostratigraphy and cyclostratigraphy will assist in the quantification of key processes related to basin evolution. Second, at reservoir scale we aim at constructing 3D geological models and forward numerical models (4D) with application to management of natural resources and innovative research on sedimentary basin analysis. Third, at the scale of petrophysics, we aim to characterize rock porosity and permeability, properties which are crucial in modeling of flow in sedimentary reservoirs. An ideal context where to apply the proposed methodology is found in the south-pyrenean foreland basins. The region underwent dramatic paleogeographic changes which included the basin partitioning associated to the emplacement of the South Central Pyrenean Unit, and transitions between open to closed drainage conditions. These changes had a strong impact on basin filling, overfilling and later erosion, evolution which was ultimately marked by the variable role of tectonics, climate and eustatism. In this context, the project targets a number of specific objectives which represent a wide range of scenarios, from the early axial sediment transfer system opened to the ocean during the Early-Middle Eocene, to the rapid aggradation and overfilling in an internally drained basin starting in the Late Eocene, and the fluvial incision, opened drainage and erosion from Late Miocene to present. The different disciplines and working scales involved in this project are merged to assist the construction of better constrained realistic geological models.

Work done

From the basin scale perspective, main actions during 2016 were focused on the building of a robust magnetostratigraphy-based chronostratigraphic framework across the Ainsa, Jaca and the northern margin of the Ebro Basin. Targeted stratigraphic units and areas included the fluvial sediments of the Escanilla Formation at the Olson section (Bartonian-Priabonian, Ainsa Basin) (Fig. 1), the marine to continental shallowing sequence of the Yebra de Basa section (Lutetian to Priabonian, Jaca Basin), the fluvial sediments of the Campodarbe and Uncastillo Fms at the Fuencalderas and San Marzal sections (Sierras Exteriores, Ebro basin).

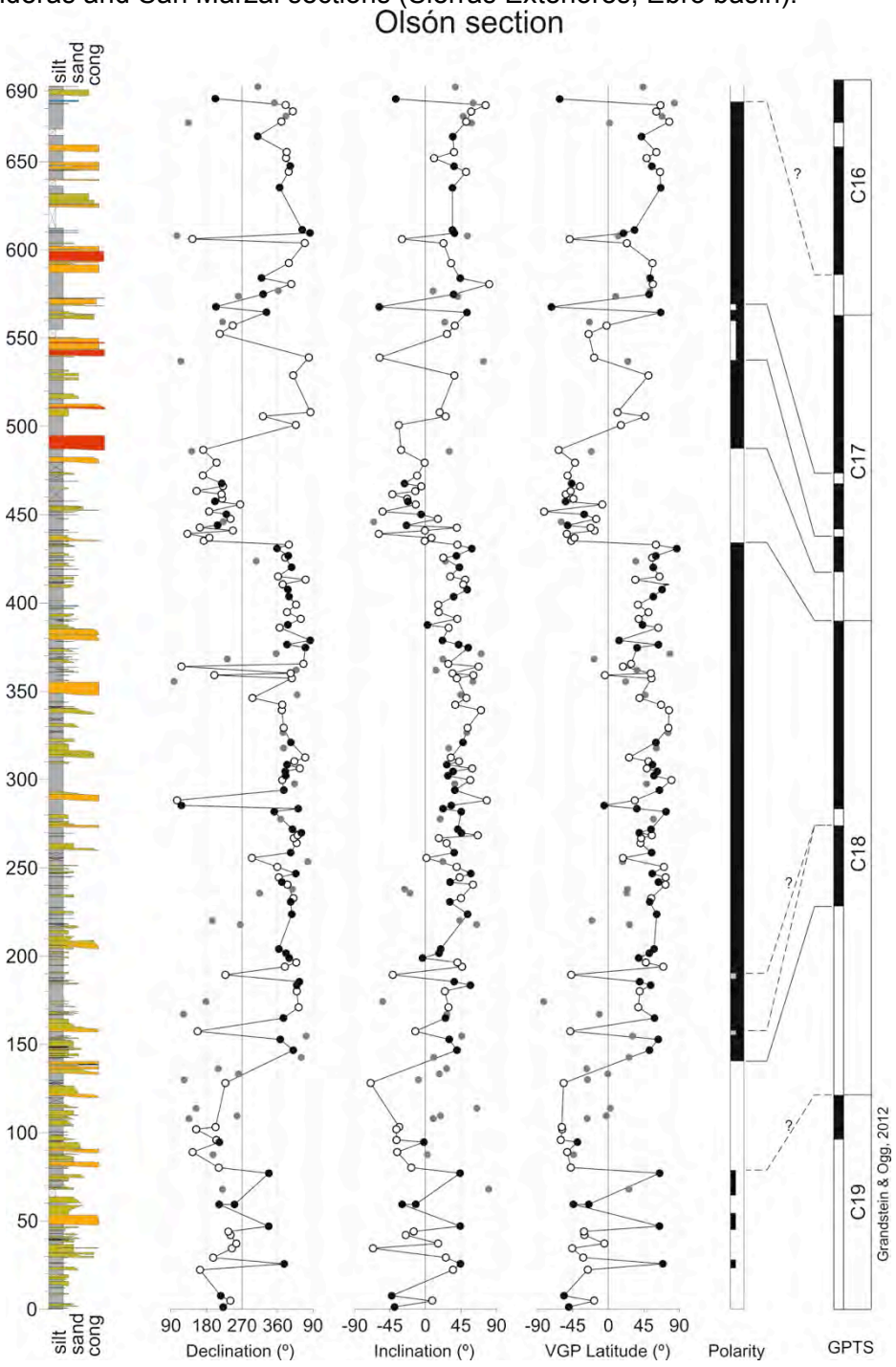

Figure 1. Magnetostratigraphy of the Olson section and correlation with the Geomagnetic Polarity Time Scale

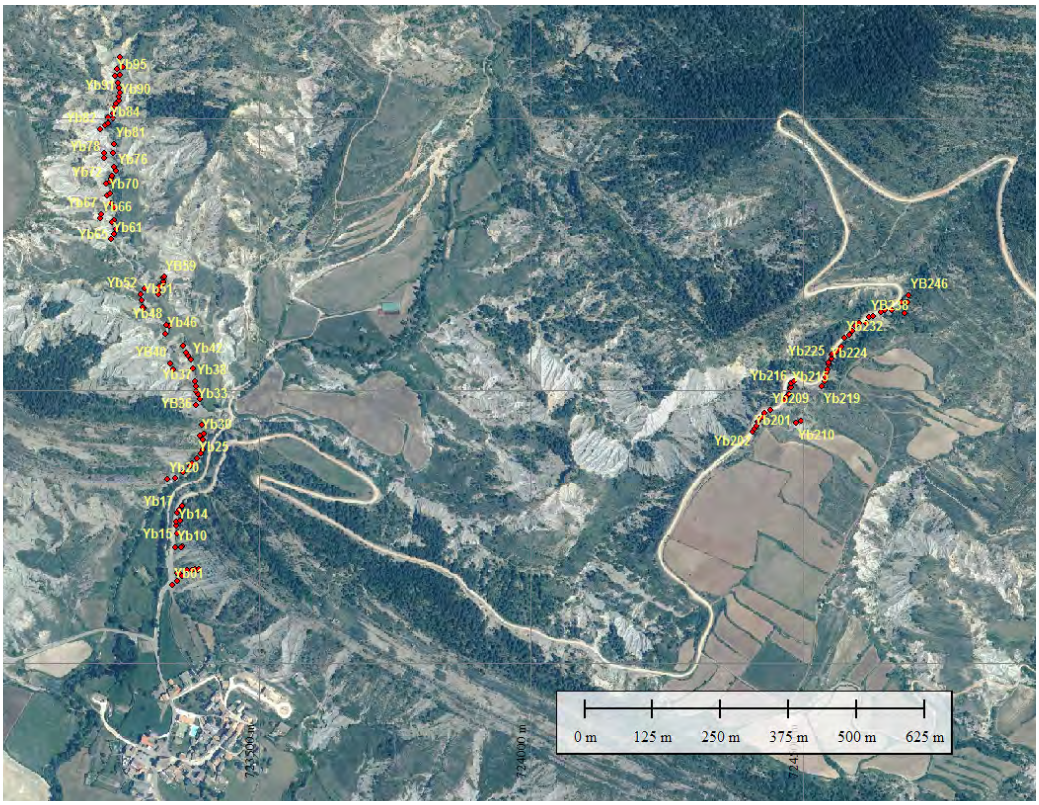

Figure 2. Magnetostratigraphic sampling ot the lower Yebra de Basa section.

Other actions related to outcrop scale characterization and models of geological reservoirs models are detailed elsewhere in this annual memory.

Conclusions

Among the studied section, magnetostratigraphic analysis has been completed in the Fuencalderas section (Sierras Exteriores) and Olson section (Ainsa Basin), and a successful correlation with the time scale has been achieved. Sampling of the Yebra de Basa section (Fig. 2) and the turbiditic sequences of the Ainsa Basin are ongoing tasks, to be completed in 2017.

In the course of this Project new colaboration with:

- The group of sedimentary geology at the University of Geneve (leaded by Sebàstien Castelltort) aiming at deciphering the climatic signatures in the turbiditic sequences of the Ainsa Basin by means of stable isotope analysis
- Josep Maria Pares, at the CENIEH (Burgos), aiming at assessing the magnetic properties of the fluvial sediments of the Escanilla Formation and its potential use as a climatic proxy record.

Future work

Magnetostratigraphic sampling of the Yebra de Basa will be completed during the first semester of 2017. Paleomagnetic processing of samples of the Yebra de Basa and San Marzal will be completed in the course of the year. In addition, sampling of new magnetostratigraphic sections spanning the turbiditic sequences of the Hecho group in the Ainsa Basin will be carried out. This will allow us assessing a firm correlation between the fluvial, deltaic and deep marine sequences of the middle to late Eocene Ainsa and Jaca Basins. This new age constrains will be used to construct new 4D forward models in order to asses the variable contribution of the different driving factors in the basin-scale stratigraphic architecture.

The Upstream and Downstream impact of Milankovitch cycles in continental nonmarine sedimentary records

[1]Luis Valero, [1]Miguel Garcés, [2]Pedro Huerta, [1]Lluís Cabrera.

[1] Grup de Geodinàmica i Anàlisi de Conques, Dept de Dinàmica de La Terra i l'Oceà; Universitat de Barcelona.
[2]Universidad de Salamanca.

Abstract.

Discerning the effects of climate in the stratigraphic record is crucial for the comprehension of past climate changes. The signature of climate in sedimentary sequences is often assessed by the identification of Milankovitch cycles, as they can be recognized due to their (quasi) periodic behaviour. The integration of diverse stratigraphic disciplines is required in order to understand the different processes involved in the expression of the orbital cycles in the sedimentary records.
New advances in Stratigraphy disclose the different variables that affect the sedimentation along the sediment routing systems. These variables can be summarized as the relationship between accommodation and sediment supply (AS/SS), because they account for the shifts of the total mass balance of a basin. Based in these indicators we propose a synthetic model for the understanding of the expression of climate in continental basins. Sedimentation in internally drained lake basins is particularly sensitive to net precipitation/evaporation variations. Rapid base level oscillations modify the AS/SS ratio sufficiently as to mask possible sediment flux variations associated to the changing discharge. On the other hand, basins lacking a central lacustrine system do not experience climatically-driven accommodation changes, and thus are more sensitive to archive sediment pulses. Small basins lacking carbonate facies are the ideal candidates to archive the impact of orbital forcing in the landscapes, as their small-scale sediment transfer systems are unable to buffer the upstream signal. Sedimentation models that include the relationship between accommodation and sediment supply, the effects of density and type of vegetation, and its coupled response with climate are needed to enhance their reliability.

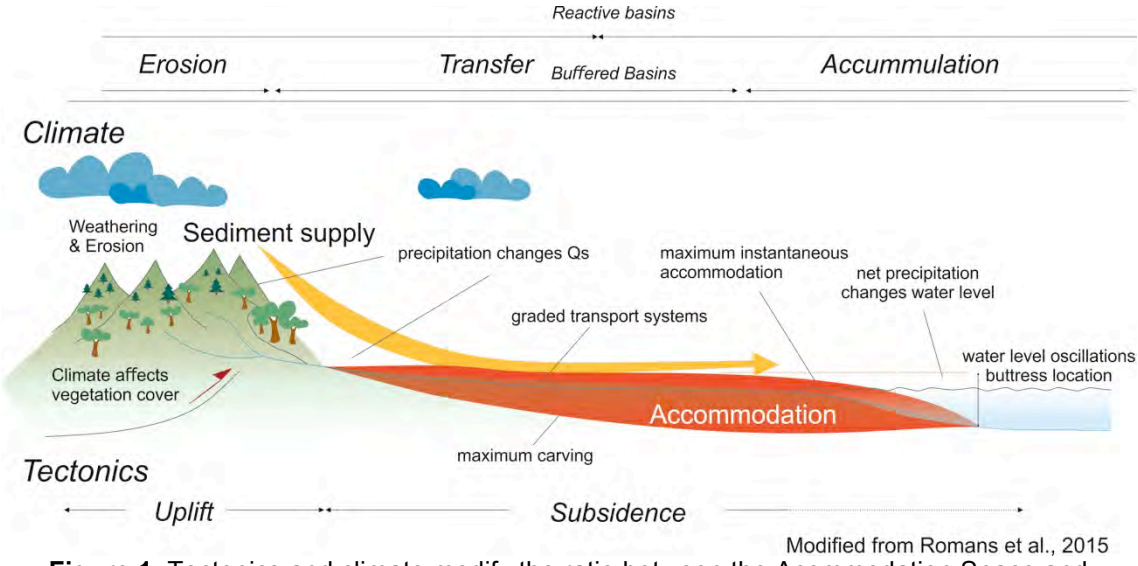

Figure 1. Tectonics and climate modify the ratio between the Acommodation Space and Sediment Supply, which in its turn control the sedimentary architecture.

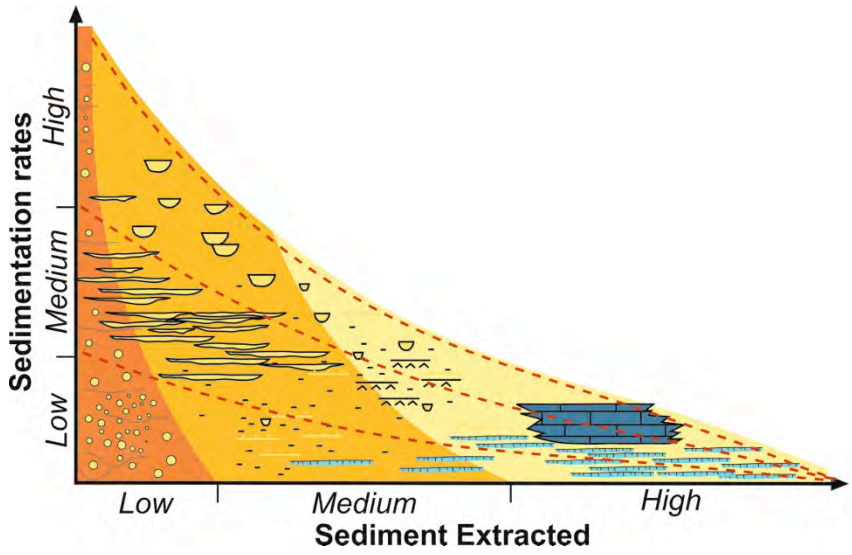

Figure 2. Sedimentary architecture as a function of the ratio between sedimentation rates and the amount of sediment extracted along the basin. Both sedimentation rates and sediment extracted depend on the ratio between accommodation space and sediment supply.

The Building of a Magnetostratigraphic Framework: Lessons Learned from the Ebro Foreland Basin (Paleogene-Neogene, NE Spain)

Miguel Garcés
Grup de Geodinàmica i Anàlisi de Conques, Dept de Dinàmica de La Terra i l'Oceà, Universitat de Barcelona.

Introduction.

Magnetostratigraphic correlation consist of a search for a best match between the local magnetic polarity zonation and the Geomagnetic Polarity Time Scale (GPTS) that agrees with some external (biostratigraphic and/or radiometric) age constrains. But solutions to this exercise do not always satisfy both conditions. Because true uncertainties associated to both biostratigraphic and radiometric ages often fall within the 100 kyr to one million year range, the final correlation is ultimately guided by the best fit between the local magnetostratigraphy and the GPTS. In doing this we rely on the questionable assumption that sediment accumulation occurs at approximately steady rates.

The extensive rock outcrops spanning the complete basin fill of the South-Pyrenean foreland make this region best suited for magnetostratigraphic analysis. Over the last decades, a biochronological framework, based fundamentally on fossil benthic foraminifera and vertebrates, is being replaced with a magnetostratigraphy-based chronology. The increasing length of the composite record has allowed magnetostratigraphic correlation to work with decreasing dependence on existing biostratigraphic constraints. This has provided integrated basin studies with a time frame of unprecedented resolution, crucial to unravel the interactions and causal relationships between the diverse forcing mechanisms involved in basin formation and filling. In the ideal progress towards an independent magnetochronological framework, a fundamental issue arises recurrently: To which extent biochronological information should limit the solutions of magnetostratigraphy? The answer to this question is not simple since the chronostratigraphic significance and age accuracy of key bioevents needs to be addressed in a case-by-case basis. In the other hand, the continuity and steadiness of the sedimentary record, which is hardly assessed a priori, reveals crucial for magnetostratigraphic correlation to work. Examples from the Eocene to Miocene of the Ebro Basin illustrate the need for an effort of a basin-scale integration of all (lito-, bio- and magneto-) stratigraphic disciplines.

Here we present a compilation of magnetostratigraphic studies from the Ebro Basin (Fig. 1) which allowed independent correlations with the GPTS. We explore the range and variability of sedimentation rates in different scenarios, from foredeep, wedge-top and passive margin basinal settings, from underfilled to overfilled conditions, and from open to closed drainage network. From compiled data we analyse the factors controlling sediment accumulation at the different spatial and temporal scales.

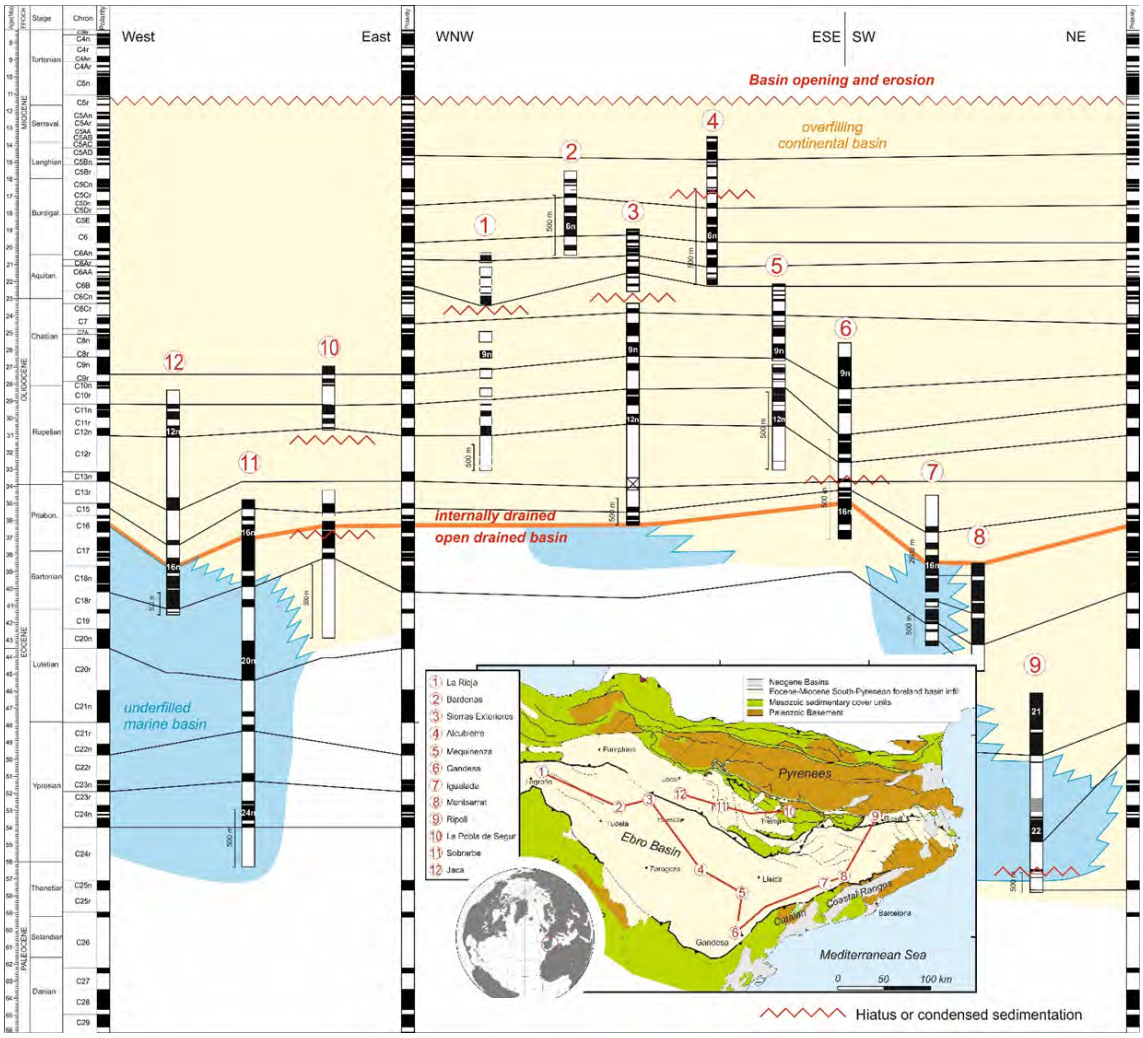

Figure 1. A compilation of key long sections in the Ebro Basin which allow the construction of a magnetostratigraphy-based time frame for the basin infill.

Conclusions

Average sedimentation rates are calculated for time increments corresponding to the duration of geomagnetic chrons, which typically range between 0.1 to 1 myr. All compiled data from the Ebro Basin yields sedimentation rates that range over two orders of magnitude, between 0.01 and 1.0 m/kyr. The amplitude of these variations is not dependent on the averaging time interval (=chron duration), thus indicating that high amplitude variations associated to the natural episodic behavior of sedimentary processes in clastic systems are compensated at the time resolution of magnetostratigraphy.

An analysis at the site level yields sedimentation rates ranging over less than an order of magnitude. Smooth long-term sedimentation trends as observed in the Stratigraphic thickness vs Age plots are related to the evolution of regional subsidence and supply (Fig. 4). These trends are only rarely interrupted, when a critical re-organization of the tectonic, climatic and geomorphic conditions takes place. Rapid shifts in sedimentation trends may be related to the onset of flexural subsidence in the foredeep, the uplift of wedge-top settings at times of thrusting and piggy-back basin generation, and changes in the configuration of the basin drainage network.

The amplitude of the short-term sedimentation changes is analysed by calculating the rate of change between adjacent magnetozones. Results indicate that the change of sedimentation rate is lower than a factor 2 for almost 80% of the complete dataset. This contrasts with the relative duration of adjacent chrons of the time scale, which is lower than a factor of 2 for only 40% of the dataset (Fig. 7). These results show that the duration of geomagnetic chrons is much more variable than sedimentation rates: Thus, the probability of having the correct correlation by searching the best match with the GPTS is high in most circumstances. This challenges a common view that the natural unsteadiness of sedimentation processes discourages stablishing independent magnetostratigraphic correlations. But magnetostratigraphic sections spanning a long sequence of well-defined magnetozones (>15 reversals defined by more than 8 sites/magnetozones) are favourable to yield a unique correlation with the time scale which is only based on the best-fit with the geomagnetic reversals of the GPTS.

B Laboratori de Modelització Analògica

Analogue modelling Laboratory

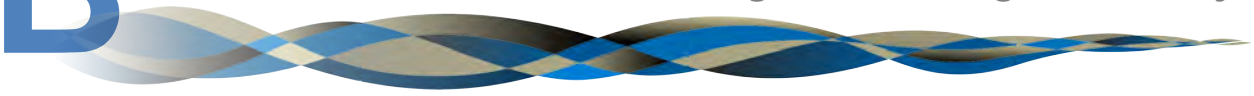

geomodels

institut de recerca

Modeling the interaction between pre-salt seamounts and gravitational failure in salt-bearing passive margins: the Messinian case in the northwestern Mediterranean basin

[1]Oriol Ferrer, [1]Oscar Gratacós, [1]Eduard Roca, [1]Josep Anton Muñoz

[1]Geomodels Research Institute, Grup de Geodinàmica i Anàlisi de Conques, Departament de Dinàmica de la Terra i de l´Oceà, Facultat de Ciències de la Terra, Universitat de Barcelona, C/ Martí i Franquès s/n, 08028 Barcelona, Spain

Abstract

The Northwest Mediterranean Basin includes a thick Messinian salt sequence composed of three evaporitic units (Figure 1). From these the intermediate unit, which is dominantly composed of halite, acted as a gravitational detachment favoring the downslope failure of the overlying sediments in a thin-skinned deformation regime. As a result, the structure of the margin is characterized by an upper extensional domain with basinward-dipping listric normal faults and a lower contractional domain that accommodates upslope extension by folding, salt inflation or diapir squeezing. Lower to middle Miocene volcanic seamounts (pre-salt reliefs) located at the upper extensional domain locally disrupted the evaporitic units and produced salt flow perturbations. They acted as passive buttresses during the gravitational failure modifying the structural zonation of the margin.

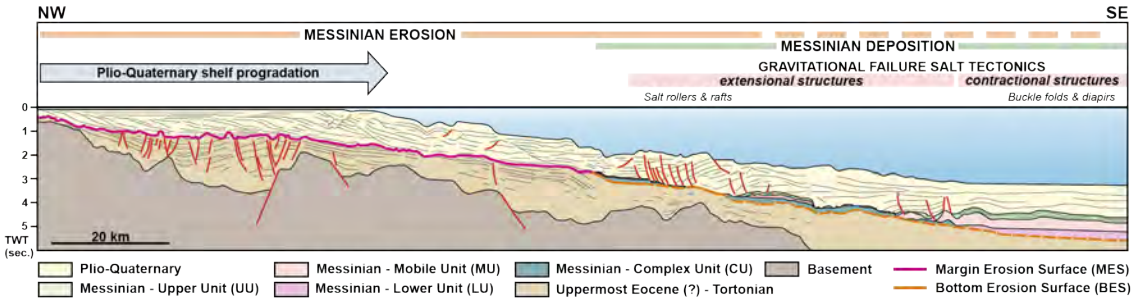

Figure 1. Line-drawing across the central part of the northwestern margin of the Liguro-Provençal Basin (southeast of the Gulf of Lions) showing the structure and the sedimentary architecture of the basin infill (modified from Lofi *et al*., 2011b after Bache *et al*., 2009).

Using an experimental approach (sandbox models) this study analyses the role played by seamounts during the kinematic evolution of passive margins and how they alter salt flow and suprasalt deformation during gravitational gliding. The experiments show that seamounts locally interrupt the structural zonation of the margin as they hindered downdip salt flow during early deformation (Figure 2). Seamounts initially compartmentalize the margin architecture, resulting in the development of two gravitational sub-systems with two extensional/contractional pairs that are subsequently re-connected when the accumulation of salt analogue upslope of the relief is enough to overthrust it. From this point onwards, the cover is passively translated downslope as a regional system. The changes in the viscous layer flow velocity related to the dip differences between the flanks and edges of the seamount determine the kinematic evolution of this system. The experiments also provide

geometrical constraints to consider during interpretation of these structures, which are commonly poorly imaged in seismic data.

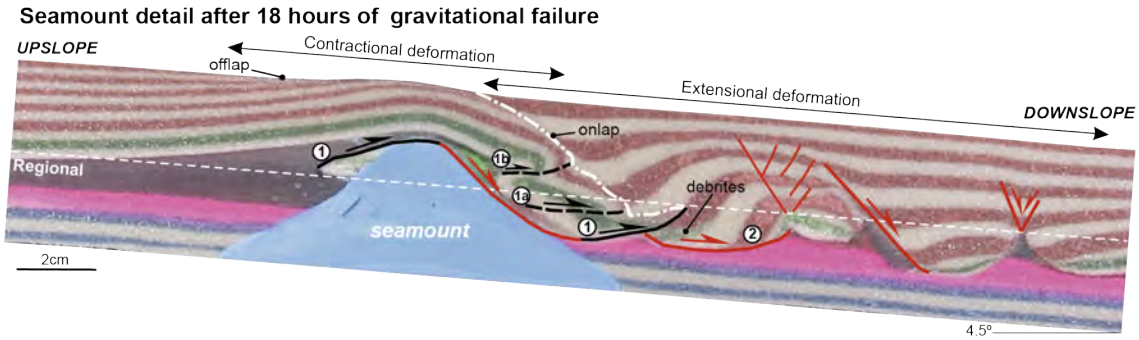

Figure 2. Detailed cross-sections showing the main structures developed around the seamount during gravitational gliding after polymer overthrusting. Cross-section of experiment 3 after 18 hours of gravitational gliding.

Work done

At the begining of 2016 was interpreted the 2D seismic of the Liguro-Provençal basins. After their interpretation different questions related to the origin of several structures remained unanswered. For this reason an experimental programme including eight analogue models was carried out on the Geomodels Analog Modeling Laboratory from March to May 2016. The aim of this experimental programme was to analyze how the height of a pre-salt seamount modifies the downslope failure of a salt-bearing passive margin. Different models with the same setup have been used to examine the temporal evolution of the System. Seamounts were built manually with plasticine in order to facilitate the slicing of the models at the end of the experiment. They were glued to a basal mylar sheet that remained fixed throughout the experiment. The shape of the basal seamount section was the same in all the experiments, consisting of a rectangle with a semicircle on each short side. All of them had a triangular section but with different heights, and consequently with different average slope angles of their flanks

The results of this research were presented in different meetings and were included in a manuscript that has been submitted to the peer-review Interpretation journal.

Conclusions

The presence of pre-salt relief in the form of a seamount can modify the typical three domain structural zonation of salt-bearing passive margins into a system that develops two gravitational sub-systems separated by the seamount.

The structural style and kinematics of both margin-wide and local structures may change during gravitational gliding if the amount of salt upslope of the seamount is sufficient to overtake the relief. Thus, depending on the seamount height with respect the top of the evaporitic unit, seamounts act as temporary barriers during margin evolution, resulting in two different evolutionary stages. During the first stage, the seamount initially hinders salt flow, forcing salt migration around the relief. As a consequence of the buttress upslope of the seamount, a thrust develops and gradually

uplifts the cover. When the cover reaches the height of the relief, the seamount is overthrusted, and falls rapidly downslope along the seamount flank. A significant increase in salt flow velocity occurs coeval with overthrusting. The development of a primary weld below the basin downslope of the seamount and the flow velocity decrease that occurs at the edge of the seamount favors the formation of a local fold and thrust system.

Divergent flow patterns are observed on the updip side of the seamount as the salt analog is diverted around the flow barrier. Flow deviation also occurs where there are diapirs allowing salt to escape vertically from beneath the basins. In contrast, flow in areas without seamounts or diapirs describe dominantly linear traces parallel to the dip direction of the passive margin.

The experimental results provide a set of geometrical constraints that can be used in seismic interpretation of similar structures (e.g., Eastern Mediterranean, Red Sea, offshore Morocco.

Future work

A new collaboration started at the end of 2016 with Spectrum Geo. This surveys company has provided new 2D seismic data of the Western Mediterranean in order to continue investigating the role of pre-salt relief on the supra-salt deformation of the area. A BSc. and a MSc. project will be carried out during 2017 focused on this topic.

Inversion of hangingwall synclinal basins over ductile décollements as illustrated by analog modeling and kinematic restoration.

[1]Maria Roma, [1]Oskar-Vidal Royo, [2]Ken McClay, [1]Oriol Ferrer, [1]Josep Antón Muñoz

[1] GEOMODELS Research Institute - Group of Geodynamics and Basin Analysis, Earth and Ocean Dynamics Department, Faculty of Earth Science, University of Barcelona, C/ Marti i Franques s/n 08028, Barcelona, Spain
[2] Fault Dynamics Research Group. Earth Sciences Department. Royal Holloway University of London. TW20 0EX, Egham, United Kingdom.

Introduction

Scaled analog models of hangingwall synclinal basins with syn-kinematic ductile silicone polymer layers above a ramp-flat detachment fault have been constructed. These successfully simulated the structural styles of natural extensional and inverted extensional basins with syn-kinematic salt sections. These models produced a main breakaway with upward propagation of the main detachment forming a hangingwall roll-over as well as an extensional fault-propagation fold. Above the main ramp a hangingwall fault-bend anticline developed with an adjacent ramp synclinal basin. The syn-kinematic ductile polymer layer changed thicknesses in response to the extension with formation of reactive diapirs and polymer walls. Serial cross-sections through the models indicate 3D flow of the polymer with significant variations in structural styles. Inversion of the ramp flat models produce shortening that particularly focused on the polymer walls and diapirs that were squeezed producing surface extrusion, and vertical welds. The complex structural styles formed in the analogue models are templates that are directly comparable to the salt bearing, hangingwall basins found in the Mesozoic basins of the Iberian Peninsula. Restoration of the sandbox models has demonstrated that this is a powerful tool to unravel the complex structures in the models and this may similarly be applied to the seismic interpretation of the natural complex salt structures.

Work done

1) Two experiments, Experiment 1 and Experiment 2 (Figure 1 & 2), are presented in this memoir, and are part of a larger modeling program (that have been done during 2014-2015 period in the *Royal Holloway University of London, at Earth Sciences Department)* designed to investigate the evolution of synclinal basins containg salt layer. Both experiments were extended initially by 7 cm, at which point a silicone polymer layer was added, and followed by a further 8 cm of extension (total extension 15 cm). Experiment 1 was terminated at the end of the extension whereas Experiment 2 was inverted by 8 cm of shortening after the end of extension.
2) The experiment cross-sections were systematically captured using a photograph camera. Those photographed sections (Figure 1 & 2) were then transferred and georeferenced into a local 3D framework using the software Petrel 2013, in order to obtain a synthetic seismic line and a 3D seismic cube (Figure 3a & b). From these cubs we have been obtained a 3D Model (Figure 3b & c).
3) Cross-sections 58 and 87 of Experiment 2 were sequentially restored to illustrate the structural evolution of the two main domains across the model, a) areas in which polymer walls form and pierce through the overburden (Section 58, Figure 4), and b) areas where no extruded polymer walls occur (Section 87,

Figure 5). The sequential restoration also shows the change in geometry and area of the

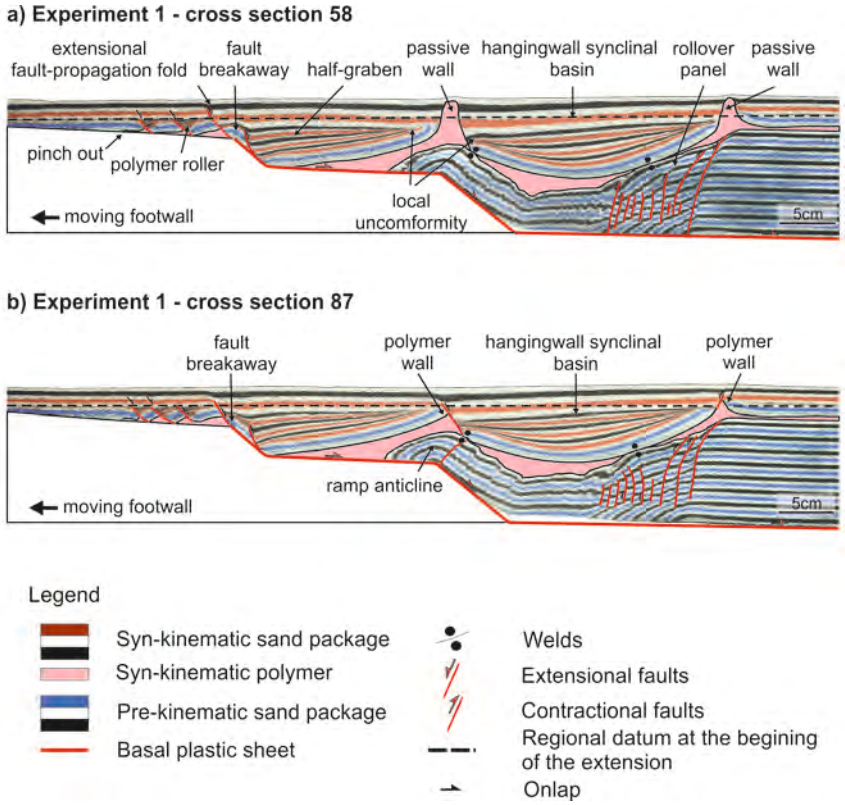

polymer as a result of extension, positive inversion and diapirism,

Figure 1. Interpreted cross section of the structures obtained in the Experiment 1 at the end of the second phase of extension (after 8 cm of lengthening) and with the terminology used in this article. a) cross section 58; and b) cross section 87.

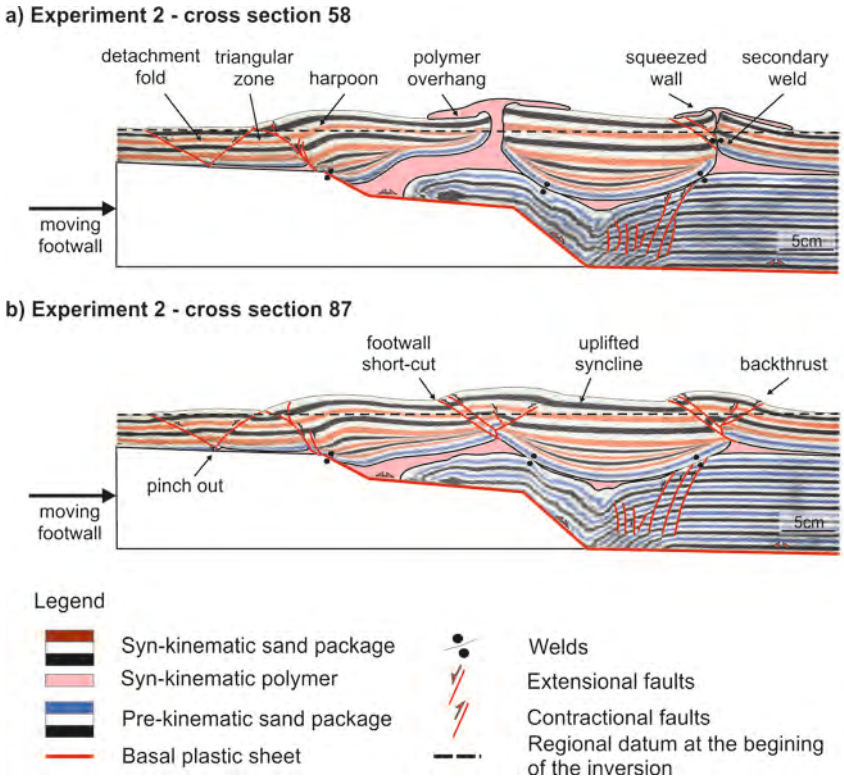

Figure 2. Interpreted cross section of the structures obtained in the Experiment 2 at the end of the inversion (after 2 phases of extension followed by 8 cm of contraction) and with the terminology used in this article. a) cross section 58; and b) cross section 87.

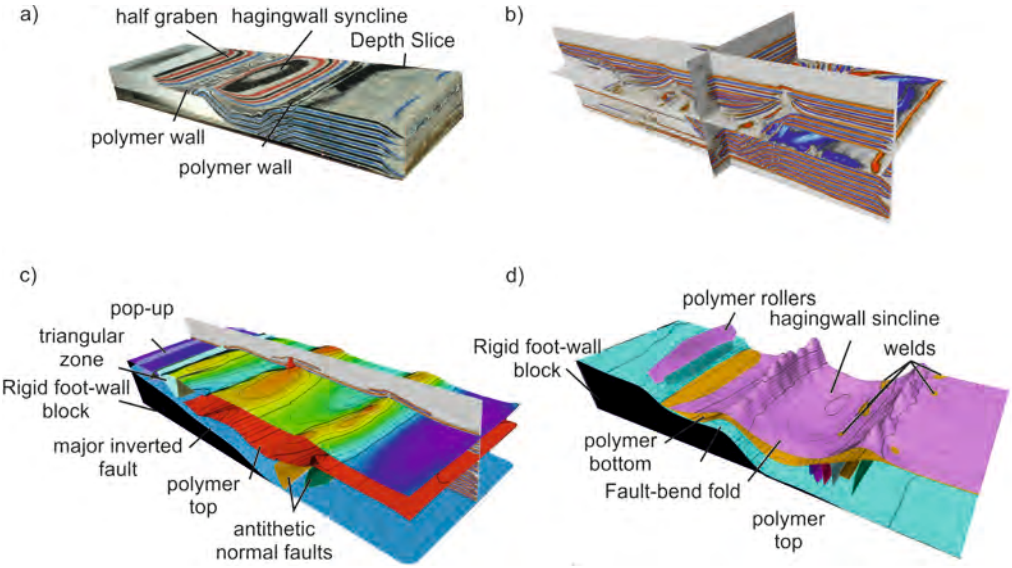

Figure 3. a) 3D volume reconstruction based on sections of Experiment 1; b) Synthetic 3D seismic obtained from the cross-sections of the Experiment 1; c) 3D structure reconstruction of the main horizons of Experiment 2; d) 3D structure reconstruction of the main horizons of Experiment 2.

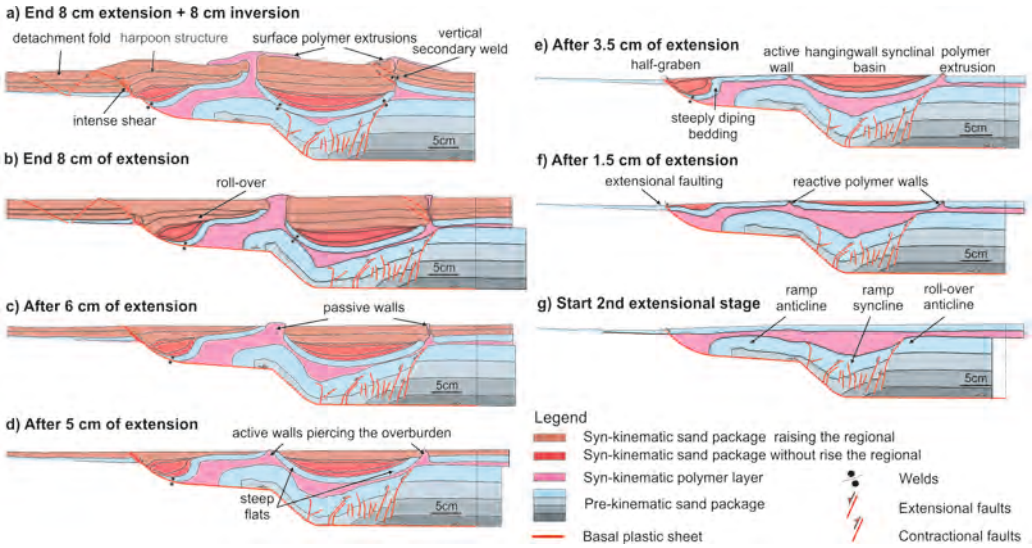

Figure 4. Sequential restoration of cross section 58 from Experiment 2 illustrating the structural evolution during the second phase of extension.

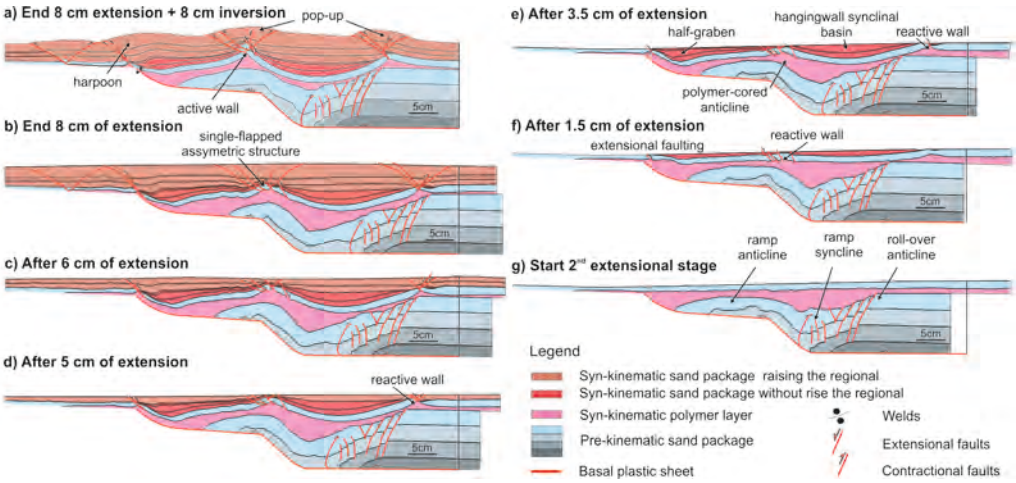

Figure 5. Sequential restoration of cross section 87 from Experiment 2 illustrating the structural evolution during the second phase of extension.

and highlights the different responses to deformation of the supra- and sub-polymer units.

4) Variations in the area of the polymer section between the lower and upper sequences in the models have been calculated for each stage of the restorations (Figures 6 & 7).

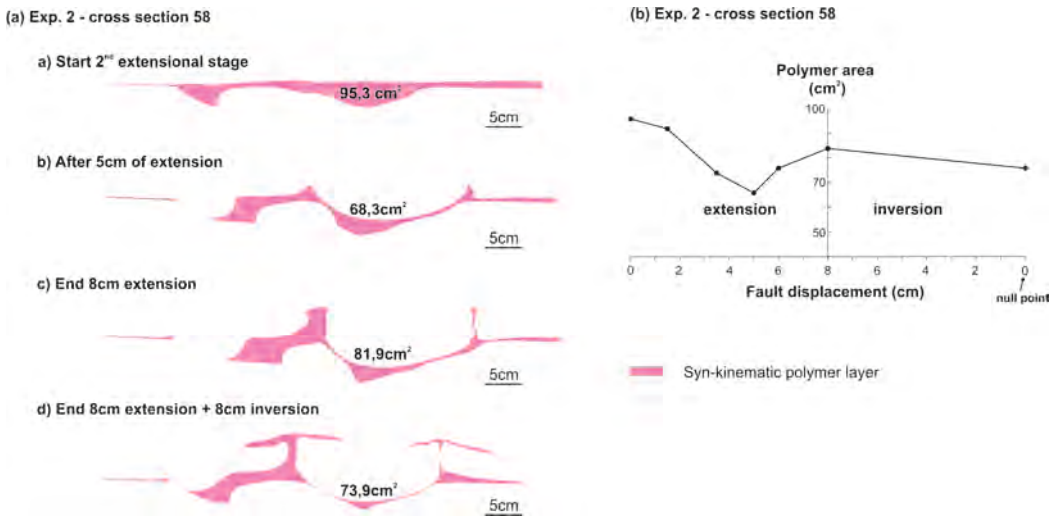

Figure 6. a) Restoration of polymer area for section 58 from Experiment 2; and b) plot of polymer area vs. fault displacement during extension (left-hand side of the graph) and inversion (right side of the graph).

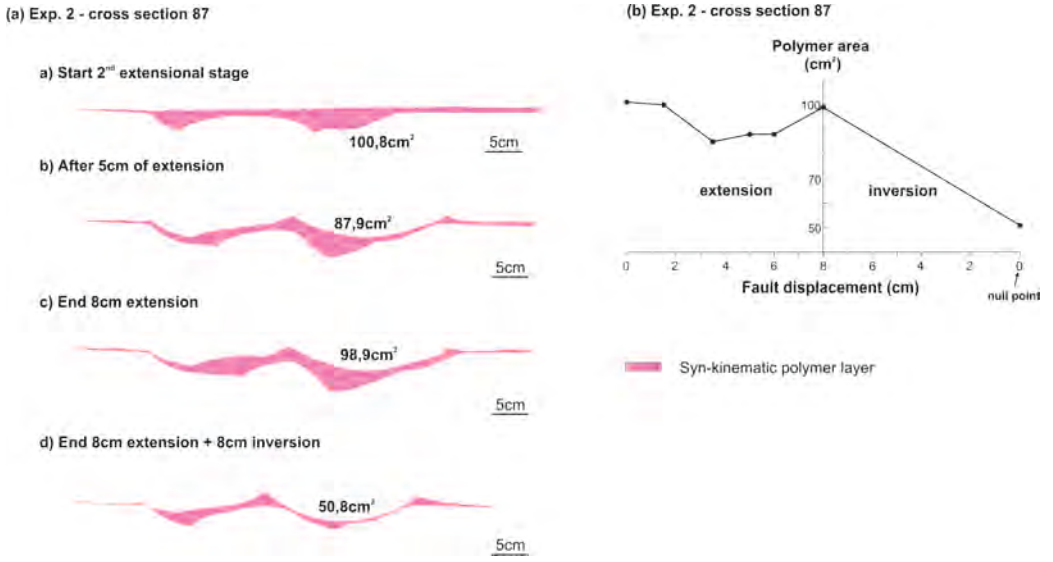

Figure 7. a) Restoration of polymer area through extension and inversion events for section 87 from Experiment 2; and b) plot of polymer area vs. fault displacement during extension (left-hand side of the graph) and inversion (right side of the graph).

5) The results of the analog model of the inverted hangingwall synclinal basin and an inverted extensional fault-propagation fold are compared with natural examples of inverted structures with salt sections from Lusitania basin, offshore Portugal and from the Parentis basin, Bay of Biscay (Figures 8a & b).

Scaled analog models of hangingwall synclinal basins with syn-kinematic ductile polymer layer above a ramp-flat fault have successfully simulated the structural styles of natural extensional and inverted basins with syn-kinematic salt sections. The complex structural styles in the analogue models are directly comparable to the salt bearing, hangingwall basins as found on the southern margin of the Bay of Biscay, in the Pyrenees and in the Lusitanian basin offshore Portugal.

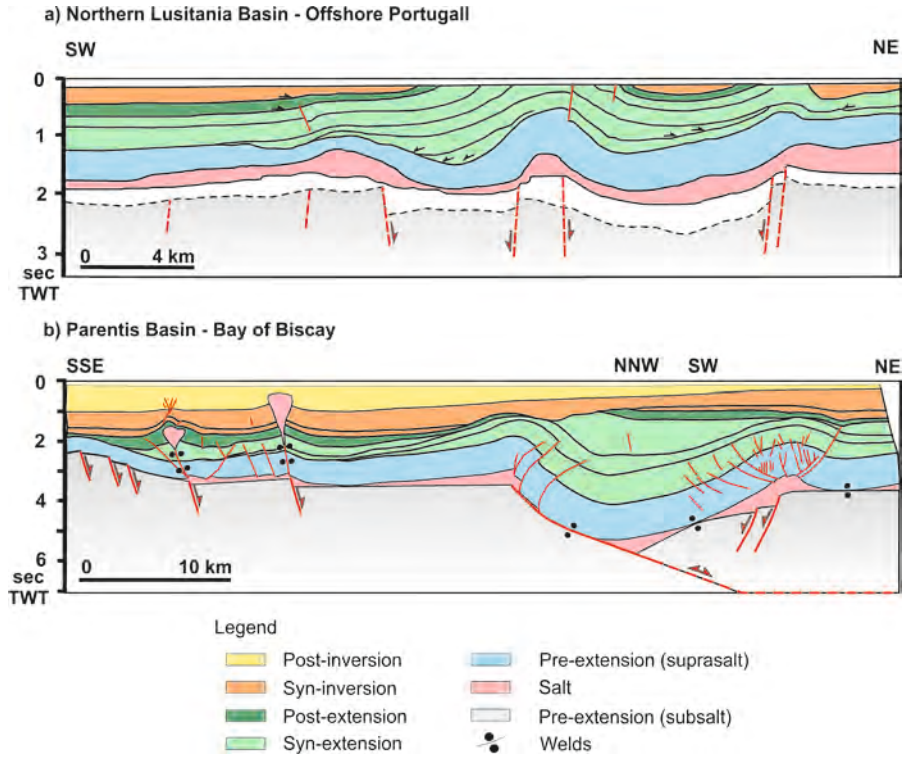

Figure 8. Natural examples of inverted basins. a) Interpreted seismic line S84-23, modified from Soto *et al* (2007), of Northern Lusitania Basin (offshore Portugal) containing syn-stretching salt (according to Rowan, 2014) and subsequent pronounced period of inversion according to Alves *et al* (2002); b) Line drawing of a seismic section of the inverted Parentis Basin (Bay of Biscay) with a pre-kinematic salt unit. Modified from Ferrer *et al* (2016).

Restoration of the sandbox models has demonstrated that this is a powerful tool to unravel the complex structures in the models and this may also be applied to the seismic interpretation of the natural prototypes.

The hangingwall syncline basin structures in the supra-polymer strata in the models may be either totally decoupled from the sub-polymer strata where the ductile polymer remains relatively thick and continuous, or may be partially coupled where the polymer thins or is breached and where there are welds, by propagating faults such as at the breakaway fault system. Comparisons and restorations of serial sections through individual models show large variations in structural styles and polymer thicknesses indicating 3D polymer flow within the model.

The sandbox models and their restorations demonstrate the evolution of the ramp-flat basin systems. Key structural features are:

a) A footwall breakaway formed at the top of the upper section of the main detachment fault and as extension proceeded an extensional fault-propagation fold developed in the adjacent hangingwall of the breakaway;

b) A fault-bend anticline develops in both the pre-kinematic as well as the syn-kinematic strata above the crest of the basement ramp. The intervening ductile layer layer accommodates the folding initially thinning across the crest of the anticline and thickening into the adjacent synclines. Outer arc extension however triggers reactive diapiric rise allowing the formation of polymer walls at this location;

c) The hangingwall syncline basin was formed decoupled from the sub-polymer units, but its development was controlled by the geometry of the basement-involved fault (thick-skinned extension). Regardless, the polymer withdrawal is the main factor responsible of the final geometry and vertical-stacking depocenter of the basin. ;

d) The outer margin of the ramp syncline is characterized by an antithetic extensional fault system that induces thinning of the polymer and localized footwall extensional faulting in the units above the polymer. This may generate a polymer wall in this position;
e) Contraction and inversion of the ramp-flat extensional architecture shortens the upper and lower sand packages and in particular squeezes the polymer layer such the polymer walls absorb most of the shortening. Where there is sufficient ductile material in the walls extrusion onto the surface may occur. Contraction drives polymer vertically up thought and the polymer walls stems and out of the wall until produced vertical, secondary welds. Continued shortening at this stage produced low-angle thrusts developed from the welds.
The results of this research can be applied to the seismic interpretation of complex salt structures in both extensional basins and inverted salt bearing basins. The models and their restorations indicate that both 2D and 3D changes in salt thicknesses and salt dispositions must be taken into account in interpreting these hangingwall structures in salt basins.

Future work

In order to understand the evolution and distribution of the strain stages, we want to use the software Davis_8 from La Vision; Digital Image Correlation (DIC) through the top photos of experiments.

Finally, we are working in the other experiments which form part of the same experimental program, in order to check the role of different factors (rate of fault slip, syn-inversion deposits,). We want to analyse these experiments in the same way and with the same detail than these ones published.

Through this experimental program, we have built new ideas to make a new powerful article.

Formation and inversion of extensional ramp syncline basins with pre-kinematic salt layer. Experimental results and application to the Mesozoic Columbrets Basin (Western Mediterranean).

[1]Maria Roma, [1]Eduard Roca, [1]Oriol Ferrer, [1]Oriol Pla, [1]Mireia Butillé

[1]GEOMODELS Research Institute - Group of Geodynamics and Basin Analysis, Earth and Ocean Dynamics Department, Faculty of Earth Science, University of Barcelona, C/ Martí i Franquès s/n 08028, Barcelona, Spain

Introduction

The widespread extensional deformation that took place during Jurassic to Cretaceous times in the Western Europe and north-Atlantic realm resulted in the formation of several rift systems. Some of the basins associated to these rifts show broad syncline-shapes filled by thick sedimentary successions. The development of these basins has been associated to the extensional motion of flat/ramp extensional faults, generate the so-called ramp synclines. The shape and kinematics of such faults have been usually established using the architecture of syn-kinematic layers and assuming a complete coupling of the hanging wall rocks. Therefore, they are fault interpretations that do not consider or neglect the role played by the deep pre- or syn-kinematic Permian or Triassic salts, which clearly act as effective décollement decoupling the sub- and supra-salt deformation. During latest Cretaceous and Cenozoic times these basins were partially inverted and often incorporated into thrust-and-fold belts.

Based on analogue models and using the Mesozoic Columbrets Basin as a case study (Figure 1), the aim of this research is twofold: to decipher the role played by a pre-rift salt layer in the syncline development above a low angle extensional fault with both convex-up and concave-up bends and to infer how ramp syncline basins are subsequently inverted considering different salt thickness.

To achieve this goal an experimental program includes 8 different sandbox models. Their results show that; the main structure formed within syn-kinematic sediments is a ramp syncline and its geometry depends on the fault segments dip and length, and also of the fault displacement; the ramp syncline geometry is strongly conditioned by the presence of salt, which generates diapiric structures, and because it behaves as a very efficient decoupling layer, and the tectonic inversion of ramp synclines is mainly characterized by the formation of a major anticline, and the development of thin-skinned contractional structures.

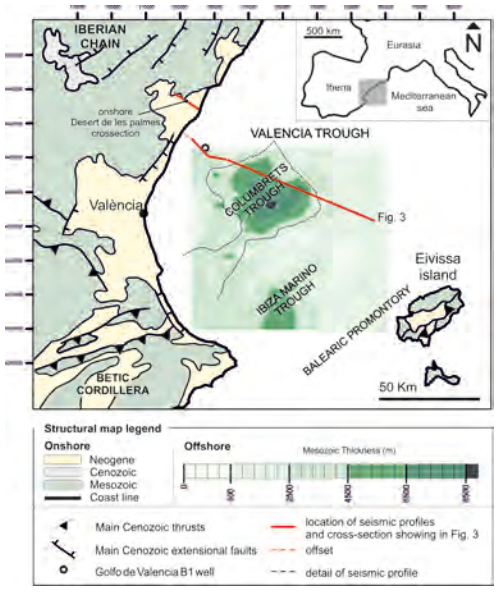

Figure 1. Simplified structural map of south-western Valencia Trough and surrounding onshore areas (modified from Roca, 2001). The position of the Columbrets Basin is highlighted by the isocore map of the Mesozoic successions in the offshore areas inferred from the seismic interpretation of the SGV01 survey.

Work done

1) The last 2014-2015 annual Geomodels memoir has included 7 experiments. During 2015-2016 we have been working on increase the experimental program (Table 1) in order to understand the main factors that control basin formation. Also we repeated some experiments in order to improve the quality of the results. The results are showing in this report, are better than the last memoir.

*erosion of any growing topographic high

Experiment	Pre-kinematic thickness (cm)	Polymer thickness (cm)	Extension Stretching (cm)	Compression Shortening (cm)	Experiment duration (hr)
1	11.8	-	20*	-	70
2	11.8	-	20	9	93
3	11.8	0.5	20*	-	70
4	11.8	0.5	20	9	93
5	12.3	1	20*	-	70
6	12.3	1	20	9	93
7	11.8	0.5	10*	-	35
8	11.8	0.5	20*	9*	93

Table 1. Summary table showing the main characteristics of the experimental program of this research.

2) It has been proposed three different mechanisms to explain the formation of these extensional syncline basins: (1) drape folding of a pre-kinematic overburden over a rotational planar or concave-up bended extensional fault with a salt layer accommodating the difference in geometry (Figure 2a) (Soto *et al*., 2007); (2) extensional fault-propagation folding (Figure 2b) (Withjack *et al*., 1990); and (3) fault-bend folding associated to an extensional fault with an upper convex-up and a lower concave-up fault bends (Figure 2c) (McClay & Scott, 1991). In these latter cases, the shape and kinematics of the extensional faults have been usually stablished using the geometry of the shallow folded pre- and syn-kinematic layers and assuming a complete coupling of the hanging wall rocks. Therefore, they are fault interpretations that do not consider or neglect the role played by the deep pre- or syn-kinematic Permian or Triassic salts as a decoupling layer. This clashes with the data that shows that these salts, present in some syncline basins, clearly act as effective décollements decoupling the sub- and supra-salt deformation

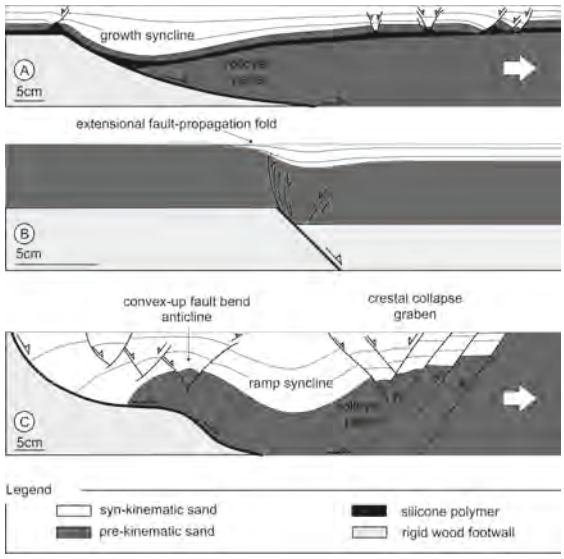

Figure 2. Simplified cross-sections of sand-box models illustrating the geometries resulting from A) a listric extensional fault with a polymer layer located close to the top of the pre-kinematic sand pack (modified from Soto et al., 2007), B) an extensional fault-propagation folding (modified from Withjack & Callaway, 2000) and C) a 2D extensional ramp-flat listric fault without silicone polymer layers analogue of salt (modified from McClay & Scott, 1991).

3) The main purpose of this submitted paper is precisely to decipher the role played by a pre-rift salt layer in the syncline development above a low angle extensional fault with both convex-up and concave-up bends. Aside, the presented work also claims to ascertain what the main deformational features are developed in these synclines during a later contractional reactivation of these kind of basement faults.
4) The geometry of the basement fault and applied deformation rates have been defined from the Columbrets Basin which belongs to a partially inverted syncline extensional basin formed above a kinked basement fault (Figure 3). This Mesozoic basin is located in the Western Mediterranean and is used in this work as a real analogue to test the validity and applicability of the obtained modeling results.

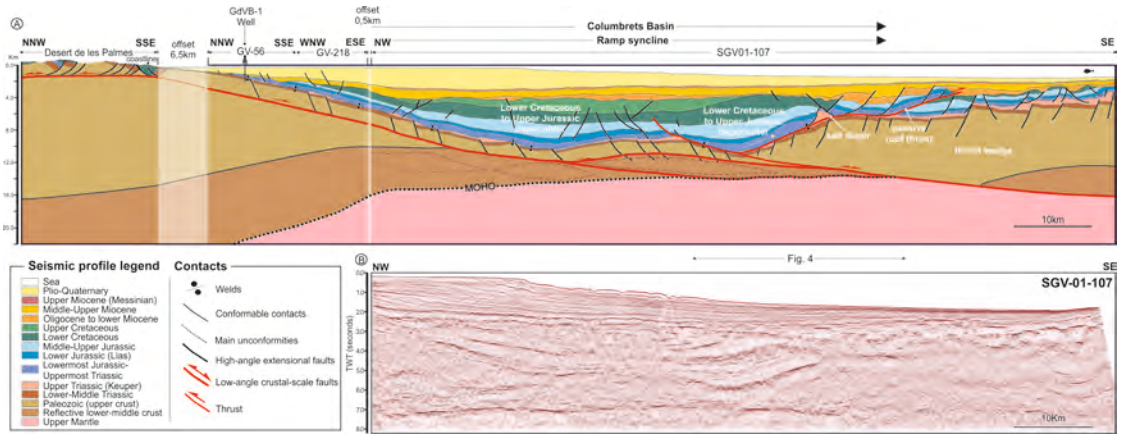

Figure 3. *Crustal cross-section trough the Columbrets Basin (onshore structure based on Zeyen et al., 1985, Martín & Suriñach, 1988; Roca et al., 1994; Vidal et al., 1998 and Ayala et al. 2003) and B) Time-migrated seismic line used to define the offshore structure of the Columbrets basin in the central part of the Valencia Trough.*

5) To achieve these goals, an experimental program of seven sandbox models has been designed (Table.1). These consider without or different silicone polymer thicknesses (analogue of salt in nature, Figure 4), fixed basement fault geometry and a constant amount of extension and shortening (Figure 5).
6) The comparison between the Columbrets Basin (Figure 3) and the experimental results (Figure 4 & 5) presented in this research show quite clearly that the structure of this basin is compatible with an inverted ramp syncline basin that: a) involved a ductile pre-kinematic salt layer; and b) developed over a master south-east dipping low angle fault which includes, at least, three planar panels separated by an upper bend with a convex-up shape and a lower one that is concave-up.

Conclusions

The experimental program presented in this article including extension and later inversion above a kinked planar fault formed by three different panels and with a pre-kinematic polymer layer, suggests that the main structure formed within syn-kinematic sediments is a broad ramp syncline. Its geometry is mainly controlled by the dip and length of the fault segments, but also for the fault displacement.
Besides to control the geometry of the basin, these three parameters also determine the thickness of the syn-kinematic layers during extension, which will strongly condition the lateral migration of the salt layer and the formation of salt structures in the overlying sand pack.

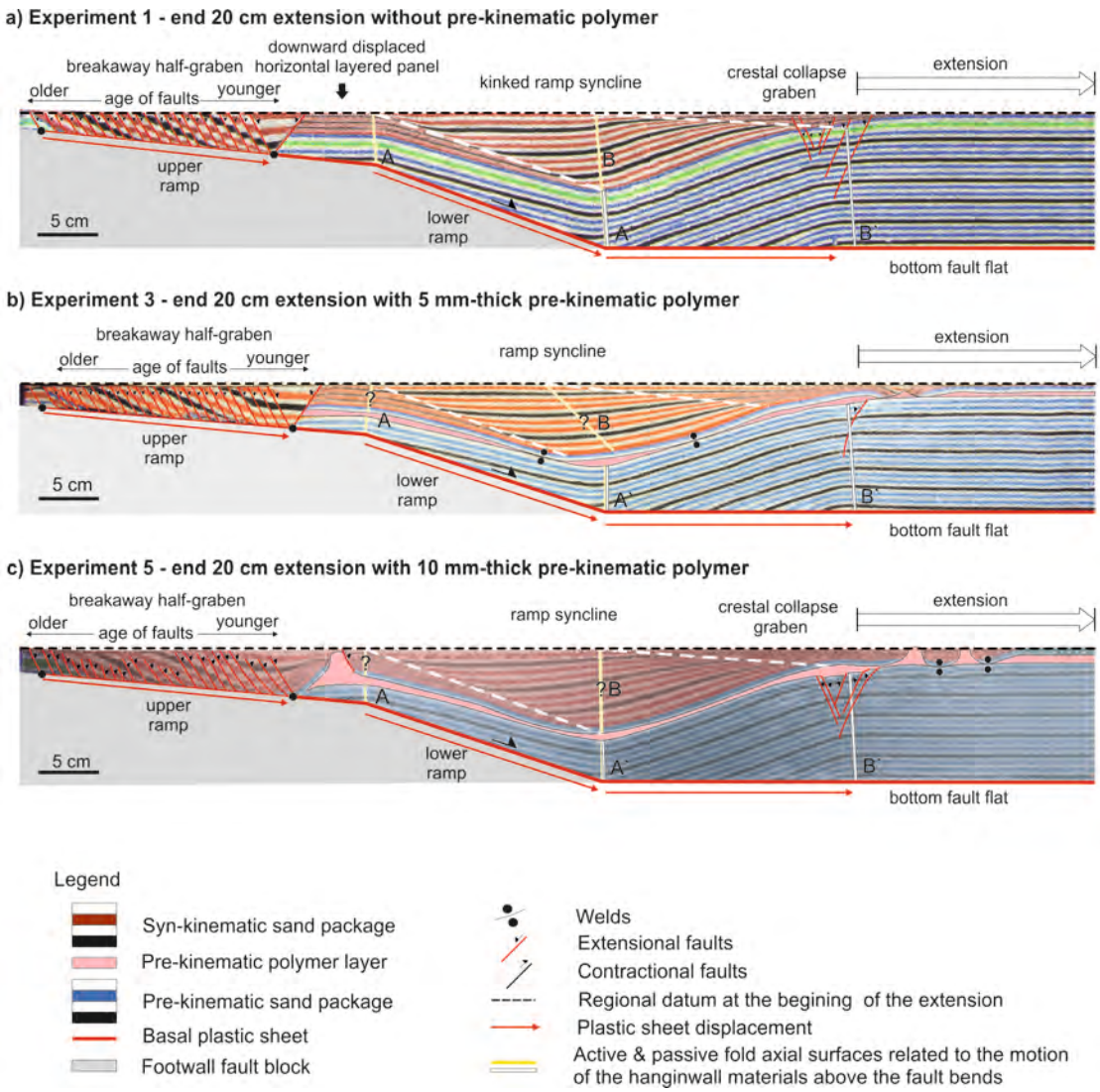

Figure 4. Cross-sections of the experiments with and without a pre-kinematic polymer layer after 20 cm lengthening. a) model without polymer (experiment 1), b) model with a 0.5 cm thick polymer layer (experiment 3) and c) model with a 1 cm thick polymer layer (experiment 5).

While extension progresses, salt preferably migrates towards the syncline edge associated to the less dipping panel (syncline forelimb), where the syn-kinematic cover was thinner. According to our results the development and evolution of salt structures will be determined by the thickness of the source layer.

During inversion, the contractional displacement and the length of the intermediate fault segment would determine the geometry of the resulted anticline, reaching its highest relief (anticline hinge) above the stepper fault panel. Our results show, that the inversion of ramp synclines is also characterized by thin-skinned contractional structures (after the squeezing the pre-existing diapir/wall in experiments with polymer) which can occur when the syncline is displaced above this intermediate panel that produced shortening of the syncline backlimb and a decreasing of the fold amplitude, related to the syncline forelimb dip changes.

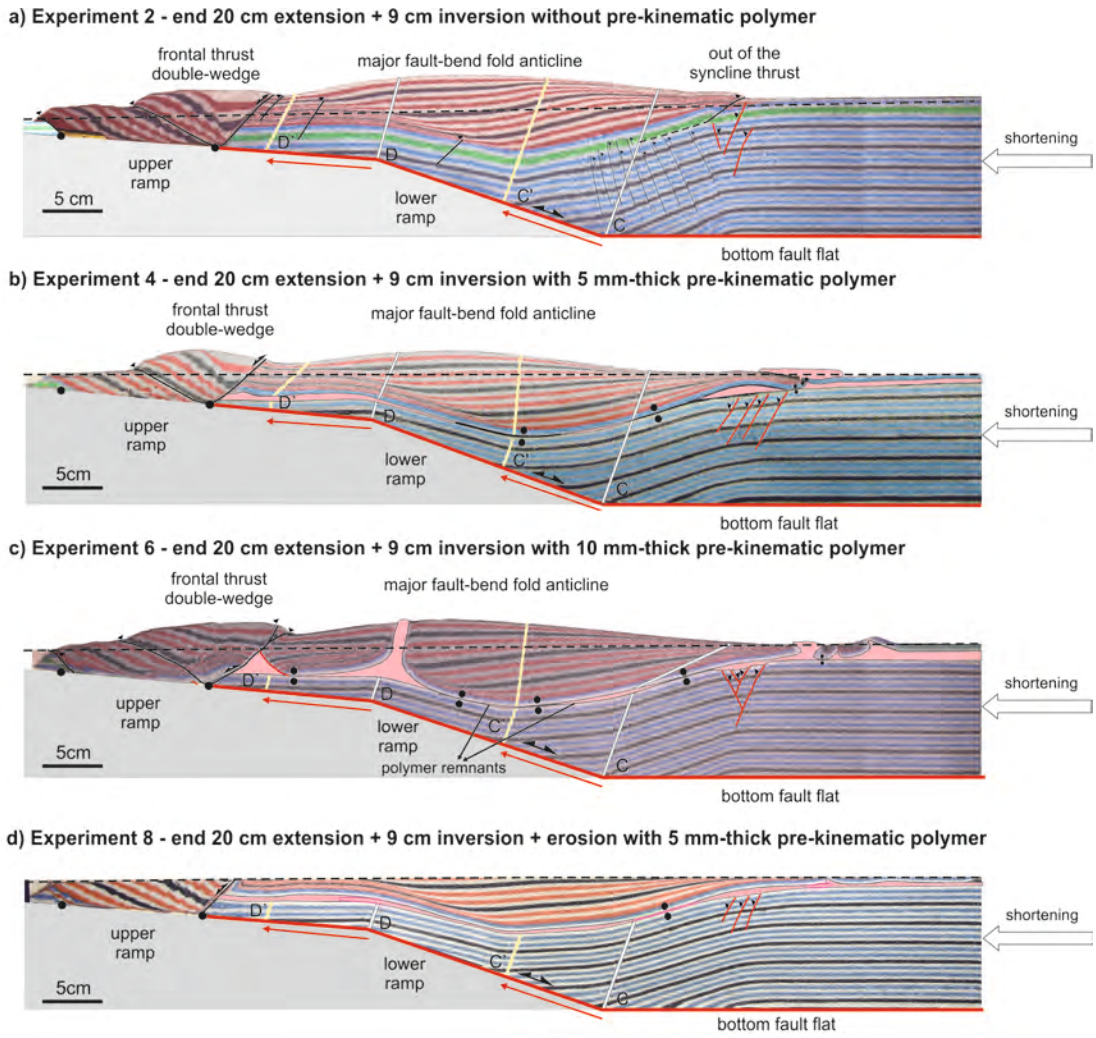

Figure 5. Cross-sections of the experiments with and without a pre-kinematic polymer layer after 20 cm lengthening and 9 cm of subsequent shortening. . a) model without polymer (experiment 2), b) model with a 0.5 cm thick polymer layer (experiment b), c) model with a 1 cm thick polymer layer (experiment 6) and d) model with a 0.5 cm thick polymer layer and erosion during shortening (experiment 8). See legend in Figure 4.

That last, occurs when the hanging wall rollover moved from the lower to the upper steeper panel of the master bounding fault.

Both during extension and inversion, salt layer act as an efficient decoupling layer, developing thin-skinned deformation and blurring the syncline geometry above it. Whereas beneath the salt, the hanging wall structure is only defined by the geometry and displacement of the fault, above the salt, this one appears significantly modified by deformation that are driven by lateral salt migration (welds in the syncline limbs and diapirs in syncline edges). Consequently, the experiments with a pre-kinematic polymer layer depicted more shortening in the upper layer of the ramp syncline.

Despite some differences, the results of the experimental program might be applied to reduce the uncertainty about the origin and kinematics of the Columbrets Basin, showing an inverted ramp syncline basin that, involved a ductile pre-kinematic salt layer and developed over a master south-east dipping low angle fault which includes three planar panels separated by an upper bend with a convex-up shape and a lower one that is concave-up.

Basin inversion in tectonic wedges: a comparative approach from sandbox analogue modelling and the Alpine-Carpathian fold-and-thrust belt

[1]Granado, P., [1]Ferrer, O., [1]Muñoz, J.A., [2]Thöny, W., [2]Strauss, P.

[1]Institut de Recerca Geomodels, Dept. de Dinàmica de la Terra i de l'Oceà, Universitat de Barcelona, Barcelona, Spain

[2]OMV Exploration and Production GmbH, Trabenstraße 6-8.1020, Vienna, Austria.

Inversion of segmented half-graben basins has been simulated by means of scaled physical analogue models. In our modelling, we have firstly focused on characterizing the formation of a half-graben basin from a segmented discontinuity striking at 90º, 45º and 15º to the extension direction. Then, we have used different angles for the basal detachment and the topographic slope, and have included a shallow polymer layer to test the effect of wedge geometry, related load, and strength profile on the inversion of the underlying half-graben. The experiments have been analysed by means of time-lapse photography, topography scans and image-based voxels from serial cross-sections. These tools have allowed constraining a deformation sequence which included layer-parallel compaction, thrusting and folding and reactivation of extensional faults. The modelling results have been fundamentally controlled by the vertical load gradient imposed by the geometry of the tectonic wedges, their pre-shortening strength profiles and by the inherited basin architecture. Basin inversion is linked to the layer-parallel compaction related with slipping along the basal detachment. This work has been inspired by the recent recognition of basin inversion beneath the Alpine-Carpathian fold-and-thrust belt in the Höflein High, a major deeply buried gas field. Results are compared to this structure and other inverted basins of the Alps. This work is in under review in the journal *Tectonophysics.*

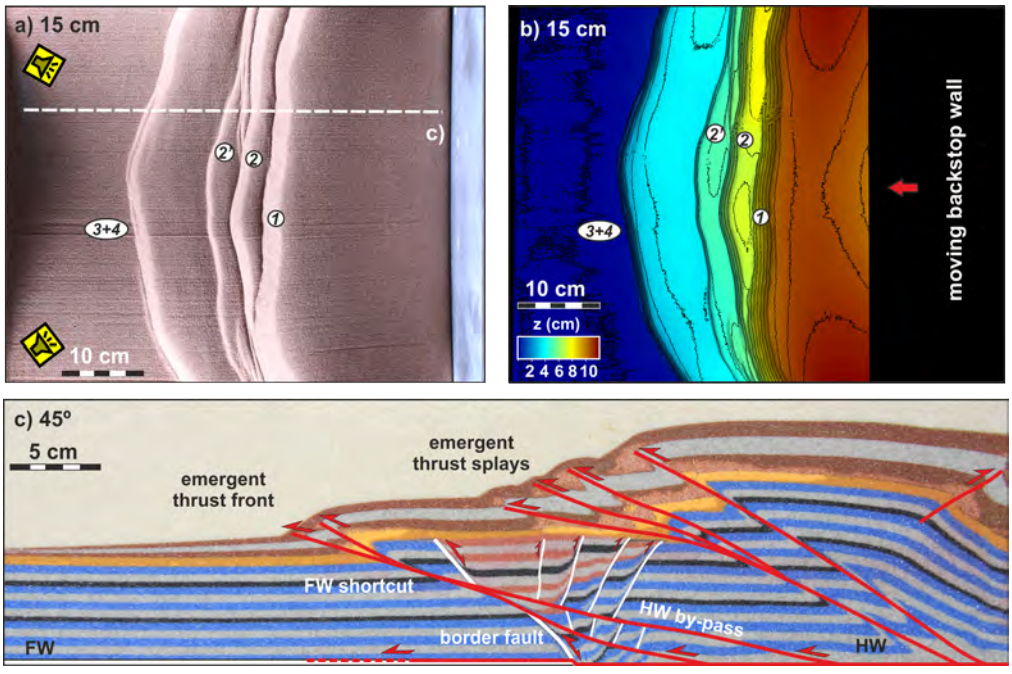

Figure 1. Summary of model 5. A) Top view after 15cm of shortening. B) Topography scan after 15 cm of shortening. C) Cross section (see A for location) illustrating the inverted rift basin within the tectonic wedge and associated structural styles.

C Modelització numérica de cossos i procesos geològics

Numerical modelling of geological bodies and processes

geomodels
institut de recerca

Numerical modelling of syntectonic subaqueous sedimentation: the effect of normal faulting and a relay ramp on sediment dispersal.

O. Gratacós[1], A. Carmona[1], R. Clavera-Gispert[1], J.A. Muñoz[1] y S. Hardy[1]

GEOMODELS Research Institute, RISKNAT Research Group,
Department of Dynamic of the Earth and the Ocean
University of Barcelona

Relay ramps and transfer fault zones are common in extensional settings and play a significant role in sediment dispersal. Unlike for subaerial settings, the impact of subaqueous relay ramps on sediment dispersal is less studied. In these cases, numerical approximations could be a good approach to understand the syntectonic sedimentation. Considering this, a novel numerical model (which merges tectonic deformation and sedimentation) is used to study the sedimentary infill related to a two-overlapped extensional faults and the related transfer zone. To perform the test study, three main parameters were considered: (1) fault configuration; (2) fault displacement rates; and (3) source area location. Our results, allow us to conclude that, although the coarse and medium-grained sediments shows not only differences perpendicular to faults, but also differences parallel to faults (conditioned by the left stepped fault geometry). Although, the dominant grain-size trends are linear and parallel to faults without reflecting the fault configuration. Furthermore, the relationship between the relay ramp dip and the sediment transport direction, strongly influences the grain-size arrangement. Complex stratigraphic architecture could be obtained with apparent stratigraphic beds terminations and erroneous conclusions could be deduced in those cases where lithological information is poor or inexistent.

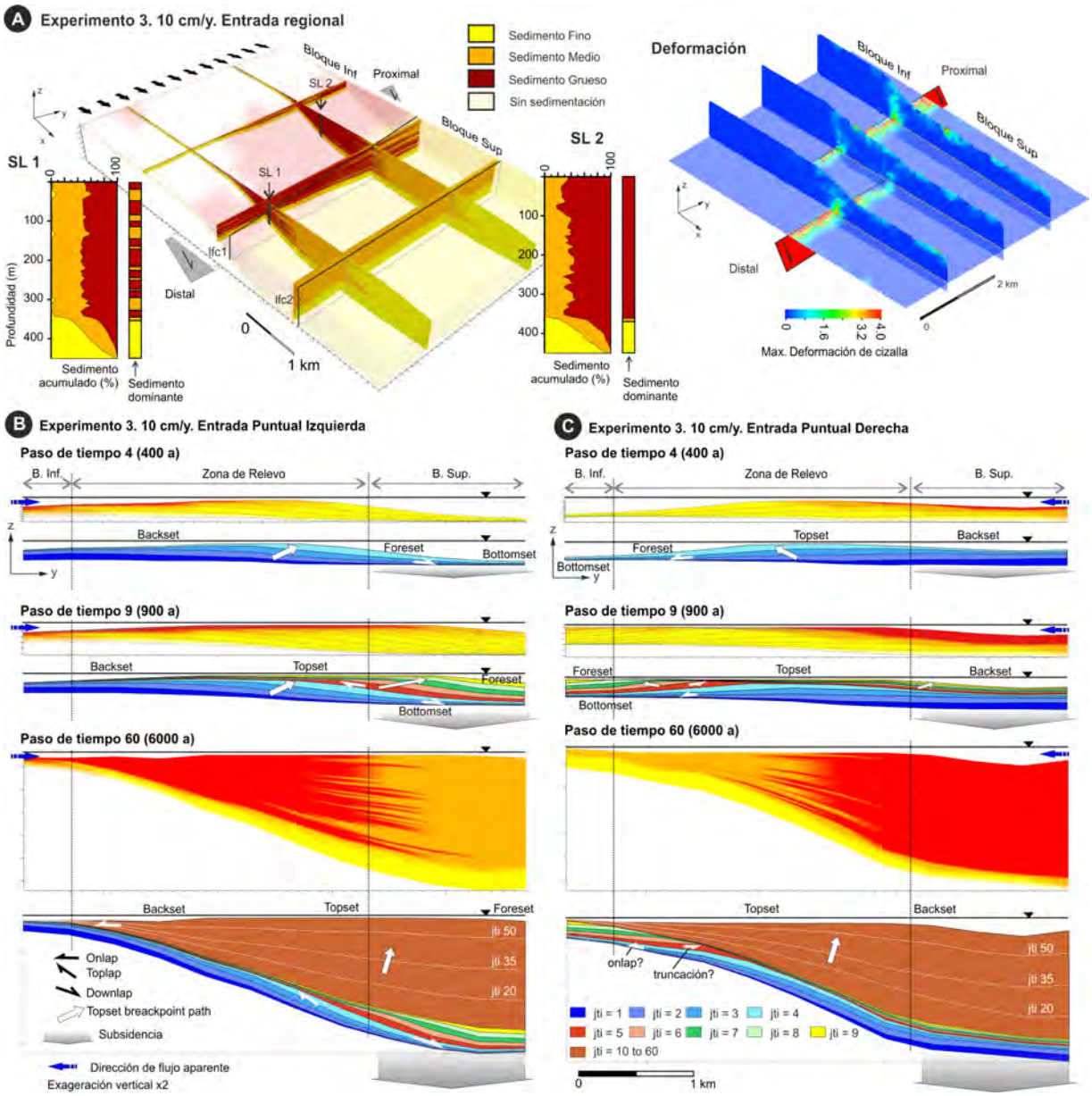

Output results for the syntectonic sedimentation and the pretectonic deformation taking into account: A. two normal faults an a relay ramp. B. Cross-section following the relay ramp and considering a left source area. C. Cross-section following the relay ramp and considering a right source area.

The Effect of syntectonic sedimentation on fold geometry: Insights from numerical modelling

O. Gratacós[1], A. Carmona[1], Miguel López[1], Josep Anton Muñoz[1], Roger Clavera-Gispert[1], Pau Arbues[1], Stuart Hardy[1,2]

GEOMODELS Research Institute, RISKNAT Research Group,
Department of Dynamic of the Earth and the Ocean
University of Barcelona

Introduction

Syntectonic sediments have been widely studied to decipher the kinematic evolution of different geological systems and structures. For example, the control of the syntectonic sedimentation on fold-and-thrust belts (for both geometry and thrusting sequence). Nonetheless, the control of these sediments on the structural style or on fold geometry is less studied. It is difficult to derive directly from the geological record as we can only observe the final stage. In this sense, in this contribution a numerical model is used to study the effect of syntectonic sedimentation on fold geometry. Specifically related to a delta progradation surrounded by two growing folds. The study is performed using a numerical model (Carmona et. al 2010) that merges deformation (DE code, Hardy et al. 2009) and sedimentation (SFM code, Gratacós et al., 2009).

Initial set-up and boundary conditions

The initial DE model (figure 1A) is defined with initial cohesion and a detachment level in the base of the model (with low cohesion). The model is tilted 1.6 degrees with an increasing bathymetry in ***y*** direction ranging from 51 to 861 m. Different shortening rates are defined perpendicular to ***y***-axis from right to left, corresponding to fold growth rates of 0.1, 0.5, 1 and 2 mm/y. At the bottom, two velocity discontinuities (figure 1B) perpendicular to the shortening direction are defined acting as breaking points, which unleash in the formation of two folds. Total simulation time is 800ky. To this initial configuration, three different cases are considered, one without sediments, and two with three different clastic sediments types and two different sea-level rise, 0.25mm/y and 0.5mm/y. The incoming water and sediment points are located in the boundary with lower bathymetry (figure 1A)

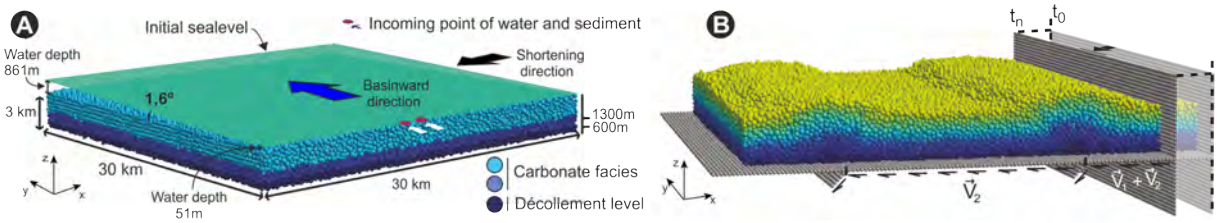

*Figure 1: A - Initial set-up: the 3D DEM model colored by facies, tilted 1,6º. The reddish dots indicate the incoming point for water and sediment. B - DEM after **n** years illustrating the shortening direction and the discontinuities in the bottom. DEM is colored by layers, which are just for a visualization purpose, and they does not attend to any mechanical property.*

Results and conclusions

Without sedimentation: two detachment folds with box-fold geometry are obtained over the discontinuities defined at the bottom of the model (figure 2A).

With sedimentation and a sea-level rise of 0.25m/y (figure 2B): the deposition of the new materials is conditioning clearly the geometry of the left fold, showing a left-

vergent asymmetric wide fold. Moreover, the strain suggests that the left fold is passing from a detachment fold to a fault propagation fold basinwards, being clearer where sediment settled is higher.

With sedimentation and a sea-level rise of 0,5 mm/y (figure 2C): the control of the syntectonic unit over the left fold geometry it is also appreciated and more evident as a consequence of the accommodation space increase, e.g. the more proximal cross-section a-a' now is showing a fold-propagation fold instead of a detachment fold. Furthermore, the right fold now is showing a right-vergent asymmetric geometry (cross-section b-b' figure 2C)..

Summing up, the syntectonic sedimentation is controlling the fold style and the fold geometry. As a consequence, the inner syncline and the related sedimentary basin is also changing in transversal and longitudinal direction, being wider with a syntectonic sedimentation and a higher sea-level rise.

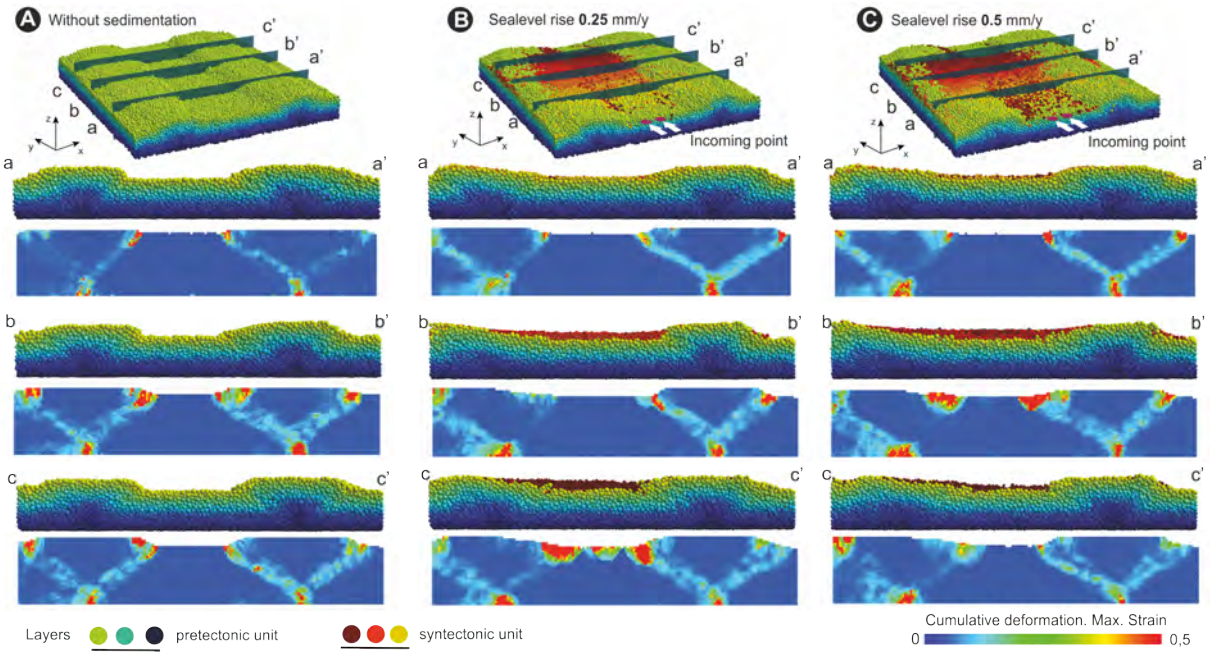

Figure 2- Cross-sections from the DE model for each sample experiment considering a fold growth rate of 1mm/y: without sediments (A) and two with syntectonic sedimentation considering two different sealevel rise, 0,25mm/y (B) and 0,5mm/y (C). Pretectonic unit is colored by layers,. Yellow and reddish layers represent the syntectonic sediments added by SFM. The maximum strain for the pretectonic unit is also computed using the SSPX program.

References

Carmona A., Clavera-Gispert R., Gratacós O., Hardy S., 2010. Modelling syntectonic sedimentation: combining a discrete element model of tectonic deformation and a process-based sedimentary model in 3D. Mathematical Geoscience, 42, 519-534

Gratacós O., Bitzer K., Cabrera L., Roca E., 2009. SIMSAFADIM-CLASTIC: a new approach to mathematical 3D forward simulation modelling for clastic and carbonate sedimentation. Geologica Acta, 7, 311-322

Hardy S., McClay K., Muñoz J.A., 2009. Deformation and fault activity in space and time in high-resolution numerical models of doubly vergent thrust wedges. *Marine and Petroleum Geology*, 26, 232-248

D Models d'alta resolució i sensors remot

High Resolution Models and remote sensing

geomodels
institut de recerca

Terrestrial laser scanner
Scanning campaigns 2016

García Sellés, D.

GEOMODELS Research Institute, RISKNAT Research Group,
Department of Dynamic of the Earth and the Ocean
University of Barcelona

- Caspe (Huesca): Scanning of three alluvial fan outcrops in Caspe; Stratigraphic examples.Tasks of Scanning, positioning, alignment and assist to processing data. I.P.: Miguel Garces.

- Montserrat (Barcelona): 8 Monitoring scanning. I.P.: Joan Manuel Vilaplana. U.B. and Emma Suriñach

- Puigcercos (Lleida): 2 Monitoring scanning. I.P.: Emma Suriñach. U.B.

- Rialp (Lleida): 1 Monitoring scanning. I.P.: Emma Suriñach. U.B.

Hexacopter
Flying Campaigns 2016

García Sellés, D.

GEOMODELS Research Institute, RISKNAT Research Group,
Department of Dynamic of the Earth and the Ocean
University of Barcelona

- Elda (Alacant): 2 Flying for image acquisition of the basin around Elda. Minibasin outcrop. Creating Orthoimage. I.P.: Eduard Roca.

- Puigcercos (Lleida): 2 Test flying for aerial image acquisition, software and hexacopter calibration.

- St. Corneli Anticline (Lleida): 2 Flying for image acquisition of the basin around the back limb of St Corneli anticline. Creating Orthoimage. I.P.: Josep Anton Muñoz.

Fracture System in an Andesite Lava Flow from Terrestrial Laser Scanning, Ruuapehu Volcano: Towards Reservoir Models

[1]Massiot, C., [2]Nicol, A., [1]Townend, J., [3]McNamara, D., [4]Garcia-Sellés D., [1]Conway, C., [3]Archibald, G.

[1]Victoria University of Wellington, New Zealand.
[2]University of Canterbury, New Zealand.
[3]GNS Science,New Zealand.
[4]University of Barcelona, Geomodels Research Institute, Spain.

Introduction

Numerous geothermal, groundwater, CO_2 storage, radioactive storage, and more recently hydrocarbons reservoirs are hosted in lava flows (Bertani, 2012). In these reservoirs, fluid flow is inferred to be controlled by fractures and faults, but the identication of permeable fracture networks often remains problematic. Fracture models can help with the management of resources by predicting preferentia low pathways. Discrete fracture network (DFN) approach models fluid flow processes through rock masses via a series of connected fractures. These models rely on the input of fracture geometries (orientation, size, frequency, aperture), typically estimated from 1D scanlines in boreholes and outcrops, or 2D window samplings in outcrops. Terrestrial laser scanner (TLS) datasets allow a comprehensive fracture analysis of an entire outcrop in 3D, which is therefore less subject to observation biases than scanlines or window surveys of limited sizes (though specific bias have to be considered), and supports more reliable statistics on fracture geometries. The delineation of fractures from TLS has gained interest, e.g. for slope stability analysis, fracture density statistics in sedimentary and plutonic formations, and input for reservoir simulation model or DFN models in the hydrocarbon industry. The large fracture datasets obtained from TLS sometimes questions empirical relationships defined from scanlines only and are more appropriate for reservoir analogue studies. TLS has been applied to volcanological settings: to monitor eruptions, reconstructing volcanic facies in 3D, characterising flow roughness and lava flow sequence or characterising dyke swarm geometries. The characterisation of fracture networks in volcanic products from TLS has recently been used to evaluate slope stability in rhyolitic ignimbrite (Agliardi et al., 2013) and as analogue to basalt lava-ow hosted reservoirs for CO_2 sequestration projects , but not in andesite lavas.
The Rotokawa geothermal reservoir located in the Taupo Volcanic Zone (TVZ), New Zealand, is an example of andesite-hosted geothermal reservoir, where hydrothermally altered andesites have low porosity (4.4-16.3%), high strength (unconfined compressive strength -UCS- of 70-211 MPa) and fluid flow is structurally controlled.
Several approaches have been developed to extract fractures from a TLS point cloud, with various computational strategies and degree of user interaction. Fracture traces or faces can be delineated manually on photographs draped over the point cloud before or after draping over the point cloud (called digital outcrop model, DOM, Buckley et al. (2008)). Fully- or semi-automatic detection of fracture faces typically depend on the a-priori definition of fracture sets of specic orientations and define patches of finite extents, with or without meshing of the point cloud (García-Sellés et al. (2011)).

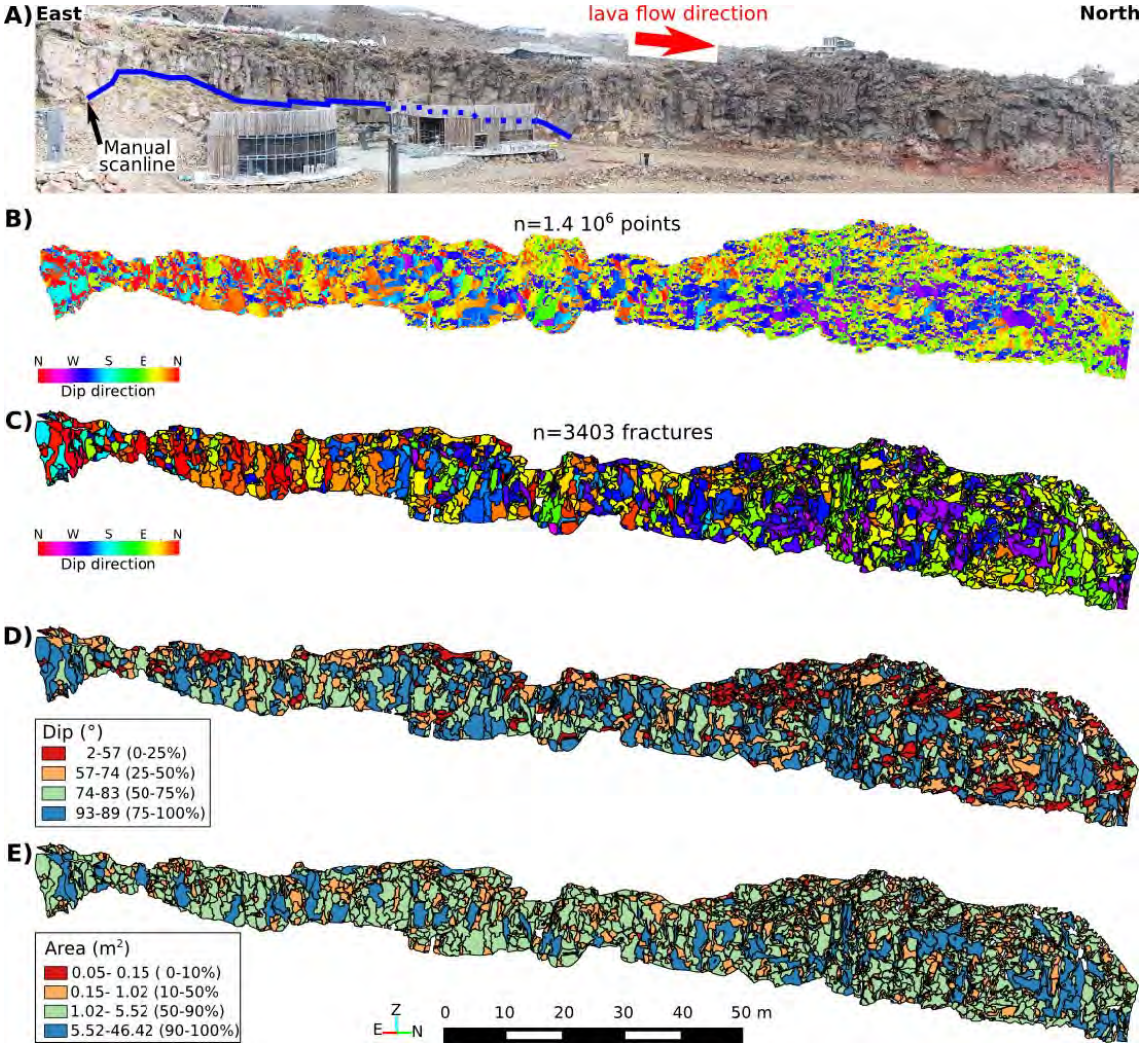

Figure 1. Fracture delineation of the Happy Valley TLS cloud. A) Gigapan panoramic picture composed of 430 individual photographs with the trace of the manual scanline (solid/dashed blue line) and the lava flow direction. B) Point cloud zone used for the fracture delineation and resampled every 4 cm, coloured by the local dip direction. C) Fracture delineated from the FACET plugin, coloured by dip direction. D) Fracture dip magnitude. E) Fracture area. Note the non-regular ranges for the dip magnitude and area scales; the percentage of fractures falling into each category is indicated in brackets. C-E: 3D fractures projected onto a NW-SE striking, vertical plane. Each colour patch represents a single fracture.

The morphology of fractures in lava flows have been extensively studied in basalts (e.g., Degraff and Aydin (1987)) and in andesites. The most prominent fracture type in the flow interior are column-forming joints formed by the thermal stress caused by the cooling of the flow by water or atmosphere from the margins to the interior of the ow (Degraff and Aydin, 1987). Column-forming fractures form when the tensile strength of the lava is exceeded by the thermal contraction and propagate perpendicular to the maximum thermal gradient (Degraff and Aydin, 1987).

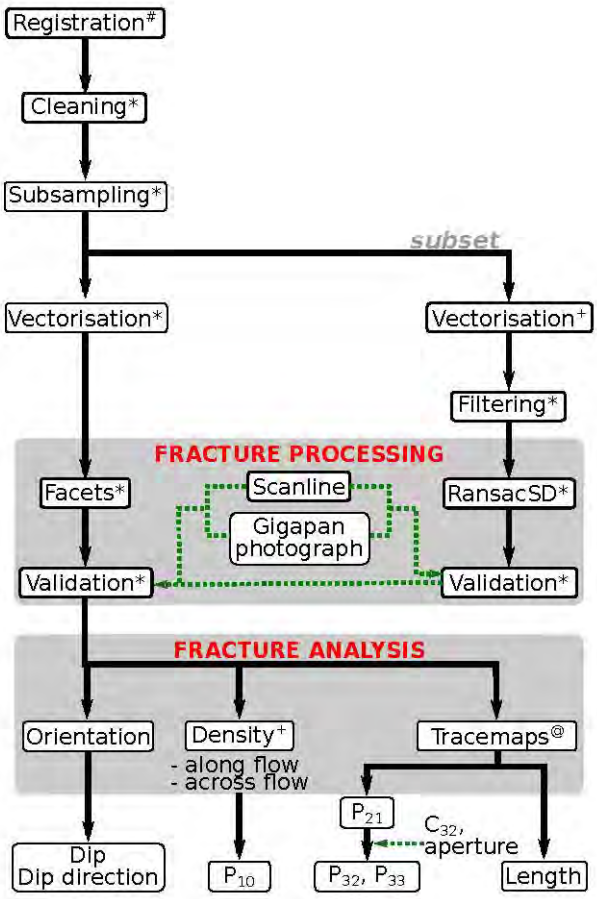

Figure 2. Flowchart of the TLS data processing and fracture using a combination of Riegl RiscanPro (#), Project120 (+), CloudCompare v2.7.0 (*) software with the RansacSD (Schnabel et al., 2007) and FACETS plugin (T. Dewez, in prep.) and Fracman software (@).

In this paper, we aim to provide constraints on DFN models of the fracture system in an andesitic lava ow based on the analysis of a TLS dataset. We test the applicability of a recently developed methodology to extract fractures from a TLS point cloud which is based solely on the shape of the outcrop. We discuss the implications of the fracture geometries obtained from the TLS dataset for the permeability in andesite-hosted reservoirs, using synthetic DFN models.

TLS Processing Workow

Fractures are extracted from the TLS dataset solely based on the shape of the 3D point cloud. Fractures are defined by portions of the 3D point cloud which are approximatively coplanar. The resulting fracture dataset contains the geometry of the planes forming the outcrop: the XYZ coordinates in the centre of each plane, together with the orientation and size of the locally fitted plane. Figure 2 presents the processing workow of the TLS to extract fracture parameters. The first step consist of merging and aligning different scans of a same outcrop using the GPS measurements (Buckley et al., 2008) in the RiScanPro software. At Happy Valley, the merged point cloud has >6.3 million points. The merging was adjusted with a plane patch filter algorithm resulting in a precision of 2 cm. Few blind areas remain in the final dataset. Zones of the point cloud that captured vegetation or buildings were manually deleted in the CloudCompare v.2.7 software (CloudCompare, 2016). Finally, the merged scan was sub-sampled to ~1.4 million points with a 4 cm regular spacing which provides the support to extract fracture planes (Figure 1). The extraction of fractures from the TLS

point cloud is performed using the Facets plugin in CloudCompare. The first step, “vectorisation" consist of calculating on each point the normal to the best-fitting plane of a local neighbourhood with a local radius of 0.15m (Figure 1B). The second step is the Facets plugin it-self with the fast marching method. Tests with the kd-tree were not satisfying with this dataset. The Facets plugin generates a series of point sets on which a polygon is automatically fitted. The orientation (dip, dip direction) and size (area, length horizontally and vertically of the bounding rectangle) is calculated for each polygon (Figures 1C-E). The choice of parameters and validation of the fracture processing with the Facet plugin is done in three ways. Firstly, the extent and orientation of fractures processed from the Facet plugin are compared to the manual scanline where available; secondly, the extent of the processed fractures are compared to the Gigapan panoramic photographs over the whole interval; and thirdly, the delineation of fractures is compared to the results of the shape detection algorithm RansacSD plugin.

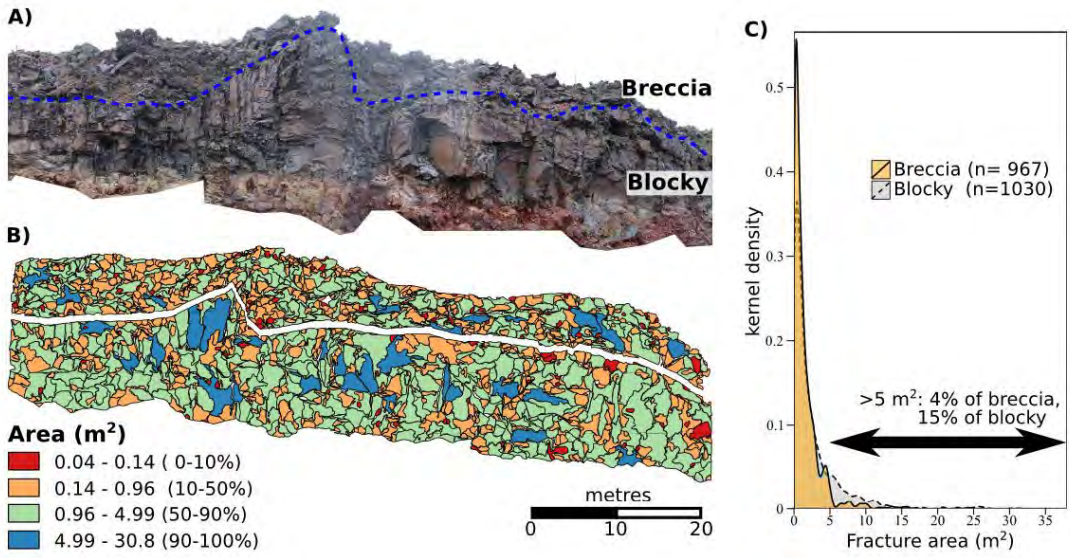

Figure 3. Variation of fracture area between the blocky and the upper brecciated zone in the northern end of the outcrop. A) Panoramic photograph. B) TLS-processed fractures coloured by fracture area. The brecciated and blocky zones are separated by a white band to help visualisation. C) Kernel density plot of the fracture area in the breccia and blocky zones.

The RansacSD method occurs in several steps: (1) vectorisation in Project120 software (García-Sellés et al., 2011) to calculate the normals to each point and compute local geometrical parameters; (2) filtering out the points of low planarity and high collinearity which correspond to fracture edges in CloudCompare; (3) run the RansacSD algorithm looking for planes and spheres, which segments the point cloud into a series of subsets of points; and (4) post-processing: manually check each subset, and subdivide them as necessary to match scanline and Gigapan observations. Similarly to Ferrero et al. (2009), the filtering of fracture edges (steps 1-2) was necessary to obtain good results in RansacSD; without filtering the fracture edges, RansacSD generates very large fractures which requires significantly more post-processing, including removing the shape generated along the fracture edges. The parameters used for the RansacSD step were iteratively selected by comparing the results to the scanline data and the Gigapan panoramas. The RansacSD method has one major advantage compared to Facets: it detects spheres as well as planes, which allows the detection of curved fractures common in the Happy Valley outcrop. However, the additional steps of filtering fracture edges before running RansacSD, checking and modifying each subset individually, and the plane fitting to each point

subset, makes it time-consuming. On the other hand, the Facets method does not allow the de-lineation of curved fractures, but is significantly faster and provides good results. The regular resampling of the point cloud prior to the fracture extraction ensures that the processing parameters are constant throughout the point cloud. Based on visual checks of the processed fractures, a minimum of 25 points per fracture was imposed during the Facets processing to limit the false detection of noiseinstead of fractures. This threshold, equivalent to a fracture area of 0.04m2, is similar to those

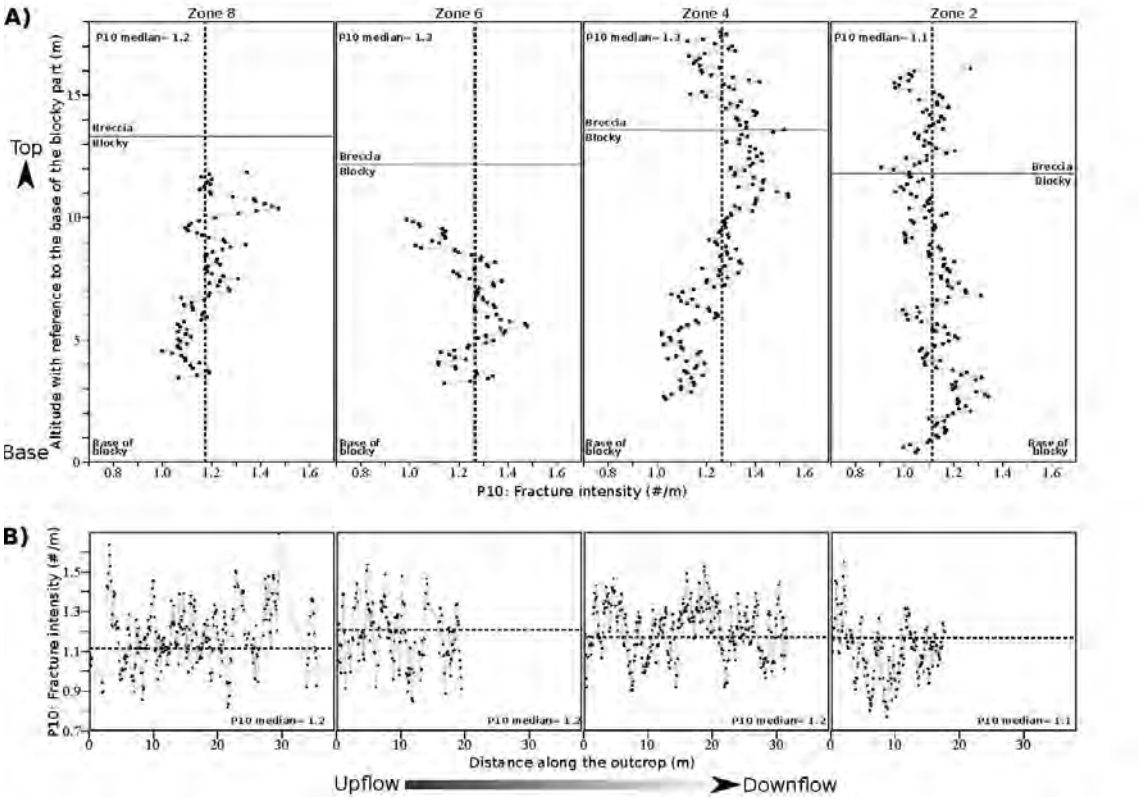

Figure 4. Linear fracture intensity (P10) along series of scanlines in different zones. A) Series of sub-horizontal scanlines measured every 10 cm along a sub-vertical axis, plotted with reference to the base of the blocky interior. B) Series of sub-vertical scanlines measured every 10 cm along a sub-horizontal axis, plotted with reference to the start of the series of the scanline, from north (up-flow) to south (down-flow).

recommended by Sturzenegger and Stead (2009a). Overall, 3403 fractures were delineated from the TLS point cloud covering an area ~3090m^2.

Linear Fracture Intensity: P_{10}

The P_{10} measured along series of virtual scanlines intersecting the TLS-processed dataset shows that the median P_{10} is 1.1 to 1.3m^{-1} across the whole outcrop, with local variations between 0.7-1.7m^{-1} (Figure 4). There is no clear variations between the P_{10} value and the location within the lava ow from the base to the top of the blocky part of the outcrop, nor in the breccia which is intersected in zones 2 and 4 (Figure 4A). The increase and decrease of the P_{10} in the middle of the blocky part of zone 6 is not reproduced in the other outcrops; measurements in zone 6 may not be as reliable as in the other zones because the scanline length is shorter. There is no clear variations of P_{10} between the up-ow and down-ow parts of the outcrop, where sub-vertical scanlines sample the whole thickness of the outcrop (Figure 4B) The P_{10} of the column-bounding fractures measured along the manual scanline is 1.92m^{-1}, which is slightly higher than

the P_{10} obtained from the TLS-processed dataset and reect the additional sampling of small fractures.

Areal (P_{21}) and Volumetric (P_{32}) Intensity, Fracture Porosity (P_{33})

The P_{21} of the steeply-dipping column-bounding fractures for the blocky zone of this outcrop is estimated to be ~1.8-2.0m^{-1}. The P_{21} evaluated directly from the surface of the outcrop ranges between 1.78-1.97m^{-1} in the blocky parts of the outcrop. P_{21} in the breccia zone of zones 2-4 is 2.56m^{-1} which reects the smaller size of fractures tan in the blocky region, and hence the higher total fracture edge length. The P_{21} evaluated on the planes parallel to the breccia base has similar values (1.7-2.2m^{-1}) and does not show any clear correlation to the position within the outcrop. The P_{21} evaluated from planes perpendicular to the breccia base are less constrained than those measured from planes parallel to the breccia base because of the lower number of fractures intersected, but have a similar range of values and the same median. The two lowest values, in zones 5 to 8, are measured in the thinnest part of the outcrop (10m high) and thus the least reliable. The evaluation of the C_{32} parameter relies on the assumption that fracture sets define clusters with a mean orientation. In this outcrop, there is a uniform distribution of dip directions, and hence no cluster. Although the dip magnitude distribution is not uniform, we use the C_{32} value of 1.27 applicable to the isotropic case (Wang, 2005) as an approximation. The resulting P_{32} is 2.3-2.5m^{-1}. A few manual scanline measurements show that the fracture aperture is _5 mm. The fracture aperture is not measurable from the terrestrial laser scanner as it is smaller than the resolution of the points cloud. Following these assumptions on C_{32} and aperture, the P_{33} of steeply dipping column-bounding fractures ranges between 0.011-0.013, equivalent to 1.1-1.3% fracture porosity.

Conclusions

The acquisition, processing and analysis of the TLS point cloud outlined in this paper are suitable to study the fracture system of blocky lava ows formed during the emplacement and cooling of the lava. The algorithm extracting fracture planes is semi-automatic and allows a uniform processing of the dataset across a large outcrop, while requiring suficient user input and calibration from other measurements to ensure its validity. The Happy Valley lava ow outcrop studied here is representative of young, 5{20m thick lava flow of andesitic composition which owed over a gently dipping paleo-topography. The fracture system is composed of column-forming fracture which form the blocky part of the outcrop, platy fractures which increase locally the fracture density and have efects on the propagation of column-forming fractures, and auto-breccias. Column-forming fractures have a uniform strike and are either gently or steeply dipping. The length of steeply-dipping column-forming fractures, which is well sampled by the TLS, is modelled as a negative exponential distribution which reects either a feedback process during fracture propagation, or inherent scales of the system either linked to the size of the lava flow, cooling rate, or feedback processes between neighbouring fractures. The areal and volumetric fracture intensity reveal a well-connected system within the blocky region, at least partially connected to the breccias. The implications of the fracture system on reservoir permeability hosted in andesitic lava ows are discussed. Discrete fracture network models generated from parameters obtained from the TLS processing and analysis provide results in agreement with the conceptual model.

References

Buckley, S. J., J. Howell, H. Enge, and T. Kurz (2008), Terrestrial laser scanning in geology: data acquisition, processing and accuracy considerations, Journal of the Geological Society, 165(3), 625-638.

Degraff, J. M., and A. Aydin (1987), Surface morphology of columnar joints and its signi_cance to mechanics and direction of joint growth, Geological Society of America Bulletin, 99(5), 605..

Ferrero, A. M., G. Forlani, R. Roncella, and H. I. Voyat (2009), Advanced geostructural survey methods applied to rock mass characterization, Rock Mechanics and Rock Engineering, 42(4), 631-665.

García-Sellés, D., O. Falivene, P. Arbués, O. Gratacos, S. Tavani, and J. Muñoz (2011), Supervised identification and reconstruction of near-planar geological surfaces from terrestrial laser scanning, Computers & Geosciences, 37(10), 1584-1594.

Sturzenegger, M., D. Stead (2009), Close-range terrestrial digital photogrammetry and terrestrial laser scanning for discontinuity characterization on rock cuts, Engineering Geology,106(3-4), 163-182.

Characterization of geological structures with technical improvements in acquisition and processing

[1]García-Sellés, D., [1]Gratacós, O., [1]Muñoz, J. A., [2]Sarmiento, S.

[1]GEOMODELS Research Institute. Faculty of Earth Sciences. University of Barcelona, 08028 Spain
[2] REPSOL 245 Technology Forest Blvd, The Woodlands, TX, USA, TX 77381

The characterization of fracture systems comprises, on one hand, the individual characterization of fractures by their orientation (strike and dip), type, length, height, roughness, aperture and in-filling, and the other their relationship expressed as spacing between fractures, the coefficient of variation (Gillespie, 1999), parameters of abundance (Dershowitz and Herda, 1992) and fracture length and height distribution among the most used classical parameters. Fracture systems characterization is commonly done by fracture measurements along scan-lines in layered rock units and often confined in discrete horizons defined by their mechanical properties (Gross, 1993).
In last decade, improvements in software and hardware referred to Terrestrial Laser Scanner or photogrammetry data have become widely used with the aim to complement the existent techniques of fracture characterization. In this line, our group have developed algorithms to measure along the virtual scan-lines the properties of modelled fracture system (Santana, 2012). Fracture intensity along the outcrop is repeatedly measured in parallel with centimetric vertical distances to represent the fracture stratigraphy (Laubach, 2009). In consequence, is possible subdivide the rock mass according its fracture stratigraphy behaviour. The identified units are surveyed again with new virtual scan-lines and window samples to characterize geometrically the outcrop.

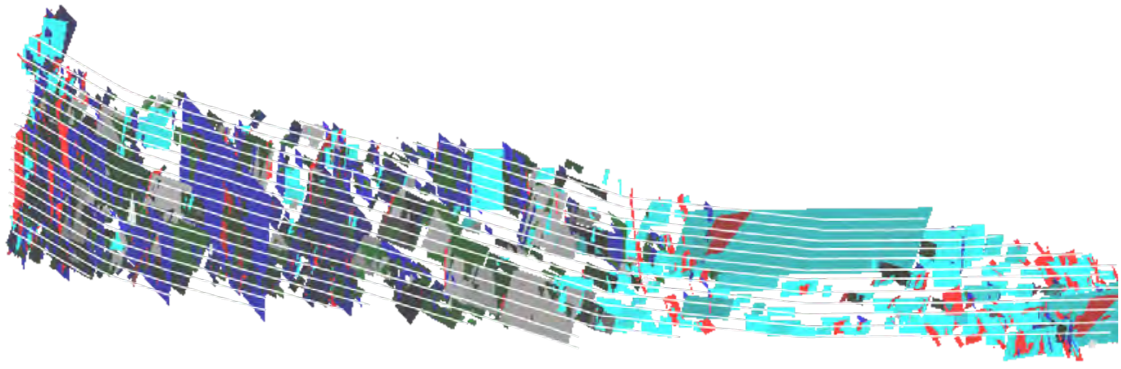

Figure 1: Image of multiple scan-lines along the fracture model to elaborate Fracture Stratigraphy.

Abra del Condor (Bolivia) is a reservoir analogue outcrop placed at the SubAndean range, with an extension of 1.7 km of tight sandstones in 350 m sequence of Huamampampa formation. The Backlimb position offers an excellent opportunity to identify the different mechanical responses and characterize it with the new developed tool.

Acknowledgements

This research is supported by Geomodels Research Institute, and financed by the projects CGL2014-54118-C2-1-R (SALTECRES), CGL2013-40828-R (CHARMA) from the Spanish Ministry of Science and Technology.

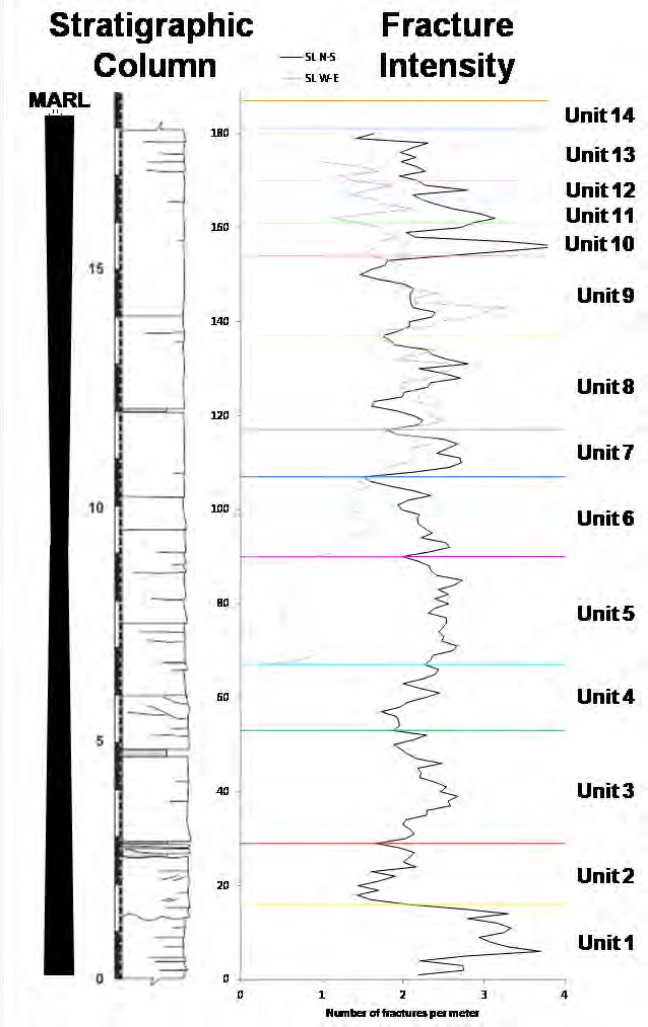

***Figure 2**. Example of correlation between fracture stratigraphy and stratigraphic column.*

References

Dershowitz, W. S. and Herda H. H. (1992). Interpretation of fracture spacing and intensity. In: Tillerson, J. R. and Waversik, W. R. (eds) *Rock Mechanics*. Balkema, Rotterdam, 757–766.

Gillespie, P. A., Johnston, J. D., Loriga, M. A., McCaffrey, K. L.W., Walsh, L. L. & Watterson, L. (1999). Influence of layering on vein systematics in line samples. In: McCaffrey, K.J.W., Lonergan, L., Wilkinson, J.J. (Eds.), Fractures, Fluid Flow and Mineralization. *Geological Society, London, Special Publication* 155, pp. 35-56.

Gross, M. R. (1993). The origin and spacing of cross joints: examples from the Monterey Formation, Santa Barbara coastline, California. *Journal of Structural Geology,* 15: 737-751.

Laubach, S. E., Olson, J. E. and Gross, M. E. (2009). Mechanical and fracture stratigraphy. *AAPG Bulletin*, 93, 11: 1413-1426.

Santana, D., Corominas, J., Mavrouli, O. & García-Sellés, D. (2012). Magnitude-frequency relation for rockfall scars using a Terrestrial Laser Scanner. *Engineering Geology,* 145-146: 50–64.

Geometrical characterization of fracture systems in rock mass by means of Terrestrial Laser Scanner

García-Sellés, D., Granado, P., Gratacos, O., Muñoz, J.A.

Institut de Recerca Geomodels, Departament de Geodinàmica i Geofísica, Facultat de Geologia, Universitat de Barcelona, Martí i Franquès s/n, 08028 Barcelona, Spain

Objectives

The measurement of individual geometrical characteristics on each fracture is a common practice among geologists and engineers when defining fracture systems in rock mass. This procedure is a slow field task generally truncated by the inaccessibility of the outcrop. Here, we propose a Terrestrial Laser Scanner (TLS) data processing technique to increase the fracture system characterization quality by means of a new set of detection and measurement algorithms followed by statistical procedures. These algorithms aim to characterize the geometry of fracture systems to be used in Discrete Fracture Networks (DFNs) construction.

Procedures

TLS data needs to be acquired with enough resolution as to capture fracture surfaces. The developed algorithms measure orientation, position and size (i.e., length and height) of fractures geometrically simplified by planar structures. The relationship between these characteristics are hereafter used to obtain a series of geological and engineering parameters according to the position, quantity or size of fractures within previously- defined Mechanical Units (M.U.). Fracture spacing, fracture impedance, number of fractures, P_{10}, P_{11}, P_{20}, P_{21}, P_{22}, P_{32}, Fracture Spacing Ratio (FSR) and Fracture Spacing Index (FSI) can be deducted. Finally, statistical procedures are applied to the results.

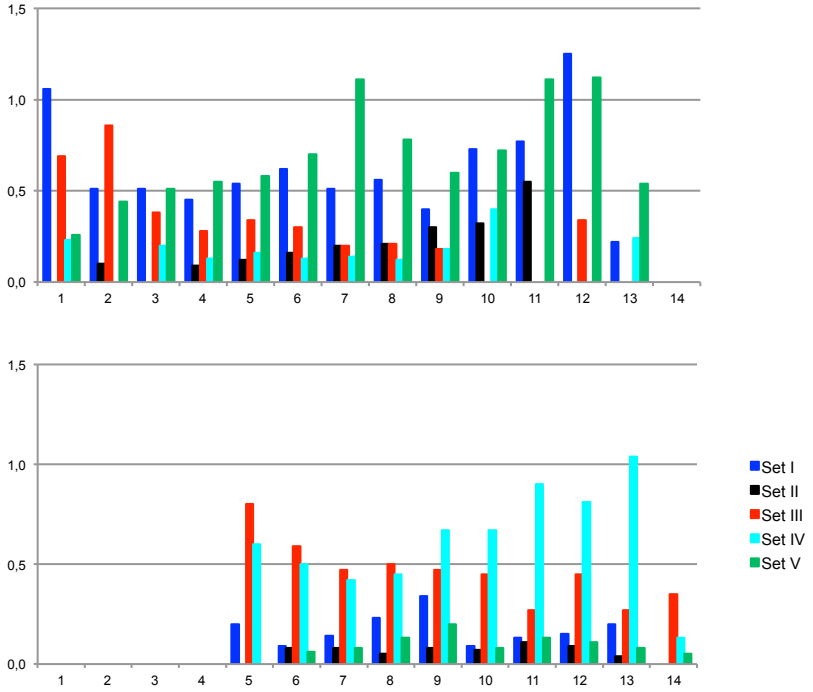

Figure 1. Parameter P32C23 calculated for each Mechanical unit and fracture sets, in the outcrop. Upper graphic correspond to the N-S outcrop orientation and the lower to the NW-SE outcrop orientation.

Results

The methodology has been applied for several case studies in selected outcrops from the Spanish Pyrenees represented by fractured limestones within macro-scale thrust-related anticlines. The outcrops characterization was used to modelling reservoir analogues. The results are summarised in a datasheet with graphical information arranged by fracture set and M. U.

Conclusions

Mechanical Units

Identified fracture surfaces are reconstructed and classified by a supervised process. Fracture system characterization algorithms used a non-supervised process. These automatic algorithms provide a rapid way to characterize the fracture systems geometry in rock mass; however, the previous tasks to define fracture sets or supervise the reconstructed fractures increase the time consuming. Despite the careful previous tasks, the improvements achieved increasing the number of statistical data and the surveyed area are of great use to characterize fracture system geometry.

Fracture analog of the subandean Devonian of southern Bolivia: LIDAR applied to abra del condor

[1]García-Sellés, D., [2]Sarmiento, S. [1]Gratacós, O., [1]Granado, P., [1]Carrera, N., [2]Lakshmikantha, M. R., [3]Cordova, J. C., [1]Muñoz, J. A.,

[1]GEOMODELS Research Institute. Faculty of Earth Sciences. University of Barcelona, 08028 Spain
[2] REPSOL 245 Technology Forest Blvd, The Woodlands, TX, USA, TX 77381

[3] REPSOL Bolivia

Introduction

Outcrops of the Devonian Huamampampa Formation at the Abra del Condor area offers the opportunity to study a natural fractured reservoir analog, which plays an important role in the modeling of the hydrocarbons fields of the Subandean range of Argentina and Bolivia. The Abra del Condor area is located 60 km (40 mi) west of productive reservoirs and previous work shows that in these outcrops for the most part near-surface fractures can be identified and discounted and that the properties and fracture attributes in outcrop and subsurface are close enough matches to make the outcrops excellent analogs for the subsurface (Iñigo, 2009). The exposed Devonian Huamampampa Formation is composed by quartzitic sandstones with primary permeability less than 2% (Moretti et al., 2002, Iñigo 2009) but it is affected by natural fractures systems that enhance the effective permeability. Therefore, the understanding of natural fractures is a key factor to model the Subandean range reservoirs and delineate high productivity areas.

Natural fractures in rock masses are produced when the rock fail under stress conditions, creating a surface of failure oriented with respect to the principal stress directions. Fractures are referred as joints, veins, dykes or small faults.

This study is based on outcrops corresponding to Abra del Condor Anticline which was formed under a fold and thrust belt tectonic setting. Fractured sandstones of the Huamampampa Formation are exposed dozens of kilometers along the backlimb of the structure in small cliffs and have been studied previously by various authors. Florez-Niño et al. (2005) described and proposed an interpretative model of faults and fractures, Iñigo (2009) and Iñigo et al. (2012) focused their work in the characterization of microfracture apertures. This study is aimed in describing quantitatively the fracture pattern of the Abra del Condor Anticline, in an area of about 1.7 km long by 1 km wide. This study has been accomplished by means of LIght Detection And Range (LIDAR) and its applicability for fracture characterization. High resolution DOM detects fracture surfaces with enough level of detail to capture and reconstruct them digitally, keeping most of their geometrical characteristics (García-Sellés et al., 2011).

The presented workflow is related to the detection, measurement and modeling discontinuities and fractures. State of the art methods are applied in this study, based on recent developments in TLS fracture measurements (García-Sellés et al., 2016). As a result, a virtual fracture model is produced and used to characterize the spatial distribution of fractures in rock masses at Abra del Condor outcrop.

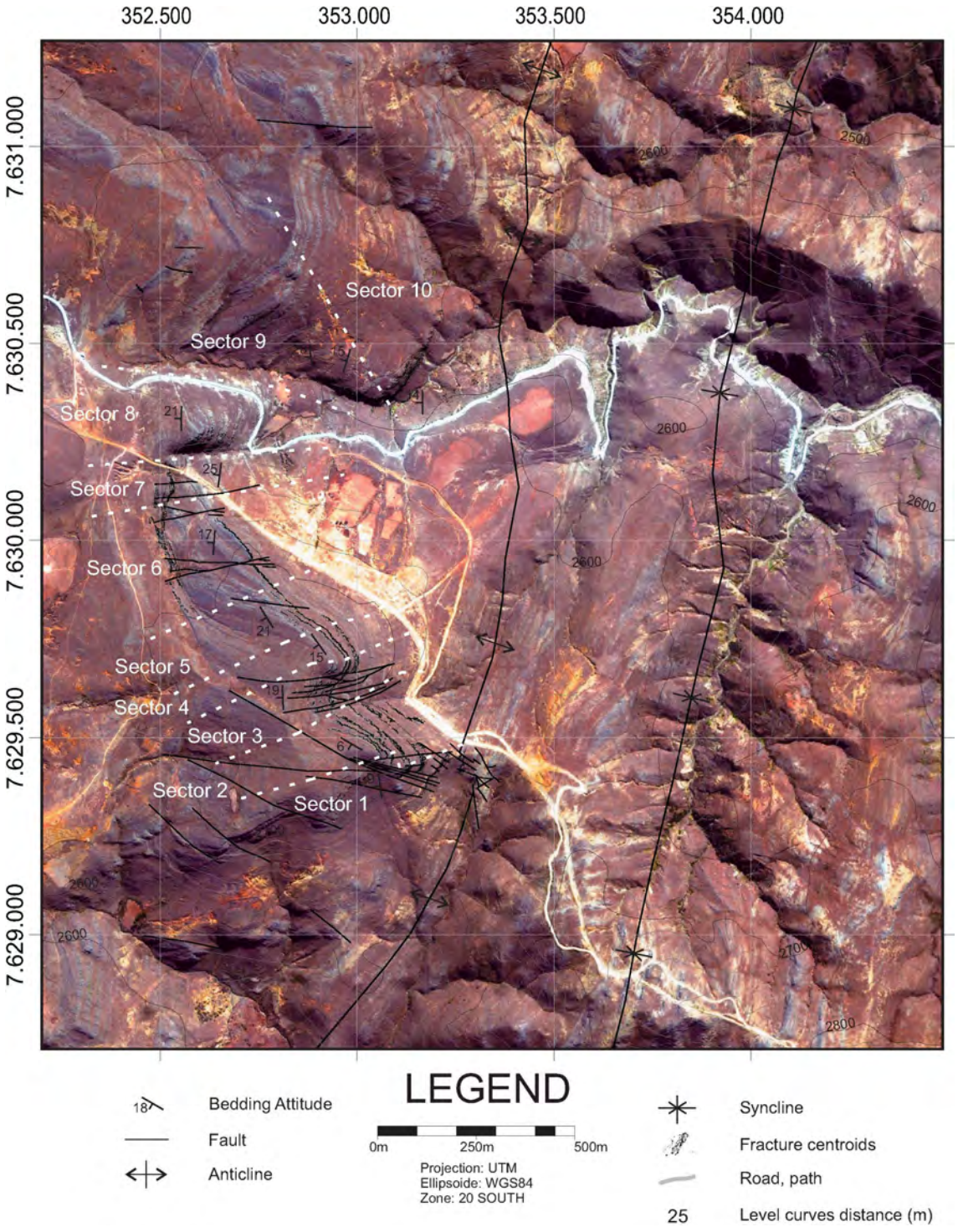

Figure 1. Orthoimage of Abra del Condor. Area division by outcrop orientation and sectors

Parameters in Fracture Characterization

Fractures are exposed at the outcrop showing directly their surface or can also been observed as traces from their intersection with the outcrop surface. For the last case, these fractures are undetectable in this methodology.

Individual fractures are characterized by the coordinates of its surface central position or centroid, fracture length, height and area, aperture (not detected in our virtual fracture model) and surface orientations grouped by orientation set. Moreover, at the rock mass characterization level, the relationship of the individual fractures is

determined by spacing between fractures sets, coefficient of variation -level of fracture clustering, mean values of length, height and area as well as their frequency distributions that reflect their best fit function.

Virtual fracture models are used to measure fracture abundance parameters and to calculate fracture density, intensity and porosity per scanline length and per window sample area (i.e. linear and areal measures). These measurements depend on the sampled scanline or area orientation with the exception of P_{32} value. P_{32} measures the fracture area per unit of volume. This parameter cannot be directly measured from the outcrop surface and must be calculated indirectly from the extrapolation of other abundance measurements.

This study measures fracture intensity in the virtual fracture model, parallel to bedding every few centimeters allowing recognition of changes in intensity trends and establishment of limits for fracture stratigraphic units (FSU). These units are used to measure properties along the virtual scanlines and virtual window samples. From the fracture virtual model a measurement of degree of impedance of each FSU is determined from the percentage of fractures that exceed the limits of the FSU or the stratabound properties of the fracture set. In this way, Fracture Spacing Ratio (FSR) is measured, dividing the FSU thickness per the median fracture set spacing with the aim to find a correlation between confined fractures in FSU and the Fracture Spacing Index (FSI). FSI value corresponds to the slope measurement of the best fit for the plotted relation between FSU thickness and joint spacing. In this study, fracture intensity is measured and used like attribute to identify FSUs.

The term fracture stratigraphy (Laubach et al., 2009) is used to subdivide the rock mass in units based on fracture attributes (Laubach et al., 2009). Heterogeneities of the rock plus bedding, faults and strata are the points of growth for fracture development which are triggered by changes in stress affecting the rock mechanical properties. Nelson (2001) identified lithology, grain size, porosity, bed thickness and structural position as the geological factors that control the mechanical properties of the rock. Burial, diagenesis or tectonic process can also modify the mechanical properties of the rock mass from their original depositional condition to the time of fracturing, making difficult the identification of mechanical units when fracturing have taken (Laubach et al., 2009).

Fractures surveyed by TLS correspond to fractures exposed completely or partially over the outcrop surface and therefore are conditioned by the outcrop orientation. Virtual scanlines or simply scanlines are 2D measurements constrained by the outcrop orientation. For this reason, Abra del Condor outcrop has been divided in sectors, according to its surface orientation. In this way, results are analyzed in the same matter. Accordingly, measurements are presented as data set population by sector by fracture set and by FSU with the aim to characterize fractures as correctly as possible and establish relations of control between fracture and structural, stratigraphic or diagenetic processes.

Discussion

The data set processing reveals the co-existence of five fracture sets. Fracture set I and II are arranged orthogonally to Abra del Condor Anticline, being perpendicular and parallel respectively to the fold axis although in some places this arrangement is not rigorously orthogonal. Both sets are the most abundant in the outcrop as is indicated in the stereoplots, frequency diagrams, frequency distributions and the rest of the derived parameters. Graphs indicate a narrow relation in terms of characterization similarity between sets I and II and rest of fracture sets. Apart from the very close angular relation between fracture sets I and III, both sets have similar characteristics respect to size distributions, spacing and abundance. These similarities also hold for fracture set I respect to sets IV and V.

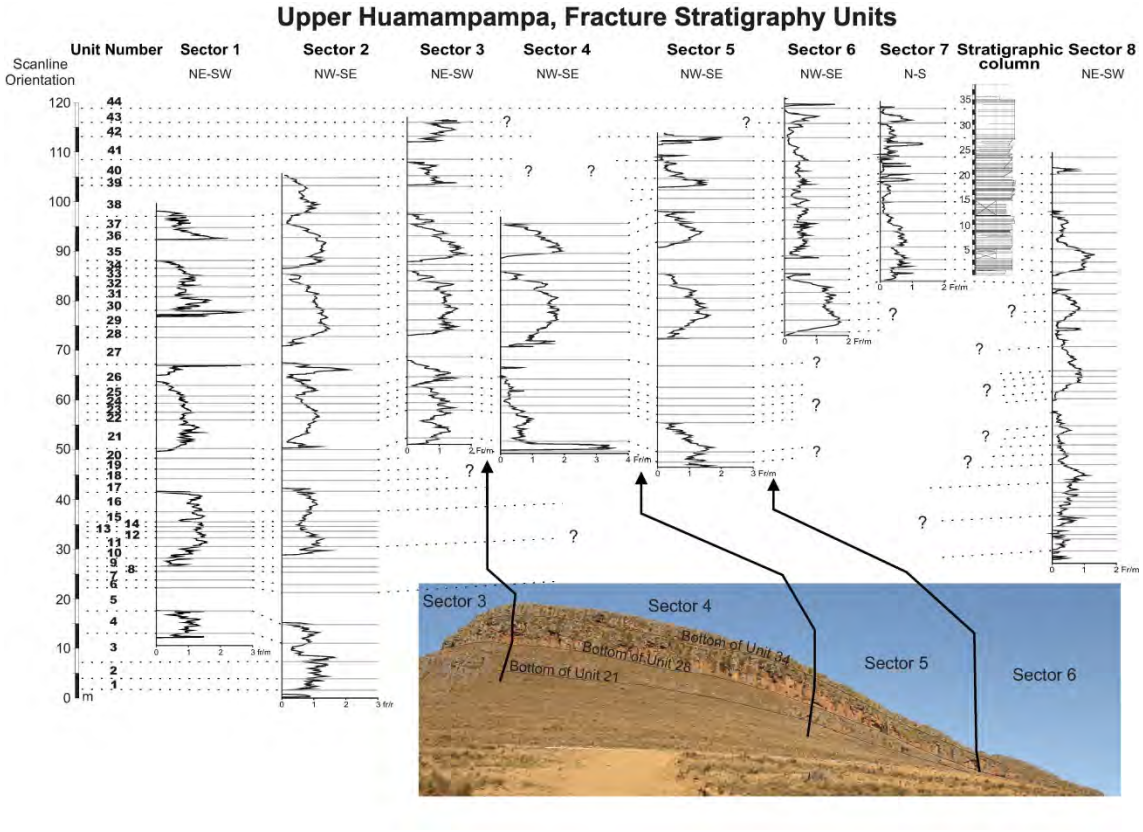

Figure 2. Correlation between the different sectors of the intensity attribute columns to identify the fracture stratigraphy units for the upper Huamampampa Formation. A stratigraphic column measured during the field works is included between Sector 7 and 8. Image represents the position of some fracture stratigraphic units in sector 4 and 5.

In relation to their genesis, fracture sets I and II are consequence of the stress regime changes that affected the studied area. Thereby, fractures sets I and II were formed during a pre-folding extensional stress regime that was followed by a strike-slip stress regime where set I was shear reactivated, inducing the growth of fracture zones and the generation of the rest of fractures sets as splay fractures. During folding strike-slip and reverse stress regimes, set II was reactivated as reverse shear fractures and thrust-related fractures. Post-folding regime induced a trough-going splay fractures that affected the studied area (Florez-Niño et al., 2005, Iñigo et al., 2012).

Outcrops orientation conditions the fracture sets surface measurements employed by this methodology. Our optimal geometry is an outcrop surface orientation perpendicular to the exposed fracture set surface, in this case parallel fracture set surfaces can be occluded. For this reason, measured values need to be carefully interpreted.

Forty four fracture stratigraphy units have been identified for upper Huamampampa section, according to the measured fracture intensity values. They have been grouped into units, depending of their similar characteristics and limits. With the same criteria, in lower Huamampampa section thirty four fracture stratigraphic units have been identified. In general, for the whole outcrop, the fracture intensity can be considered as low with a mean of 1 fracture/meter.

Notwithstanding the above, the studied area is not homogeneous respect to individual and collective fracture properties and presents differences. The long extension of the surveyed area, allows finding trends along the outcrop, which have been recorded and analyzed. In Abra del Condor Anticline, the most evident trend is a decrease in fracture intensity from the fold hinge toward the backlimb, i.e. from sector 1 to sector 8. The mean fracture intensity decreases gradually between these sectors, whereas the bedding increases in dip from 0º, at the hinge) to 30º (backlimb) in upper Huamampampa section. Sectors 9 and 10 in lower Huamampampa section present the same trend. Therefore, fracture intensity is directly related with the structural position along the anticline profile and not with the lithology.

The majority of the FSUs measured about 2.6 m of height with exceptional maximums about 6 m or even 7 m and minimums around a meter. The thickness of each FSU are greater than the mean fracture heights in each FSU, accordingly these fractures can be considered as contained within FSU and do not develop or occupy the total FSU thickness. Also fractures show values of impedance very low and in general only a low percentage of fractures, fewer than 10% cross the FSU limits. In the same way, FSR and FSI do not show low coefficients to find a correlation between fracture spacing and FSU thickness. Fracture spacing coefficients of variation generally are located over the unit, revealing a fracture clustering distribution in the FSU. Thus, fracture distribution is not regular and independently of the FSU thickness.

Calculated mean fracture length for upper Huamampampa section ranges around the 1 – 1.5 m and can be considered as homogeneous, however in lower Huamampampa section, with lower fracture intensities, the mean lengths are longer around 2-2.5 m. Frequency distribution for each sector have been truncated by longest fractures around 6 m for a few cases. It is difficult to assure that in areas of lower intensity as the back limb of lower Huamampampa, fractures can be longer than areas of higher intensity as the upper Huamampampa because the difference is small and not gradual as for the fracture intensity.

Faults observed in the study area with N-S orientation are perpendicular to the dominant structures present in the Abra del Condor Anticline and the thrust sheet of Piedra Larga. Faults in Abra de Condor described previously by Florez-Niño et al. (2005) and Iñigo et al. (2012) were incorporated in this study and were subdivided into three categories: fault zones, intermediate and small faults. The fault zone is placed at the backlimb, close to the hinge and recognizable by the high fault concentration (Figure 2) with a wide damage area made by normal conjugate faults and several interconnected faults of small offset. Intermediate and small faults are present in the rest of the back limb but with a minor intensity and with a small offsets and sometimes isolated, dividing the back limb in regions free of faults.

These types of faults can influence in different ways, increasing or decreasing the fractures connectivity. Case of decreasing can be produced when damage zones play a sealing mechanism between fractures. In the study area, damage zone is in the backlimb around the hinge zone, where the fracture intensity is higher but length and aperture are small. Instead, intermediate and small faults can play as corridors, increasing the connectivity owed to longer fractures in areas of minor fracture intensity and with similar aperture that in damage zones. The above, supports that rather than higher fracture intensities, it is longer lengths and larger apertures, the factors that play a more significant role in fractured reservoir connectivity and permeability. What it was observed in Abra del Condor is that away from the backlimb close to the hinge, a larger drainage area or connectivity was present due to longer fractures.

Characterization trends of Huamampampa Formation divided by FSUs allow considering the outcrop as homogeneous in terms of sizes, spacing and abundance. The FSUs have similar values, always in small ranges, without standing out any FSU

unit independent of the lithology. It is possible to assume that processes of burial and diagenesis have contributed to the rock mass homogenization, affecting and influencing fracture creation in the studied area (Laubach et al., 2009).

Porosity is measured and considered as extremely low (Iñigo, 2009) and the fractures presence increases the total porosity of the area, although perhaps heterogeneously. The values produced in this study as an input into a Discrete Fracture Network (DFN) would allow to measuring the total porosity in different areas of the outcrop and measure the real connectivity of the system.

References

Florez-Niño, J. MAydin, A. Mavko, G., Antonellini, M. Ayaviri, **A. (2005)**, Fault and fracture system in a fold and thrust belt: An example from Bolivia: The American Association of Petroleum Geologist Bulletin. v. 34, p. 471-493.

García-Sellés, D., Falivene, O., Arbués, P., Gratacós, O., Tavani, S., Muñoz, J. A., (2011), Supervised identification and reconstruction of near-planar geological surfaces from terrestrial laser scanning: Computers & Geosciences. v. 37, p. 1584-1594.

Iñigo, J. F., (2009), Structural Model and Fracture Analyses for Major Gas Emplacement in Devonian Sandstones of the Subandes: M.S. Thesis, The University of Texas, Austin, Texas, 297 p.

Iñigo, J. F., Laubach, S. E., Hooker, J. N., (2012), Fracture abundance and patterns in the Subandean fold and thrust belt Devonian Huamampampa Formation petroleum reservoirs and outcrops, Argentina and Bolivia: Marine and Petroleum Geology, v. 35, p. 201-218.

Laubach, S. E., Olson, J. E., Gross, M. R., (2009), Mechanical and fracture stratigraphy: American Association of Petroleum Geologist Bulletin, v. 93, p. 1413-1426.

Moretti, I., Labaume, P., Sheppard, M. F., Boulègue, J., (2002), Compartmentalisation of fluid migration pathways in the sub-Andean Zone, Bolivia: Tectonophysics v. 348, p. 5-24.

Nelson, R. A., (2001), Geologic Analysis of Naturally Fractured Reservoirs:, second edition Gulf Publishing, Houston, 320 p.

E Dinàmica i caracterització de moviments de vessants

Dynamics and evolution of landslides

geomodels
institut de recerca

E1. Mass movement analysis

[1,2]Manuel Jesús Royan, [1,2]Joan Manuel Vilaplana, [1,2,3]Antonio Abellán, [1,2]Marta Guinau, [1,2]Jaume Calvet [1,2]Emma Suriñach, [1,2]Glòria Furdada, [1,2]Maria Ortuño, [4]Mar Tàpia, [1,2]Cristina Prérez, [1,2]David García-Sellés, [1,2]Jaume Bordonau, [1,2]Anna Echeverria, [5]Pere Roig, [5]Marta Torné, [5]Xabier Blanch, [6]AntonioRuiz, [7]Miquel Camafort, [5]Verónica Náquira

[1] RISKNAT Group, Departament de Dinàmica de la Terra i l'Oceà, Secció de Geodinàmica i Geofísica, Facultat de Ciències de la Terra, Universitat de Barcelona, C/Martí i Franquès s/n., 08028 Barcelona, Spain
[2] GEOMODELS Institute, Departament de Dinàmica de la Terra i l'Oceà, Secció de Geodinàmica i Geofísica, Facultat de Ciències de la Terra, Universitat de Barcelona, C/Martí i Franquès s/n., 08028 Barcelona, Spain
[3] Scott Polar Reasearch Institute, Geography Department, University of Cambridge, Lensfield Road, CB2 1ER, Cambridge, UK
[4] Laboratori d'Estudis Geofísics Eduard Fontserè (LEGEF-IEC), Barcelona 08001, Spain
[5] Departament de Dinàmica de la Terra i l'Oceà, Secció de Geodinàmica i Geofísica, Facultat de Ciències de la Terra, Universitat de Barcelona, C/Martí i Franquès s/n., 08028 Barcelona, Spain
[6] ICGC, Institut Cartogràfic i Geològic de Catalunya, Parc de Montjuïc, 08038 Barcelona, Spain
[7] Centre Mediterrani d'Investigacions Marines i Ambientals-CSIC, Psg. Marítim de la Barceloneta, 37-49, 08003 Barcelona, Spain

Introduction.

Mass movements and torrential activity are the most significant geomorphological processes in steep slopes and constitute a major natural hazard in mountainous areas. RISKNAT Research is focused on the development of methodologies to analyze the phenomenon and to evaluate the susceptibility, the hazard and the exposure to these processes.

The main areas of the RISKNAT research are listed below:

- *LiDAR (TLS) rockslope monitoring, in turn focusing on two aspects; on the one hand, the spatial location of rockfalls and quantification of their magnitude and frequency, and on the other, the spatial prediction of rockfalls based on the detection of precursory indicators. This monitoring is now focused in two localities: Puigcercós and Montserrat Mountain.*
- *Reconstructing landslide dinamics and characteristics using remote sensing data (photogrammetry, LiDAR and seismic data): comparison between different techniques and complementary data analysis. This research was developed in la Riba, Tarragona, Spain.*
- *Detection of early stage large scale landslides in forested areas by sub-5 m LiDAR DEM analysis. This research was foccused last year in Portainé, Central Pyrenees.*
- *Characterising and dating flash floods and debris flows through dendrogeomorphological methodologies in Portainé stream, Eastern Pyrenees (this item is treated in a separated chapter, related to torrential activity and floods).*
- *LiDAR data application to the study of the torrential dynamics and evolution of the Portainé and Reguerals streams Eastern Pyrenees (this item is treated in a separated chapter, related to torrential activity and floods).*
- *Implementation of a methodology of risk analysis related to flood hazard: Sud-East Haïtí.*
- *(this item is treated in a separated chapter, related to torrential activity and floods).*

- *Seismic studies on mass movements: Lahars, debris flows, snow avalanches. (this item is treated in a separated chapter).*

The rapid development of the techniques (LiDAR and photogrammetry) that support the research methods is expected to lead to substantial improvements in mass movement hazard assessment and risk mitigation strategies.

Work done

Rock slope monitoring and characterization by TLS

[1,2]Manuel Jesús Royan, [1,2]Joan Manuel Vilaplana, [1,2,3] Antonio Abellán, [1,2]Jaume Calvet, [1,2]Marta Guinau, [2]Xabier Blanch, [1,2]David García-Sellés

[1] RISKNAT Group, Departament de Dinàmica de la Terra i l'Oceà, Secció de Geodinàmica i Geofísica, Facultat de Ciències de la Terra, Universitat de Barcelona, C/Martí i Franquès s/n., 08028 Barcelona, Spain
[2] GEOMODELS Institute, Departament de Dinàmica de la Terra i l'Oceà, Secció de Geodinàmica i Geofísica, Facultat de Ciències de la Terra, Universitat de Barcelona, C/Martí i Franquès s/n., 08028 Barcelona, Spain
[3] Scott Polar Reasearch Institute, Geography Department, University of Cambridge, Lensfield Road, CB2 1ER, Cambridge, UK

Early detection of rock slope failures using precursory rockfalls along cracks

Little is known about the spatial location and temporal occurrence of small scale rockfall events preceding larger slope failures. In this study we show how the location of future rock slope instabilities can be early detected through the analysis of previous signs of activity that occurred along certain tensile cracks, identified such as "precursory rockfalls". The rockfall database (figure 1) used in this research was obtained through repeated terrestrial LiDAR scanning during a time-span of almost 9 years over the Puigcercós rock face (Catalonia, Spain). Our data shows both an aggregation of small scale rockfalls along certain cracks and a non-stationary rockfall occurrence along time. Interestingly, the clustering of rockfalls was linked with those areas of the slope affected by a progressive failure, as it was confirmed by the concurrent detection of slope deformation and a subsequent rock slope failure (figure 2). We were able to detect these unconventional precursory signs of activity over six unstable areas, helping to improve our understanding on the spatio-temporal clustering of precursory rockfalls. These findings could be used for early detection and real-time forecasting of progressive failures in the near future.

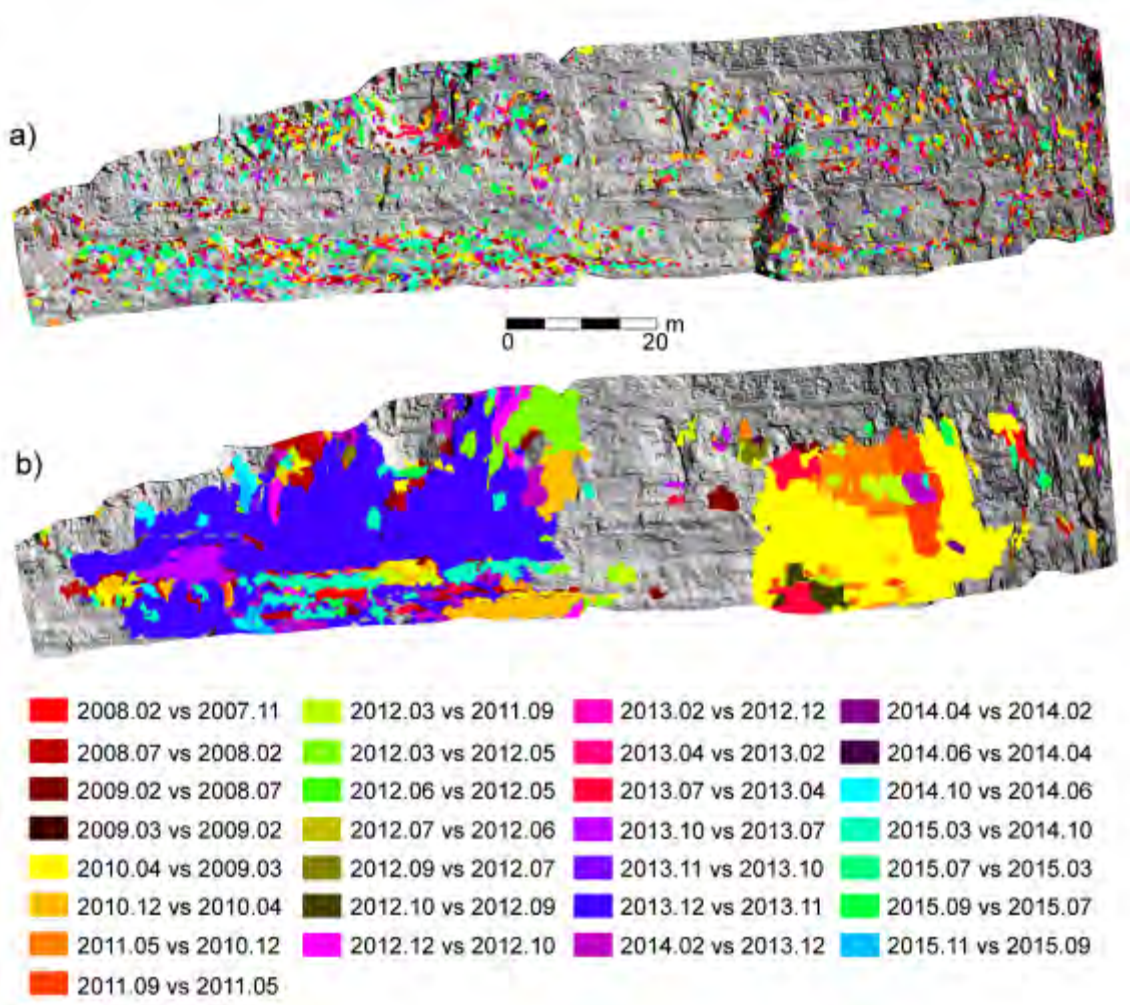

Figure 1: Rockfalls occurred in Puigcercós scarp during the timespan of this research, classified by volume and dates. (a) Group A of rockfalls corresponding to small-scale events (3240 rockfalls with volume ≤ 0.1 m^3). (b) Group B of rockfalls corresponding to medium and big-scale events (313 rockfalls with volume > 0.1 m^3).

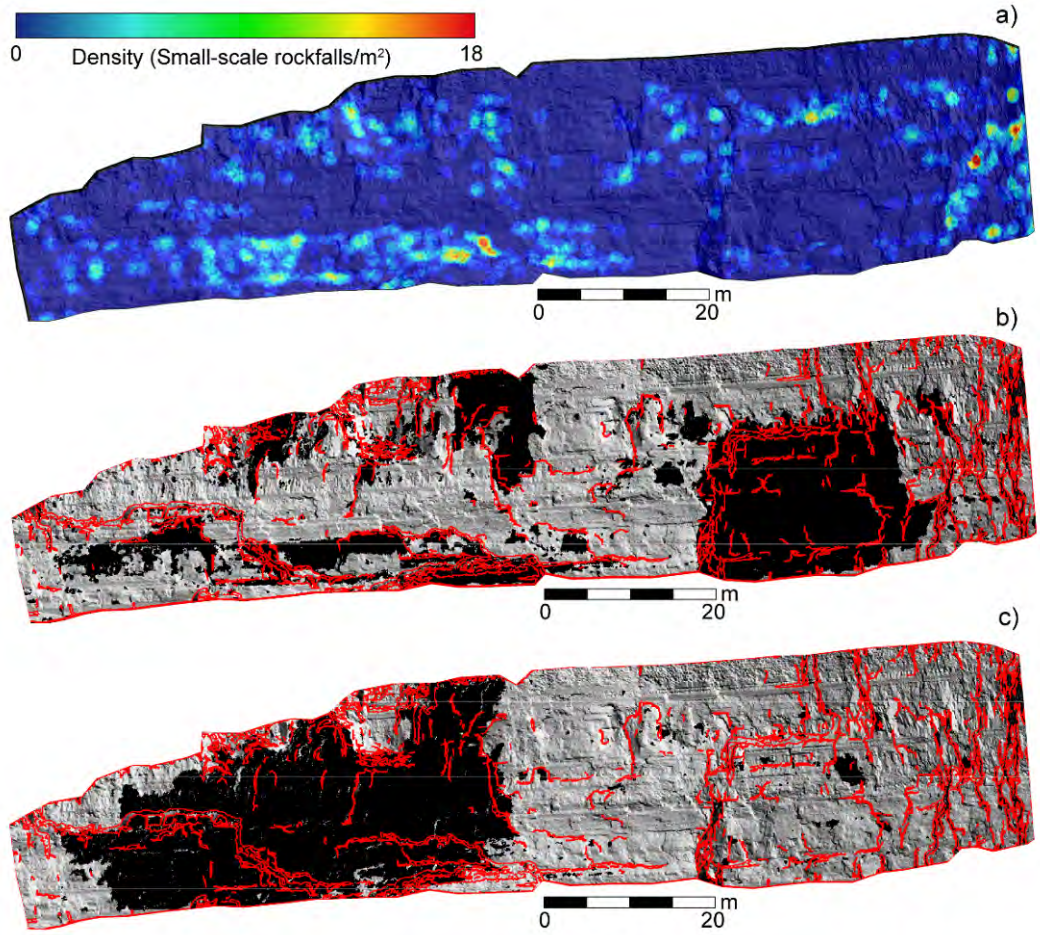

Figure 2: Validation test: (a) Density map of small-scale rockfalls (group A). (b) Active cracks plotted against rockfalls occurred until period G (1841-2143 days). (c) Active cracks plotted against rockfalls occurred from period H (2143-2217 days).

Analysis of LiDAR aplications in rockfalls detection and characterization at Montserrat Mountain

The different methodologies developed and successfully applied in the pilot study area of Puigcercós were employed then in an area with a high rockfall risk for both buildings and vehicles and people, Montserrat Mountain. Specifically two critical sites were chosen, the cliffs located just behind Montserrat Monastery, whose monitoring started in 2011; and Degotalls rock face, located behind the parking of the Monastery, whose monitoring started in 2007. This monitoring has allowed obtaining a rockfall inventory with an unprecedented level of detail (figure 3). Therefore, the continuation of this research will allow improving our comprehension of the geomorphologic behavior of these conglomerate cliffs. Furthermore, the methodologies applied have allowed the detection of pre-failure deformation in two unstable blocks. The analysis of this pre-failure deformation in one of these instabilities has demonstrated its critical condition close to the rockfall (figure 4).

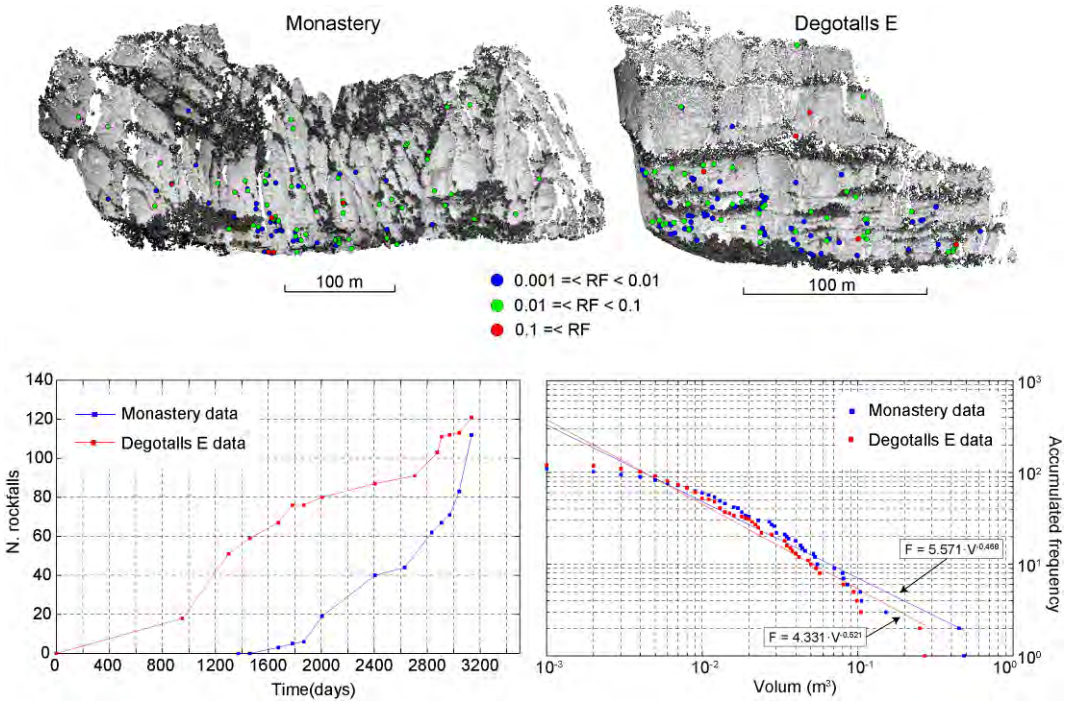

Figure 3: Rockfalls detection with TLS monitoring in the Monastery and Degotalls E study areas.

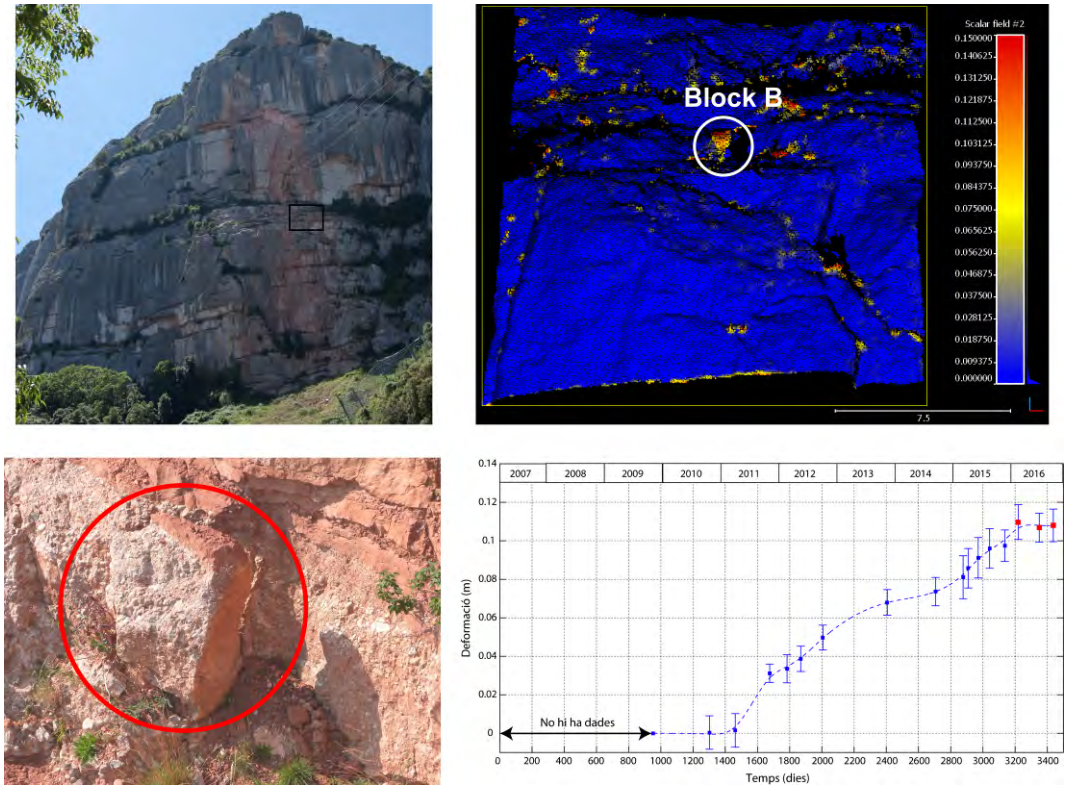

Figure 4: Pre-failure deformation analysis of an unstable block located at Degotalls rock face.

Moreover, during the year 2016, 5 new localities in the Montserrat Mountain where included in the study (Sant Benet cliff, Guilleumes cliff, Can Jorba, La Salut and Collbató road at the kilometric point 3.5). Whereas in all of those locations the LiDAR data have not been analyzed yet, in the last location the study was centered on characterizing rockfall source areas by analyzing 3D discontinuity sets identified from

TLS data, in order to describe the mechanisms and possible features and volumes of potential rockfalls. The Colbató road study site includes rock faces affecting one of the most exposed access roads, characterized by an area of 2 ha and a maximum height of 90 m.

A first approach on the detection and characterization of the rockfall source zones is developed by visual inspection at the field. Subsequently, the discontinuity sets are analysed from TLS point clouds, by using the SEFL (Surface Extraction From LiDAR) application developed by GEOMODELS. Briefly the SEFL application is based on the planar regression of the point cloud that allowed the computation of the dip and dip direction of the different continuous surfaces. The computation of a series of quality parameters of the resulted data and a clustering process allows the individual extraction of discontinuity sets (Figures 5 and 6) and the obtaining of a morphometric model of the discontinuities. Afterward the mean surface length and the mean spacing are calculated for each discontinuity set. Field measurements and observations are used to validate the discontinuity sets characteristics defined from TLS data, since TLS point cloud is normally affected by occlusion and certain biases.

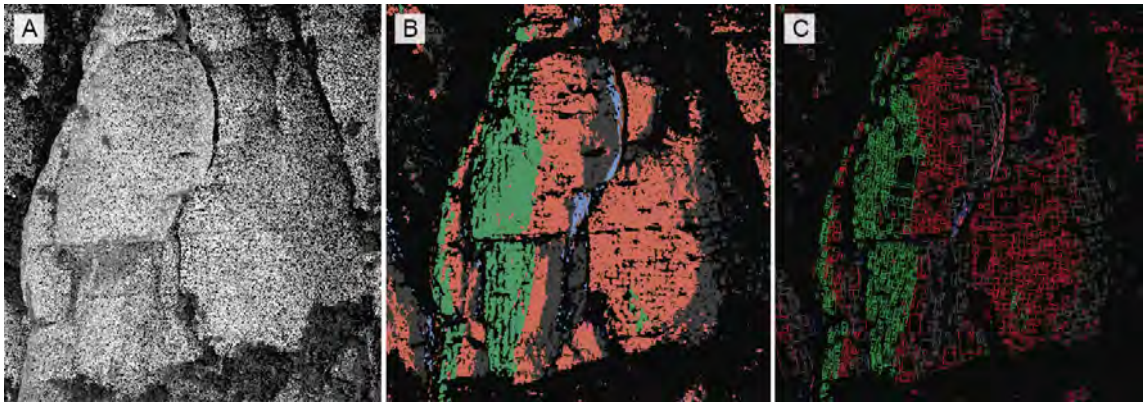

Figure 5. Results from the SEFL application to obtain the discontinuity sets affecting the rock cliff. A: TLS point cloud. B: Points showed in different colors depending on which discontinuity set they belong. C: Morphometric model.

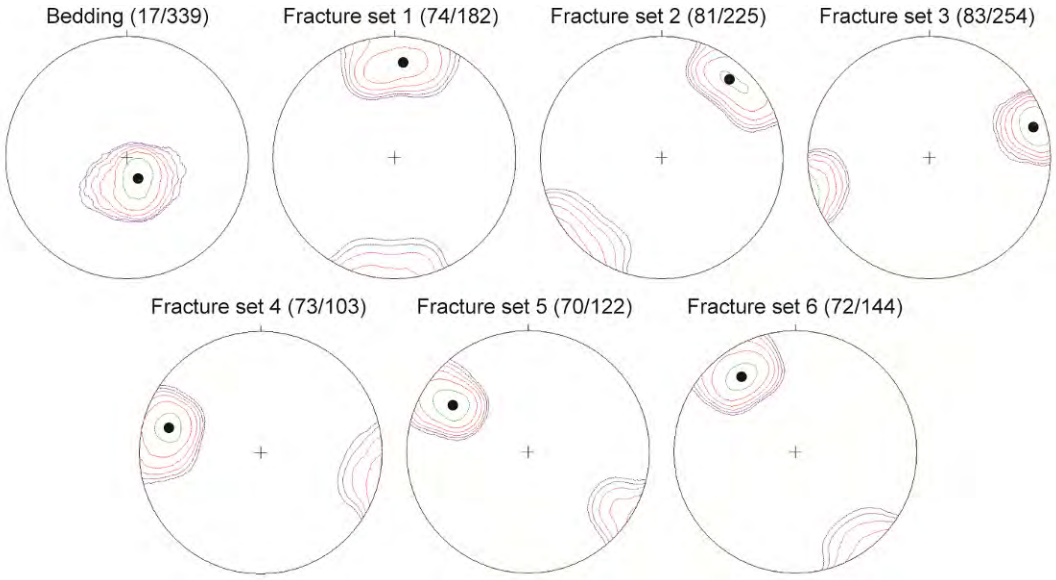

Figure 6. Pole density stereographic representations and mean dip and dip direction for each discontinuity set and bedding.

The results are compared with the ones obtained in further works developed in other sectors of the Montserrat Mountain, in order to detect possible differences in the morphometry of the rockfalls. The characterization of the source zones attained provides compulsory information for the design and implementation of protective measures to reduce the rockfall risk in the study area.

Reconstructing landslide dinamics and characteristics using remote sensing data (photogrammetry, LiDAR and seismic data)

[4]Marta Torné, [1,2]Marta Guinau, [3]Mar Tàpia, [1,2]Manuel Jesús Royan, [1,2]Emma Suriñach, [1,2]Cristina Pérez, [1,2]Anna Echeverria, [4]Pere Roig

[1] RISKNAT Group, Departament de Dinàmica de la Terra i de l'Oceà, Secció de Geodinàmica i Geofísica, Facultat de Ciències de la Terra, Universitat de Barcelona, C/Martí I Franquès s/n., 08028 Barcelona, Spain
[2] GEOMODELS Institute, Departament de Dinàmica de la Terra i de l'Oceà, Secció de Geodinàmica i Geofísica, Facultat de Ciències de la Terra, Universitat de Barcelona, C/Martí I Franquès s/n., 08028 Barcelona, Spain
[3] Laboratori d'Estudis Geofísics Eduard Fontserè (LEGEF-IEC), Barcelona 08001, Spain
[4] Departament de Dinàmica de la Terra i de l'Oceà, Secció de Geodinàmica i Geofísica, Facultat de Ciències de la Terra, Universitat de Barcelona, C/Martí I Franquès s/n., 08028 Barcelona, Spain

The purpose of this study is to characterize the rock planar landslide that occurred in the village of La Riba (Catalonia) on May 5th 2013, using different techniques such as photogrammetry, terrestrial LiDAR data, and seismic data. After the May 5th natural landslide, a controlled blasting was carried out to stabilize the slope. Using this programmed blasting as a benchmark, two photogrammetric models and two terrestrial LiDAR data models corresponding to the pre and post blast were made to compute the rock volume involved in the blast (figure 7). The blasting process was recorded with two HD video cameras and by two temporary seismic stations deployed close to the site.
With the aim to characterize the artificial triggered rockslide flow, this last year, the seismic record was studied to identify different instants of the evolution of the

rockslide, its dynamics, the energy released and its relationship with the triggered volume. To do this, amplitudes, energy content, frequency content, polarization and others were measured and the results are compared with video frames (figure 8).
Moreover, information about the natural landslide was obtained from the records of a permanent seismic station 10 km from the site. Data such as the estimated fallen volume, the landslide mechanism and time of occurrence are information that would otherwise not be obtained.

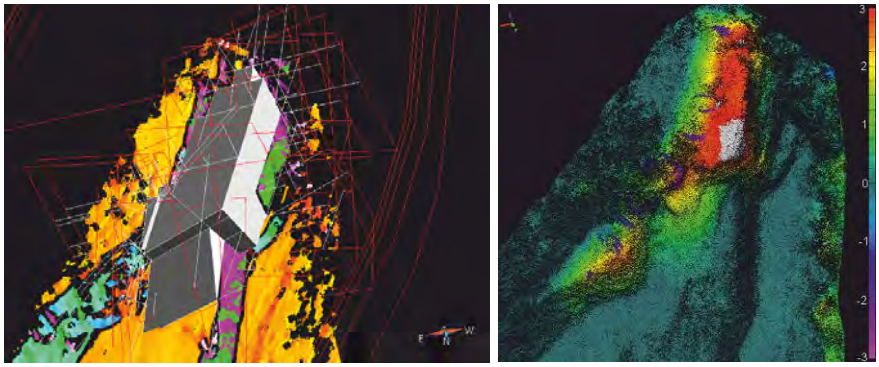

Figure 7: Left, Blasted volume reconstructed and calculated by combining simplified surfaces using GOCAD software (Paradigm – www.pdgm.com). Right, the volume involved in the blast was calculated from the difference between pre and post LiDAR data sets using the Surface to Plane tool of PolyWorks.

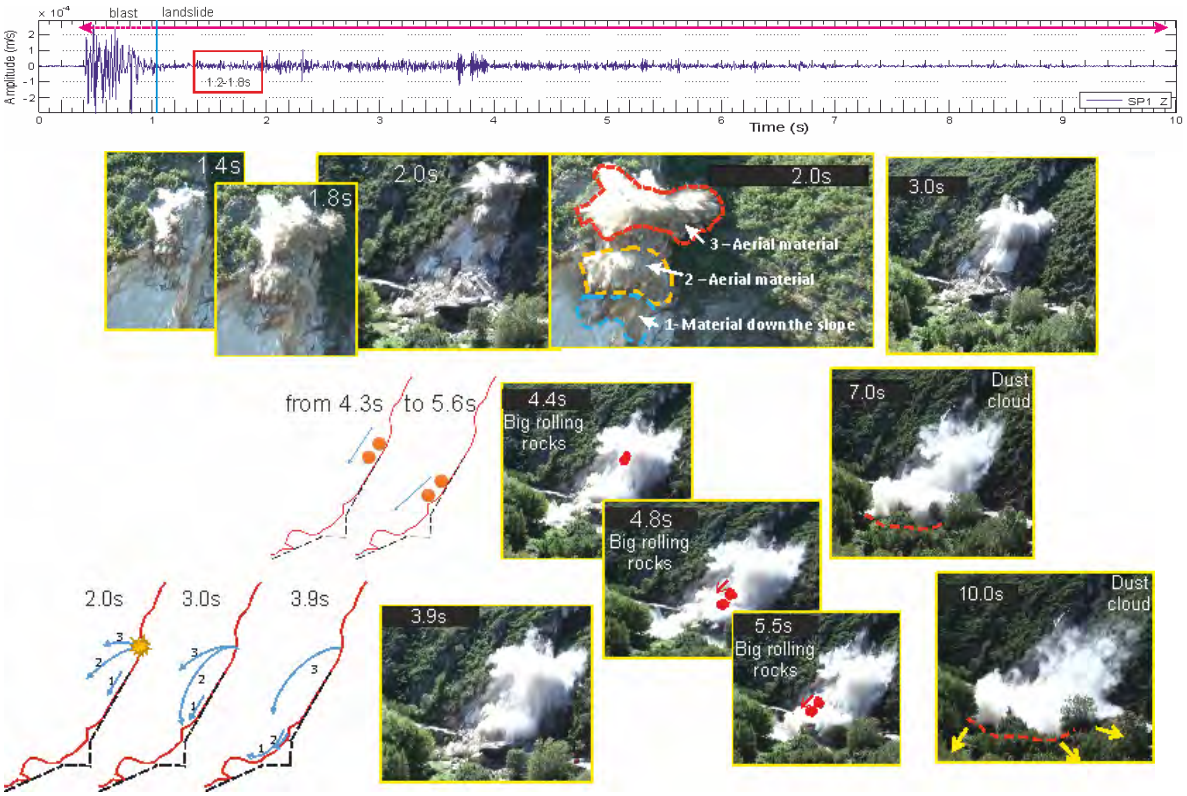

Figure 8: The video recordings together with the seismic signals allow us to identify different instants in the landslide and provide information about their dynamics. Note the different amplitude and frequency content of each part of the landslide. Different parts of the landslide could be identified: 1) small materials falling down the slope, 2) some individual rock impacts and 3) large rocks rolling down the slope. Signals are filtered according to the frequency content of each phenomenon. Particle motions are consistent with the directionality of the different parts of the landslide.

This research is done in collaboration with the Laboratori d'Estudis Geofísics Eduard Fontserè (LEGEF).

Detection of early stage large scale landslides

[1,2]*Maria Ortuño,* [1,2]*Marta Guinau,* [1,2]*Jaume Calvet,* [1,2]*Glòria Furdada,* [1,2]*Jaume Bordonau,* [3]*AntonioRuiz,* [4]*Miquel Camafort,* [5]*Verónica Náquira*

[1] RISKNAT Group, Departament de Dinàmica de la Terra i de l'Oceà, Secció de Geodinàmica i Geofísica, Facultat de Ciències de la Terra, Universitat de Barcelona, C/Martí I Franquès s/n., 08028 Barcelona, Spain
[2] GEOMODELS Institute, Departament de Dinàmica de la Terra i de l'Oceà, Secció de Geodinàmica i Geofísica, Facultat de Ciències de la Terra, Universitat de Barcelona, C/Martí I Franquès s/n., 08028 Barcelona, Spain
[3]ICGC, InstitutCartogràfic i Geològic de Catalunya, Parc de Montjuïc, 08038 Barcelona, Spain
[4]Centre Mediterrani d'Investigacions Marines i Ambientals-CSIC, Psg. Marítim de la Barceloneta, 37-49, 08003 Barcelona, Spain
[5] Departament de Dinàmica de la Terra i de l'Oceà, Secció de Geodinàmica i Geofísica, Facultat de Ciències de la Terra, Universitat de Barcelona, C/Martí I Franquès s/n., 08028 Barcelona, Spain

Mass movements have been classically detected by field inspection and air-photo interpretation. However, airborne LiDAR has significant potential for generating high-resolution digital terrain models, which provide considerable advantages over conventional surveying techniques. In this work, we present the identification and characterization of six slope failures previously undetected in the Orri massif, Portainé zone (Figure 9) and Tirvia zone (Figure 10), at the core of the Pyrenean range.

The landforms had not been previously detected and were identified by the analysis of high resolution 2 m LiDAR derived bared earth topography. Most of the scarps within these failures are not detectable by photo interpretation or the analysis of 5 m resolution topographic maps owing to their small heights (ranging between 0.5 and 2 m) and their location within forest areas. 2D and 3D visualization of hillshade maps with different sun azimuths, allowed to obtain the overall picture of the scarp assemblage and to analyze the geometry and location of the scarps with respect to the slope and the structural fabric.

Near 120 scarps were mapped and interpreted as part of slow gravitational deformation, incipient slow flow affecting a colluvium, rotational rock-sliding and slope creep. Landforms interpreted as incipient slow flow affecting a colluvium have headscarps with horse-shoe shape and superficial (< 20 m) basal planes whereas sackung features have open headscarps and basal planes that are likely located at 200-250 m maximum depth. Other distinctive features are toppling or extensive scarps, double ridges and rock rotational landslides. The sharpness of the scarps suggests their recent activity, which may pose a potential risk for the Port-Ainé sky resort users and facilities.

These results suggest that the systematic analysis of 2 m LIDAR derived bared earth topography would significantly help in the rapid detection and mapping of early stage slope deformations in high mountain areas, which could contribute to 1) a better understanding of the spatial controlling factors and 2) obtaining rapid diagnosis of the state of the slopes, critical for the proper forecast of future catastrophic failures.

This presentation is supported by the Spanish Ministry of Science and Innovation project CHARMA: CHAracterization and ContRol of MAss Movements. A Challenge for Geohazard Mitigation (CGL2013-40828-R).

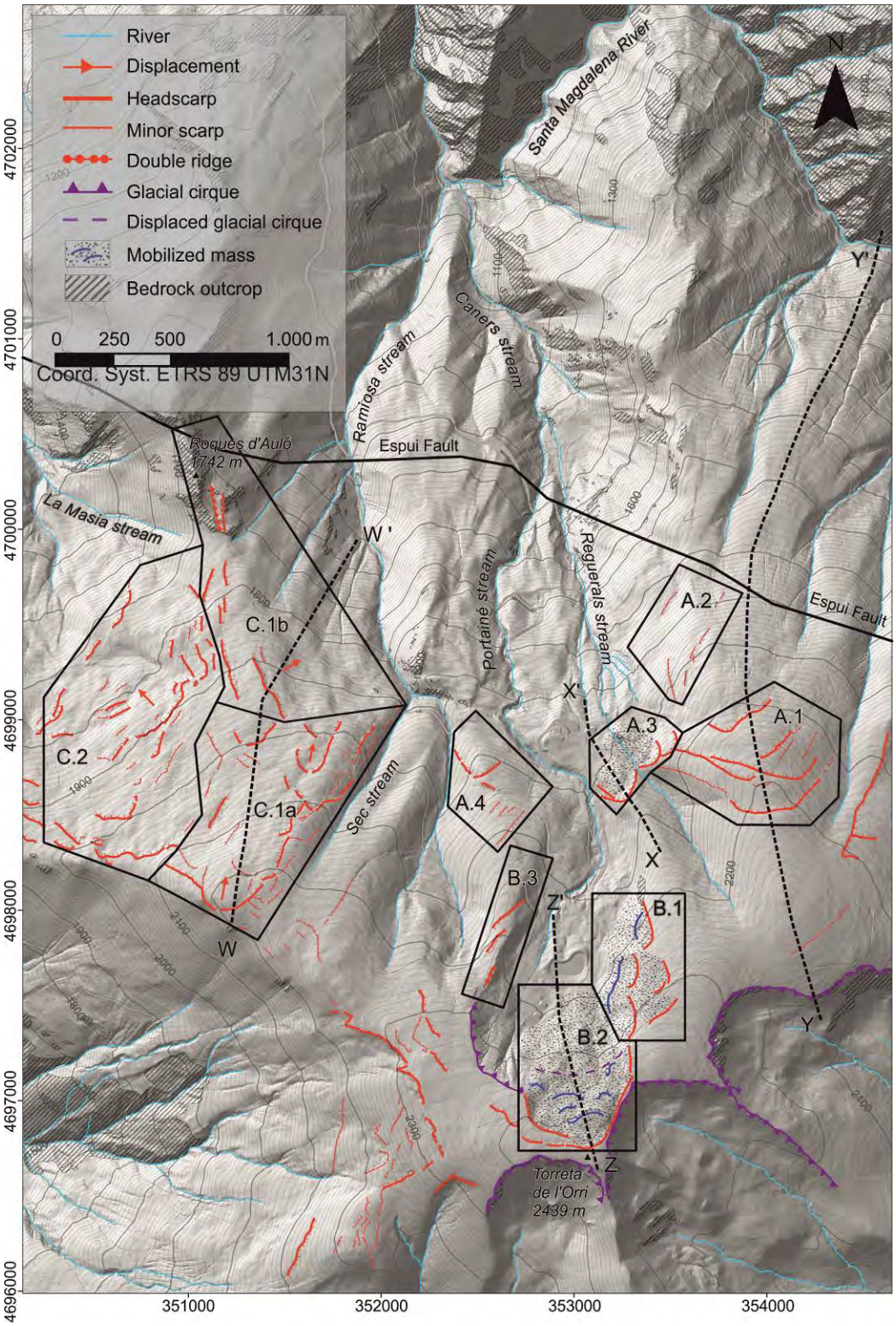

Figure 9: Detected geomorphological features and subdivision in zones in the Portainé zone over a hillshade map (sun at 45º elevation and 315º azimuth).

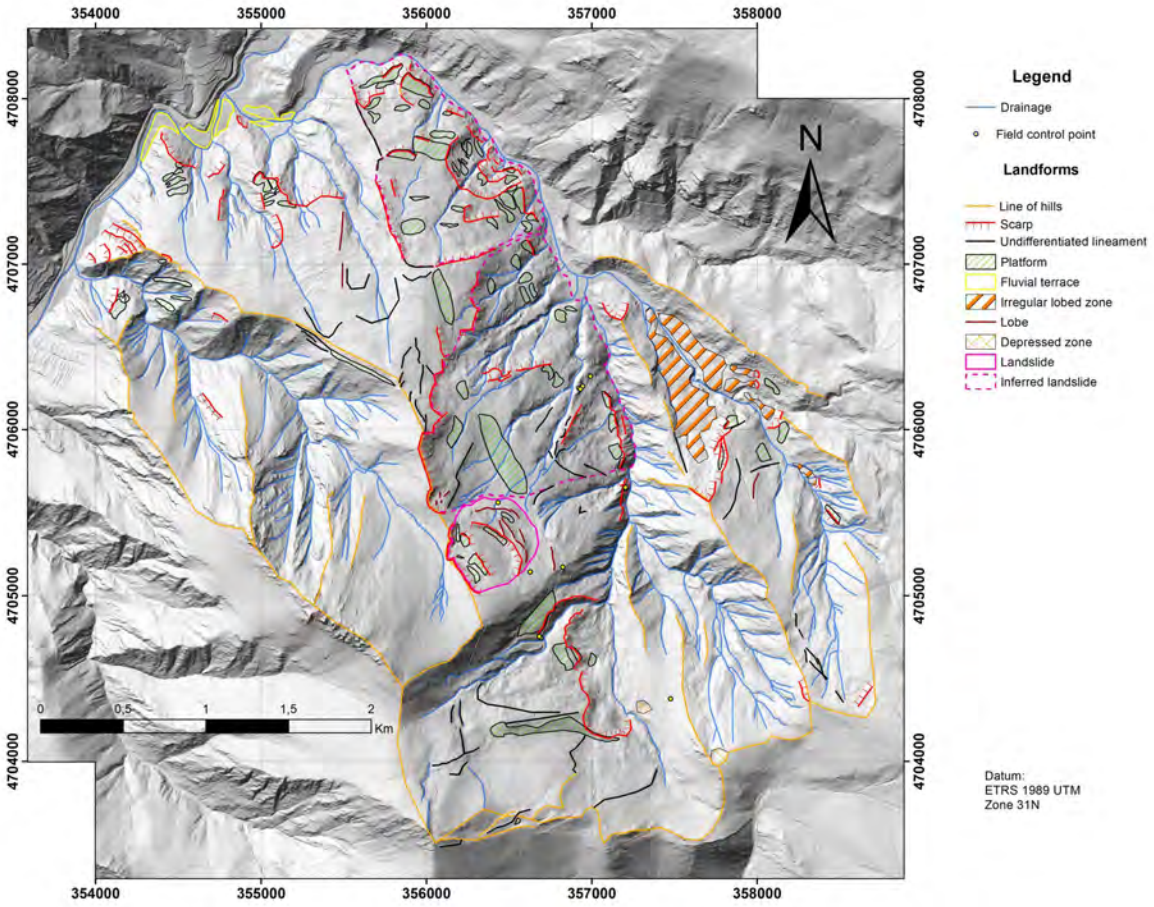

Figure 10: Detected geomorphological features in the Tírvia zone over a hillshade map (sun at 45º elevation and 315º azimuth).

Future work

Rock slope monitoring by TLS

As regards to rock slope monitoring, we are going to continue with the monitoring of Puigcercos and Montserrat rock faces by TLS for detecting the future rockfalls events and to predict it. One of the goals is to stablish a magnitude/frequency analysis of the rockfalls. Also, we are going to do a seismic, GPS and fotogrametric monitoring of Puigcercos rock face to relate this data with the TLS and weather data. Futhermore a continuous and permanet photographic monitoring is being carried out at Puigcercós Scarp with the aim of improve the temporal resolution of rockfalls detection.

Reconstructing landslide dinamics and characteristics using remote sensing data (photogrammetry, lidar and seismic data)

As regards to landslide dynamics and characteristics analyzed by remote sensing techniques, we are going to continue with the data acquisition and analysis in other locations in order to purchase new knowledge on data interpretation in different contexts (lithologies, landslide mechanisms, etc.).

Detection of early stage large scale landslides

On this context, we are going to develop the analysis of high resolution DTM (obtained from ariborn LiDAR data) in other location on the Pyrenees, in orther to obtain a thorough knowledge on large scale landslide distribution in the Pyrenees region. Moreover, we are going to develop new methods focused on the semi-authomatic identification of morphologies associated with large scale landslides.

E2. Torrential activity and floods

[1,2]Glòria Furdada, [1,2]Marta Guinau, [1,2]Ane Victoriano, [3]Mar Génova, [4]Andrés Díez-Herrero, [1,2]Giorgi Khazaradze, [1,2]Jaume Calvet, [5]Álvaro de las Heras, [6]Mariló Cabré, [6]Miriam Moysset [1,2]M. Angels Marqués.

[1] RISKNAT Group, Departament de Dinàmica de la Terra i de l'Oceà, Facultat de Ciències de la Terra, Universitat de Barcelona. C/Martí I Franquès s/n., 08028 Barcelona, Spain
[2] GEOMODELS Institute, Departament de Dinàmica de la Terra i de l'Oceà, Facultat de Ciències de la Terra, Universitat de Barcelona. C/Martí I Franquès s/n., 08028 Barcelona, Spain
[3] Departamento de Sistemas y Recursos Naturales, Universidad Politécnica de Madrid, Spain
[4] Instituto Geológico y Minero de España, Spain
[5] ECOGESFOR Research Group; ETSI de Montes, Forestal y del Medio Natural; Universidad Politécnica de Madrid.
[6] ICGC, Institut Cartogràfic i Geològic de Catalunya, Spain.

Introduction.

Torrential activity, floods and mass movements are the most significant geomorphological processes in steep slopes and constitute a major natural hazard in mountainous areas. RISKNAT Research is focused on the development of methodologies to analyze the phenomenon and to evaluate the hazard and the exposure to these processes.
In this chapter we will focus on the following research lines:

- *Characterising and dating flash floods and debris flows through the integration of dendrochronological, geomorphological and historical methods; the Portainé stream, Eastern Pyrenees.*
- *LiDAR data application to the study of the torrential dynamics and evolution of the Portainé and Reguerals streams, Eastern Pyrenees.*
- *Implémentation d'une méthodologie d'analyse de risque lié à l'aléa inondation : Sud-Est d'Haïtí.*

Work done

Characterising and dating flash floods and debris flows through the integration of dendrochronological, geomorphological and historical methods; the Portainé stream, Eastern Pyrenees.

[1,2]Glòria Furdada, [1,2]Marta Guinau, [1,2]Ane Victoriano, [3]Mar Génova, [4]Andrés Díez-Herrero, [1,2]Giorgi Khazaradze, [1,2]Jaume Calvet, [5]Álvaro de las Heras,

[1] RISKNAT Group, Departament de Dinàmica de la Terra i de l'Oceà, Facultat de Ciències de la Terra, Universitat de Barcelona. C/Martí I Franquès s/n., 08028 Barcelona, Spain
[2] GEOMODELS Institute, Departament de Dinàmica de la Terra i de l'Oceà, Facultat de Ciències de la Terra, Universitat de Barcelona. C/Martí I Franquès s/n., 08028 Barcelona, Spain
[3] Departamento de Sistemas y Recursos Naturales, Universidad Politécnica de Madrid, Spain
[4] Instituto Geológico y Minero de España, Spain
[5] ECOGESFOR Research Group; ETSI de Montes, Forestal y del Medio Natural; Universidad Politécnica de Madrid.

The ski resort of Port-Ainé opened in 1986. It is located in the Pallars Sobirà county (Central Pyrenees, northern Lleida province) (Fig. 1) and is a key infrastructure in this mountainous region. The flank of the mountain range, on whose head the ski station is located, is drained northward by the Portainé, Reguerals (tributary of Portainé) and Ramiosa streams. Its maximum and minimum altitudes are 2439 m a.s.l. (Torreta de l'Orri peak) and 950 m a.s.l. (confluence with the Romadriu River). The access road runs along the slope, and traverses them at various points. Between 2006 and 2015 ten torrential floods occurred in Portainé and Reguerals streams, and nine of them affected the road, causing significant damage involving considerable reconstruction and maintenance economic costs.

In order to know if the torrential floods had destructive activity prior to 2006 and to understand the recent intense torrential activity, the evolution of the torrents and their catchments was studied since the mid-twentieth century, with special detail during the last decade. The methodology used integrates: 1) historical data collection of floods and anthropogenic activities, including hydrological correction measures applied in Portainé and Reguerals torrents; 2) study of the evolution of vegetation cover in the headwaters of the watersheds (fig. 2); 3) study of anthropogenic changes in the area of the ski resort, especially the tracks and the snow-melt water drainage channels; 4) study of trees affected by torrential floods in the lower reaches of the Portainé river (dendrogeomorphology) (fig. 3), and 5) GIS mapping using total station and *Global Navigation Satellite System* (GNSS) advanced techniques (fig. 4).

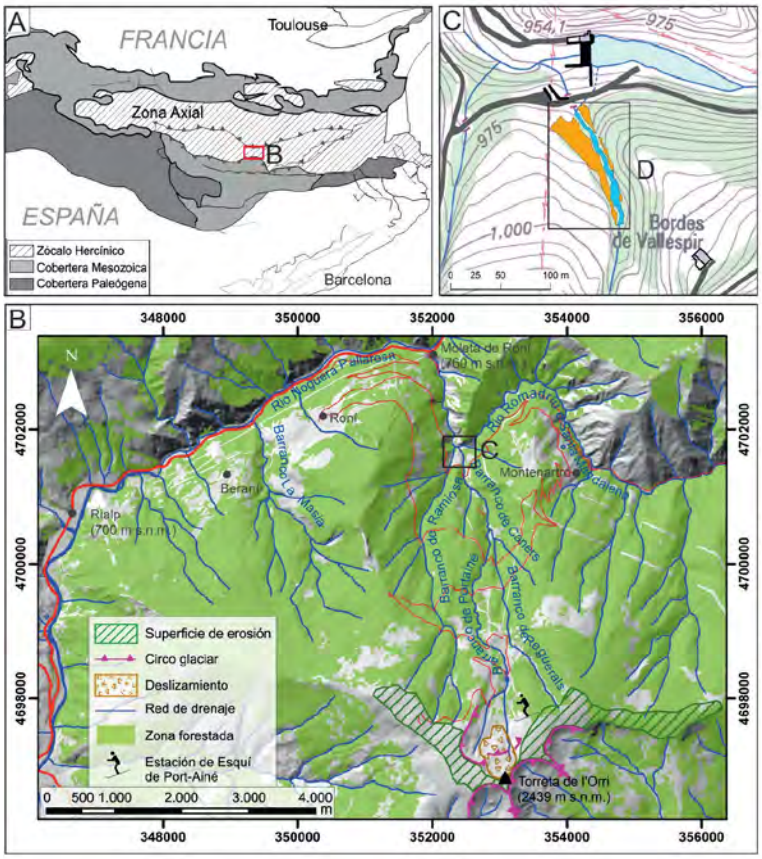

Figure 1: A). Geological context of the study area: axial zone, Eastern Pyrenees. B). Geomorphological framework: elements that characterize the headwaters of Portainé Stream, drainage network and major access routes (Hillshade performed from de DTM 2x2 m from the ICGC). C). Outline of the location of the study area at the confluence of

the Portainé Stream with Romadriu River. Vallespir dam and Portainé Stream artificial channel that carries ordinary water to reservoir (topographic map from the ICGC).

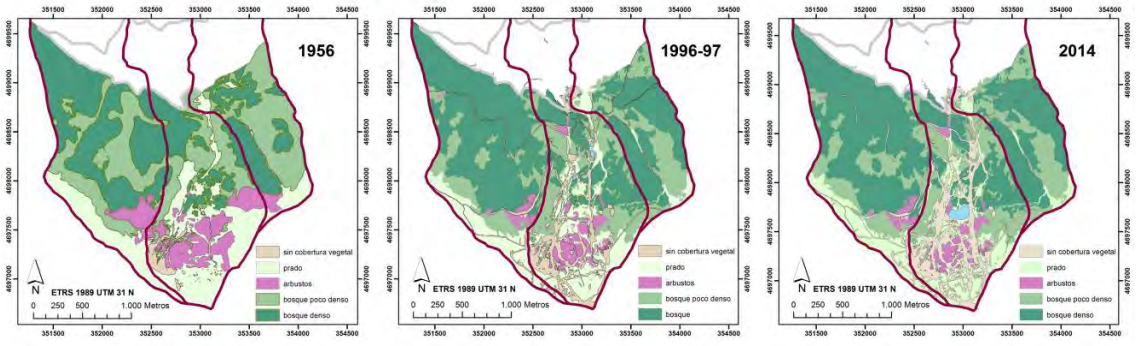

Figure 2. Three examples of the land use cover changes from 1956 to 2014 ata the headwaters of the Portainé watershed

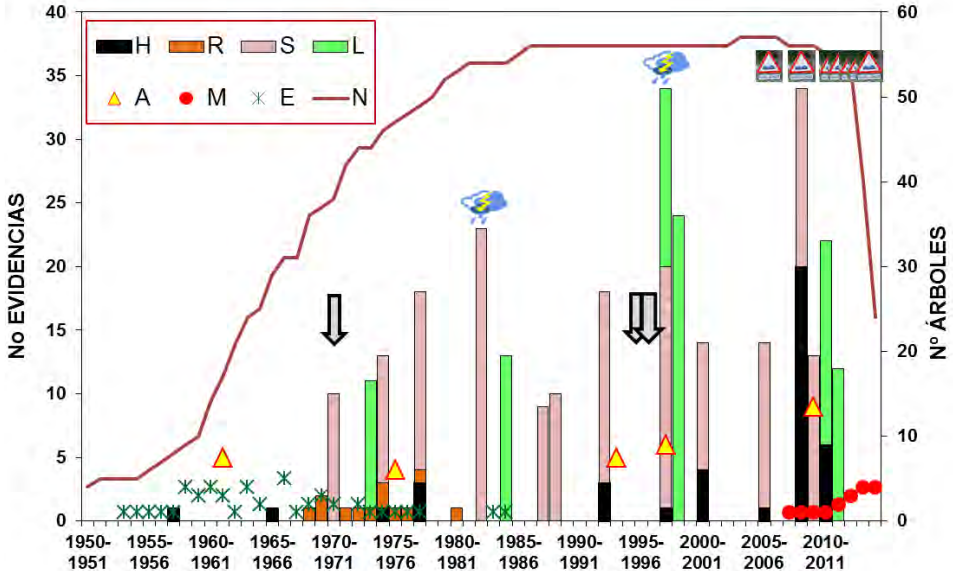

Figure 3. Number of dendrogeomorphological evidence dated in the Portainé ravine. H/M: Injuries and deaths. A: asymmetries in the tree ring sequences. R: development of secondary branches. S/A: supressions or missing rings. L: releases. Clouds: historical data about major rainfalls. Signals: historical data about damages ion infrastructures. Arrows dates related to infrastructures development.

Conclusions on this research:
11 events dated by dendrogeomorphological methods, half of them coinciding with historic events registered since 2006. These results highlight an increased frequency of events in the last decade, which is most likely related to the works made at the headwaters of the basin occupied by the ski station. The major event of 2008 caused the overcoming of a geomorphological equilibrium threshold and, since then, the hydrological behavior of these streams dramatically changed and induced severe erosion and deposition processes.
The geomorphological threshold overcoming and the processes change was clearly enhanced by the increase in peak discharges demonstrated in this work.

This research which is done within the project “Caracterización y Control de Movimientos de Masa. Un Reto para la mitigación del Riesgo Geológico” CGL2013-40828-R, and is developed in collaboration with researchers of the Instituto Geológico y Minero de España (IGME) and Universidad Politécnica de Madrid (UPM).

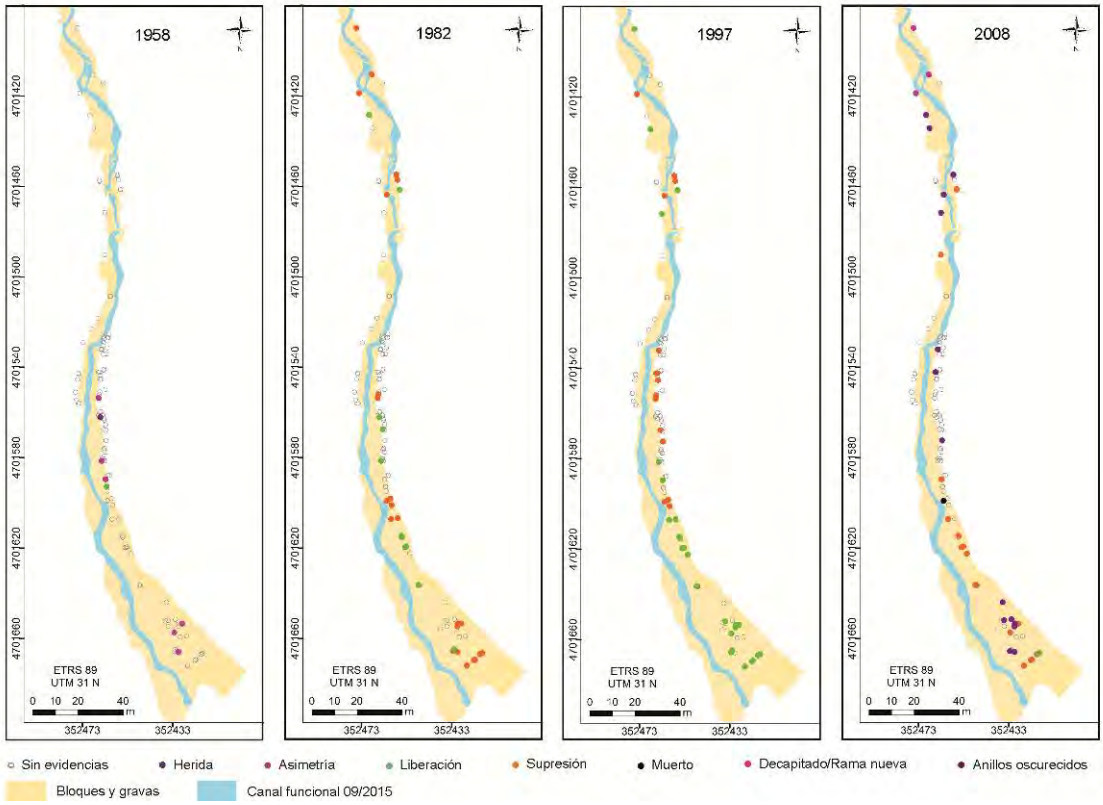

Figure 4. Geomorphological mapping of the study area with geomorphological features and deposits that characterize the alluvial fan, and the location of trees present in the area, the situation of the sampled units and different types of damages at different detected years.

LiDAR data application to the study of the torrential dynamics and evolution of the Portainé and Reguerals streams Eastern Pyrenees.

[1,2]Glòria Furdada, [1,2]Marta Guinau, [1,2]Ane Victoriano, [1,2]Jaume Calvet, [6]Mariló Cabré, [6]Miriam Moysset.

[1] RISKNAT Group, Departament de Dinàmica de la Terra i de l’Oceà, Facultat de Ciències de la Terra, Universitat de Barcelona. C/Martí I Franquès s/n., 08028 Barcelona, Spain
[2] GEOMODELS Institute, Departament de Dinàmica de la Terra i de l’Oceà, Facultat de Ciències de la Terra, Universitat de Barcelona. C/Martí I Franquès s/n., 08028 Barcelona, Spain
[6] ICGC, Institut Cartogràfic i Geològic de Catalunya, Spain.

The Portainé and Reguerals streams (Pallars Sobirà, Lleida) are characterized by a high activity of torrential and debris flows. These events produce significant economic losses in infrastructures, especially where the access road to the Port-Ainé ski station, located in the headwater area, crosses the streams. In order to reduce these impacts, VX-160 sediment retention barrier systems were installed along the channels since

2009 (fig. 5.), but the problem remains. The interference of defense measures with the natural river evolution has resulted in a complex erosion-sedimentation dynamics. 2009 and 2011 LiDAR data series were available in the study. Three events occurred and nine barriers were also installed during this period of time, altering flow dynamics. The spatio-temporal comparison of LiDAR data allows identifying, quantifying and interpreting the river morphological changes. Erosion is widespread along valley bottoms, but it also concentrates in specific areas (margins, lateral landslides and downstream of anthropic structures). Accumulation mainly occurs upstream of anthropic structures and the confluence with the Romadriu River (fig. 6). The mobilized material during this period of time was quantified.

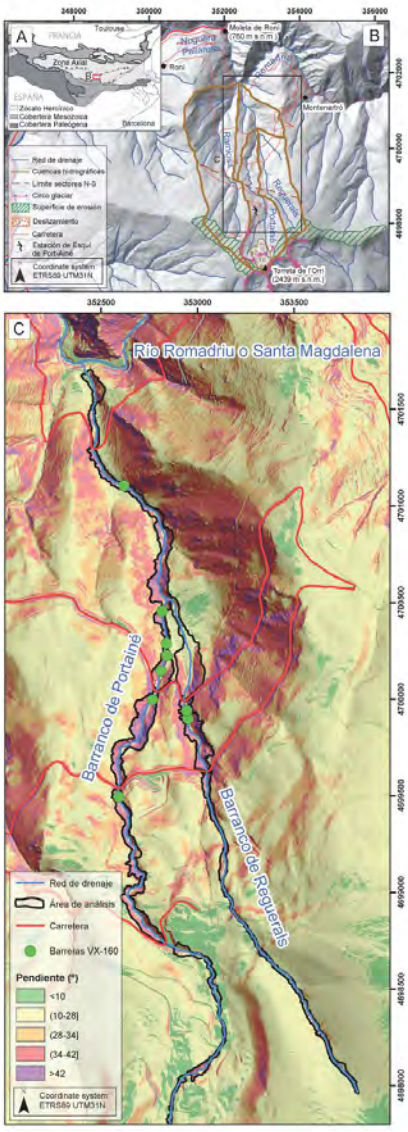

Figure 5. A) Location of the area on the Pyrenees. B) Geomorphological setting of the Portainé basin. C) Slope map with the límits of the studied area, drainage network and location of the sediment retention barrier systems installed between the obtention of the ICGC LiDAR data.

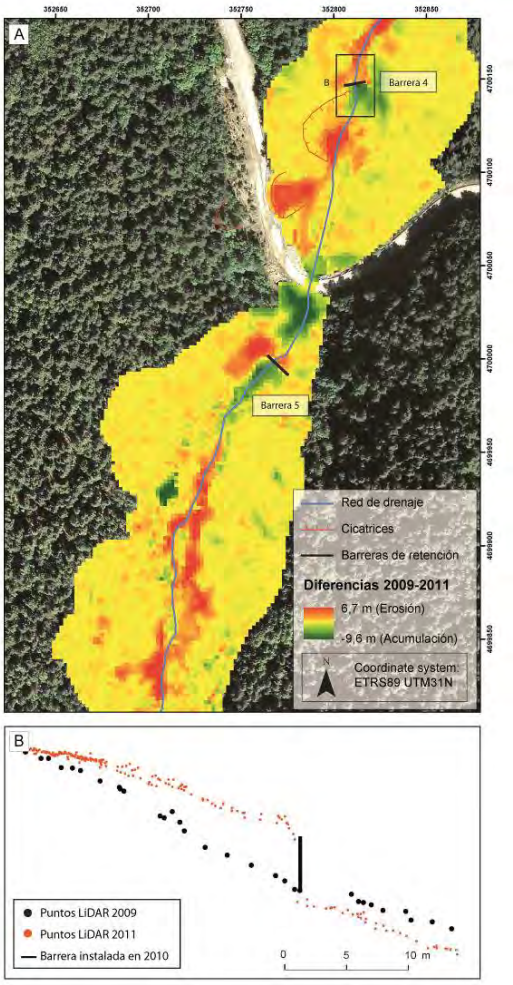

Figure 6. . A) DEM of differences of the medium stretch of the Portainé stream. B) 2009 and 2011 LiDAR points; they correspond to a longitudinal profile of the stream (30 m long and 3 m wide) crossing the barrier 4; the sediment filling of the barrier is clearly observed

Conclusions on this research:
The sediment budget is negative, indicating that part of the eroded material is exported outside the Portainé basin towards the Romadriu River, despite the installed barriers. The results fit with the apparent present erosive tendency of the increasingly entrenched streams. Characterization of this dynamics is essential to understand the geomorphological evolution of the fluvial system, but also to assess the effectiveness of the retention barriers, and therefore for an adequate risk management and mitigation of the area.

This research which is done within the project “Caracterización y Control de Movimientos de Masa. Un Reto para la mitigación del Riesgo Geológico” CGL2013-40828-R, and is developed in collaboration with researchers of the Institut Cartogràfic i Geològic de Catalunya (ICGC).

Implementation of a methodology of risk analysis related to flood hazard: Sud-East Haïtí.

[1,2]Glòria Furdada, [1,2]M. Angels Marqués.

[1] RISKNAT Group, Departament de Dinàmica de la Terra i de l’Oceà, Facultat de Ciències de la Terra, Universitat de Barcelona. C/Martí I Franquès s/n., 08028 Barcelona, Spain
[2] GEOMODELS Institute, Departament de Dinàmica de la Terra i de l’Oceà, Facultat de Ciències de la Terra, Universitat de Barcelona. C/Martí I Franquès s/n., 08028 Barcelona, Spain

The objective of this work is to test, improve and validate an analysis methodology useful to characterize the flood hazard, the Integrated Geomorphologycal Method, by adapting it to the Haití conditions and constraints. In parallwel, this Method is transferred to the Haitian experts by means of formation and collaborative field work.
This Method is specially usefil in context of lack of basic topographical data, hydrological data and detailed DEMs, needed to simulate floods with hydraulic models. It is a pragmatic method, simple, based on existing data and also the participative approach is valued. it includes the following steps: vertical aerial photointerpretation, fieldwork and geomorphological ‘‘silent witnesses’’, definition of the reference flood, historical data and inquiries, consideration of the anthropic interactions, community workshop, elaboration of the integrated geomorphological map with geomorphological criteria, analysis of the integrated data, interpretation of the hazard level and generation of the hazard map.

Photointerpretation

Photointerpretation

Photointerpretation

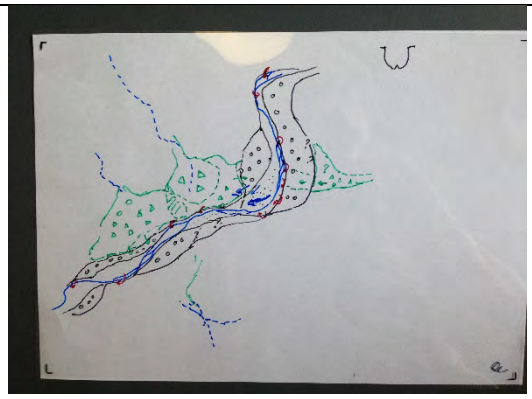

Photointerpretation

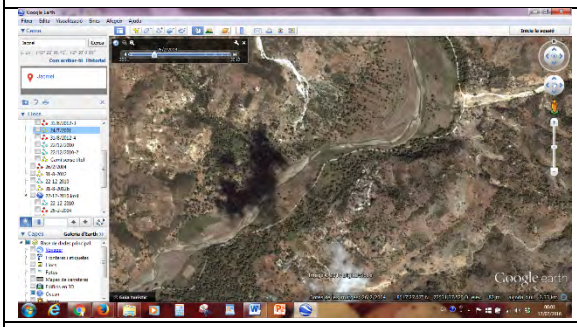

Historical images

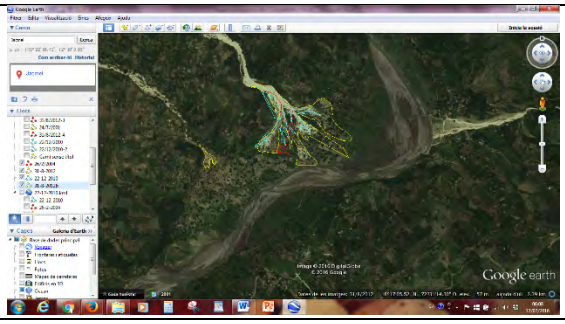

Digitizing of the flood indices

Figure 7. Photointerpretation of all kind of available data in order to generate the integrated geomorphological map

Field work

Field work

Enquiries

Participative approach

Figure 8. Fieldd work, enquiries and participative approach

Conclusions on this research:
The method is very well adapted to the constraints and characteristics of the developing countries and, in addition, it is simple, economic and efficient. The main contribution of the method is the use of detailed orthophotographs as the base of the work as well as the final product. The use of orthophotographs proved very useful both for the development of the work and for the presentation of the final maps. The resulting products are more up-to-date, precise, efficient, and easy to understand than those that could be produced on the available 1:50,000 maps. The first product of the work is the Integrated Geomorphological map, which compiles all the real data obtained. The great value of this map is that it is objective, as far as possible, and it is not subject to change depending on different interpretations. Therefore, it is a map that can always be used as a basis for new interpretations or, in the future, to calibrate calculations made with more sophisticated techniques.

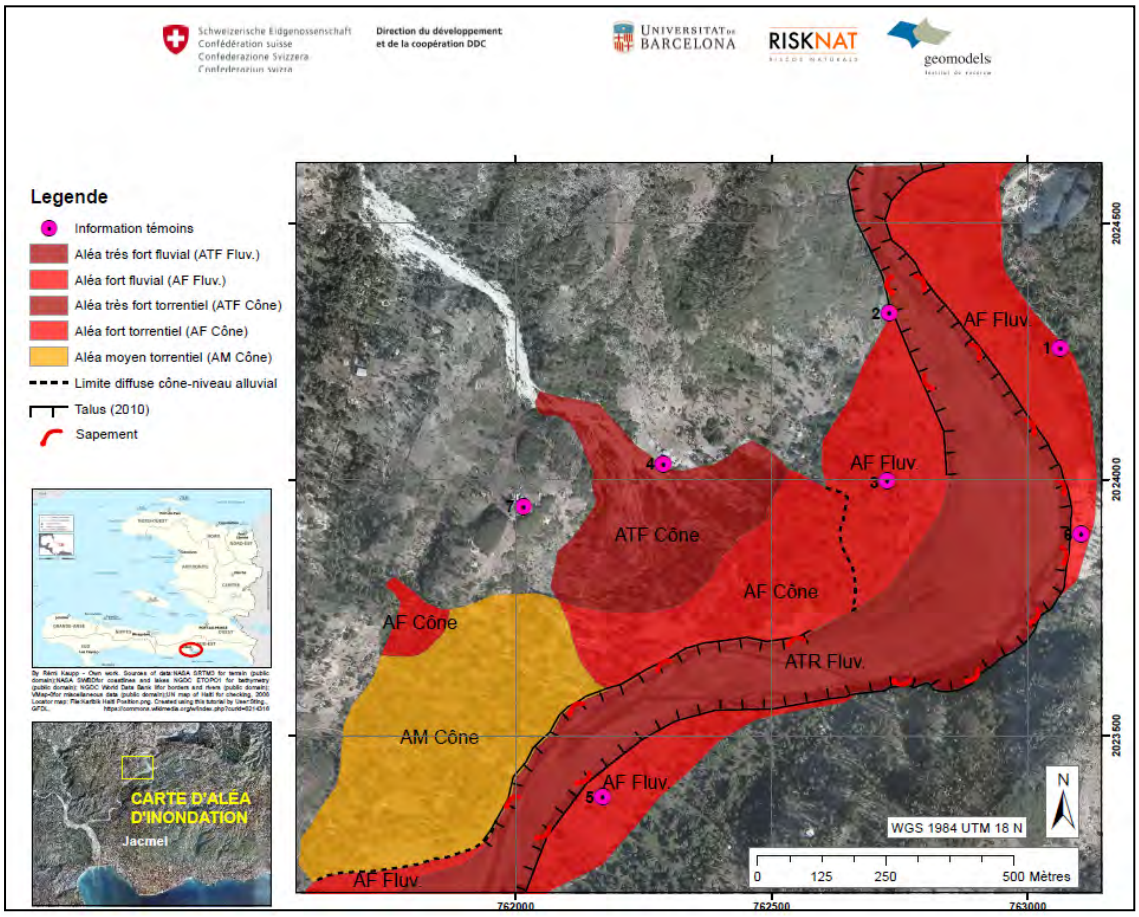

Figure 9. Flood hazard map

Future work

Characterising and dating flash floods and debris flows through dendrogeomorphological methodologies in Portainé stream, Central Pyrenees.
Regarding the torrential activity in the Portainé stream, we are going to continue acquiring and analysing dendrogeomorphological data, in orther to improve the knowledge about the relationship between the events frequency and the man-made changes on the headwaters of the stream. Also, we are going to apply hydrological models at the head of the basin and hydraulic models at the lowest stretch in order to relate dendrochronology, geomorphology and hydraulics.

LiDAR data application to the study of the torrential dynamics and evolution of the Portainé and Reguerals streams Eastern Pyrenees.
The next step is to do the same type of work and compare the new ICGC acquired LiDAR data (2016) in order to obtain an evolution of the erosion and sedimentation and a more complete sediment balance. Also, models are being applied in order to integrate all the existing data.

Implementation of a methodology of risk analysis related to flood hazard: Sud-East Haïtí.
Due to the occurrence of the hurricane Mathew (october 2016) the.continuity of the project is not clearly focused. The firs idea was to integrate knowledge about floods, mass movements (experts fro Switzerland) and droughts (experts from France), in order to put the basis for a sustainable developpement at this Southern Haiti region. Due to the priorities arised because of the hurricane, the focus of future work has to be discussed.

E3. Using seismic signals to characterize mass movements

[1, 2]Suriñach, E., [1,2] Pérez- Guillén, C., [1, 3]Tapia, M., [1, 2]Pere Roig, [1, 2]Khazaradze, G.

[1] RISKNAT Group, Departament de Dinàmica de la Terra i l'Oceà, Secció de Geodinàmica i Geofísica, Facultat de Ciències de la Terra, Universitat de Barcelona, C/Martí i Franquès s/n., 08028 Barcelona, Spain
[2] GEOMODELS Institute, Departament de Dinàmica de la Terra i l'Oceà, Secció de Geodinàmica i Geofísica, Facultat de Ciències de la Terra, Universitat de Barcelona, C/Martí i Franquès s/n., 08028 Barcelona, Spain
[3] Laboratori d'Estudis Geofísics Eduard Fontserè - Institut d'Estudis Catalans (LEGEF-IEC), Barcelona 08001. e-mail: mtapia@iec.cat

Introduction

Our group is interested in take advantage of the information contained in the seismic signals generated by mass movements to obtain information of the dynamics of the phenomena. We study snow avalanches, debris flows, fall rocks and lahars. The methodology used consist of cartography, modelling and physic-mathematical analysis of seismic and infrasound signals generated by avalanches.

Work done

Seismic characterisation of lahars at Volcán de Colima, Mexico

[1]VázquezR., **[2,3] Suriñach, E.,** [1]Capra, L., [4] Arámbula-Mendoza R., [5] Reyes-Dávila G.

[1] Centro de Geociencias, UNAM-Campus Juriquilla, Blvd. Juriquilla No. 3001, C.P. 76230, Querétaro, México
[2] Grup d'Allaus (RISKNAT Group), Departament de Dinàmica de la Terra i l'Oceà, Secció de Geodinàmica i Geofísica, Facultat de Ciències de la Terra, Universitat de Barcelona, C/Martí i Franquès s/n., 08028 Barcelona, Spain
[3] GEOMODELS Institute, Departament de Dinàmica de la Terra i l'Oceà, Secció de Geodinàmica i Geofísica, Facultat de Ciències de la Terra, Universitat de Barcelona, C/Martí i Franquès s/n., 08028 Barcelona, Spain
[4] Facultad de Ciencias, Universidad de Colima, Av. Bernal Díaz del Castillo No. 340, Col. Villas San Sebastián, C.P. 28045, Colima, Colima, México
[5] Centro Universitario de Estudios e Investigaciones en Vulcanología, Av. Bernal Díaz del Castillo No. 340, Col. Villas San Sebastián, C.P. 28045, Colima, Colima, México

Abstract

Volcán de Colima is one of the most active volcanoes in Mexico, not only for its eruptive history, but also for its annual occurrence of lahars. This makes the volcano a natural laboratory for the monitoring and study of lahar processes. Since 2011 monitoring instruments have been deployed along the highly active Montegrande ravine, with at least three lahar events per year. Here we report the datasets of three events collected during the 2012 and 2013 seasons and interpret our findings. An event classification scheme based on lahar magnitude, duration and seismic characteristics is presented to distinguish "single-pulse" events (SPEs) from "multi-pulse" events (MPE). SPEs lasted approximately 60 minutes, had average velocities of ~2 m/s and mean peak discharges of ~24 m^3/s. MPEs endured for more than 3 hours, reached mean velocities of ~4.5 m/s and peak discharges of ~60 m^3/s (related to block-rich surges). The

analysis of the seismic signals also allowed us to discriminate among the physical flow fluctuations of the lahars, i.e. between the block-rich fronts and the variations in flow discharge. The exponential regression analysis conducted, showed a best fit with correlation coefficients around 0.93 and exponential coefficients of ~0.01 s for the block-rich fronts, with increasing seismic amplitudes from 4.8 $\times$ 10^{-4} to 2.3 $\times$ 10^{-3} m/s and frequency ranges from 10 to 20 Hz; the variations in flow discharge showed a distinguishable tendency, rather linear, with lower amplitudes of ~5.7 $\times 10^{-4}$ m/s compared with the block-rich fronts and ranges of frequencies of 10-40 Hz. The results presented in this paper demonstrate that it is feasible to describe and discriminate types of flows and fluctuations among them using mainly the seismic records of events, which represent a useful investigation tool for those events which lack direct observation, but having a record of seismic data with which to be analysed. Considering this, it could be feasible to propose an early warning system to help civil protection authorities in hazard mitigation strategies.

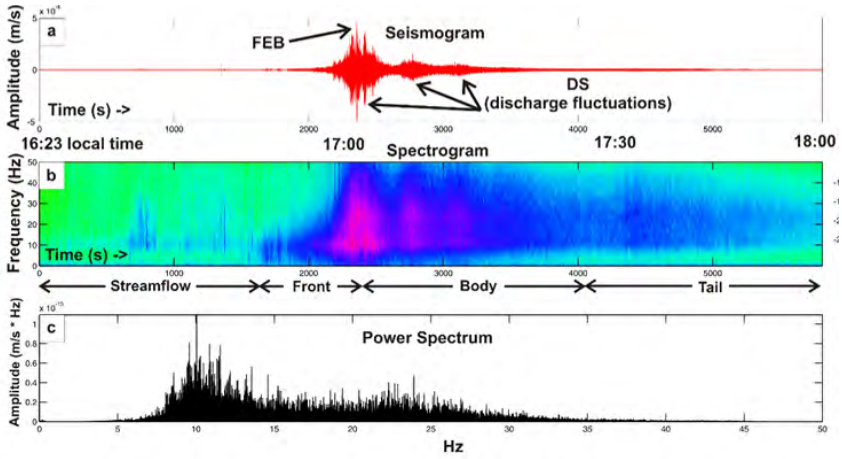

Contribution of the cross- correlation of seismic and infrasound waves generated by snow avalanches to the knowledge of their temporal evolution and characteristics.

[1, 2] Suriñach, E., [1, 2] Pérez- Guillén, [1, 3] C., Tapia, M., [1, 2] Khazaradze, G. and [1, 2] Roig, P.

[1] Grup d'Allaus (RISKNAT), Departament de Dinàmica de la Terra i l'Oceà, Secció de Geodinàmica i Geofísica, Facultat de Ciències de la Terra, Universitat de Barcelona, C/Martí i Franquès s/n., 08028 Barcelona, Spain

[2] GEOMODELS Institute, Departament de Dinàmica de la Terra i l'Oceà, Secció de Geodinàmica i Geofísica, Facultat de Ciències de la Terra, Universitat de Barcelona, C/Martí i Franquès s/n., 08028 Barcelona, Spain

[3] Laboratori d'Estudis Geofísics Eduard Fontserè - Institut d'Estudis Catalans (LEGEF-IEC), Barcelona 08001. e-mail: mtapia@iec.cat

Abstract

Snow avalanches are a source of waves that are transmitted through the ground and the air. These wave fields are detected by seismic and infrasound sensors. During the winter seasons 2008 -2016, a good quality database of avalanches was acquired at Vallée de la Sionne (VDSL, Switzerland) test site with an accurate instrumentation. These avalanches were both natural and artificially triggered and were of varying types and sizes. Distances involved were 0.5 -3 km. Seismic signals were acquired using three seismometers (3-components, 1Hz) spaced 600 m apart along the avalanche track. One infrasound sensor (0.1Hz) and one seismometer (3-components, 1Hz) were placed one next to the other with a common base of time on the slope opposite the path. The data base obtained enables us to compare the different signals generated. Differences in the frequency content and shape of the signals depending on the type and size of the avalanche are detected. A clear evolution of the recorded seismic signals along the path is observed. The cross correlation of the infrasound and seismic signals generated by the avalanches allows us to determine different characteristics for powder, transitional and wet

avalanches concerning their wave fields. The joint analysis of infrasound and seismic waves enables us to obtain valuable information about the internal parts of the avalanche as source of each wave field. These results have repercussions on avalanche dynamics and on the selection of the appropriate avalanche detection system.

Recovering the seismic energy transmitted to the ground by snow avalanches.

[1,2] Emma Suriñach, [3,5] Anne Mangeney, [3,4] Clara Levy and [1,2]Pere Roig

[1] Grup d'Allaus (RISKNAT), Departament de Dinàmica de la Terra i l'Oceà, Secció de Geodinàmica i Geofísica, Facultat de Ciències de la Terra, Universitat de Barcelona, C/Martí i Franquès s/n., 08028 Barcelona, Spain
[2] GEOMODELS Institute, Departament de Dinàmica de la Terra i l'Oceà, Secció de Geodinàmica i Geofísica, Facultat de Ciències de la Terra, Universitat de Barcelona, C/Martí i Franquès s/n., 08028 Barcelona, Spain
[3] Institut de Physique du Globe de Paris, CNRS UMR 7154, Université Paris Diderot-Paris 7, Paris, France,
[4] Bureau des Recherches Géologiques et Minières, Orleans, France,
[5] ANGE team, CEREMA, INRIA, Laboratoire Jacques-Louis Lions, Paris, France,

Abstract

The energy transmitted into the ground by flowing snow avalanches was estimated by using the seismic signal recorded at two different sites by UB LE-3D/5s seismic sensors. One sensor was located on the avalanche path, so that the avalanche passes over it. The second one was placed at about 400 m from the runout zone. The energy was recovered at each position of the path taking into account the attenuation factors (intrinsic attenuation and geometrical spreading) as in Vilajosana et al. (2008). Seismic characteristics of the ground, Digital Elevation Model of the area were taking into account for this calculation. The coincidence of the recovered energy at each position coming from the two sensors validates the approach.
We then simulated the avalanches that occurred in 2004-2008 at the Ryggfonn experimental site (Norway) (Gauer and Kristensen, 2016) using the data obtained in collaboration with the Norwegian Geotechnical Institute. Dense and Mixed (artificially triggered and spontaneous) avalanches of large and medium size were studied. Video images and characteristics of the snow helped in the determination of the characteristics of the avalanches. The approximate length of the path was 2 km and the vertical drop was 900 m. The transmitted energy shows a good correspondence with the outputs of the SHALTOP numerical model that we used to simulate the snow avalanche along the real topography. We also show a correlation between the seismic energy and the fluctuations of the topography along the avalanche path. Moreover, for the two sites and different parts of the avalanche we recovered similar power laws relating the seismic energy and the signal duration than those observed in a very different environment with different gravitational flows (i. e. rockfalls and pyroclastic flows in La Réunion by Hibert et al., 2011 and Montserrat by Levy et al., 2015).

Characterization of snow avalanches applying the Hough transform to the spectrograms of the seismic signals generated by the avalanches.

[1]Elsa Leticia Flores Márquez, [2,3] **Emma Suriñach**

[1]Instituto de Geofísica de la Universidad Nacional Autónoma de México. Circuito Institutos S/N, C. U. 04510 Mexico D. F.
[2] Grup d'Allaus (RISKNAT), Departament de Dinàmica de la Terra i l'Oceà, Secció de Geodinàmica i Geofísica, Facultat de Ciències de la Terra, Universitat de Barcelona, C/Martí i Franquès s/n., 08028 Barcelona, Spain
[3] GEOMODELS Institute, Departament de Dinàmica de la Terra i l'Oceà, Secció de Geodinàmica i Geofísica, Facultat de Ciències de la Terra, Universitat de Barcelona, C/Martí i Franquès s/n., 08028 Barcelona, Spain

Abstract

The ground motion generated by a snow avalanche is a complex natural phenomenon produced by the interaction of the avalanche with the snow cover and the terrain. The interest in the application of seismic methodology to the field of avalanche research has increased considerably due to the advantages of providing data from remote areas at a relative low economic cost.
While much progress has been made in the field, is still much to do in the study of the dynamics of snow avalanches. We present a first attempt to characterize quantitatively some patterns of the spectrograms of the seismic signals obtained from different types (powder, transitional and wet) of snow avalanches. Specifically, in the triangle shape obtained at the beginning of the spectrograms when the avalanche is approaching to the seismic sensor. We are interested in the determination of the exponential low, based on the Generalized Hough Transform (GHT), which is related to the approaching speed of the avalanche to the sensors.
The proposed methodology is an interactive method to quantify the slope of the images of the spectrogram by using Hough transform; its advantage is the easy algorithm that allows finding a numerical relationship between the spectrogram and the type of avalanche. As deduced from these preliminary approaches, we can conclude that exist a range of velocities inherent to the type of materials forming the avalanches.

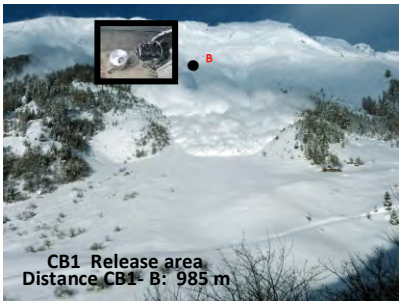

Powder/transitional avalanche

Wet avalanche

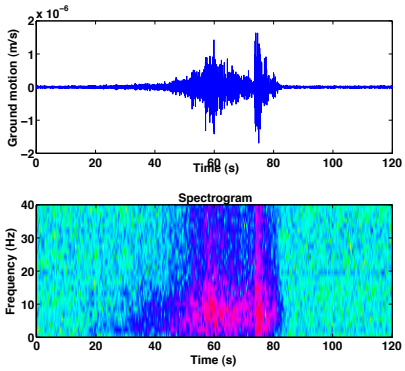

Example of a seismic signal and spectrogram of a powder snow avalanche

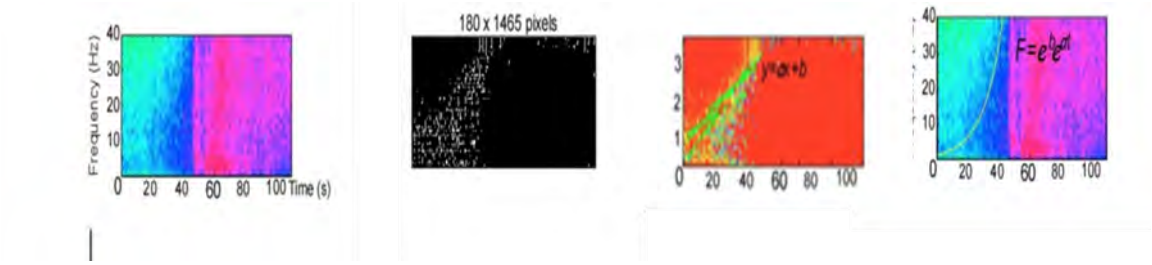

Example of the Application of the Generalized Hough Transform (GHT) to the spectrogram of a seismic signal generated by a snow avalanche

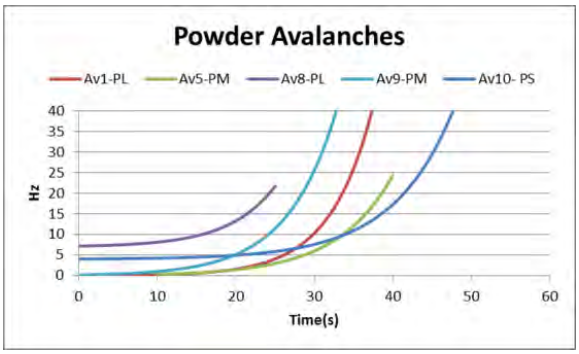

Result of the process: different curves corresponding to different sized powder snow avalanche

Snow avalanches studies using seismic signal and numerical modelling tools

[1, 2] Roig P., [1, 3]Tapia, M., [1,2] Pérez- Guillén, C. [1, 2]Suriñach, E.

[1] Grup d'Allaus (RISKNAT), Departament de Dinàmica de la Terra i l'Oceà, Secció de Geodinàmica i Geofísica, Facultat de Ciències de la Terra, Universitat de Barcelona, C/Martí i Franquès s/n., 08028 Barcelona, Spain
[2] GEOMODELS Institute, Departament de Dinàmica de la Terra i l'Oceà, Secció de Geodinàmica i Geofísica, Facultat de Ciències de la Terra, Universitat de Barcelona, C/Martí i Franquès s/n., 08028 Barcelona, Spain
[3] Laboratori d'Estudis Geofísics Eduard Fontserè (LEGEF-IEC), C. Del Carme, 47. Barcelona 08001, Spain (mtapia@iec.cat)

Abstract

The avalanches investigation group from the University of Barcelona (RISKNAT – UB) manages a seismic and infrasound installation in the experimental site *Vallée de la Sionne*, Switzerland (VDLS), in collaboration with the Swiss Institute for Snow and Avalanche Research (SLF). Using the seismic data, the avalanches investigation group achieve to know velocities, dissipated energy, recognise the flow type and determinate the avalanche dimension. The seismic signal only shows information from the inner and denser parts of the flow. The infrasound signal shows information from the outer and less dense parts of the flow, completing its observation.
RAMMS is a 3D mass movement modelling software developed by the SLF. It uses the hydraulic Voellmy-Salm model and only represents the dense part of the snow avalanches. This study wants to incorporate the seismic data as an external observer of the avalanches for improving and validating the synthetic models generated with RAMMS, trying to assimilate the modelled flow as much as we can with the observed flow. Using all the available field information, two reference avalanches are modelled, as precise as we could.
From the temporal relation between the modelled flow data and the seismic data, and thanks to radar data, we achieve to validate or dismiss the generated model.

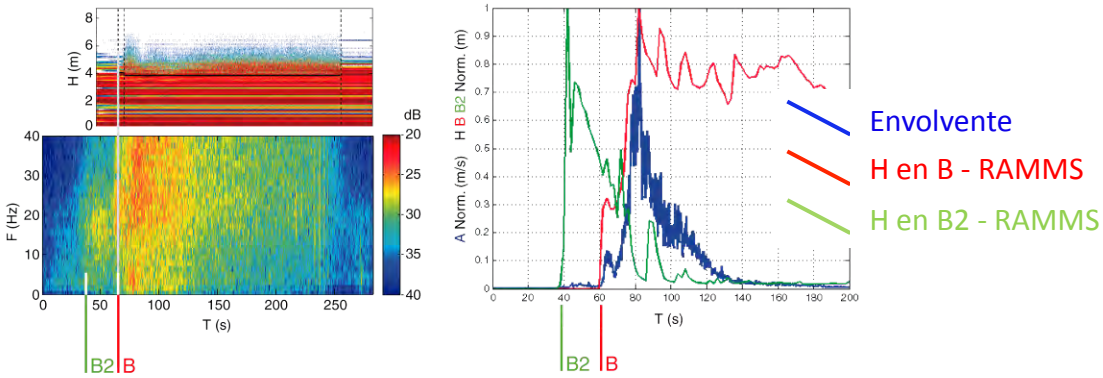

Example of the output of avalanche RAMMS modelling compared to the seismic and radar data.

Advanced seismic methods applied to the study of Snow avalanche dynamics and avalanche formation

[1,2] Cristina Pérez-Guillen

[1] Grup d'Allaus (RISKNAT), Departament de Dinàmica de la Terra i l'Oceà, Secció de Geodinàmica i Geofísica, Facultat de Ciències de la Terra, Universitat de Barcelona, C/Martí i Franquès s/n., 08028 Barcelona, Spain

[2] GEOMODELS Institute, Departament de Dinàmica de la Terra i l'Oceà, Secció de Geodinàmica i Geofísica, Facultat de Ciències de la Terra, Universitat de Barcelona, C/Martí i Franquès s/n., 08028 Barcelona, Spain

Abstract

Snow avalanches are extended moving sources of infrasonic and seismic energy. The acoustic and seismic wave fields generated by an avalanche are a complex natural phenomenon produced by the interaction of the flow with its environment. Seismic waves are mainly generated by friction and the impacts of the flow on the snow cover and terrain features; whereas the infrasound waves are generated by the interaction of the powder cloud with the air. Nowadays, avalanches are recorded using seismic and infrasound sensors that provide data that can be used to obtain information about the characteristics of the source and the basis processes that govern avalanche dynamics such as erosion and deposition. So far, the knowledge of how all these dynamical processes and the inherent characteristics of avalanches affect the signatures of the signals is limited and thus more quantitative data are require. Additionally, seismic and infrasonic monitoring systems can provide information on the avalanche triggering mechanisms such as, for example, the shaking produced by an earthquake. Few earthquake-generated avalanches have been documented to date, all of them visually or statistically identified. Hence, a complete dataset of such events does not exist. This study aims to enlarge the current application of seismic methods, mainly for snow avalanche research, which in turn, is relevant to improve monitoring systems. A catalogue of thirty-three snow avalanches of different natures is analysed using the seismic signals recorded with a set of seismic sensors at the Vallée de la Sionne test site in Switzerland. A comparative analysis of the seismic measurements and data acquired with other instrumentation such as infrasound sensor, several frequency-modulated continuous wave radars, and weather stations, is presented in each case to complement and validate the results.

This thesis presents novel contributions using seismic methods in the research field of avalanche dynamics and in the field of avalanche formation, specifically in the field of avalanche induced by earthquakes. As a first step, the joint analysis of seismic and infrasound data, correlated with radar measurements, provides data of the onset of an avalanche with the arrival of an earthquake. Seismic data were used to quantify energy parameters and changes in the elastic stress field within the snowpack due to the earthquake. This event was compared with two stronger earthquakes that did not trigger any avalanche. The study was complemented by nivo-meteorological data and snow cover simulations. I conclude that when the snowpack is only marginally stable, then the displacement caused by even a small earthquake could be enough to trigger an avalanche. In addition, the analysis of the other two, even stronger, earthquake shows that in stable conditions no avalanche was triggered.

Furthermore, in order to better understand the connection between seismic signals and avalanche dynamics, I quantify the seismic signals in a set of seismic indices. For each seismic signal, the duration, peak ground velocity of the envelope, and both the intensity and the frequency content were compared with the avalanche flow regimes and the thicknesses of the snow cover measured using radar measurements, as well as with the avalanche size. The frequency content of the seismic signal can be used to infer the avalanche flow regime and to characterize its internal parts. Furthermore, the seismic signal duration can be correlated to the avalanche size. If the snow cover absorption does not significantly weaken the intensity of the signal, the avalanche size can also be deduced from the peak ground velocity and its intensity. These results show that avalanche characteristics can be feasible inferred using only seismic data. Such analysis can be usefully employed in avalanche monitoring and management.

Future work

Using seismic signals to characterize mass movements specially snow avalanche by means of:

- Incorporation of the infrasound measurements to study avalanches of different type and size.
- Development of specific algorithms for the comparison of seismic signals and infrasound signals.
- Collection of avalanche data in VDLS experimental site.
- Transferring know-how on snow avalanches seismic monitoring to Nagoya University avalanche group through one of the members of our group (C.P-G) because she has a post- doctoral grant there.
- Collaboration with the Instituto de Geofísica, UNAM in the development and application of mathematical methods to extract information of the seismic signals generated by avalanches
- Collaboration with the IPG Paris with the aim to evaluating the energy released by the snow avalanches in comparison to other mass movements
- Collaboration with the IPG Paris with the aim to validate avalanche modelling using SHALTOP program.
- Collaboration with SLF (Davos) with regard the use of seismic signals to validate avalanche modelling using RAMMS

Conclusions

The use of seismic signals to characterize mass movements permits:

- Seismic characterisation of lahars at Volcán de Colima, Mexico
- Contribution of the cross-correlation of seismic and infrasound waves generated by snow avalanches to the knowledge of their temporal evolution and characteristics.
- Recovering the seismic energy transmitted to the ground by snow avalanches.
- Characterization of snow avalanches applying the Hough transform to the spectrograms of the seismic signals generated by the avalanches.
- Snow avalanches studies using seismic signal and numerical modelling tools

Collaborations:

- WSL Institute for Snow and Avalanche Research SLF, Flüelastrasse 11, CH-7260 in Vallée de la Sionne experimental site. Incorporation of the infrasound measurements to study avalanche different its type and size. Collecting avalanche data in VDLS experimental site. Experiments participation.
- Centro de Geociencias, UNAM-Campus Juriquilla, Blvd. Juriquilla No. 3001, C.P. 76230, Querétaro, México. Paper on lahar seismic signals interpretation.
- Instituto de Geofísica, UNAM in the development and application of mathematical methods to extract information of the seismic signals generated by avalanches.2 weeks of E. Leticia Flores in UB. Member of the Jury of PhD. Thesis Cristina Pérez-Guillén.
- Collaboration with the IPG Paris with the aim to evaluating the energy released by the snow avalanches in comparison to other mass movements and validation of avalanche modelling using SHALTOP. 2 weeks stay of Pere Roig in Paris
- Collaboration with SLF (Davos) with regard the use of seismic signals to validate avalanche modelling using RAMMS. 1 week stay of Pere Roig in Davos
- Laboratori d'Estudis Geofísics Eduard Fontserè (LEGEF-IEC), C. Del Carme, 47. Barcelona 08001, Spain. One of the members of our group (M.T.) belongs to this institution. She collaborates in the seismic research.

F Estudi i incorporació de dades geofísiques

Analysis and incorporation of geophysical data

geomodels
institut de recerca

Magnetotelluric characterization of the Alhama de Murcia Fault (Eastern Betics): preliminary results

[1]Anna Martí, [1]Pilar Queralt, [1]Juanjo Ledo, [1]Alejandro Marcuello, [2]Julen Alvarez-Aramberri, [3]José Jesús Martínez-Diaz

[1]Departament de Dinàmica de la Terra i de l'Oceà, GEOMODELS Research Institute, Facultat de Ciències de la Terra, Universitat de Barcelona, c/Martí i Franquès s/n 08028, Barcelona, Spain.
[2]BCAM - Basque Center for Applied Mathematics, 48009 Bilbao, Spain
[3]Departamento de Geodinámica, Facultad de Ciencias Geológicas, Universidad Complutense, 28040 Madrid, Spain

Abstract

The Lorca Earthquake (11/5/2011, Mw 5.2) stands as the most destructive in Spain over the last 50 years. It was interpreted as having occurred in an intersegment zone of the strike-slip Alhama de Murcia Fault (AMF). The project "Intergeosima" is carrying on a multi parametric characterization and monitoring of the fault structure aiming to develop a future Near Fault Observatory (NFO). We present preliminary results of a magnetotelluric (MT) survey carried out along the Rambla de la Torrecilla (SW of Lorca) to characterize the electrical resistivity of the AMF, to constrain the information from the borehole drilled in the area, and to extend the geological interpretation SE of the fault gauge.

Geodynamic and geophysical settings

The AMF is a left lateral strike-slip fault located at the eastern part of the Internal Betics (figure 1). The major tectonic complexes (Nevado-Filábride, Alpujárride and Maláguide) were reactivated through low-angle normal faults subject to regional extensional tectonics. In the last 9 My a compressional NNW-SSE stress field became dominant and high-angle faults such as the AMF formed, which have been active since Late Miocene. Most of the damaging historical earthquakes (Mw > 6.5) are related to the structure of the AMF (figure 1).

The 3D structure of the AMF is being characterised through LIDAR, ERT, and seismics. The borehole FAM-1 (174 m) drilled in the shear zone with the highest exhumation rate, and several trenches allowed to determine that the fault gouge has a minimum width of 150 m and dips 70º NW. From NW to SE the observed units are a wide damage zone affecting paleozoic graphitic schists (Alpujárride), a clay-rich fault gouge containing graphite, a block of unaltered protolith (schist), a melange of blue-gray phyllite fault gauge with Miocene marls, Miocene sandstones and Quaternary alluvial limes and gravels. In order to better constrain this interpretation and to obtain more information on the structure under the Quaternary deposits, an MT survey was carried out (figure 1).

Magnetotelluric Survey in the Rambla de la Torrecilla (SW Lorca)

MT data were acquired across the AMF at 15 sites (figure 1). Time series were recorded using Metronix systems, measuring horizontal electric and magnetic fields at different sampling rates, with a total duration between 2 h and 18 h. Some pairs of stations were recorded simultaneously, with magnetic sensors in only one of both. The location of the survey is close to the highway and an industrial zone hence the time series were highly affected by noise. To mitigate this effect, some sites were recorded

over night, when anthropogenic activity is lower and which allowed to get enough samples and better statistics for the data processing. The contact resistivity between the electrodes and the soil presented high values, due to the low compaction of the terrain.

Time series were processed using Mapros and MTproc Metronix software based on a robust method. Data with poor quality were removed and the resulting transfer functions correspond to a period range between 10^{-3} s and 1s to 10 s (and 100 s at some sites). Dimensionality analysis shows that data have 3D effects althought fitting data to a NE-SW direction (geological strike) shows a similar mistift. Hence, responses were rotated 45º E in order to invert and obtain a geoelectrical model. Static shift was also corrected, according to the high contact resistances and ERT data.

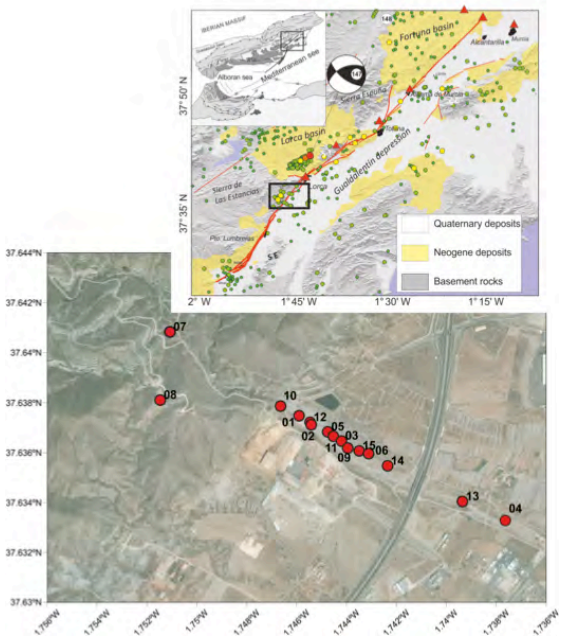

Figure 1: Top: Inset and geological map of the AMF (red) with shallow historical earthquakes (circles), damaging historical ones (red triangles) and Mw 5.2 Lorca focal mechanism. Labels 147 and 148 indicate the location of long period MT data previously acquired in the Sierra de las Estancias. Black rectangle limits the survey area of this study (modified from Martínez-Díaz et al. 2016). Bottom: Aerial view of the rambla de la Torrecilla area and location of the MT sites.

Geoelectrical model

MT data from 8 central sites and site 7 (Sª Estancias) were inverted (2D Mackie code, Winglink), using TE and TM modes resitivity and phases from 1 ms to 1s, 10% errors in apparent resistivities and 5º error in phases. The mesh used had 114 x 134 cells and topography was taken into account.

The initial resistivity was 1000 ohm·m and the inversion was constrained to values between 1 and 3000 ohm·m. Initial rms was 20 and was reduced to 4.8 after a couple hundred iterations. Figure 2 shows the vertical section of the top 1000 m of the model. Figure 5 shows the pseudosections of measured data and model responses.

An inversion of the determinant data was carried out as well (program ZondMT) in order to delineate the main large scale geoelectrical structure. The resulting model (figure 2, top) presents a top resistive layer (400 m), with a thin conductive body under sites 1 and 2, underlained by a conductive area, with lower resistivity values towards

the WNW. Figure 2 is also completed with the resistivity log from FAM-1 (up to 100 m depth), which shows a decrease of resistivity with depth from approximately 100 ohm·m to 20 ohm·m.

Discussion and conclusions

Below sites 10, 1 and 2 there is a NW dipping sequence (limited by two 70º NW dipping red discontinuous lines) formed by a moderately conductive zone (C1, 200 m thickness), a resistor (R1), and a highly conductive zone (C2) underlain by another moderately conductive zone. We interpret this area as the main fault gouge zone, where resistor R1 is interpreted as a block of palaeozoic protolith.

Below sites 5, 11, 9, 15 and 14, there is a shallow alternation of resistive and conductive zones (RC, blurred area). Given the lack of resolution at the shallowest depths (i.e., at the shortest measurd period, 1 ms, the skin depth for a 100 ohm·m medium is of 150 m), we interpret this area from ERT data, which gives a resistivity of 1000 ohm·m and is linked to the low compacted quaternary deposits. Below these, there is a conductive area (C3), which is interpreted as marls and sandstones. Under it, the resistive (R2) palaeozoic basement appears at between -200 and -300 masl.

The MT study has allowed to differentiate the fault gauge zone and to identify depth of the basement. Further studies will include a joint inversion with ERT data and the acquisition of a new profile.

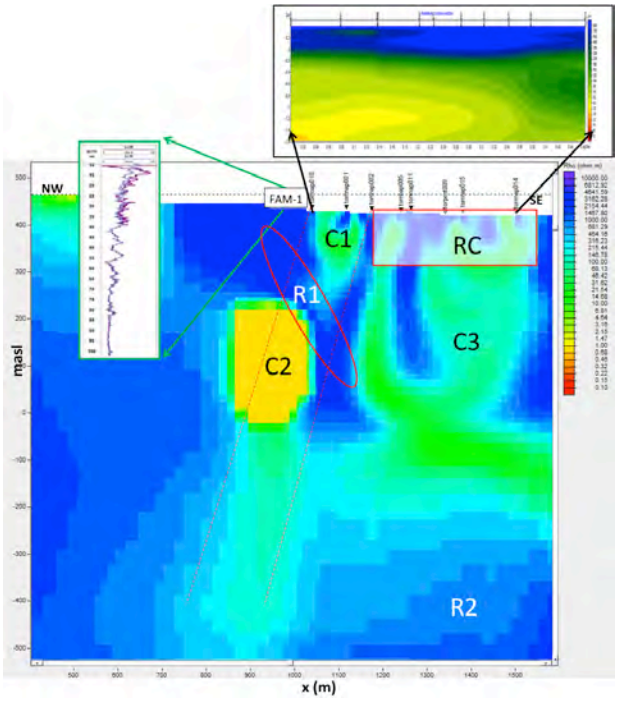

Figure 2: Section of the central part of the 2D geoelectrical model. On top there is the model obtained from the inversion of the determinant. Green arrows point to the resistivity log obtained from the well FAM-1. Conductive (C) and resistive (R) areas are indicated. Red dotted lines mark the fault gouge area.

CSEM monitoring at the Hontomín CO_2 storage site: modeling, experimental design and baseline results

PhD Thesis

[1]*Eloi Vilamajó Llobera*
Advisor: [1]*Pilar Queralt Capdevila*
[1] *Departament de Dinàmica de la Terra i de l'Oceà, GEOMODELS Research Institute, Facultat de Ciències de la Terra, Universitat de Barcelona, c/Martí i Franquès s/n 08028, Barcelona, Spain.*

Abstract

This thesis is devoted to the development of a land-based controlled-source electromagnetics (CSEM) experimental methodology to be applied to the monitoring of CO_2 storage at the Technological Development Plant (TDP) of Hontomín (Burgos, Spain). The main objectives of the thesis are 1) the evaluation of the feasibility of performing a CSEM monitoring at Hontomín, 2) the design of the CSEM monitoring experiment, and 3) the acquisition of the baseline (pre-injection) data set and the processing of the data to obtain the geoelectrical response of the structure.

A modeling experiment has been performed simulating the resistivity changes in the reservoir caused by the storage and evaluating the ability of the method to detect them. The study analyzes the capabilities of different experimental configurations (source/receiver location and relative orientation, emission frequencies...) in order to decide the appropriate configuration in views of the real experiment. The study considered the simulation of an experimental configuration in two different moments of the storage process (pre- and post-injection). It compares the synthetic results obtained in each case and seeks the differences to infer the presence of CO_2. A wide range of scenarios of increasing complexity were simulated, from 1D models with an infinite CO_2 plume to models with a 3D plume in a medium that contains the casings of the injection and monitoring wells and considers the noise conditions at the Hontomín TDP. The CO_2 effect on the synthetic data was analyzed with two different approaches: quantifying the signal caused by the CO_2 on the data, *TLS* (time-lapse signal), and comparing it with the noise conditions in the study area, *D* (detectability). A borehole-to-surface configuration is sensitive to the presence of CO_2, to its saturation and to the relative position source/plume. Furthermore, it was observed that the steel casings installed in the injection and monitoring wells affect the EM propagation from the transmitter to the surface. The study concluded that the CSEM monitoring is suitable at Hontomín given that measurable changes will occur between time-lapsed data sets.

Considering the results obtained in the modeling study, the CSEM monitoring experiment was designed. The baseline acquisition was carried out between April 21st and 26th 2014. A borehole-to-surface configuration was used with three different transmitter dipoles: 1) vertical dipole in the injection well HI (dVED-1), 2) vertical dipole in the monitoring well HA dVED-2), and 3) horizontal dipole using one electrode in each well (dHED). Receivers were distributed at the surface in two different patterns: cross-shape and circular-shape. During each emission, 86 surface dipoles were measuring the electric field.

Data processing focused on the obtaining of the geoelectrical response of the subsurface for each source/receiver configuration and for each processed frequency. To this goal, time series were divided into segments and, for each one, the transfer function between source transmission and receiver electric field were calculated. Experimental data were analyzed in terms of experimental uncertainty (error associated to each measurement) and experimental repeatability.

Experimental results allowed to characterize the geoelectrical response of the Hontomín structure (including steel casings). Baseline data quality is high: experimental errors are lower than 1% in amplitude and 1º in phase for most of the data points. Repeatability is high (differences lower than 1% in most of the cases). Figure 1 shows the results obtained with source dVED-1 in the permanent elèctrodes and Figure 2 presents the experimental uncertainties associated to each data point.

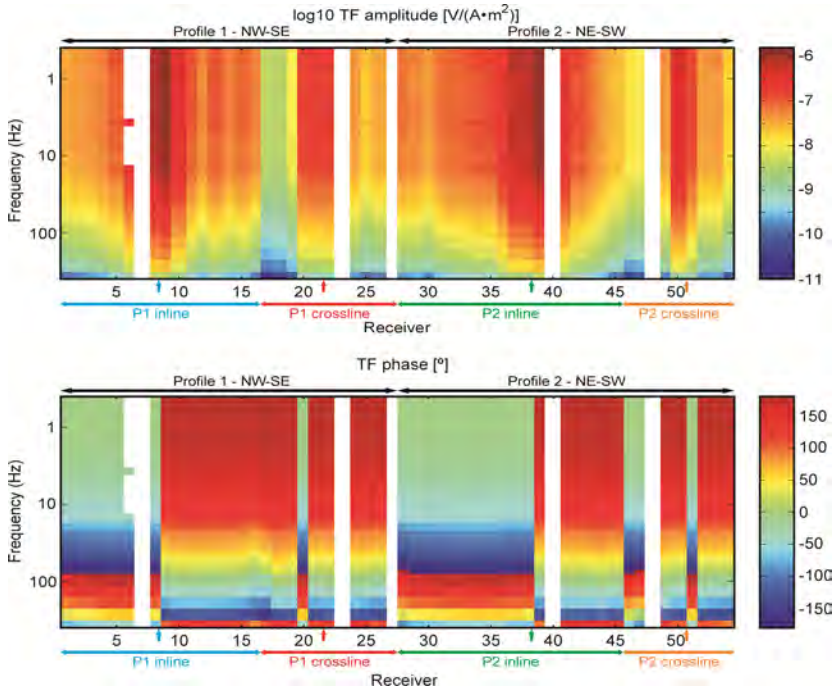

Figure 1. Transfer Function (TF) produced by source dVED-1 at permanent receivers. Top: amplitude data. Bottom: phase data. Results are grouped in inline/crossline data along profiles 1 or 2. Arrows indicate the position of well HI within each group.

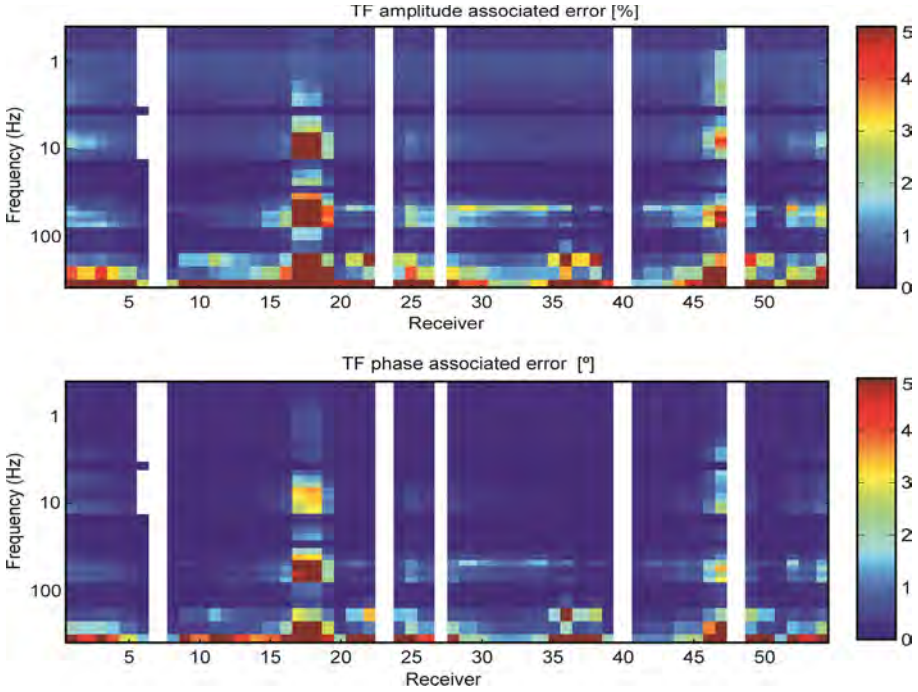

Figure 2. Experimental errors at permanent receivers during emission with source dVED-1. Top: amplitude data. Bottom: phase data. Data collected at profile 1 correspond to receivers 1-16 (inline) and 17-27 (crossline). Data collected at profile 2 correspond to receivers 18-45 (inline) and 46-54 (crossline).

The casing influence over the experimental data was investigated. We tested the hypothesis that a current was induced along the casing of the injection well. To reproduce the experimental behavior of the data, a number of scenarios have been simulated. For low frequencies, the hypothesis can explain the experimental data.

Considering the high data quality obtained and the results of the modeling study, we consider that the CSEM experiment will be able to detect the CO_2-caused resistivity changes in the reservoir after the post-injection repetition of the experiment.

Three-Dimensional Modeling of the Casing Effect in Onshore Controlled-Source Electromagnetic Surveys

[1]Vladimir Puzyrev, [2]Eloi Vilamajó, [2]Pilar Queralt, [2]Juanjo Ledo, [2]Alex Marcuello

[1] Department of Applied Geology, Western Australian School of Mines, Curtin University, Kent Street, Bentley, Perth, WA 6102, Australia
[2] Departament de Dinàmica de la Terra i de l'Oceà, GEOMODELS Research Institute, Facultat de Ciències de la Terra, Universitat de Barcelona, c/Martí´ i Franquès s/n 08028, Barcelona, Spain.

Abstract

The presence of steel-cased wells and other infrastructure causes a significant change in the electromagnetic fields that has to be taken into consideration in modeling and interpretation of field data. A realistic and accurate simulation requires the borehole casing to be incorporated into the modeling scheme, which is numerically challenging. Due to the huge conductivity contrast between the casing and surrounding media, a spatial discretization that provides accurate results at different spatial scales ranging from millimeters to hundreds of meters is required. In this paper, we present a full 3D frequency-domain electromagnetic modeling based on a parallel finite-difference algorithm considering the casing effect and investigate its applicability on the borehole-to-surface configuration of the Hontomín CO2 storage site. To guarantee a robust solution of linear systems with highly ill-conditioned matrices caused by huge conductivity contrasts and multiple spatial scales in the model, we employ direct sparse solvers. Different scenarios are simulated in order to study the influence of the source position, conductivity model, and the effect of the steel casing on the measured data. Several approximations of the real hollow casing that allow for a large reduction in the number of elements in the resulting meshes are studied. A good agreement between the modeled responses and the real field data demonstrates the feasibility of simulating casing effects in complex geological areas. The steel casing of the well greatly increases the amplitude of the surface electromagnetic fields and thus improves the signal-to-noise ratio and the sensitivity to deep targets.

Work done

This article explores the sensitivity of a borehole-to-surface CSEM configuration with a deep electric dipole installed in the injection well and compares the modeling results with the baseline data set collected at the Hontomín CO2 storage site, Spain. We begin with the description of the geophysical setup at Hontomín and the acquired data set. Then we describe the modeling algorithm used to simulate the experimental configuration with an accurate representation of the injection well casing and we conduct a set of numerical simulations, compare them with the real field data and investigate the effect of the source distance to the base of the casing and variations in the resistivity model on CSEM data. Finally, we simulate several post-injection scenarios and the time-lapse changes expected in CSEM data are determined.

In the numerical simulations, the steel casing is represented in a realistic way resulting in the smallest cell dimensions of 8 mm. The casing should feature with many fine elements due to two main reasons: the huge conductivity contrast between the casing and the surrounding media, and the approximation of the curvilinear thin walls of the casing with a staircase finite-difference or a straight-sided finite-element model. The cells gradually grow away from the well, and largest elements along the boundaries of the domain are several kilometers thick. The growth rate of the cells is chosen

empirically to reduce the number of unknowns in the problem and at the same time keep the accuracy of the numerical scheme within reasonable bounds. Figure 1 shows plane XY views of the central part of the discretization grids. The most accurate representation of the casing and tubing (Fig. 1a) has been used in the subsequent simulations. Two approximations (Fig. 1b, c) have been used only to study the accuracy loss and computational gain of using coarse casing representations.

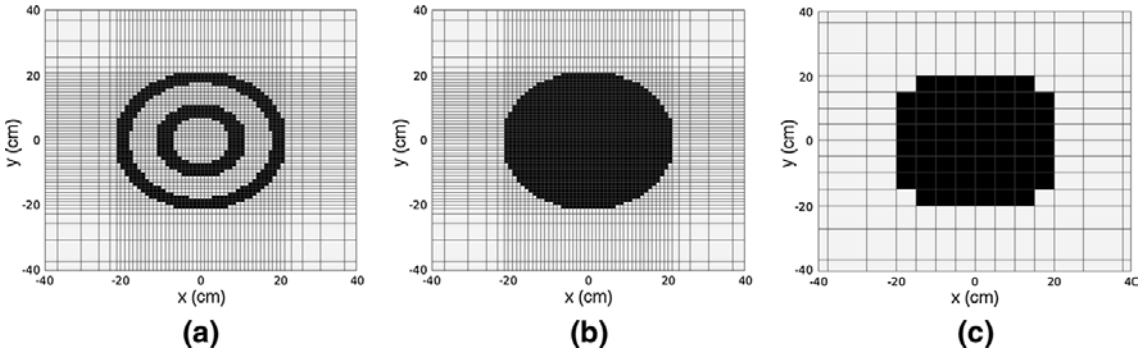

Figure 1. Plane XY view of the discretization grids near the casing. (a) The most accurate representation. (b) The solid casing approximation using the same grid as in the previous case. (c) The solid casing approximation on a coarse grid.

Figure 5 shows the electric field amplitude in the vertical plane y = 0 when the realistic representation of the casing is included in the model. As a source we consider a vertical electrical dipole (VED) located below the HI injection well at a depth of 1500 m. We can see a large amount of current channeling along its casing toward the surface. For the 4-Hz frequency, almost no decay in the amplitude along the casing is observed. For the highest frequency of 128 Hz, the EM signal attenuates more. The casing serves as a channel through which electrical currents flow to the surface and produce large perturbations in the measured surface electric field. In the near-casing zone and up to several hundred meters away, the amplitude of the horizontal electric field is 2–3 orders of magnitude larger than the simulation results without the casing.

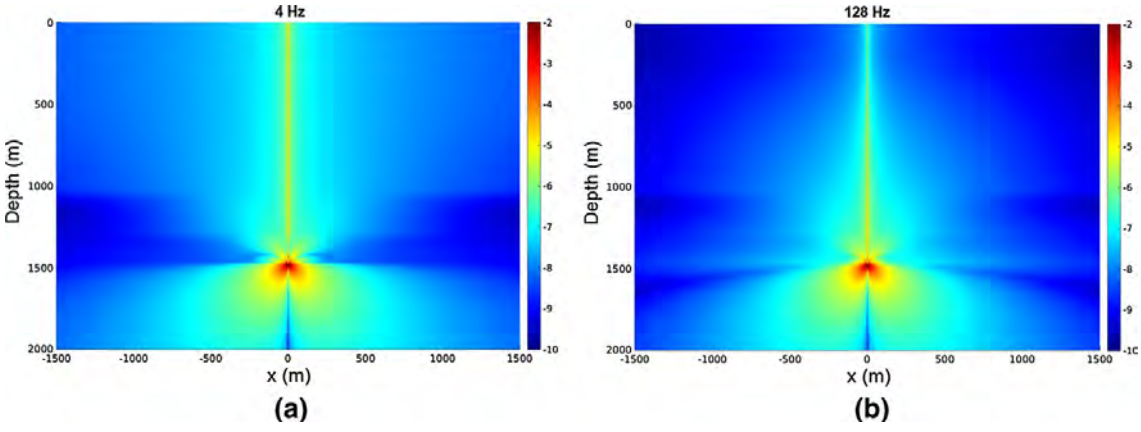

Figure 2. Electric field amplitude at logarithmic scale in the central vertical plane (y = 0) for the case when the casing is included in the model. Results for the frequencies of 4 Hz (left) and 128 Hz (right) are shown.

Figure 3 illustrates dependence of the amplitudes of the surface electric field on the depth of the vertical source. It can be easily noted that when the VED source is located in the vicinity of the well's tubing (1460 m deep), the surface responses are much stronger than for the sources located just 20 and 40 meters deeper. Locating the

vertical electric source closer to the casing results in an increase in the amplitude of the electric field at the surface and can improve the signal-to-noise ratio. We should note that, for all four frequencies, the amplitudes of the real data are located between the curves for the 1460- and 1480-m sources. The real data would be a good match to the simulation results when the VED is located approximately 1470 m deep.

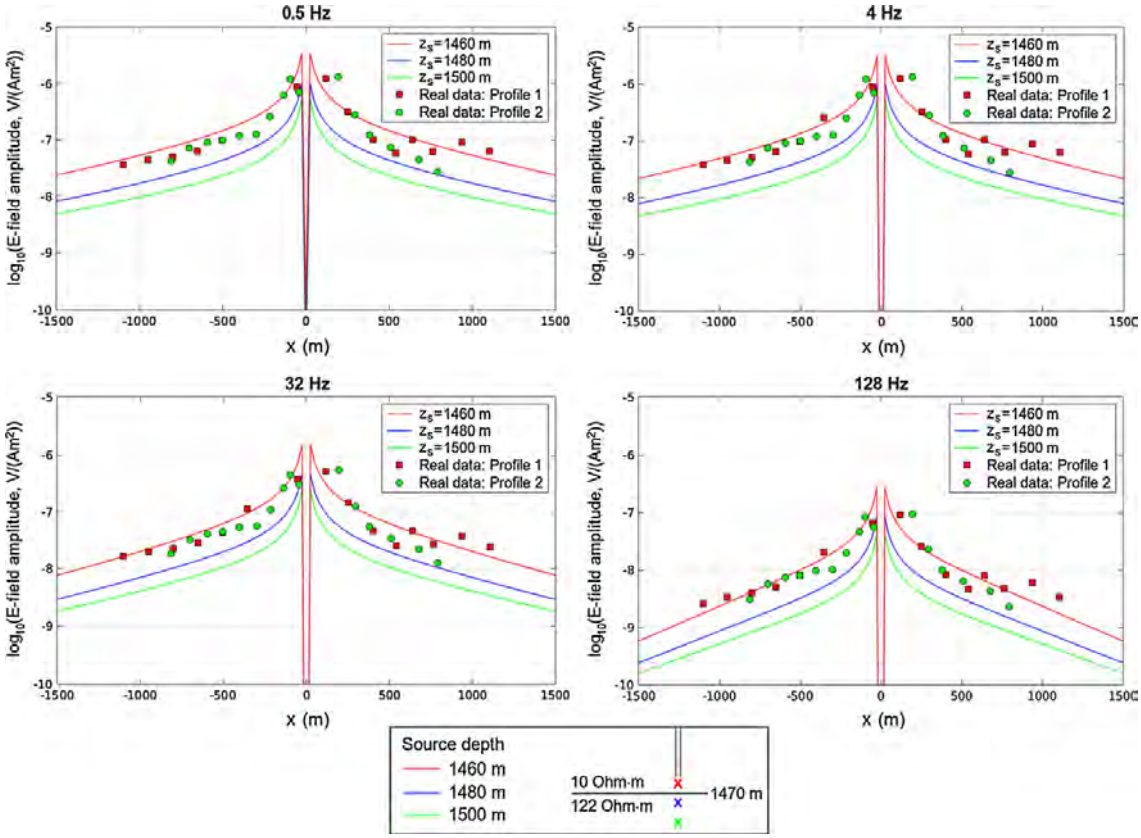

Figure 3. Amplitudes of the horizontal surface electric field for three different source depths (see the sketch at the bottom of the figure) for the frequencies of 0.5 Hz (top left), 4 Hz (top right), 32 Hz (bottom left), and 128 Hz (bottom right).

Conclusions

Realistic 3D modeling of the casing effect on the borehole-to-surface Hontomı´n setup is able to produce results that are quantitatively similar to the real experimental data. Two hypotheses have been proposed and tested to reproduce the experimental data: a lack of knowledge of the exact depth of the source electrodes and an inaccurate characterization of the geoelectrical response. Both of them are able to quantitatively reproduce the experimental data. A combination of these hypotheses may explain the discrepancy between the data and the simulation results.

The casing greatly amplifies the signal and enlarges the signal-to-noise ratio, making the surface measurements more sensitive to conductivity changes near the bottom of the well. In noisy areas, this may greatly increase the efficiency of CO2 monitoring with a borehole-to-surface configuration. This is similar to the results of other studies where the conductive casing is used for better characterization of deep zones using surface-to-surface and surface-to-borehole configurations.

A magnetotelluric study in La Rosa diapir (Murcia, Spain)

E. Górriz, A. Marcuello, F. Escosa, P. Queralt, A. Martí, J. Ledo & E. Roca

GEOMODELS Research Institute, Departament of Dynamics of the Earth and the Ocean, University of Barcelona. C/Martí Franquès s/n, 08028 Barcelona (Spain).

Abstract

The knowledge of salt structures is an important challenge today by its economic implications because they are suitable to accommodate geological reservoirs. However, the singular physical properties of the salt, both electrical and mechanical, give to these structures a high structural complexity. The magnetotelluric (MT) mehod has been proven as a suitable method to characterize these structures to constrain their geodynamic evolution (Rubinat et al., 2010)

In this work La Rosa Diapir has been taken as an example of salt structure because is still active showing an outcrop in good conditions. This diapir is located on Eastern External Prebetic (in Jumilla, SE Spain). The Prebetic Zone of Jumilla is located in the outermost part of Betic Range (Figure 1A and 1B). It is constituted by Mesozoic to Middle Neogene materials detached from the Paleozoic basement by the Triassic evaporites and mudstones. La Rosa Diapir is located northwest of El Carche Mountain, in the junction between the Internal and External Prebetic Zone (Figure 1C). This area represents the most external part of the foreland fold-and-thrust belt in the Betic Cordillera. The extrusion of the diapir is controlled by La Rosa Fault, oriented NW-SE, which belongs to a fault system oblique to the main shortening direction of the Betic System (red faults in Figure 1C). La Rosa Diapir is the largest diapir of the region, with a surface of 5,5 km^2 and a topographic slope of 227 m (Navarro & Rodríguez, 1985), so it has a great relevance to observe its evolution level. Actually, here is located the most productive exploitation of salt in the region from the production of saturated brine. This area is moderately populated and its geological structure is complex. The aim of this work was to perform a MT survey to obtain a first interpretation of the diapir area with this technique.

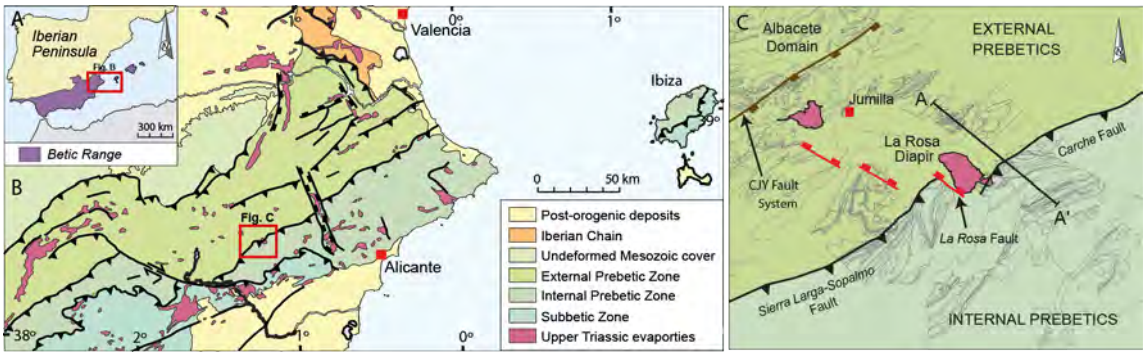

Figure 1. A) Western Mediterranean map indicating the location of the Betic Range in the Iberian Peninsula. Note the red-square pointing out the location of the Eastern Prebetics. B) Geological map of the Eastern Prebetics. C) Structural sketch indicating the orientation of the main structures that are deforming the Prebetic of Jumilla (Eastern External Betics). Note the different colors representing the two different palaeogeographical domains: the Internal Prebetics and the External Prebetic with the Albacete domain.

Work done

In January 2016, the MT data was acquired along a profile perpendicular to the La Rosa Diapir structure and it was 10.6 km-long. A remote MT station was installed 5 km away of the profile to the west. 16 stations were recorded in the profile, and the distance between them was approximately 800 m (red dots in Figure 2). Two different datalogger were used: Metronix ADU06 and Worldsensing Spider. The recording time were between 14 to 24 hours per station. In the measurements the magnetometers and the dipoles were along NS and EW directions. As it was pointed before the area is moderately populated and some EM sources that can affect MT data were identified: a 400kV power line (green dashed line in Figure 2), which runs approximately parallel to the profile (the MT stations were located from it as far as possible, >0.5 km), houses and farms in the basin, and a plant exploitation of salt in the diapir, JUMSAL, S.A.

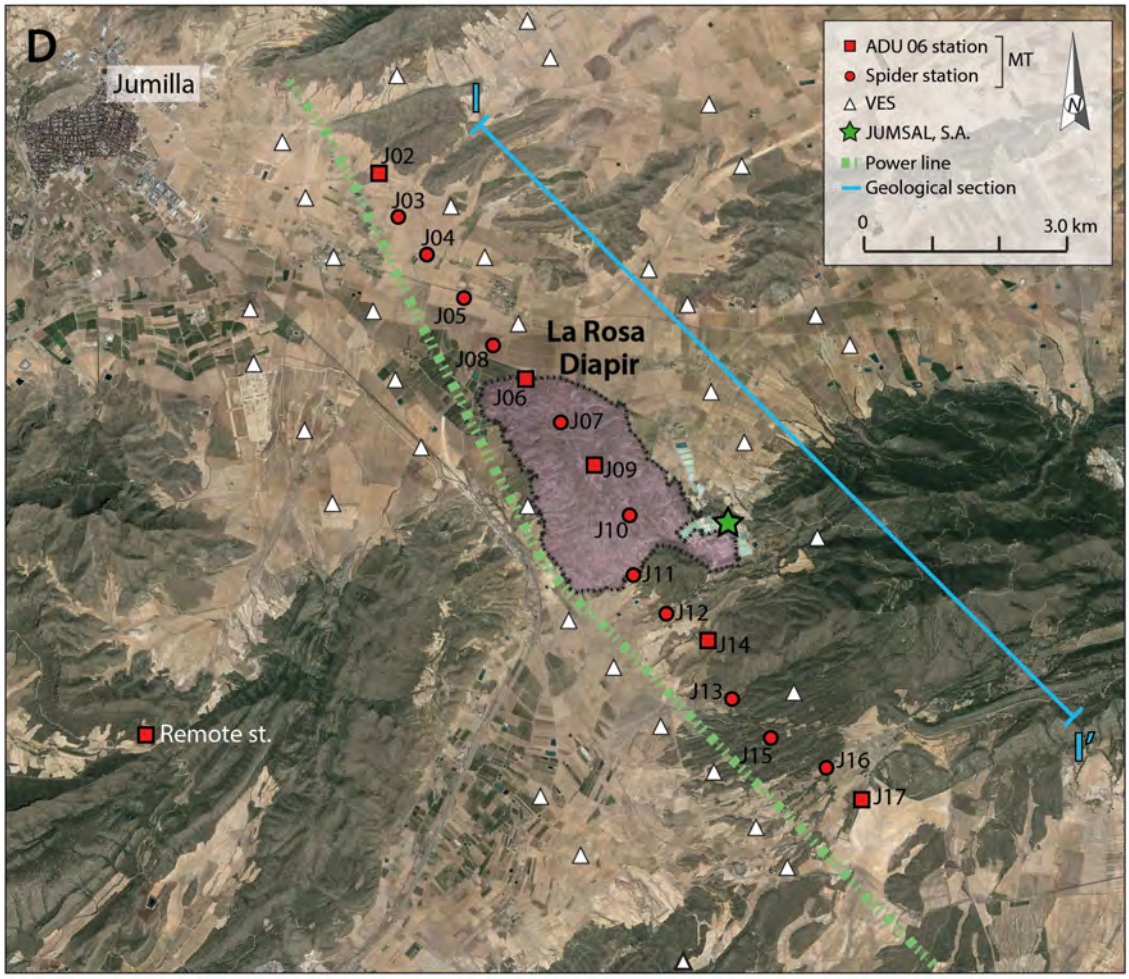

Figure 2. Location of MT stations, VES and some EM sources in the study area.

Despite these precautions, the effect of the power line was clearly recognized with very high harmonic amplitudes (> 1000 nT) (upper panel, Figure 3), which were filtered with shift filters to reduce this undesired behavior (lower panel of, Figure 3). After the processing, the dimensional analysis was performed with the software WALDIM (Martí et al. 2009), indicating that the geoelectrical structure behaves as 3D in the period range [0.01;10] s. However, a primary interpretation was obtained from a 2D model along the profile (upper panel, Figure 5), whose responses are shown in the Figure 4 with a RMS of 1.7.

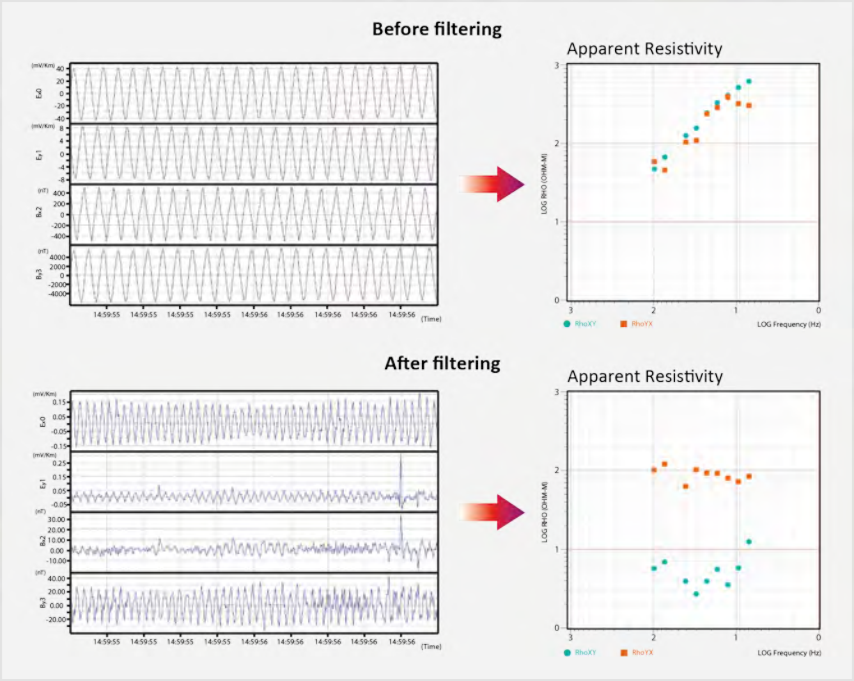

Figure 3. Example of Aparent Resistivity before and after filtering to reduce the undesired signal

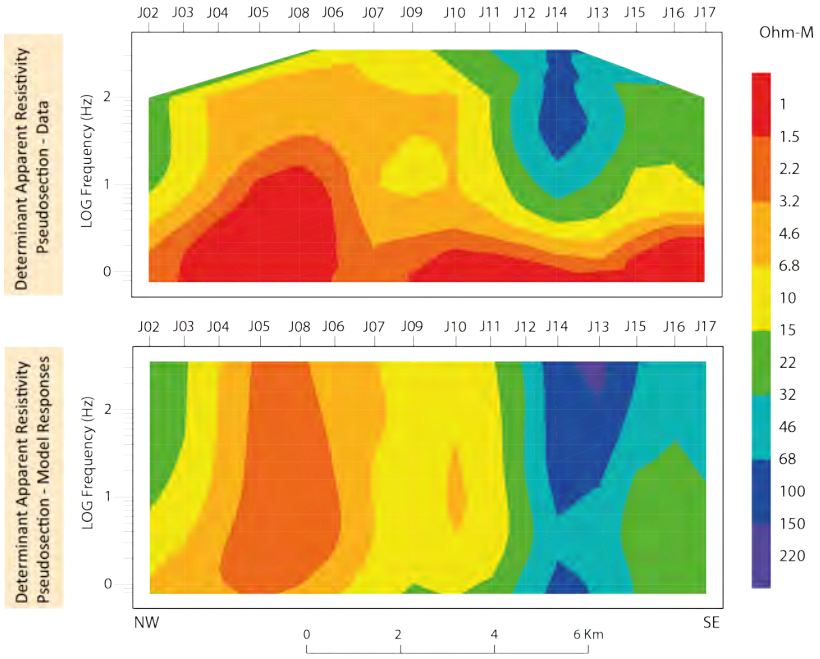

Figure 4. Determinant Apparent Resistivity Pseudosection of the data and the model responses.

Taking into account a geological cross-section in the study area (Figure 1C), the following structures can be interpreted (Lower panel, Figure 5):

(I) Approximated location of basement according to geological and gravity data.

(II) The carbonate Mesozoic layers denotes significant resistivity contrasts along to the profile. Note that conductive and resistive layers in the Internal Prebetics are SE-dipping consistent to geological data.

(III) The diapir shows both resistive and conductive surface anomalies that could

be related to mining exploitation activities.

(IV) In depth the diapir present a high-resistivity area.

(V) A central-septentrional conductive body which could correspond to a Mesozoic basin.

(VI) Interpreted base of caprock of the diapir.

(VII) Mesozoic anticlinal cored by Triassic evaporates.

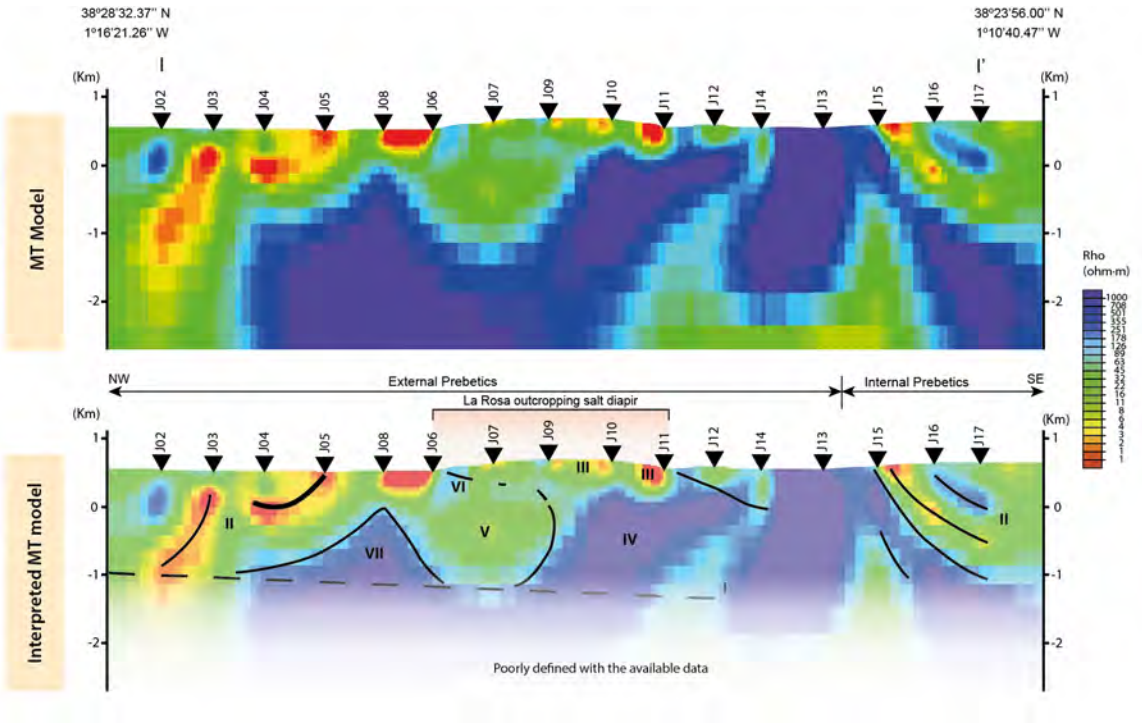

Figure 5. 2D MT Model and interpretation of MT Model

A new fieldwork was performed at La Rosa Diapir to acquire passive seismic to constrain the geolectrical data recorded before. The processing of this new data is in progress. This work was done in collaboration with the geophysical group of the Institut Cartographic i Geologic de Catalunya (ICGC).

Conclusions

The main results identified in this work have been:

1) The effectiveness of the shift filters to reduce the effect of the power lines and its harmonics on the apparent resistivity curves,
2) The confirmation that this area is geoelectrically complex (3D) as it is shown by the dimensional analysis, and more stations should be acquired for further studies.
3) Despite the complexity of the zone, the presented 2D geoelectrical structure of La Rosa diapir showed a good agreement with the geological cross-section.

All of these aspects must be taken into account in further surveys in this region.

Future work

Future work will be focused on new fieldworks to complete the current data and spread, strengthen and densify the geophysical data (geoelectrical and seismic) to interprete the geological model.

F Tectònica Activa

Active Tectonics

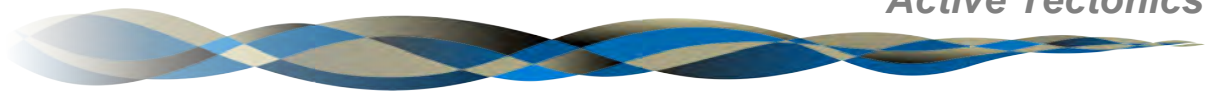

geomodels

institut de recerca

Refining seismic parameters in low seismicity areas by 3D trenching: the not so slow Alhama de Murcia fault, SE Iberia

[1]Marta Ferrater, [1]Maria Ortuño, [1]Eulàlia Masana, [1]Raimon Pallàs, [2]Hector Perea, [3]Stephane Baize, [4]Eduardo García-Meléndez, [5]José J. Martínez-Díaz, [1]Anna Echeverria, [6]Thomas Rockwell, [7]Warren D. Sharp, [8]Alicia Medialdea, [8]Edward J. Rhodes

[1]RISKNAT Group. GEOMODELS. Departament de Geodinàmica i Geofísica, Facultat de Geologia, Universitat de Barcelona, c/ Martí i Franquès, s/n, 08028 Barcelona, Spain. Email: marta.ferrater@ub.edu
[2]Barcelona Center for Subsurface Imaging (B-CSI), Departament de Geociències Marines - Institut de Ciències del Mar - CSIC, 08003 Barcelona, Spain
[3]Institut de Radioprotection et Sûreté Nucléaire - Seismic Hazard Division (BERSSIN), BP 17, 92262 Fontenay-aux-Roses, France
[4]Área de Geodinámica Externa, Facultad de CC. Ambientales, Universidad de León, Campus de Vegazana s/n 24071 León, Spain
[5]Departamento de Geodinamica, Universidad Complutense, Instituto de Geociencias IGEO (UCM, CSIC), 28040 Madrid, Spain
[6]Department of Geological Sciences, San Diego State University, San Diego, CA 92182, USA
[7]Berkeley Geochronology Center, Berkeley, CA 94709, USA
[8]Landscape Dynamics, Department of Geography, University of Sheffield, Sheffield S10 2TN, UK

Abstract

Three-dimensional paleoseismology in strike-slip faults with slip rates less than 1 millimeter per year involves a great methodological challenge. We adapted 3D trenching to track buried channels offset by the Alhama de Murcia seismogenic left-lateral strike-slip fault (SE Iberia). A fault net slip of 0.9 ± 0.1 mm/yr was determined using statistical analysis of piercing lines for one buried channel, whose age is constrained between 15.2 ± 1.1 ka and 21.9-22.3 cal BP. This value is larger and more accurate than the previously published slip rates for this fault. The minimum number of five paleo-earthquakes identified since the deposition of dated layers suggests a maximum average recurrence interval of approximately 5 ka. The combination of both seismic parameters yields a maximum slip per event between 5.3 and 6.3 m. We show that accurately planned trenching strategies and data processing may be key to obtaining robust paleoseismic parameters in low seismicity areas.

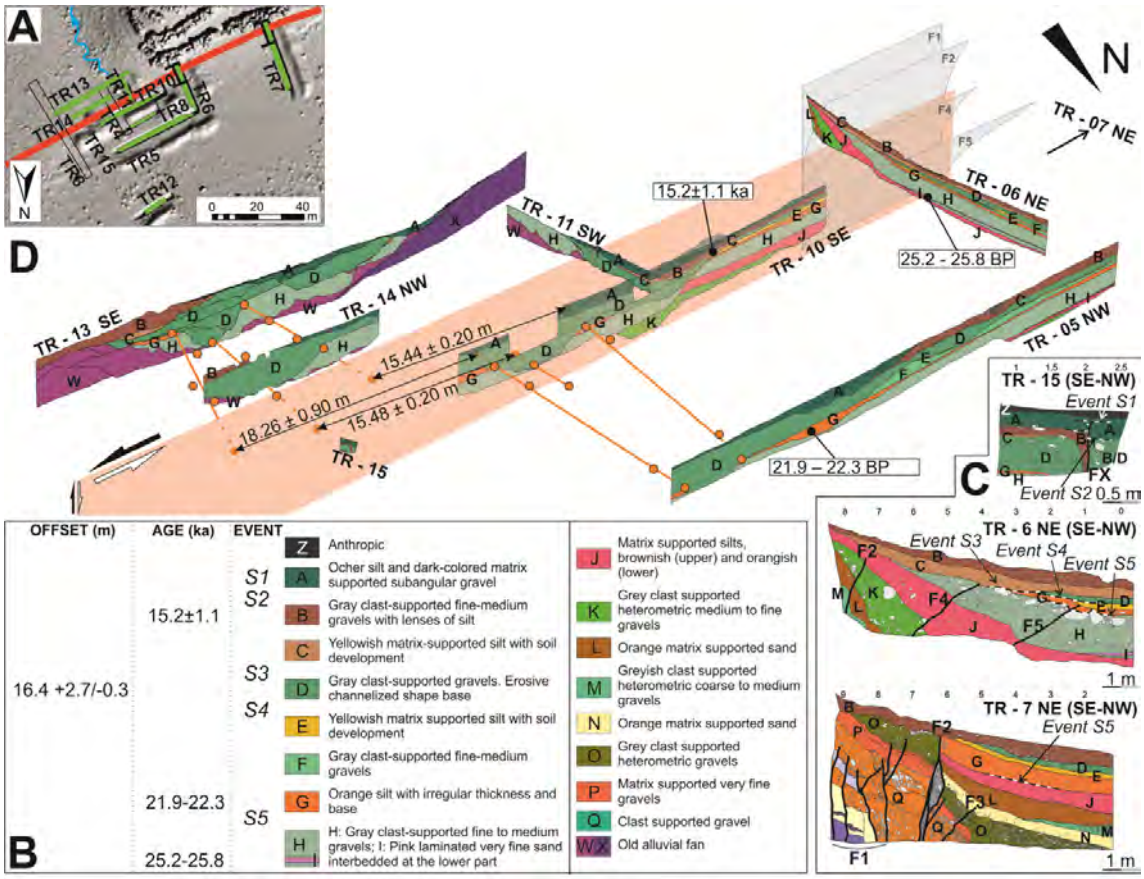

Figure 1. Results at El Saltador site. A) Map with the trench locations of this study in green (the position of the trenches 3 and 4 in Masana et al., 2004 is highlighted), the fault zone in red, and the position of the active channel (blue). B) Legend summarizing units' description, offset measurements, numerical ages and identified events. C) Partial logs of the trenches dug across the fault showing deformed stratigraphic units (TR 6, 7 and 15, position indicated in 2A and D) with indication of the event horizons (dashed black and white lines, S1 to S5). Interpretation of events is based on: event S1: unit A is offset while unit Z shows no deformation (Trench 15); event S2: unit B is more strongly folded than unit A (Trench 15); event S3: angular discontinuity between units D and C (Trench 6); event S4: unit D is not affected by the deformation that folds unit G and E (Trench 6); events S5: the base of unit H dips more that the base of unit G (Trench 6); D) Perspective block diagram showing the location of some trench walls (TR 5 NW, 6 NE, 10 SE, 11 SW, 13 SE, 14 NW and 15; the others are not included for clarity), the reconstructed fault plane and the samples position. Orange dots on channels in the trench walls represent the position of all reference points. In orange, piercing lines and piercing points for channel D. The piercing lines have been adjusted using two to four reference points for each channel feature (rims or thalweg). Piercing lines are regression lines and thus do not necessarily contain the reference points due to channel irregularities.

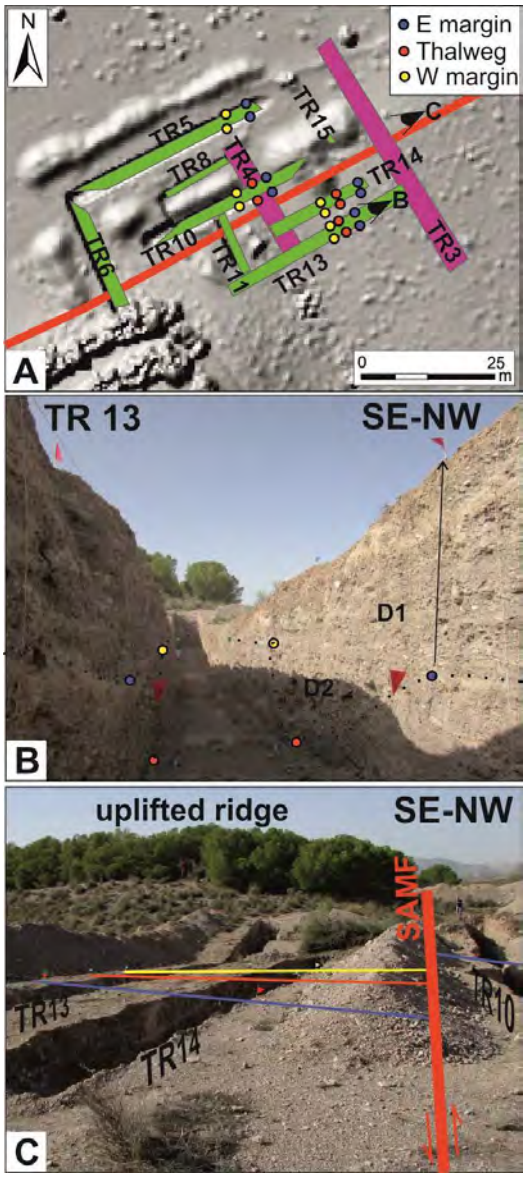

Figure 2. Reference points identified in the trenches. A) Map of the trenches with respect to the surface projection of the reference points identified in the trench walls, the solid red line is the fault zone (the eye symbols indicate the perspectives of the pictures B and D); B) example of the identified reference points of unit D in the trench 13, and their projections on surface; C) field photograph of the trenches and the projection of the reference points indicated with flags (the approximation of the piercing lines is shown).

Future work

We plan to analyse in detail the paleoseismic evidences identified in the trenches in order to calculate the recurrence period of the Alhama de Murcia fault in this segment between Lorca and Totana.

A 3D measurement of the offset in paleoseismological studies

[1]Marta Ferrater, [1]Anna Echeverria, [1]Eulàlia Masana, [2]José J. Martínez-Díaz, [3]Warren D. Sharp

[1]RISKNAT Group. GEOMODELS. Departament de Geodinàmica i Geofísica, Facultat de Geologia, Universitat de Barcelona, c/ Martí i Franquès, s/n, 08028 Barcelona, Spain. Email: marta.ferrater@ub.edu
[2]Departamento de Geodinamica, Universidad Complutense, Instituto de Geociencias IGEO (UCM, CSIC), 28040 Madrid, Spain
[3]Berkeley Geochronology Center, Berkeley, CA 94709, USA

Abstract

The slip rate of a seismogenic fault is a crucial parameter for establishing the contribution of the fault to the seismic hazard. It is calculated from measurements of the offset of linear landforms, such channels, produced by the fault combined with their age. The three-dimensional measurement of offset in buried paleochannels is subject to uncertainties that need to be quantitatively assessed and propagated into the slip rate. Here, we present a set of adapted scripts to calculate the net, lateral and vertical tectonic offset components caused by faults, together with their associated uncertainties. This technique is applied here to a buried channel identified in the stratigraphic record during a paleoseismological study at the El Saltador site (Alhama de Murcia fault, Iberian Peninsula). After defining and measuring the coordinates of the key points of a buried channel in the walls of six trenches excavated parallel to the fault, we a) adjusted a 3D straight line to these points and then extrapolated the tendency of this line onto a simplified fault plane; b) repeated these two steps for the segment of the channel in the other side of the fault; and c) measured the distance between the two resulting intersection points with the fault plane. In doing so, we avoided the near fault modification of the channel trace and obtained a three-dimensional measurement of offset and its uncertainty. This methodology is a substantial modification of previous procedures that require excavating progressively towards the fault, leading to possible underestimation of offset due to diffuse deformation near the fault. Combining the offset with numerical dating of the buried channel via U-series on soil carbonate, we calculated a maximum estimate of the net slip rate and its vertical and lateral components for the Alhama de Murcia fault.

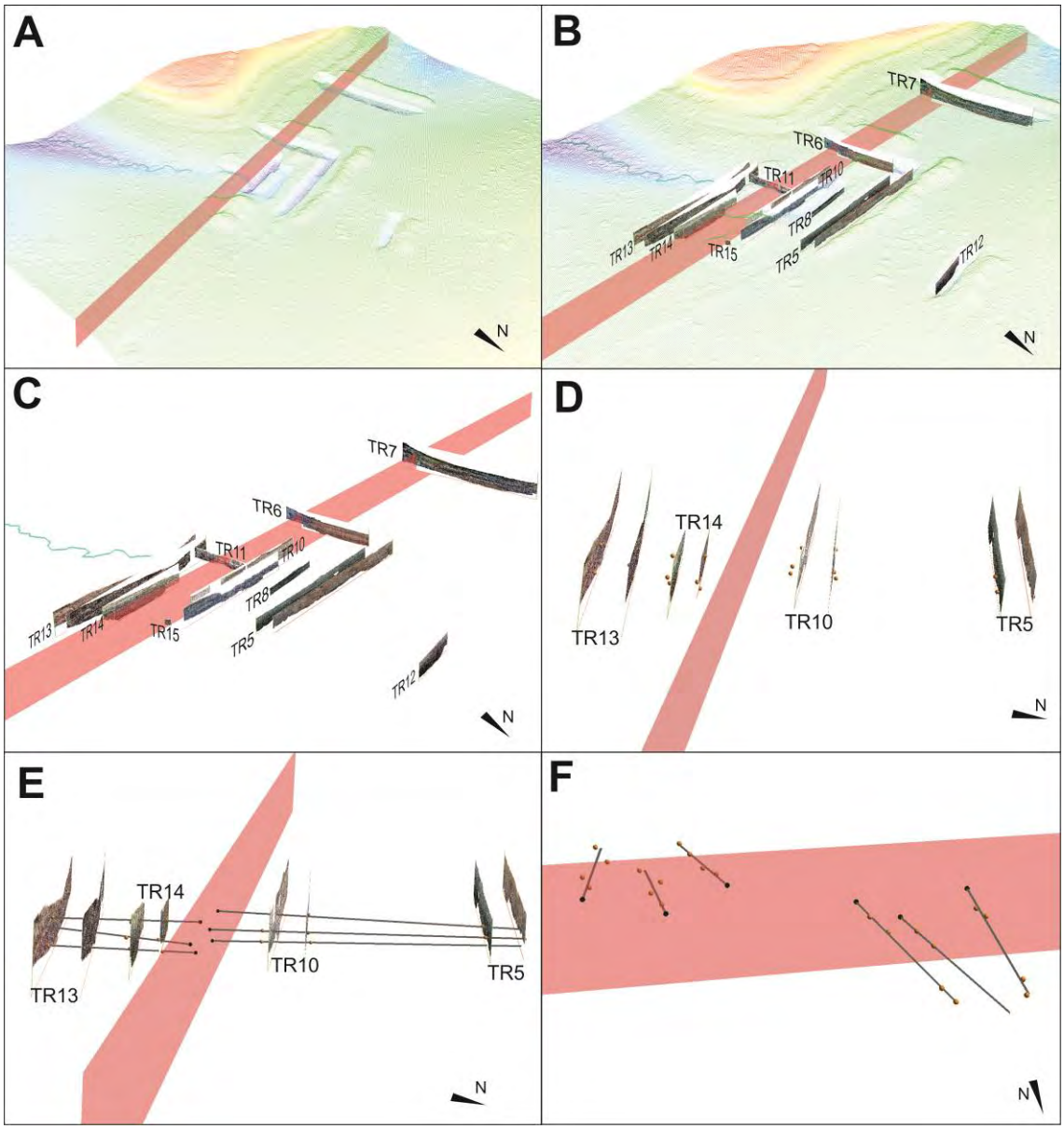

Figure 1. Visualization of the 3D trenching. A) Point cloud acquired from airborne lidar data in 2013 including the simplified vertical fault plane; B) photomosaics and orthophotography of the exposed trenches in the point cloud; C) photomosaics and orthophotography of the exposed trenches; D) parallel view of the trenches in which the channel was identified (reference points in orange); E) position of the adjusted 3D straight piercing lines (grey lines) with respect to the trench walls; F) simplified fault, reference points (in orange), straight piercing lines (in grey) and piercing points (in black). Notice that the straight piercing lines do not contain the reference points.

Lateral slip rate of Alhama de Murcia fault (SE Iberian Peninsula) by a morphotectonic analysis: comparison with paleoseismological data

[1]Marta Ferrater, [1]Maria Ortuño, [1]Eulàlia Masana, [2]José J. Martínez-Díaz, [1]Raimon Pallàs, [3]Hector Perea, [4]Stephane Baize, [5]Eduardo García-Meléndez, [1]Anna Echeverria, [6]Thomas Rockwell, [7]Warren D. Sharp, [8]Ramon Arrowsmith

[1]RISKNAT Group. GEOMODELS. Departament de Geodinàmica i Geofísica, Facultat de Geologia, Universitat de Barcelona, c/ Martí i Franquès, s/n, 08028 Barcelona, Spain. Email: marta.ferrater@ub.edu
[2]Departamento de Geodinamica, Universidad Complutense, Instituto de Geociencias IGEO (UCM, CSIC), 28040 Madrid, Spain
[3]Barcelona Center for Subsurface Imaging (B-CSI), Departament de Geociències Marines - Institut de Ciències del Mar - CSIC, 08003 Barcelona, Spain
[4]Institut de Radioprotection et Sûreté Nucléaire - Seismic Hazard Division (BERSSIN), BP 17, 92262 Fontenay-aux-Roses, France
[5]Área de Geodinámica Externa, Facultad de CC. Ambientales, Universidad de León, Campus de Vegazana s/n 24071 León, Spain
[6]Department of Geological Sciences, San Diego State University, San Diego, CA 92182, USA
[7]Berkeley Geochronology Center, Berkeley, CA 94709, USA
[8]School of Earth and Space Exploration, Arizona State University, Tempe, AZ 85287-6004, USA

Abstract

To define the seismic potential of the left-lateral strike-slip Alhama de Murcia fault (SE Iberian Peninsula), we calculated its slip rate by measuring offset linear features of known age using a morphotectonic analysis. The Lorca-Totana section of the fault yielded a minimum slip rate of 1.0 ± 0.2 mm/a for the past 30 ka, based on a channel whose age is estimated by OSL technique. The minimum left-lateral slip rate of the Goñar-Lorca section is 1.6-1.7 mm/a for the past 200 ka, based on eight offset surface channels, previously mapped alluvial fans dated by TL, and by new U-series dating of pedogenic carbonate. The U-series technique was used here for first time in the Iberian Peninsula to date small amounts (mg) of pedogenic carbonate. According to the newly estimated slip rate values, the Alhama de Murcia fault is one of the most active faults in the Eastern Betics Shear Zone. These values are larger and have fewer uncertainties in comparison with previous slip rates estimations. In the Lorca-Totana section, the new lateral slip rate is compared with a slip rate calculated by means of a paleoseismic study showing good agreement between the values obtained with the two approaches. We encourage the combination of paleoseismology and morphotectonic analysis to obtain reliable slip rates for faults with scarce evidence of late Holocene slip.

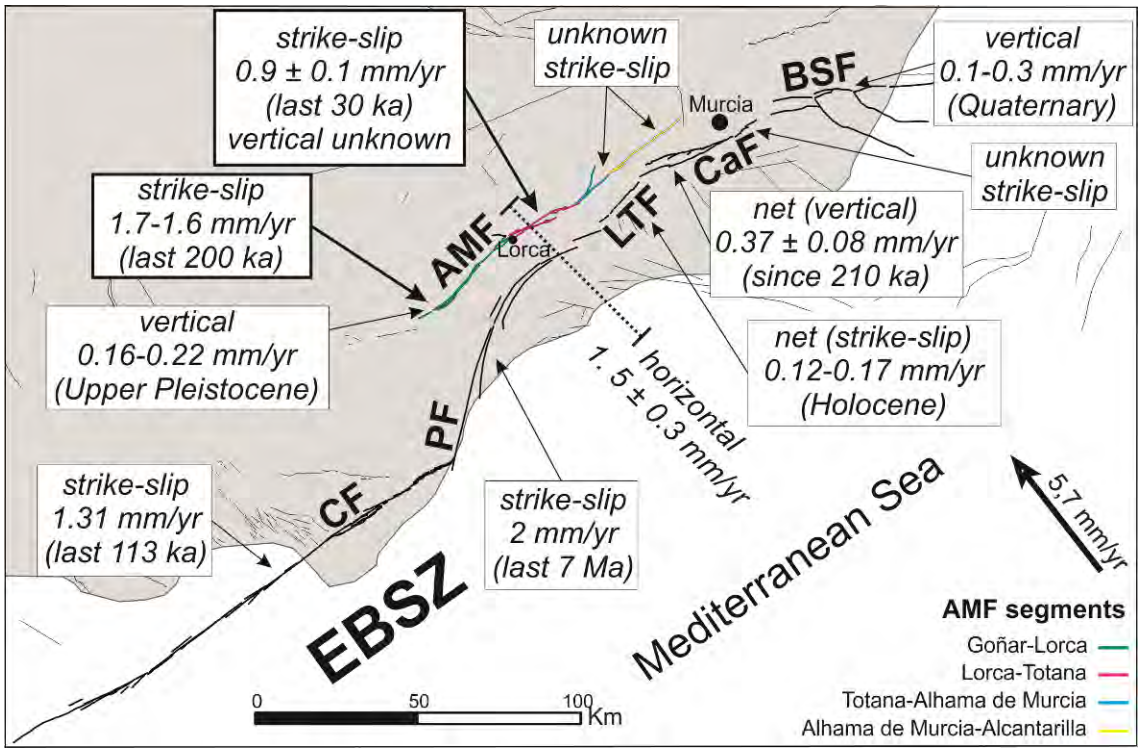

Figure 1. Summary of available slip rates for the Eastern Betics Shear Zone (EBSZ) faults (Weijermars, 1987; Alfaro et al., 2012; Ortuño et al., 2012; Echeverria et al., 2013; Moreno et al.,2015; Martín-Banda et al., 2015; this study). Legend: CF, Carboneras fault; PF, Palomares fault; LTF, Los Tollos fault; CAF, Carrascoy fault; BSF, Bajo Segura fault. Quaternary Active Faults Database of Iberia from IGME (2015). The dot line is the profile where Echeverria et al. (2013) projected the geodetic velocities. The arrow indicates the convergence direction between the Eurasian and African plates according to NNR-MORVEL56 model (Argus et al., 2011).

Evolution of morphotectonic parameters in an experimental wedge

Marc Viaplana-Muzas[1,2], María Ortuño[1], Vicente Perez-Peña[3], José Pedro Galve[3], Julien Babault[2], Jean Van Den Driessche[4] and Stephane Dominguez[5]

1) RiskNat and Geomodels groups. Universitat deBarcelona. Facultat de Geologia, 08028, Barcelona, Spain.

2) UniversitatAutònoma de Barcelona. Departament de Geologia, 08193 Bellaterra, Spain

3) Universidad de Granada. Campus de Fuentenueva, 18071 Granada, Spain.

4) Université de Rennes 1. Géosciences Rennes, Campus de Beaulieu, Rennes, France.

5) Université Montpellier. Géosciences Montpellier,I I, F-34095, Montpellier, France.

Abstract

The morphometry of geomorphological features along mountains front has been classically applied to characterize the regional degree of tectonic activity. The analysis of the shape and slope of alluvial fans as well as the geometry and distribution of the rivers and drainage basins is useful to detect enhanced/decreased uplift and ongoing tectonic deformation on mountain areas worldwide. The most common calculated parameters refer to the sinuosity of mountains front (Smf), the valley floor to width ratio (Vf), the stream-length gradient index (SL) or the percentage of dissection (Fd). In the last decades, new morphotectonic parameters, such as the Chi parameter (which weights up the river slope in relation with the drainage area), have permitted to better localize interest areas of tectonic activity. All the previous studies, however, have analyzed the morphometry of the present-day landscape, this is, a snapshot of the whole history of changes experienced in active areas. Thus, the spatial comparison between areas undergoing different tectonic activity has been the only way to infer the expected changes in morphometry in the landscape. This “static” approach has to face the limitations related to controlling factors that vary in space such as lithology, structure and climate.

We propose to use the Digital Elevation Models (DEMs) obtained for a set of experiments generating an artificial synthetic mountain front evolving with time. The system experienced orogenic growth at different rates and under different rainfall conditions, allowing us to reproduce and to monitor the interactions between tectonics, erosion and sedimentation. During the experiments, wedges were monitored by an optical measurement bench composed of photograph cameras coupled to a laser interferometer that allows quantifying surface deformations and generating DEMs. The experimental set-up used is adapted from the setup used by Graveleau and Dominguez, (2008). The deformation device is constituted by a basal film pulled beneath a static buttress. The film is overlaid by the analogue material, composed of glass microbeads, silica powder and plastic powder (PVC), which models the upper part of the crust. Shortening induces material deformation and generates an accretionary wedge composed of imbricated thrusts (Fig.1). The rainfall system is composed of sprinklers that deliver water micro-droplets over the model.

The experimental channels adjust to uplift rate by both increasing their slope and narrowing their channels as it is observed in nature above active faults.This analogyis evidenced by the values, in the erosion law, ofexponents on the slope “n”, that is 1.5±0.2, and on the drainage area “m”, that is 0.8±0.2 (Viaplana-Muzas et al., 2015). A set of 8 different analogues models coupling deformation and erosion were analyzed and changes in morphotectonic parameters were studied following, among others, the approach proposed by Pérez-Peña et al. (2009) for natural systems inspected using

GIS tools. Results confirm that this type of modeling reproduce accurately the erosion dynamics of an active natural setting. Thus, morphotectonics of mountain fronts are analyzed for the first time in an experimental approach. This methodology emerges as a powerful way to study quantitatively the evolution of the landscape and permits to get some insights in the changes of active tectonics through the analysis of the different DEMs obtained synthetically.

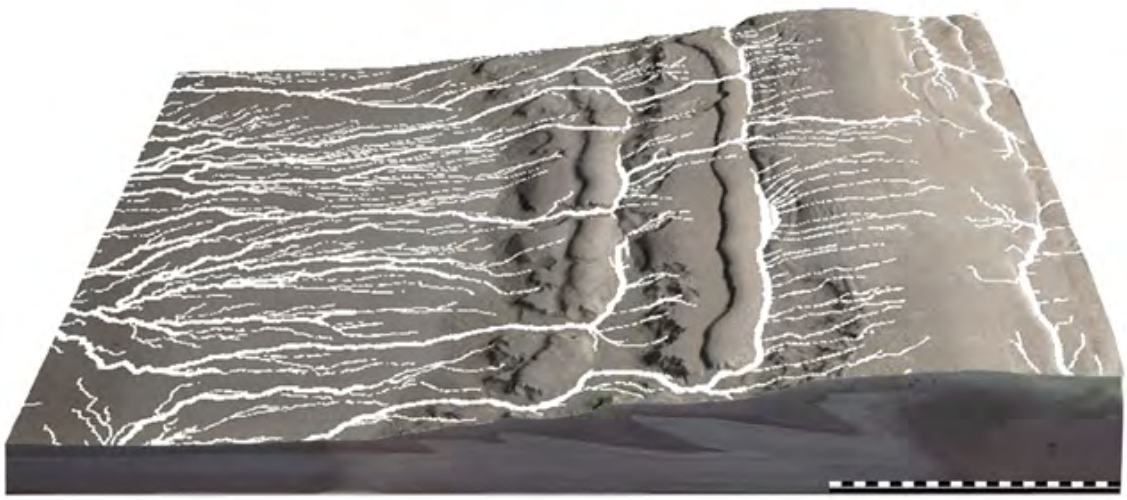

Figure 1. 3D view of a model run under 8 cm/h of shortening rate and 9 mm/h of rainfall rate, after the third thrust activity. The photographs are overlapped on the DEM. Drainage network is superimposed in white.

Future work

We plan to quantify the variations of several morphometric parameters such as the Chi, Ksn and SL in tectonic mountains fronts of different activity in order to explore how the incission migrates up to the mountain belt. This research will be applied to better understand the development of the landscape within the postorogenic phase of the Pyrenean range.

General Future research in Active Tectonics

1) We will start new paleoseismic research at Carboneras fault (trenching and geomorphologic analyses), where slip.rates are scarce and need to be obtained along strike to define possible segment boundaries onshore. Longer seismic sequences are also seeked to bon¡tein better constraines recurrence times and timing for the last event.
2) Paleoseismic studies will also started at Alhama de Murcia fault to elongate the seimsic history of the fault at Lorca-totana segment and to obtain slip-rates along the fault (including Goñar-Lorca segment).
3) A further sedimentological and experimental analysis of the co-seismic significance of ponded strata found at La Hoya-El Saltador site (Lorca, Alhama de Murcia fault) will be performed.
4) Collaborations with the InterGeo project (coordinnated by Dr. Jose Martínez Diaz) are planned to develop paleoseismological investigation south of Lorca city, at La Torrecilla site (Alhama de Murcia fault) in the light of recent findings of possible historical ruptures.
5) New GPS stations will be constructed both for permanent and non-permanent observations along selected profiles at Carboneras and Alhama de Murcia faults.
6) Dissemination activities will start with the design of a divulgation video on the fault activity and its relationship with seismicity in the Eastern Betic Shear zone.
7) We'll develop a research to analyze the development of the fluvial network at Pyrenees and Sierra nevada (Betic Cordillera) with the aim to detect active faulting and disitribution of potentially hazarous land, in the frame of a collaboration with the ARPA research group (Univ. of Granada).

PUBLICACIONS

Publications

3

geomodels

institut de recerca

Albert-Villanueva, E., Permanyer, A., Tritlla, J., Levresse, G., Salas, R. (*2016*). Solid hydrocarbons in Proterozoic dolomites, Taoudeni Basin, Mauritania. *Journal of Petroleum Geology*. 39(1), 5-27

Bartolome, R., Górriz, E., Dañobeitia, J., Cordoba, D., Martí, D., Cameselle, A. L., Núñez-Cornú, F., Bandy, W.L., Mortera-Gutiérrez, C.A., Núñez, D., Castellón, A., Alonso, J.L. (2016). Multichannel seismic imaging of the Rivera Plate subduction at the seismogenic Jalisco Block area (Western Mexican margin). *Pure and Applied Geophysics*, 173(10-11), 3575-3594.

Beamud, E., Soto, E., Roca, E., Carola, E., Almar, Y. and Escosa, F. (2016). Paleomagnetic data in syn-diapiric Aptian to Albian rocks (Vasc-Cantabrian basin). *Geo-Temas*, 16 (1), 793-796.

Belaustegui, Z., Puddu, C., Casas, J.M. (2016). New ichnological data from the lower Paleozoic pf the Central Pyrenees: presence of Artrophycus Brogniartii (Harlam, 1832) in the Upper Ordovician Cava Formation*. Geo-Temas,* 16 (1), 271-274.

Bellmunt, F., Marcuello, A., Ledo, J., Queralt, P. (2016). Capability of cross-hole electrical configurations for monitoring rapid plume migration experiments**.** Journal of Applied Geophysics.124, 73-82.

Blanch, X., Royán, M.J., Guinau, M. (2016). Análisis de la evolución de desprendimientos a partir de datos LiDAR en el escarpe de Puigcercós (Pallars Jussà – Cataluña). *Geo-Temas*, 16 (1), 597-600.

Bosch, D., Ledo, J., Queralt, P., Bellmunt, F., Luquot, L., Gouze, P. (2016). Core-scale Electrical Resistivity Tomography (ERT) monitoring of CO2-brine mixture in Fontainebleau sandstone, Journal of Applied Geophysics, 130, 23-36. doi:10.1016/j.jappgeo.2016.03.039

Bover-Arnal, T., Moreno-Bedmar, J.A., Frijia, G., Pascual-Cebrian, E., Salas, R. (2016). Chronostratigraphy of the Barremian-Early Albian of the Maestrat Basin (E Iberian Peninsula): integrating strontium-isotope stratigraphy and ammonoid biostratigraphy. *Newsletters on Stratigraphy*. 49, 41-68.

Cabello, P., López, C., Dussán, M. I., Gamba, N., Calvo, R., Vázquez, Y., Ramos, E. (2016). Definición de trampas estratigráficas en cuencas petrolíferas maduras: Estudio integrador de la Cuenca del Valle Medio del Magdalena, Colombia. *Geo-temas*. 16(1), 459-462.

Cabello, P., López, C., Dussán, M. I., Gamba, N., Torres, E., Ballesteros, C., Cantisano, M. T., Marfisi, N., Calvo, C., Vázquez, Y., Ramos, E. An integrated approach to define new stratigraphic plays in the mature oil Middle Magdalena Valley Basin (Colombia). Submitted to be published in AAPG Bulletin.

Canora, C., Roca, C., Martínez-Díaz, J.J., Insua-Arévalo, J.M., Martín-González, F., Gómez-Ortiz, D., Martínez-Pagan, P., Masana, E., Ortuño M., Ferrater, M., Medialdea, A., (2016). Nuevos datos de actividad paleosísmica de la falla de Alhama de Murcia en el abanico de La Salud (segmento Lorca-Totana de la Falla de Alhama de Murcia), Béticas orientales. *Geo-Temas*, 16 (2), 563-566.

Carola, E., Ferrer, O., Vidal-Royo, O., Muñoz, J.A. (In press). Interpretation of salt-cored frontal structures in the Southern Pyrenees guided by analog modeling, surface and subsurface data. *Interpretation* / February 2017.

Casanovas-vilar, I., Anneke Madern, Alba, D. M., Cabrera, L., García-Paredes, I., Van Den Hoek Ostende, L. W., Moyà-solà, S. **(2016).** The Miocene Mammal Record of the Vallès-Penedès Basin (Catalonia). Comptes Rendus Palevol, 15, 791–812.

Casanovas-Vilar, I., Garcés, M., Dam, J. van, García-Paredes, I., Robles, J. M., & Alba, D. M. **(2016).** An updated biostratigraphy for the late Aragonian and Vallesian of the Vallès-Penedès Basin (Catalonia). Geologica Acta, 14(3):195-217.

Cañellas-Boltà, N.; Rull, V.; Sáez, A.; Margalef, O:, Pla-Rabes; S.; Valero-Garcés, B.; Giralt, S. (2016). Vegetation dynamics at Raraku Lake catchment (Easter Island) during the past 34,000 years. Palaeogeography Palaeoclimatology Palaeoecology 446: 55 - 69

Capape, S., Martín-Vide, J.P., Colombo., F. (2016). Subaqueous Barchans and Plane Beds from Deposition of Quartz silt. Journal of Hydraulic Engineering, 142 (12). doi: http://dx.doi.org/10.1061/(ASCE)HY.1943-7900.0001212

Carmona, A., Gratacós, O., Clavera-Gispert, R., Hardy, S., Muñoz, J.A. (2016). Numerical modelling of syntectonic subaqueous sedimentation: The effect of normal faulting and a relay ramp on sediment dispersal. *Tectonophysics*, 684, 100-118.

Castelltort, X., Balasch, J.C., Cirés, J., Colombo, F. (2016). Evolución del drenaje en cuencas erosivas durante el Neógeno-Cuaternario. Margen oriental de la Cuenca del Ebro. Geogaceta 60: 19-22.

Clavera-Gispert, R., Carmona, A., Gratacós, O., Tolosana-Delgado, R. (*Under review*). Process-based forward numerical ecological modelling for carbonate sedimentary basins. Submitted to Computational Geosciencies (under review).

Colombo, F., Alonso, J.L., Limarino, C.O., Quintana, R., Cardó, R., Césari, S.N. (2016). Características estratigráficas y estructurales de un paleovalle glacial Mississipiense. Precordillera Andina, San Juan (Jáchal), Argentina. *Geo-Temas*, 16 (1), 435-438.

Cruset, D., Cantarero, I., Travé, A., Vergés, J., John, C.M. (2016) Crestal graben fluid evolution during growth of the Puig-reig anticline (South Pyrenean fold and thrust belt). Journal of Geodynamics, 101, 30-50.

Escosa, F. O., Roca, E., Ferrer, O. (2016). Role of the pre-existing thick-skinned extensional faults in the thin-skinned deformation of a salt-bearing passive margin (the Eastern Prebetic). *Geo-Temas*, 16(1), 37-40.

Farrés, F., Carnevale, G., Colombo, F., Cabello, P., Belaústegui, Z., Domènech, R., Vidal, A., Martinell, J. (2016). Peces fósiles en el Eoceno Superior de La Plana de Vic (Barcelona): Nuevos yacimientos y significado sedimentario. Geogaceta 60: 79-82.

Ferrater, M.; Echeverría, A., Masana, E.; Martínez-Díaz, T.; Sharp, W.D. (2016). A 3D measurement of the offset in paleoseismological studies. *Computers & Geosciences.* 90, 156-163

Ferrater, M.; Ortuño, M.; Masana, E.; Pallàs, R.; Perea, H.; Baize, S.; García-Meléndez, E.; Martínez-Díaz, J.J.; Echeverría, A., Rockwell, T.; Sharp, W.D. (2016). Refining seismic parameters in low seismicity areas by 3D trenching: the not so slow Alhama de Murcia fault, SE Iberia. *Tectonophysics, 680, 122-128.*

Ferrater, M.; Ortuño, M.; Masana, Martínez-Díaz, J.J.; E.; Pallàs, R.; Perea, H.; Baize, S.; García-Meléndez, E.; Echeverría, A., Rockwell, T.; Sharp, W.D., Arrowsmith, R. (*submitted*) Lateral slip rate of Alhama de Murcia fault (SE Iberian Peninsula) by a morphotectonic analysis: comparison with paleoseismological data. Submitted to Quaternary International.

Ferrater, M., Ortuño M., Masana, E., Martínez-Díaz, J.J., Pallàs, R., Medialdea, A., Perea, H., Baize, S., García-Meléndez, E., Echeverría, A., Rockwell, T., Sharp, W.D., Rhodes, E., Arrowsmith, R. (2016). Velocidad de desplazamiento de la falla de Alhama de Murcia calculada mediante técnicas paleosismológicas y morfotectónicas. *Geo-Temas*, 16 (2), 511-514.

Ferrer, O., Gratacós, O., Roca, E., Muñoz, J.A. (accepted). Modeling the interaction between pre-salt seamounts and gravitational failure in salt-bearing passive margins: the Messinian case in the northwestern Mediterranean basin. *Interpretation*.

Ferrer, O., Gratacós, O., Roca, E., Muñoz, J.A. (2016). Influencia de volcanes o altos submarinos en la deformación supra-sal en márgenes pasivos con tectónica gravitacional: Resultados experimentales y aplicación al Mediterráneo Occidental. *Geo-Temas*, 16(1), 53-56.

Furdada, G.; Génova, M.; Guinau, M.; Victoriano, A.; Khazaradze, G.; Díez-Herrero, A.; Calvet, J. (2016): Las avenidas torrenciales de los barrancos de Portainé, Reguerals y Ramiosa (Pirineo Central): evolución de las cuencas y dinámica torrencial. Comprendiendo el relieve: del pasado al futuro. Juan José Durán Valsero, Manuel Montes Santiago, Alejandro Robador Moreno y Ángel Salazar Rincón, eds. IGME: 315-322.

Gabàs, A., Macau, A., Benjumea, B., Queralt, P., Ledo, J., Figueras, S., Marcuello, A. (2016). Joint Audio-Magnetotelluric and Passive Seismic Imaging of the Cerdanya Basin. Surveys in Geophysics. 37, 897-921. DOI:10.1007/s10712-016-9372-4.

Garces, M. **(2015).** Magnetostratigraphic Dating. In W. J. Rink & J. Thompson (Eds.), Encyclopedia of Scientific Dating Methods SE - 115 (pp. 507–517). CHAP, Springer Netherlands. http://doi.org/10.1007/978-94-007-6304-3_115

Garcés, M., García-Senz, J., Muñoz, J.A., López-Mir, B., Beamud, E. (2016). Timing of magnetisation and vertical-axis rotations of the Cotiella massif (late Cretaceous, South Central Pyrenees). In: Pueyo, E. L., Cifelli, F., Sussman, A. J. & Oliva-Urcia, B. (eds). *Palaeomagnetism in Fold and Thrust Belts: New Perspectives*. Geological Society, London, Special Publications, 425, 213–232.

García-Sellés, D., Sarmiento, S., Gratacós, O., Granado, P., Carrera, N., Lakshmikantha, M.R., Cordova, J.C., Muñoz, J.A. (*accepted*). Fracture analog of the subandean Devonian of southern Bolivia: Lidar applied to Abra del Condor. In: Petroleum Basins and Hydrocarbon Potential of the Andes of Peru and Bolivia. AAPG Memoir

Gili, E., Skelton, P.W., Bover-Arnal, T., Salas, R., Obrador, A., Fenerci-Masse, M. (2016). Depositional biofacies model for post-OAE1a Aptian carbonate platforms of the western Maestrat Basin (Iberian Chain, Spain). *Palaeogeography, Palaeoclimatology, Palaeoecology*. 453, 101-114.

Granado, P., Ferrer, O., Muñoz, Thöny, W., Strauss, P. (*in press*). Basin inversion in tectonic wedges: a comparative approach from analogue modelling and the Alpine-Carpathian fold-and-thrust belt. *Tectonophysics.*

Granado, P., Thöny, W., Carrera, N., Gratzer, O., Strauss, P., Muñoz, J.A. (2016). Basement-involved reactivation in foreland fold and thrust belts: the Alpine-Carpathian Junction (Austria). *Geological Magazine, 153 (5-6), 1110-1135.* Special volume "Tectonic evolution and mechanics of basement-involved fold-and-thrust belts". doi: 10.1017/S0016756816000066.

Granado, P., Urgeles, R., Sàbat, F., Albert-Villanueva, E., Roca, E., Muñoz, J.A., Mazzuca, N., Gambini, R. (2016). Geodynamical framework and hydrocarbon plays of a salt giant: the North Western Mediterranean Basin. *Petroleum Geoscience, 22(4),* 309-321. Thematic Set: "Messinian Salinity Crisis". doi: 10.1144/petgeo2015-084

Gratacós, O., Carmona, A., Clavera-Gispert, R., Muñoz, J.A., Hardy, S. (2016) Numerical Modelling of Syntectonic Subaqueous Sedimentation: The Effect of Normal Faulting and a Relay Ramp on Sediment Dispersal. *Geo-Temas,* 16 (1), 141-144.

Guimerà, J., Rivero, L., Salas, R., Casas, A. (2016). Moho depth inferred from gravity and topography in an intraplate area (Iberian Chain). *Tectonophysics*. 666, 134–143. doi: 10.1016/j.tecto.2015.10.021.

Guinau, M.; Ortuño, M.; Calvet, J.; Furdada, G.; Bordonau, J.; Ruíz, A.; Camafort, M. (2016). Detection of early stage large scale landslides in forested areas by 2 m LiDAR DEM analysis. The example of Portainé (Central Pyrenees). Geophysical Research Abstracts Vol. 18, EGU2016.

Izquierdo-Llavall, E., Roca, E., Pla, O., Neng, Y., Muñoz, J.A., Rowan M.G., Huang, S. (2016) Geometry of a fold-and-thrust belt controlled by multiple décollements: The structureof teh central Kuqa Basin (MW China). Geo-Temas, 16 (1), 13-16.

Janeras, M., Jara, J. A., López, F., Marturià, J., Royán, M. J., Vilaplana, J. M., Aguasca, A., Fàbregas, X., Cabranes, F. and Gili, J. A. (2015): Using several monitoring techniques to measure the rock mass deformation in the Montserrat Massif. Conf. Series: Earth and Environmental Science. 26:1-19. doi.: 10.1088/1755-1315/26/1/012030

M Janeras, JA Jara, MJ Royán, JM Vilaplana, A Aguasca, X Fàbregas, JA Gili, P Buxó (2016): Multi-technique approach to rockfall monitoring in the Montserrat Massif (Catalonia, NE Spain). Engineering Geology. DOI:10.1016/j.enggeo.2016.12.010

Jaramillo-Vogel, D., Bover-Arnal, T., Strasser, A. (2015). Bryozoan beds in northern Italy as a shallow-water expression of environmental changes during the Oligocene isotope event 1. *Sedimentary Geology*. 331, 148-161.

Jegen, M., Avdeeva, A., Berndt, C., Franz, G., Heincke, B., Hölz, S., Neska, A., Marti, A., Planert, L., Chen, J., Kopp, H., Baba, K., Ritter, O., Weckmann, U., Meqbel, N., Behrmann, J. (2016). 3-D magnetotelluric image of offshore magmatism at the Walvis Ridge and rift basin. *Tectonophysics*. 683, 98-108. DOI:10.1016/j.tecto.2016.06.016.

Larrasoaña, J.C., Beamud, E., Olivares, M., Murelaga, X., Tarriño, A., Baceta, J., Etxebarria, N. (2016). Magnetic properties of cherts from the Basque-Cantabrian basin and surrounding regions: archeological implications. *Frontiers in Earth Science*. http://dx.doi.org/10.3389/feart.2016.00035.

López-Blanco, M. **(2016).** El Margen SE de la Cuenca del Ebro hace unos 40 Millones de años y la sedimentación en Montserrat y Sant Llorenç del Munt. Un paseo desde las montañas hasta el mar profundo. Monografies Tècniques, Institut Cartogràfic I Geològic de Catalunya, 6, 67–78.

López-Mir, B., Muñoz, J.A., García-Senz, J. (2016). Geology of the Cotiella thrust sheet, southern Pyrenees (Spain), Journal of Maps, 12:sup1, 323-327, DOI: 10.1080/17445647.2016.1211895

López-Mir, B., Muñoz, J.A., García-Senz, J. (2016). 3D geometric reconstruction of Upper Cretaceous passive diapirs and salt withdrawal basins in the Cotiella Basin (southern Pyrenees). *Journal of the Geological Society. 173, 616-627.* doi:10.1144/jgs2016-002

Margalef, A., Castiñeiras., P., Casas, J.M., Navidad M., Liesa, M., Linnemann, U., Hofmann, M., Gärtner, A. (2016). Detrital zircons from the Ordovician rocks of the Pyrenees: Geochronological constraints and provenance. *Tectonophysics*. 681, 124-134.

Margalef, A., Casas, J.M. (2016). Corte geológico compensado del sur de Andorra: aportaciones a la estructura varisca del Pirineo central. *Geo-Temas,* 16 (1), 61-64.

Margalef, A., Casas, J.M., Castiñeiras, P., Navidad, M., Liesa, M. (2016). Comparison between detrital zircon populations from the Ordovician rocks of the

Pyrenees and from other Perigondwanan terrains: paleogeographic implications. *Geo-Temas,* 16 (1), 21-24.

Massiot, C., Nicol, A., Townend, J., McNamara, D., Garcia-Sellés D., Conway, C., Archibald, G., *(submitted).* Fracture system in an Andeite lava flow from terrestrial laser scanning, Ruapehu Volcano: Towards reservoir models. Geochemistry, Geophysics, Geosystems

Moreno, X.; Gràcia, E.; Bartolome, R.; Martínez-Loriente, S.; Perea, H.; Gómez-Peña, L.; Lo Iacono, C.; Piñero, E.; Pallàs, R.; Masana, E.; Dañobeitia, J.J. (2016). Seismostratigraphy and tectonic architecture of the Carboneras Fault offshore based on multiscale seismic imaging: Implications for the Neogene evolution of the NE Alboran Sea. *Tectonophysics,* 689, 115-132.

Nebot, M., Guimerà, J. (2016a). Structure of an inverted basin from subsurface and field data: the Late Jurassic-Early Cretaceous Maestrat basin (Iberian Chain). *Geologica Acta*. 14(2), 155-177. DOI:10.1344/GeologicaActa2016.14.2.5.

Nebot, M., Guimerà, J. (2016b). Kinematic evolution of a fold-and-thrust belt developed during basin inversion: the Mesozoic Maestrat basin, E Iberian Chain. *Geological Magazine*. doi:10.1017/S001675681600090X.

Nebot, M., Guimerà, J. (2016c). La extensión Triásica en el substrato de la Cuenca del Maestrat, y evidencias de tectónica salina en las evaporitas en facies Muschelkalk medio (Cadena Ibérica Oriental). *Geo-Temas*, 16(1), 241-244.

Nebot, M., Guimerà, J. (2016d). Inversión cenozoica de la Cuenca mesozoica del Maestrat: evolución cinemática del cinturón de pliegues y cabalgamientos desarrollado en su margen norte (Cadena Ibérica oriental). *Geo-Temas*, 16(2), 527-530.

Ninh Nguyen, H., Vernant, P., Mazzotti, S., Khazaradze, G., & Asensio, E. (2016). 3-D GPS velocity field and its implications on the present-day post-orogenic deformation of the Western Alps and Pyrenees. *Solid Earth*, *7*, 1349–1363. http://doi.org/10.5194/se-7-1349-2016.

Oms, O., Lopez Blanco, M., **Vilaplana, JM. (2016).** Introducción a la Geología de la Cataluña Central. Monografies Tècniques, Institut Cartogràfic I Geològic de Catalunya, 6, 17–65.

Ogaya, X., Alcalde, J., Marzán, I., Ledo, J., Queralt, P., Marcuello, A., Martí, D., Saura, E., Carbonell, R., Benjumea, B. (2016). Joint interpretation of magnetotelluric, seismic, and well-log data in Hontomín (Spain). Journal of Geophysical Research – Solid Earth. 7, 943-958. DOI:10.5194/se-7-943-2016.

Ogaya, X., Ledo, J., Queralt, P., Jones, A.G., Marcuello, A. (2016). A layer stripping approach for monitoring resistivity variations using surface magnetotelluric responses**.** Journal of Applied Geophysics. 132, 100-115. DOI:10.1016/j.jappgeo.2016.06.014.

Oliva-Urcia, B., Beamud, E., Garcés, M., Arenas, C., Soto, R., Pueyo, E., Pardo, G. (2016). New magnetostratigraphic dating of the Palaeogene syntectonic sediments of the west-central Pyrenees: tectonostratigraphic implications. In: Pueyo, E. L., Cifelli, F., Sussman, A. J. & Oliva-Urcia, B. (eds). *Palaeomagnetism in Fold and Thrust Belts: New Perspectives*. Geological Society, London, Special Publications. 425, 213–232.

Oliva-Urcia, B., Beamud, E., Soto, R., Arenas, C., Garcés, M., Pueyo, E.L. (2016). Datación magnetostratigráfica de la molasa Surpirenaica (Fm Uncastillo, Oligoceno-Mioceno). *Geo-Temas*, 16(1), 857-860.

Ortuño M., Ferrater, M., Masana, E., Martínez-Díaz, J.J., Pallàs, R., Perea, H., Baize, S., García-Meléndez, E., Rockwell, T., Sharp, W.D., Medialdea, A., Rhodes, E., Cunha, P.P., Sohbati, R., Buylaert, J.P., Murray, A. (2016). Combinación de

métodos de datación en cronologías paleosísmicas: el ejemplo de El Saltador (Falla de Alhama de Murcia). *Geo-Temas,* 16(2), 551-554.

Ortuño, M., Guinau, M., Calvet, J., Furdada, G., Bordonau, J., Ruíz, A., Camafort, M. (*under revision*). Potential of airborne LiDAR data analysis to detect subtle landforms of slope failure: the example of Portainé, Central Pyrenees. Geomorphology.

Pascual-Cebrian, E., Götz, S., Bover-Arnal, T., Skelton, P.W., Gili, E., Salas, R., Stinnesbeck, W. (2016). Calcite/aragonite ratio fluctuations in Aptian rudist bivalves: Correlation with changing temperatures. *Geology*. 44, 135-138.

Pérez-Guillén, C.; Sovilla, B.; Suriñach, E.; Tapia, M.; Köhler A. (2016). Deducing avalanche size and flow regimes from seismic measurements. Cold Regions Science and Technology,121, 25 **–** 41. DOI :10.1016/j.coldregions.2015.10.004

Permanyer, A., Jorge, R., Baudino, R., Gibert, L. (2016). Organic-rich shales from internal Betic basins (SE Spain): potential source rocks analogs for the pre-Messinian Salt play in the Western Mediterranean. *Geologica Acta*, 14(4), 443-460.

Pla, O.; Ferrer, O.; Gratacós, O.; Muñoz, J.A.; Roca, E. (2016) Influencia de los niveles evaporíticos sin-orogénicos en la geometría del frente surpirenaico central: Anticlinales de Sanaüja y de La Sentiu – Almenara. *Geo-Temas*, 16(1), 65-68.

Prats, E., Busquets, P., Gallastegui, G., Césari, S.N., Cuesta, A., Limarino, C.O., Colombo, F. (2016). Bacterias fósiles con composición mineralógica diferente a la de su entorno. Formación San Ignacio, Paleozoico Superior, Cordillera Frontal, San Juan, Argentina. *Geo-Temas*, 16 (2), 423-426.

Pueyo, E.L., Beamud, E., Rodríguez-Pintó, A., San Miguel, G. (2016). Remagnetización alpina en la Serra del Cadí (Pirineo Oriental). *Geo-Temas*, 16 (1), 869-872.

Puzyrev, V., Vilamajó, E., Queralt, P., Ledo, J., Marcuello, A. (2016). Three-Dimensional Modeling of the Casing Effect in Onshore Controlled-Source Electromagnetic Surveys. *Surveys in Geophysics*. DOI:10.1007/s10712-016-9397-8.

Ramos, A., Fernández, O., Terrinha, P., Muñoz, J. A., (*2016*). Extension and inversion in the Tethys-Atlantic linkage zone, Algarve Basin, Portugal. *International Journal of Earth Sciences*, 105, 1663–1679. doi:10.1007/s00531-015-1280-1

Raposeiro, P.M.; Rubio, M.J.; González, A.; Hernández, A.; Sánchez-López, G.; Vázquez-Loureiro, D.; Rull, V.; Bao, R.; Costa, A.C.; Gonçalves, V.; Sáez, A.; Giralt, S. (2017). Impact of the historical introduction of exotic fishes on the chironomid community of Lake Azul (Azores Islands). Palaeogeography Palaeoclimatology Palaeoecology 466: 77 - 88

Roma, M.; Roca, E.; Ferrer, O.; Pla, O.; Butillé, M. (2016) Formación e inversión de cuencas sinclinales con sal pre-cinemática. Resultados experimentales aplicados a la Cuenca de las Columbretes (Mediterráneo Occidental). *Geo-Temas*, 16(1), 73-76.

Royán, M. J., Abellán, A. and Vilaplana, J. M. (2015): Progressive failure leading to the 3 December 2013 rockfall at Puigcercós scarp (Catalonia, Spain), Landslides, 12, 585–595, doi: 10.1007/s10346-015-0573-6.

Royán, M.J.; Vilaplana, J.M.; Janeras, M.; Abellán, A.(2016): Detección e inventario de desprendimientos de rocas mediante el seguimiento con lidar terrestre en la montaña de Montserrat (Catalunya, España). En: Comprendiendo el relieve: del pasado al futuro. Servicio de Publicaciones del IGME, 5:257-264

Royán, M.J.; Vilaplana, J.M.; Abellán, A. (2016). Uso del ángulo de vuelco en la predicción temporal de desprendimientos de rocas. *Geo-Temas*, 16 (1), 645-648

Rull, V.; Cañellas-Boltà, N.; Margalef, O.; Pla-Rabes, S.; Sáez, A.; Giralt, S. (2016). Three Millennia of Climatic, Ecological, and Cultural Change on Easter Island: An Integrative Overview. Frontiers in Ecology and Evolution 4 (29): 1-4.

Rull, V.; Cañellas-Boltà, N.; Margalef, O.; Pla-Rabes, S.; Sáez, A.; Giralt, S. (2016). Climate changes and cultural shifts on Easter Island during the last three millennia. 2016. PAGES MAGAZINE 24 (2) 70 - 71

Alberto Saez; Linda V. Godfrey; Christian Herrera; Guillermo Chong; Juan J. Pueyo (2016). Timing of wet episodes in Atacama Desert over the last 15 ka. The Groundwater Discharge Deposits (GWD) from Domeyko Range at 25 ºS. Quaternary Science Reviews 145: 82 – 93.

Sánchez-López, G.; Hernández, A.; Plà-Rabes, S.; Trigo, R.M.; Toro, M.; Granados, I.; Sáez, A.; Masqué, P.; Pueyo, J.J.; Rubio-Inglés, M.J.; Giralt, S. (2016). Climate reconstruction for the last two millennia in Central Iberia: the role of East Atlantic (EA), North Atlantic Oscillation (NAO) and their interplay over the Iberian Peninsula. Quaternary Science Reviews 149: 135 – 150.

Santanach, P.; Ruano, P.; Ortuño, M.; Masana, E.; Rubí, C. (2016). On the search for the source of the 1865-66 Nicaraguan earthquakes: paleoseismicdata from the Cofradía fault, Managua graben (Nicaragua). Bulletin of the Seismological Society of America, 106 (3).

Santolaria, P.; Pla, O; Soto, R.; Casas, A.M.; Gratacós, O.; Roca, E.; Ferrer, O.; Muñoz, J.A.; Pueyo, E. (2016). Along-strike structural variations of the Barbastro-Balaguer anticline. *Geo-Temas*, 16 (1), 105-107.

Soriano, C., Beamud, E., Garces, M., & Ort, M. H. (2016). "Anomalous" magnetic fabrics of dikes in the superparamagnetic/single domain threshold. Geophysical Journal International. doi: 10.1093/gji/ggv495

Soto, R., Larrasoaña, J.C., Beamud, E., Garcés, M. (2016). Early–Middle Miocene subtle compressional deformation in the Ebro foreland basin (northern Spain); insights from magnetic fabrics. *Comptes Rendus Geoscience*. 348, 213-223.

Soto, R., Beamud, B., Roca, E., Carola, E., Almar, Y. and Escosa, F. (2016). Magnetic fabrics in syn-diapiric rocks (North Vasco-Cantabrian basin). *Geo-Temas*, 16, 893-896.

Suriñach, E.; Tapia, M.; Pérez-Guillén, C.; Khazaradze, G.; Roig, P. (2016) Comparison of seismic and infrasound wave fields generated by snow avalanches. Geophysical Research Abstracts Vol.18 EGU2016-9515.

Tavani, S., Granado, P., Arbués, P., Muñoz, J.A. (*in press*). Syn-thrusting, near-surface flexural- slipping and stress deflection along folded sedimentary layers of the Sant Corneli-Bóixols Anticline (Pyrenees, Spain). *Journal of Geophysical Research – Solid Earth.*

Valcárcel, M., Soto, R., Beamud, E., Oliva-Urcía, B., Muñoz, J.A., Biete, C. (2016). Integration of paleomagnetic and structural data to characterize the obliquity of the Altomira Range and Loranca basin structures (Central Spain). In: Pueyo, E. L., Cifelli, F., Sussman, A. J. & Oliva-Urcia, B. (eds). *Palaeomagnetism in Fold and Thrust Belts: New Perspectives*. Geological Society, London, Special Publications. 425, 213–232.

Valenzuela, S., Alías, G., Casas, J.M. (2016). Superposición de pliegues hercínicos y alpinos en el Paleozoico del Priorat Central*. Geo-Temas,* 16 (1), 109-112*.*

Valero, L.; Cabrera, Ll.; Sáez, S.; Garcés, M. (2016). Long-period astronomically-forced terrestrial carbon sinks. Earth and Planetary Science Letters 444: 131- 138.

Vázquez, R.; Suriñach, E.; Capra, L.; Arámbula-Mendoza, R.; Reyes-Dávila, G. (2016). Seismic characterisation of lahars at Volcán de Colima, Mexico. Bulletin of Volcanology,78, 8. DOI: 10.1007/s00445-016-1004-9

Vázquez-Taset, Y., Ramos, E., Sàbat, F., Cabello, P., Cruz-Orosa, I. (2016). Evolución tectono-estratigráfica de la Cuenca de Cauto-Güacanayabo, Cuba. *Geo-temas,* 16(1), 189-192.

Victoriano, A., García-Silvestre, M., Furdada, G., and Bordonau, J. (2016): Long-term entrenchment and consequences for present flood hazard in the Garona River (Val d'Aran, Central Pyrenees, Spain). Natural Hazards And Earth System Sciences, Vol. 16: 2055-2070

Victoriano, A.; Guinau, M.; Furdada, G.; Calvet, J.; Cabré M.; Moysset, M. (2016): Aplicación de datos LiDAR en el estudio de la dinámica torrencial y evolución de los barrancos de Portainé y Reguerals (Pirineo Central). Comprendiendo el relieve: del pasado al futuro. Juan José Durán Valsero, Manuel Montes Santiago, Alejandro Robador Moreno y Ángel Salazar Rincón, eds. IGME: 447-455.

Vilaplana, J. M.; Royán, M.J.; Fontquerni,S.; Janeras, M.; González, M. (2016): Los desprendimientos de rocas en la montaña de Montserrat. Un riesgo geológico relevante. En: Oms, O.; Climent, F.; González,M. (Editores): Excursiones geológicas por la Cataluña Central. Monografía técnica 6. 79-96. ICGC.

PARTICIPACIONS A CONGRESSOS

Congress participations

4

geomodels

institut de recerca

Alonso-Muruaga, P.J., Limarino, C.O., Spalletti, L.A., Colombo, F. (2016). Aspectos sedimentológicos y estratigráficos del relleno de un paleovalle glacial Pennsilvaniano en el área de la Loma de los Piojos, Precordillera Central de San Juan. VII Congreso Latinoamericano de Sedimentologia. Santa Rosa, Argentina. Sesión ST 16.

Albert-Villanueva, E., Esteban, M., González, L., Salas, R., Bover-Arnal, T., Ferràndez-Cañadell, C., Fernández Carmona, J. (2016). San Luis and Churuguara carbonates (onshore Venezuela): Analogs of the offshore Perla field? International Conference and Exhibition, Barcelona, Spain, 3-6 April 2016, pp. 49-49. doi: 10.1190/ice2016-6364499.1. AAPG & SEG International Conference and Exhibition. Barcelona (Spain), 3-6/04/2016.

Aguirre, J., Bover-Arnal, T. (2015). Upper Oligocene coralline algal assemblages from the Benitatxell Range (Alicante, SE Spain). V International Rhodolith Workshop, Program 2015. V International Rhodolith Workshop. San José (Costa Rica), 27-31/07/2015.

Arbués, P., De Matteis, M., Cabello, P., Burcet, M., Demko, T., Abreu, V. (2016). The O Grao turbidite system: architectural and depositional interpretations from outcrop and well data (Middle Eocene, Ainsa Basin, Spain). 32nd IAS Meeting of Sedimentolgy. International Association of Sedimentologists. Marrakech, Mayo de 2016

Bartolomé, R., Górriz, E., Dañobeitia, JJ., Córdoba, D., Martí, D., Cameselle, A.L., Núñez-Cornú, F., Bandy, W. L., Morter, C., Nuñez, D., Prada, M., Alonso, J. L., Castellon, A. (2016). Multichannel seismic imaging of the Rivera Plate subduction at the seismogenic Jalisco Block area (Western Mexican margin). AGU Fall Meeting. San Francisco, December 2016

Rafael Bartolome, Estefanía Górriz, Juanjo Dañobeitia, Diego Cordoba, David Martí, Alejandra L. Cameselle, Francisco Núñez-Cornú, William L. Bandy, Carlos A. Mortera-Gutiérrez, Diana Nuñez, Arturo Castellón, Jose Luis Alonso. (2016) Multichannel seismic imaging of the Rivera Plate subduction at the seismogenic Jalisco Block area (Western Mexican margin). Asamblea Hispano Portuguesa de Geodesia y Geofísica. Madrid, Junio de 2016.

Beamud, E.; Soto, R.; Roca, E.; Carola, E.; Almar, Y. (2016) Datos paleomagnéticos en materiales sin-diapíricos Aptienses-Albienses (cuenca Vasco-Cantábrica, N Iberia). IX Congreso Geológico de España 12-14 Septiembre 2016

Belaustegui, Z., Puddu, C., Casas, J.M. (2016). New ichnological data from the lower Paleozoic pf the Central Pyrenees: presence of *Artrophycus Brogniartii* (Harlam, 1832) in the Upper Ordovician Cava Formation. IX Congreso Geológico de España. Sociedad Geológica de España. Huelva, Septiembre de 2016.

Blanch, X.; Guinau, M.; Royán, M.J. (2016). Análisis de la evolución de desprendimientos a partir de datos LiDAR en el escarpe de Puigcercós (Pallars Jussà – Cataluña). Congreso Geológico de España, Huelva, 2016.

Blanch, X.; García-Sellés, D.; Guinau, M.; Royán, M.J. (2016). Rockfall source areas detection and characterization from Terrestrial Laser Scanner (TLS) data. Virtual Geosciences Conference 2016, Bergen (Norway).

Bover-Arnal, T., Esteban, M., Aguirre, J., Ferràndez-Cañadell, C., Giner, J.A., Salas, R. (2016). The Miocene rhodalgal Amposta limestone in the Tarraco reservoir (offshore eastern Spain). International Conference and Exhibition, Barcelona, Spain, 3-6 April 2016, pp. 39-39. doi: 10.1190/ice2016-6364696.1. AAPG & SEG International Conference and Exhibition. Barcelona (Spain), 3-6/04/2016.

Bover-Arnal, T., Moreno-Bedmar, J.A., Frijia, G., Pascual-Cebrian, E., Salas, R. (2016). Strontium-isotope stratigraphy and ammonoid biostratigraphy of the late Barremian-early Albian succession from the Maestrat basin (E Iberia). International Conference and Exhibition, Barcelona, Spain, 3-6 April 2016, pp. 267-267. doi: 10.1190/ice2016-6364815.1. AAPG & SEG International Conference and Exhibition. Barcelona (Spain), 3-6/04/2016.

Bover-Arnal, T., Ferràndez-Cañadell, C., Aguirre, J., Albert-Villanueva, E., Esteban, M., Fernández Carmona, J., Salas, R. (2016). Anatomy of a latest Chattian carbonate ramp with larger foraminifera and coralline algae (Prebetic domain; SE Spain). International Conference and Exhibition, Barcelona, Spain, 3-6 April 2016, pp. 53-53. doi: 10.1190/ice2016-6364219.1. AAPG & SEG International Conference and Exhibition. Barcelona (Spain), 3-6/04/2016.

Cabello, P., López, C., Dussán, M. I., Gamba, N., Calvo, R., Vázquez, Y., Ramos, E. (2016). Definición de trampas estratigráficas en cuencas petrolíferas maduras: Estudio integrador de la Cuenca del Valle Medio del Magdalena, Colombia. IX Congreso Geológico de España. Sociedad Geológica de España. Huelva, Septiembre de 2016

Canora, C., Roca, C., Martínez-Díaz, J.J., Insua-Arévalo, J.M., Martín-González, F., Gómez-Ortiz, D., Martínez-Pagan, P., Masana, E., Ortuño M., Ferrater, M., Medialdea, A., (2016). Nuevos datos de actividad paleosísmica de la falla de Alhama de Murcia en el abanico de La Salud (segmento Lorca-Totana de la Falla de Alhama de Murcia), Béticas orientales. Geo-Temas 16, IX Congreso Geológico de España, Huelva, Septiembre 2016

Carmona, A., Gratacós, O., López-Blanco, M., Muñoz, J. A., Clavera-Gispert, R., Arbues, P., & Hardy, S. (2016). The Effect of syntectonic sedimentation on fold geometry: Insights from numerical modelling. In GeoMod 2016 conference. Montpellier.

Colombo, F., Alonso, J.L., Limarino, C.O., Quintana, R., Cardó, R., Césari, S.N. (2016). Características estratigráficas y estructurales de un paleovalle glacial Mississipiense. Precordillera Andina, San Juan (Jáchal), Argentina. IX Congreso Geológico de España, Huelva. Geo-Temas 16:435-438.

De Matteis, M., Belaústegui, Z., Arbués, P., Granado, P., Cabello, P., Demko, T., & Abreu, V. (2016). Ichnological analysis of the turbiditic Solitary Channel Complex from drillcore data (Miocene, Tabernas Basin, SE Spain). In ICHNIA. Idanha-a-Nova, Portugal.

De Matteis, M., Arbués, P., Belaústegui, Z., Cabello, P., Granado, P., Demko, T., & Abreu, V. (2016). Flow characteristics as inferred from core and outcrop data of a turbidite channel-fill : The Solitary Channel (Miocene, Tabernas Basin , SE Spain). In IAS 32nd Meeting of Sedimentology. Marrakech, Marruecos.

Escosa, F.O.; Roca, E.; Butillé, M.; Roma, M.; Ferrer, J.O (2016) The Mesozoic structure of the central part of the south-Iberian passive margin and its influence in the Cenozoic contractional deformation: Comparision between the eastern Prebetic zone (Betic cordillera) and the Columbrets basin (southern Valencia trough). AAPG ICE Barcelona 3-6 Abril 2016

Escosa, F. O. and Roca, E. (2016). The external eastern Prebetic: paper of basement faults in an inverted salt-bearing passive margin. Conference poster. AAPG/SEG's International Conference and Exhibition at Barcelona.

Escosa,F.O.; Roca, E.; Ferrer, O. (2016) Papel de las fallas extensivas de piel gruesa pre-existentes en la deformación de piel fina afectando a un margen pasivo invertido con tectónica salina (Prebético oriental). IX Congreso Geológico de España

Escosa, F.O.; Ferrer, O.; Roca, E.; Gratacós, O.; Muñoz, J.A. (2016) Modeling the interaction between seamounts & gravitational failure in passive margins: the Messinian case in Western Mediterranean. Salt-sediment interaction research consortium (SSIRC meeting), Cortez 24-26 Mayo 2016.

Ferràndez-Cañadell, C., Bover-Arnal, T. (2016). Chattian larger foraminifera from the Benitatxell range (Prebetic domain, SE Spain). Discussion on the characterization of Shallow Benthic Zone 23. International Conference and Exhibition, Barcelona, Spain, 3-6 April 2016, pp. 266-266. doi: 10.1190/ice2016-6361617.1. AAPG & SEG International Conference and Exhibition. Barcelona (Spain), 3-6/04/2016.

Ferràndez-Cañadell, C., Bover-Arnal, T. (2015). Chattian larger foraminifera from the Benitatxell Range (Prebetic Domain, SE Spain). Comments on the biostratigraphy utility of certain species. Ber. Inst. Erdwiss. K.-F.-Univ. Graz., p. 107. ISSN 1608-8166, Band 21. STRATI 2015. Graz (Austria), 19-23/07/2015.

Ferrater, M. (2016). Active tectonics, paleoseismology and associated methodological challenges posed by the slow moving Alhama de Murcia fault (SE Iberia). PhD Student Conference (PhDSC), Institut de Physique du Globe de Paris (IPGP), 14-18 March, 2016, Paris, France.

Ferrater, M., Ortuño M., Masana, E., Pallàs, R., Perea, H., Baize, S., García-Meléndez, E., Martínez-Díaz, J.J., Echeverría, A., Rockwell, T., Sharp, W.D., Arrowsmith, R., Medialdea, A., Rhodes, E.J. (2016). Active tectonics, paleoseismology and associated methodological

challenges posed by the slow moving Alhama de Murcia fault (SE Iberia). European Goesciences Union General Assembly 2016, Vienna.

Ferrater, M., Ortuño M., Masana, E., Martínez-Díaz, J.J., Pallàs, R., Medialdea, A., Perea, H., Baize, S., García-Meléndez, E., Echeverría, A., Rockwell, T., Sharp, W.D., Rhodes, E., Arrowsmith, R. (2016). Velocidad de desplazamiento de la falla de Alhama de Murcia calculada mediante técnicas paleosismológicas y morfotectónicas. Geo-Temas 16, IX Congreso Geológico de España, Huelva, Septiembre 2016 (ISSN: 1576-5172, Ed. Morales, J.A., Carro, B., Sarmiento, A.M., Camacho, M.A.)

Ferrater, M., Ortuño M., Pallàs, R., Perea, H., Baize, S., García-Meléndez, E., Martínez-Díaz, J.J., Echeverría, A., Khazaradze, G., Rockwell, T., Sharp, W.D., Arrowsmith, R., Medialdea, A., Rhodes, E., Masana, E. (2016). Characterizing the seismic potential of a slow moving fault by integrating different techniques: the Alhama de Murcia fault (southeastern betics, Spain). ESC General Assembly. Trieste 4-10 September, 2016

Ferrer, O.; Gratacós, O.; Roca, E.; Muñoz, J.A. (2016) Influencia de volcanes o altos submarinos en la deformación supra-sal en márgenes pasivos con tectónica gravitacional: Resultados experimentales y aplicación al Mediterráneo Occidental. IX Congreso Geológico de España, Huelva, September 2016. Oral presentation.

Ferrer, O.; McClay, K.; Sellier, N.C.; Roma, M.; Roca, E.; Muñoz, J.A. (2016) Modelizando el control de las evaporitas y la geometría de falla en desarrollo de cuencas sinclinales y en su posterior inversión: Aplicación a cuencas ibéricas. IX Congreso Geológico de España, Huelva, September 2016. Oral presentation.

Ferrer, J.O.; Roca, E.; Gratacós, O., Muñoz, J.A. (2016) Seamount control during gravity-driven extension involving multi-layered evaporites. AAPG/SEG 2016 International Conference & Exhibition. Barcelona, April 2016. Oral presentation.

Ferrer, J.O.; Carrera, N.; Roca, E.; Muñoz, J.A.; Rowan M.G.; Giles K.; (2016) Experimental approach to megaflap development during passive salt diapirism: Controlling factors and kinematics. AAPG/SEG 2016 International Conference & Exhibition. Barcelona, April 2016.

Ferrer, O, Escosa, F. O**.,** Roca, E., Gratacós, O. and Muñoz, J. A., (2016). Modeling the interaction between seamounts & gravitational failure in passive margins: the Messinian case in Western Mediterranean. Conference paper. In the Salt-sediment interaction research consortium (SSIRC meeting) Institute of Tectonic Studies (ITS) and University of Texas at El Paso (UTEP). Cortez (Colorado).

Ferrer, O., Gratacós, O., Roca, E., Muñoz, J.A. (2016). Experimental insights of the seamount control during gravity-driven extension in passive margins salt basins. 78th EAGE Conference & Exhibition 2016. Viena, June 2016. Oral presentation.

Ferrer, O.; Roca, E.; Carrera, N.; Muñoz, J.A.; Rowan, M.; Giles, K. (2016) Growth of Megaflaps during Differential Loading - Insights from Analogue Modeling. 79th EAGE Conference & Exhibition 2016

Flores-Márquez E.-L. and Suriñach, E. (2016). Characterization of snow avalanches applying the Hough transform to the spectrograms of the seismic signals generated by the avalanches. Poster. International Workshop conference on Time series Analysis ITISE2016. 27-29 June. Granada.

Furdada, G.; Génova, M.; Guinau, M.; Victoriano, A.; Khazaradze, G.; Díez-Herrero, A.; Calvet, J . (2016). Las avenidas torrenciales de los barrancos de Portainé, Reguerals y Ramiosa (Pirineo Central): evolución de las cuencas y dinámica torrencial. XIV Reunión Nacional de Geomorfología. Málaga, 22-25 June 2016.

Miguel Garcés; Luis Valero; Lluís Cabrera; Alberto Sáez; Elisabeth Beamud. Long-term Sedimentary Trends of Neogene Lake Systems of the Iberian Plate 2016 RCMNS Interim Colloquium - CGS Limnogeology Workshop, Zagreb (CROACIA) 2016

García-Selles, D.; Martínez Granado, P.; Gratacós, O.; Muñoz, J.A. (2016) Geometrical characterization of fracture systems in rock mass by means ofd terrestrial laser scanner. AAPG - ICE Barcelona 3-6 Abril 201

García-Selles, D.; Gratacós, O.; Muñoz, J.A.; Sarmiento, S.; (2016) Characterization of

geological structures with technical improvements in acquisition and processing. 2nd Virtual Geoscience Conference, Bergen, Norway, 21-23 September 2016.

Gratacós, O.; Carmona, A.; Clavera-Gispert, R.; Muñoz, J.A.; Hardy, S. (2016) Modelación numérica de sedimentación subacuática sintectónica: efecto de la presencia de fallas normales y zonas de relevo en la distribución de sedimento. IX Congreso Geológico de España 12-14 Septiembre 2016.

Gómez-Novell, O., Ortuño, M. (2016). Seismic amplification due to topography: preliminary results of a gelatin model. Geomod 2016, 17-20 October, Montpellier, Poster

Gomez-Paccard, M., Beamud, E., Bergada, M., Martínez, P. (2016). A combined archeomagnetic and microstratographic study of Neolithic anthropogenic burnt sediments from the Can Sadurni cave (NE Spain). EGU General Assembly. Viena 17-22 Abril 2016. Poster

Gorriz, E., Marcuello, A., Escosa, F., Queralt, P., Martí, A., Ledo, J. and Roca, E. (2016). A magnetotelluric study in La Rosa Diapir (Murcia, Spain). Conference poster. Near Surface Geoscience, 2016. 22nd European Meeting of Environmental and Engineering Geophysics (EAGE). Barcelona, September 2016.

Guinau, M.; Ortuño, M.; Calvet, J.; Furdada, G.; Bordonau, J.; Ruíz, A.; Camafort, M. (2016). Detection of early stage large scale landslides in forested areas by 2 m LiDAR DEM analysis. The example of Portainé (Central Pyrenees). EGU General Assembly 2016, Viena (Austria).

Heredia, N., García-Sansegundo, J., Gallastegui, G., Farias, P., Giacosa, R., Alonso, J.L., Busquets, P., Charrier, R., Clariana, P., Colombo, F., Cuesta, A., Gallastegui, J., Giambiagi, L., González-Menéndez, L., Limarino, C.O., Martínez-González, F., Pedreira, D., Ramos, V.A., Rubio-Ordóñez, A., Seggiaro, R., Serra-Varela, S., Spalletti, L.A. (2016). Orogenias paleozoicas en los Andes de Argentina y Chile, y en la Península Antártica. I Simposio sobre Tectónica Sudamericana. Santiago de Chile. Actas 1: 70.

Hernández, A.; Leira, M.; Vázquez- Loureiro, D.; Trigo, R. Carballeira, R.; Sáez, A. (2016): The impact of AMO and NAO in Western Iberia during the Late Holocene. 2016 AGU Fall Meeting. Abtracts, PP51A-2286. San Francisco (USA)

Izquierdo, E.; Roca, E.; Xie, E.; Pla, O.; Huang, S.; Muñoz, J.A.; Neng, Y.; Rowan M. (2016) The Kuga Foreland Basin (NW China) - Geometry of a Fold-and-thrust Belt Controlled by Multiple Décollements. 78th EAGE Conference & Exhibition 30 mayo a 2 Junio 2016

Izquierdo-Llavall, E.; Roca, E.; Pla, O.; Neng, Y.; Muñoz, J.A.; Rowan M.G.; Huang, S. (2016) Geometry of a fold-and-thrust belt controlled by multiple décollements: The structureof teh central Kuqa Basin (MW China). IX Congreso Geológico de España 12-14 Septiembre 2016.

Khazaradze, G; Guinau, M.; Calvet, J.; Furdada, G.; Victoriano, A.; Génova, M.; Suriñach, E. (2016). Debris flow cartography using differential GNSS and Theodolite measurements. EGU 2016, Viena (Austria), 17–22 April 2016.

Khazaradze, G., Echeverria, A., & Masana, E. (2016). Geodetic slip rate estimates for the Alhama de Murcia and Carboneras faults in the SE Betics, Spain. *Geophysical Research Abstracts*, *18*, 40828.

Khazaradze, G., Echeverria, A., Asensio, E., Masana, E., & Suriñach, E. (2015). Geodetic and geological evidence for continuing tectonic activity of the Alhama de Murcia and Carboneras faults in the SE Betics, Spain. In X. Pérez Campos (Ed.), *Sismo 85: Avances y retos en sismología, ingeniería y gestión de riesgos a 30 años del sismo de 1985* (p. SE02-2, 40). Ciudad de México, México.

López-Blanco, M. (2016). El Margen SE de la Cuenca del Ebro hace unos 40 Millones de años y la sedimentación en Montserrat y Sant Llorenç del Munt. Un paseo desde las montañas hasta el mar profundo. Excursiones Geológicas por la Cataluña Central. In XIX Simposio sobre enseñanza de la Geología. Manresa.

Machavariani, K., Khazaradze, G., Turazashvili, I., Kachakhidze, N., Kachakhidze, M., & Gogoberidze, V. (2016). The results of the pilot project in Georgia to install a network of electromagnetic radiation before the earthquake. In *Geophysical Research Abstracts, Vol. 18, EGU2016-2257-1, 2016.* (Vol. 18, p. 2257). Vienna, Austria.

A. Marcuello; E. Gorriz; F. Escosa; P. Queralt; J. Ledo; A. Martí; C. Ayala; F. Rubio; P. Martínez

Pagán; B. Benjumea; A. Gabàs; E. Roca (2016) Estudio geoeléctrico integrado de la zona del diapiro La Rosa (Murcia). 9a Asamblea Hispano-Portuguesa de Geodesia y Geofísica.

Marcuello, A, Ledo, J., Queralt, P., Vilamajó, E., Martí, A. (2016) Challenges in geoelectrical monitoring using instrumented wells. Fourth International Congress on Multiphysics, Multiscale, and Optimization Problems, Bilbao, Spain, March 2016

Marcuello, A., Gorriz, E., Escosa, F., Queralt, P., Ledo, J., Martí, A., Ayala, C., F. Rubio, F., Martínez Pagán, P., Benjumea, B., Gabàs, A., Roca, E. (2016). Estudio geoeléctrico integrado de la zona del diapiro La Rosa (Murcia). 9a Asamblea Hispano-Portuguesa de Geodesia y Geofísica. Madrid, June 2016

Margalef, A., Casas, J.M. (2016). Corte geológico compensado del sur de Andorra: aportaciones a la estructura varisca del Pirineo central. IX Congreso Geológico de España. Sociedad Geológica de España. Huelva, Septiembre de 2016.

Margalef, A., Casas, J.M., Castiñeiras, P., Navidad, N., Liesa, M. (2016). Comparison betwqen detrital zircon populations from the Ordovician rocks of the Pyrenees and from other Perigiondwanan terrains: paleogegrpahic implications. IX Congreso Geológico de España. Sociedad Geológica de España. Huelva, Septiembre de 2016.

Martí, A., Queralt, P., Ledo, J.J. (2016). DTM3 responses, dimensionality analysis of secret model data and inversion of land sites. Magnetotelluric 3D inversion workshop III. Bari (Italy), May 2016.

Martí, A., Queralt, P., Ledo, J.J., Marcuello, A., Alvarez-Aramberri, J., Martínez-Diaz, J.J. (2016). Magnetotelluric characterization of the Alhama de Murcia Fault (Eastern Betics): preliminary results. 22nd European Meeting of Environmental and Engineering Geophysics. Barcelona, September 2016

Muñoz, J.A.; Roca, E.; Ritske, H.; Suzon, J.; Ferrer, J.O.; Gratacós, O. (2016). The tectonic evolution of the north Iberian margin. The Roberts Conference - Passive Margins 2016 6-8 Abril

Muñoz, J.A.; Roca, E.; Ferrer, O.; Arbués.; Beamud, E.; Gratacós. O.; Fernández. (2016) Diapir growth during the development of a thrust salient: The Ainsa Oblique Zone (Central Pyrenees). 78th EAGE Conference & Meeting

Murillo Lopez, M. H., Dominguez, D., Cabello, P., & Arbués, P. (2016). From Conventional Outcrop Datasets to Flow Simulation : the Fluvial Strata in Pont de Montanyana (Ypresian, Southern Pyrenees). In IAS 32nd Meeting of Sedimentology. Marrakech, Marruecos.

Nebot, M., Guimerà, J. (2016c). La extensión Triásica en el substrato de la Cuenca del Maestrat, y evidencias de tectónica salina en las evaporitas en facies Muschelkalk medio (Cadena Ibérica Oriental). IX Congreso Geológico de España. Sociedad Geológica de España. Huelva, Septiembre de 2016.

Nebot, M., Guimerà, J. (2016d). Inversión cenozoica de la Cuenca mesozoica del Maestrat: evolución cinemática del cinturón de pliegues y cabalgamientos desarrollado en su margen norte (Cadena Ibérica oriental). IX Congreso Geológico de España. Sociedad Geológica de España. Huelva, Septiembre de 2016.

Oliva, B., Beamud, E., Soto, R., Pueyo, E.L., Garcés, M., Valero, L. (2016). Fábricas magnéticas en el antepaís del orógeno Pirenaico, relación con los últimos estadios de deformación (cabalgamiento de San Felices, Sierras Exteriores Aragonesas). 61 Sesión Científica de la Sociedad Geológica de España. Zaragoza, 25 noviembre 2016.

Oliva-Urcia, B., Beamud, E., Soto, R., Arenas, C., Garcés, M., Pueyo, E.L. (2016). Datación magnetostratigráfica de la molasa Surpirenaica (Fm Uncastillo, Oligoceno-Mioceno). IX Congreso Geológico de España. Huelva, 12-14 setembre 2016. Geotemas16. Oral

Oliva-Urcia, B., Beamud, E., Soto, R., Arenas, C., Garcés, M., Pueyo, E. (2016). Preliminary magnetostratigraphic dating of the South-Pyrenean Molasse (Uncastillo Fm, Oligocene-Miocene). EGU General Assembly. Viena, 17-22 Abril 2016. Poster

Olmos, P.; Furdada, G.; Garcia, A.; Polonio, T.; Palet, J.M. Evaluating natural hazards and tourist impact on mountain archaeological heritage conservation in Núria and Coma de Vaca valleys (Eastern Pyrenees). YOCOCU2016: 5th INTERNATIONAL CONFERENCE YOuth in COnservation of CUltural Heritage. Madrid. 21-23 September 2016

Ortega, D., Terradas, X., Roqué, C., Ibáñez, J., Beamud, E., Larrasoaña, J.C. (2016). Caracterización petrológica del sílex de la Formación Calizas de Montmaneu (Sector oriental de la Cuenca del Ebro). 60 Sesión Científica de la Sociedad Geológica de España. Barcelona, 20 Mayo 2016.

Ortuño M., Ferrater, M., Masana, E., Martínez-Díaz, J.J., Pallàs, R., Perea, H., Baize, S., García-Meléndez, E., Rockwell, T., Sharp, W.D., Medialdea, A., Rhodes, E., Cunha, P.P., Sohbati, R., Buylaert, J.P., Murray, A. (2016). Combinación de métodos de datación en cronologías paleosísmicas: el ejemplo de El Saltador (Falla de Alhama de Murcia). Geo-Temas 16, IX Congreso Geológico de España, Huelva, Septiembre 2016 (ISSN: 1576-5172, Ed. Morales, J.A., Carro, B., Sarmiento, A.M., Camacho, M.A.)

Ortuño, M. Aguirre, G., Lacan, P., Zúñiga, R. (2016). Seismic and volcanic events in central mexico: lesson from paleoseismological excavations. IASPEI-IAVCEI International Workshop on Earthquakes and Volcanoes, Barcelona, 8-9 November. Presentación oral.

Pascual-Cebrian, E., Bover-Arnal, T., Salas, R., Skelton, P.W., Gili, E. (2016). Sequence-stratigraphy and depositional model of an Aptian non-rimmed carbonate platform (Maestrat basin, E Spain). International Conference and Exhibition, Barcelona, Spain, 3-6 April 2016, pp. 263-263. doi: 10.1190/ice2016-6512278.1. AAPG & SEG International Conference and Exhibition. Barcelona (Spain), 3-6/04/2016.

Pavón-Carrasco, F.J., Gómez-Paccard, M., Carrancho, A., Beamud, E. (2016). Archaeomagnetism in Iberia: state-of-the-art, successes and future challenges. Cronometrías para la Historia de la Península Ibérica. Barcelona, 17-19 octubre 2016.

Pla, O., Muñoz, J.A., Ferrer, O., Roca, E., Gratacós, O. Development of detachment folds on syn-orogenic sequences including salt layers. In the EAGE-77th Conference and Exhibition 2015. Madrid, Spain.

Pla, O., Muñoz, J.A., Ferrer, O., Roca, E., Gratacós, O. Halokinetic deformations during the development of detachment folds on multilayered syn-orogenic evaporitic sequences. Results from analogue modeling and comparison with the Sanaüja Anticline (Ebro Foreldand Basin, Iberian Peninsula). In the AAPG SEG International Conference and Exhibition 2015. Melbourne, Australia.

Pla, O.; Carmona, A.; Izquierdo, E.; Roca, E.; Muñoz, J.A.; Ferrer, J.O.; Hardy, S.; Huiwen, X.; Yuan, N.; Shaoying, H.; Rowan, M.; (2016) Geometry of a fold-and-thrust belt generated by multiple décollements (Kuga basin, NW China): Insights from analogue and numerical models. AAPG - ICE Barcelona 3-6 Abril 2016

Pla, O.; Ferrer, O.; Gratacós, O.; Muñoz, J.A.; Roca, E. (2016) Influencia de los niveles evaporíticos sin-orogénicos en la geometría del frente surpirenaico central: Anticlinales de Sanaüja y de La Sentiu – Almenara. IX Congreso Geológico de España

Prats, E., Busquets, P., Gallastegui, G., Césari, S.N., Cuesta, A., Limarino, C.O., Colombo, F. (2016). Bacterias fósiles con composición mineralógica diferente a la de su entorno. Formación San Ignacio, Paleozoico Superior, Cordillera Frontal, San Juan, Argentina. IX Congreso Geológico de España, Huelva. Geo-Temas 16:423-426.

Pueyo, E.L., Beamud, E., Rodríguez-Pintó, A., San Miguel, G. (2016). Remagnetización alpina en la Serra del Cadí (Pirineo Oriental). IX Congreso Geológico de España. Huelva, 12-14 setembre 2016. Geotemas16. Oral

Puzyrev, V., Vilamajó, E., Queralt, P., Ledo, J., Marcuello, A. (2016). (2016). Steel casing effect on land CSEM monitoring. SEG International Conference and Exhibition. Barcelona, Spain, 3-6 April 2016. DOI:10.1190/ice2016-6284929.1

Ramos, A., Fernández, O., Torne, M., Terrinha, P., Muñoz, J.A., Manatschal, G., 2016. Inversion of a hyperextended passive margin. EGU General Assembly 2016, Vienna. Presented at the EGU General Assembly 2016, Vienna.

Raposeiro, P.M.; Saez, A.; Giralt, S; Costa, A.C; Gonçalves, V. Spatial distribution of subfossil diatom and chironomid assemblages' in surface sediments of a remote oceanic lake: The case of Lake Azul (Azores archipelago). 2nd International Conference on Island Evolution, Ecology and Conservation: Island Biology 2016, 18-22 July 2016. Angra do Heroísmo, Azores (PORTUGAL)

Raposeiro, P.; Saez, A.; Giralt, S.; Costa, A.C.; Gonçalves, V. Spatial distribution of subfossil diatom and chironomid assemblages' in surface sediments of a remote oceanic lake: the case of Lake Azul (Azores Archipelago). 33rd SIL Congress, July 31, 2016 - August 5, 2016. Torino (ITALIA

Raposeiro, P.; Rubio, M.J; Gonzalez, A.; Hernández, A.; Vazquez-Loureiro, D.; Rull, V.; Bao, R.; Costa, A.C.; Gonçalves, V.; Sáez, A.; Giralt, S. Impact of the historical introduction of exotic fishes on chironomid community of Lake Azul (Azores Islands) and relevance for paleolimnological reconstruction. Community ecology for the 21st century. 17-19 Oct 2016. Evora (PORTUGAL)

Roca, E.; Butillé, M.; Ferrer, J.O.; Arbués, P.; De Matteis, M.; Muñoz, J.A.; Rowan, M.; Giles, K. (2016) Salt tectonics and salt-sediment interaction around the Bakio Diapir, Basque-Cantabrian Basin, Pyrenees. AAPG - ICE Barcelona 3-6 Abril 2016

Roig, P.; Tapia, M.; Pérez-Guillén, C.; Suriñach, E. (2016). Snow avalanches studies using seismic signal and numerical modelling tools. Presentation of oral communication in 9 th Asamblea Hispano Portuguesa de Geodesia y Geofísica. Madrid 28-30 June 2016.

Roma, M.; Roca, E.; Ferrer, O.; Pla, O.; Butillé, M. (2016) Formación e inversión de cuencas sinclinales con sal pre-cinemática. Resultados experimentales aplicados a la Cuenca de las Columbretes (Mediterráneo Occidental) IX Congreso Geológico de España 12-14 Septiembre 2016

Roma, M.; Ferrer, O.; McKlay, K.; Muñoz, J.A. (2016) Rift-system features overlaying a salt layer and above a multiple bend extensional fault: inversion of hyperextended rift margins. The Roberts Conference Passive Margins 2016 6-8 Abril 2016

Royán, M.J., Vilaplana, J.M., Janeras, M., Abellán, A. (2016): Detección e inventario de desprendimientos de rocas mediante el seguimiento con LiDAR Terrestre en la Montaña de Montserrat (Catalunya, España). XIV Reunión Nacional de Geomorfología, Málaga, 2016

Royán, M.J., Vilaplana, J.M., Abellán, A. (2016): Uso del ángulo de vuelco en la predicción temporal de desprendimientos de rocas. Congreso Geológico de España, Huelva, 2016.

Rubio-Inglés, M.J.; Shanahan, T.M.; Hernández, A.; Sáez, A.; Raposeiro, P.M.; Vázquez-Loureiro, D.; Sanchez-López, G.; Gonçalvez, V.; Bao, R.; Trigo, R.; Giralt, S. (2016)The role of the NAO on the North Atlantic hydrological conditions and its interplay with the EA and SCAND atmospheric patterns. 2016 AGU Fall Meeting. Abtracts, PP51A-2287. San Francisco (USA).

Sánchez-López, G.; Hernández, A.; Pla-Rabes, S.; Toro, M.; Granados, I; Masqué, P.; Rubio-Inglés, M.J.; Sáez, A.; Giralt, S. Climate imprints and forcing mechanisms in the iberian central range during the last two millennia. 33rd SIL Congress, July 31, 2016 - August 5, 2016 Torino (ITALIA)

Sanchez-López, G.; Hernández, A.; Pla-Rabes, S.; Trigo, R.; Toro, M.; Granados, I.; Sáez, A.; Masqué, P.; Pueyo, J.J.; Rubio-Inglés, M.J.; Giralt, S. (2016). East Atlantic (EA) and North Atlantic Oscillation (NAO) interplay over the Iberian Peninsula for the last two millennia. 2016 AGU Fall Meeting. Abtracts, PP51A-2285. San Francisco (USA).

Santolaria, P.; Pla, O; Soto, R.; Casas, A.M.; Gratacós, O.; Roca, E.; Ferrer, O.; Muñoz, J.A.; Pueyo, E. (2016) Variaciones laterales de la estructura del anticlinal de Barbastro-Balaguer. IX Congreso Geológico de España

Soto, R., Beamud, E., Roca, E., Carola, E., Almar, Y., Escosa, F. (2016). Fábricas magnéticas en materiales sin-diapíricos del encajante (N cuenca Vasco-Cantábrica). IX Congreso Geológico de España. Huelva, 12-14 setembre 2016. Geotemas16. Oral

Soto, R., Beamud, E., Carola, E., Almar, Y., Roca, E. (2016). Magnetic fabrics on syn-diapiric overburden rocks: The Bakio diapir (Basque-Cantabrian basin, Northern Spain). EGU General Assembly. Viena 17-22 Abril 2016. Poster

Spalletti, L.A., Colombo, F. (2016). Arquitectura de facies intereruptivas y sineruptivas en un paleovalle andino cuaternario: Formación Huarenchenque, Neuquén, Argentina. VII Congreso Latinoamericano de Sedimentologia. Santa Rosa, Argentina. Sesión ST 14.

Suriñach, E.; Pérez-Guillén, C.; Tapia, M.; Khazaradze, G.; Roig, P. (2016). Contribution of the

cross- correlation of seismic and infrasound waves generated by snow avalanches to the knowledge of their temporal evolution and characteristics. Presentation of oral communication in 9 ª Asamblea Hispano Portuguesa de Geodesia y Geofísica. Madrid 28-30 June 2016.

Suriñach, E.; Tapia, M.; Pérez-Guillén, C.; Khazaradze, G.; Roig, P. (2016) Comparison of seismic and infrasound wave fields generated by snow avalanches. Presentation of PICO communication EGU General Assembly 2016, Viena (Austria). *Geophysical Research Abstracts*, *18*, 9515.

Suriñach, E. Mangeney, A., Levy, C., Roig P. and Durand, V. (2016). Recovering the seismic energy transmitted to the ground by snow avalanches. Presentation of oral communication in AGU Fall Meeting, (2016) San Francisco 12-16 December 2016.

Tavani, S., Granado, P., Arbués, P., Muñoz, J.A. (2016). Reactivation of a syn-growth unconformity during flexural-slip folding (Bóixols Anticline, Pyrenees, Spain). TS6.6GM4.8. Fold-and-thrust belts and accretionary wedges. *EGU General Assembly 2016*, Vienna. 2016EGUGA. 18.2096T

Tavani S., Bertok C., Corradetti A., Granado P., Vigna B. (2016). A Pyrenean mid-Cretaceous extensional fault system in the Briançonnais Domain of the Alps: implications for the eastern termination of the segmented Bay of Biscay-Pyrenean rift system. 88º Congresso della Società Geologica Italiana, Napoli, Italia.

Valenzuela, S., Alías, G., Casas, J.M. (2016). Superposición de pliegues hercínicos y alpinos en el Paleozoico del Priorat Central. IX Congreso Geológico de España. Sociedad Geológica de España. Huelva, Septiembre de 2016.

Valero, L., Garcés, M., Huerta, P., & Cabrera, L. (2016). The Upstream and Downstream impact of Milankovitch cycles in continental nonmarine sedimentary records. In EGU General Assembly (Vol. 18, p. EGU2016-16035-1). Viena.

Valero, L., Garcés, M., Cabrera, L., & Sáez, A. (2016). Long-period astronomically forced peat deposits. In EGU General Assembly (Vol. 18, p. EGU2016-16282). Viena.

Vázquez-Taset, Y., Ramos, E., Sàbat, F., Cabello, P., Cruz-Orosa, I., (2016). Evolución tectono-estratigráfica de la Cuenca de Cauto-Güacanayabo, Cuba. IX Congreso Geológico de España, 12-14 de Septiembre de 2016, Huelva, España.

Viaplana-Muzas, M., Ortuño, M., Perez-Peña, V., Galve, J.P., Babault, J., Van Den Driessche, J. and Dominguez, S. (2016). Evolution of morphotectonic parameters in an experimental wedge. Geomod 2016, 17-20 October, Montpellier, Poster

Victoriano, A.; Guinau, M.; Furdada, G.; Calvet, J.; Cabré M.; Moysset, M. (2016). Aplicación de datos LiDAR en el estudio de la dinámica torrencial y evolución de los barrancos de Portainé y Reguerals (Pirineo Central). XIV Reunión Nacional de Geomorfología. Málaga, 22-25 June 2016.

Victoriano, A.; Furdada, G. Floods in Val d'Aran and Torrential events in Portainé (Central Pyrenees). Workshop: *Update of flood research in the Mediterranean area from a multidisciplinary perspective. PREDIFLOOD Meeting 2016.* Lleida. 24-25 May 2016.

Vilamajó, E., Puzyrev, V., Queralt, P., Marcuello A., Ledo, J. (2016). Study of the casing effect on borehole-to-surface onshore CSEM. 78th EAGE Conference & Exhibition 2016. Vienna, Austria, 30 May – 2 June 2016

PROJECTES

Projects

5

geomodels

institut de recerca

Títol: Salt tectonics modelling at Kuqa foreland fold and thrust belt, Tarim oilfield
Entitat Finançadora: CNPC USA Corporation
Durada: 01/05/2014 -01/05/2017
Import Concedit: 613.240,29
Investigador Principal: Eduard Roca Abella; Josep Anton Muñoz de la Fuente

Títol: Structural and sedimentary evolution of the Valencia Basin, identification of petroleum systems
Entitat Finançadora: UCPO - UNIVERSITE DE CERGY-PONTOISE **Nº de Projecte:** FBG307750 **Durada**: 2014-2017
Import Concedit: 30.000,-€
Investigador Principal: Eduard Roca Abella

Títol: Grup de Geodinàmica i Anàlisi de Conques.
Entitat Finançadora: AGAUR **Nº de Projecte:** 2014SGR467 **Durada**: 2014-2016
Import Concedit: 63.000,-€
Investigador Principal: Josep Anton Muñoz de la Fuente

Títol: Expertise externe dans le cadre du project COLORS
Entitat Finançadora: CNRS - Centre National de la Recherche Scientifique (CNRS)
Nº de Projecte: FBG308770 **Durada**: 2016-2021
Import Concedit: 25.000,-€
Investigador Principal: Josep Anton Muñoz de la Fuente

Títol: Estudio estructural en Oriente Próximo denominado 'Proyecto Golondrinas'
Entitat Finançadora: Repsol Exploración, S.A. **Nº de Projecte:** FBG307776 **Durada**: 2014-2016
Import Concedit: 668.637,16€
Investigador Principal: Josep Anton Muñoz de la Fuente

Títol: Potential salt Plug related hydrocarbon traps in Eastern FARS-BANDER ABAS hinterland and its adjacent Iranian offshore territory in the Persian Gulf area, located in Iran
Entitat Finançadora: National Iranian Oil Company **Nº de Projecte: Durada**: 2014-2016
Investigador Principal: Josep Anton Muñoz de la Fuente

Títol: Building capacity in petroleum geoscience at University of Dodoma
Entitat Finançadora: Statoil Tanzania **Nº de Projecte:** FBG308968 **Durada**: 2016-2019
Import Concedit: 749.561,70€
Investigador Principal: Josep Anton Muñoz de la Fuente

Títol: Regularization concerning gravity and salt tectonics training course in Bilbao from 14/03/2016 to 19/03/2016
Entitat Finançadora: Total Exploration Production, S.A. (França) **Nº de Projecte:** FBG308756 **Durada**: 2016
Import Concedit: 7.500,-€
Investigador Principal: Josep Anton Muñoz de la Fuente

Títol: Structural characterization of a thrust weld, Warraweena and Mucaloona diapirs, Flinders Ranges, South Australia
Entitat Finançadora: University of Texas at El Paso **Nº de Projecte:**FBG308775 **Durada**: 2016
Import Concedit: 26.349,83€
Investigador Principal: Josep Anton Muñoz de la Fuente

Títol: Pyrenean Source-to-Sink Reasearch Project: Mapping and Sequence Correlation
Entitat Finançadora: Statoil ASA **Nº de Projecte:** FBG308803 **Durada**: 2016
Import Concedit: 122.000,-€
Investigador Principal: Josep Anton Muñoz de la Fuente

Títol: Zagros Exploration Workshop
Entitat Finançadora: Conoco Phillips Upstream **Nº de Projecte:** FBG308886 **Durada**: 2016
Import Concedit: 20.000,-€
Investigador Principal: Josep Anton Muñoz de la Fuente

Títol: Salt Tectonics in Convergebt-Margin Fold and Thurst Belts
Entitat Finançadora: ConocoPhillips Company **Nº de Projecte:** FBG308983 **Durada**: 2016
Import Concedit: 120.000,-€
Investigador Principal: Josep Anton Muñoz de la Fuente

Títol: Geological Structural Evolution and Hydrocarbon migration
Entitat Finançadora: ConocoPhillips Company **Nº de Projecte:** FBG308984 **Durada**: 2016
Import Concedit: 120.000,-€
Investigador Principal: Josep Anton Muñoz de la Fuente

Títol: Caracterización estructural y geofísica de reservorios asociados a estructuras de tectónica salina de carácter contractivo.
Entitat Finançadora: MCOC - Ministerio de Economia y Competitividad
Nº de Projecte: CGL2014-54118-C2-1-R **Durada**: 2015-2017
Import Concedit: 240.000,00 €
Investigadores Principales: Eduard Roca Abella i Alejandro Marcuello Pascual

Títol: Pilot project of establishing a radio network fore detecting Very Low Frequency (VLF) and Low Frequency (LF) electro-magnetic emissions preceding the occurrence of earthquakes.
Entitat Finançadora: Shota Rustaveli National Science Foundation of Georgia
Nº de Projecte: DI/21/9-140/13 **Durada**: 2014-2017
Import Concedit: 57.000,00€
Investigador Principal: Giorgi Khazaradze Tsilosani

Title: PREVENT: Prevención de desastres sísmicos en las Béticas Orientales mediante la integración de paleosismología, geodesia GPS, reevaluación del peligro sísmico y conscienciación social.
Funding from: Ministerio de Ciencia e Innovación
Nº project:**:** CGL2015-66263-R
Duration: 2015-2018
Budget: 193.600 **€**
Responsible: Eulàlia Masana Closa y Raimon Pallàs Serra

Title: Proyecto de actualización de la caracterización sísmica de los emplazamientos de las Centrales Nucleares Españolas
Funding from: Iberdrola España
Duration: from January 2016 to July 2016
Budget: 23.500 **€**
Responsible: María Ortuño Candela

Títol: Sediment Routing Systems: Stratigraphic Analysis And Models.
Entitat Finançadora: Ministerio de Economia y Competitividad
Nº de Projecte: CGL2014-55900-P **Durada**: 01/01/2015 al 31/12/2017
Import Concedit: 169.400,00€
Investigador Principal: Miguel Garcés, Miguel López-Blanco

Títol: Flujo de fluidos durante la evolucion de un orogeno: caracterizacion diagenetica, hidrotermal y metamorfica con aplicacion al almacenamiento de gas y exploracion de minerales.
Entitat Finançadora: Dirección General de Investigación Científica y Técnica.
Proyectos de I+D+I, del programa estatal de investigación, desarrollo e innovación orientada a los retos de la sociedad.
Nº de Projecte: CGL2015-66335-C2-1-R **Durada**: 2016-2018
Import Concedit: 81.000€
Investigador Principal: Anna Maria Travé Herrero

Títol: Synthesis and Comparison of Phanerozoic Carbonate Depositional Systems and Impact of Diagenesis on Reservoir Preservation/Improvement.
Entitat Finançadora: Repsol Exploración S.A. **Nº de Projecte:** JK002 **Durada**: 2016-2017
Import Concedit: 52.740,00€
Investigador Principal: Telm Bover-Arnal

Títol: Oligocene-Miocene red-algal limestones of the Prebetic domain (SE Spain).
Entitat Finançadora: Repsol Exploración S.A. **Nº de Projecte:** JK002 **Durada**: 2015-2016
Import Concedit: 52.740,00€
Investigador Principal: Telm Bover-Arnal

Títol: Identificació i distribució dels diferents nivells de calcàries a l'àrea SE Bages.
Entitat Finançadora: Generalitat de Catalunya, Empresa i Coneixement, Direcció General d'Energia, Mines i Seguretat Industrial **Nº de Projecte:** FBG 308961 **Durada**: 2016
Import Concedit: 2.925,01€
Investigador Principal: Miguel López Blanco

Títol: Reconstrucción de la NAO durante los periodos de Cambio Climático Rápido del Holoceno
Entitat Finançadora: Ministerio de Economia y Competitividad
Nº de Projecte: CGL2013-40608-R **Import Concedit:** 166.000,00 **Durada:** 2014**-**2016
Investigador Principal: Alberto Saez Ruiz

Títol: Caracterizacion y control de movimientos de masa. Un reto para la mitigacion del riesgo geologico
Entitat Finançadora: MINECO **Nº de Projecte:** CGL2013-40828-R **Durada**: 2014-2016
Import Concedit: 121.000,00€
Investigador Principal: Emma Suriñach Cornet

Títol: Arctic Geo-hazards, Geo-fluids and Climate Change (Arctic Geo-hazards)
EU. PIEF-GA-2012-332043
Import Concedit: 156.957,00. **Durada**: 2013 - 2018
Investigador Principal: Joan Manuel Vilaplana Fernandez

Títol: Aplicacions LiDAR (TLS) en l'estudi de despreniments de roques a Montserrat
Entitat Finançadora: ICGC
Nº de Projecte: FBG-308328 **Durada**: 2015-2016
Import Concedit: 17.082,36
Investigador Principal: Joan Manuel Vilaplana Fernandez

Títol: Suport al Grup de Recerca Consolidat de Riscos Naturals (RISKNAT)
Ajuts de Suport als Grups de Recerca de Catalunya (SGR)
GENERALITAT DE CATALUNYA I CONSELLERIA DE INNOVACIÓ, UNIVERSITAT I EMPRESA. **Nº de Projecte:** 2014SGR1243 **Durada**: 2014 **-** 2016
Import Concedit: 0
Investigador Principal: Joan Manuel Vilaplana

Títol del projecte/contracte: Assessorament i investigació aplicada en el camp de la Geofísica
Empresa/Administració finançadora: BOGI - Fundació Bosch i Gimpera
Durada: des de 2008 **fins** 2050
Investigador/a Principal Juan Jose Ledo Fernandez
Import (despeses indirectes incloses): 4.784,49

Títol del projecte/contracte: Monitoratge de camps elèctrics naturals i fenòmens associats
Empresa/Administració finançadora: GCEN - Geoma Cen S.L.
Durada: des de 2015 **fins** 2016
Investigador/a Principal: Pilar Neus Queralt Capdevila

Títol del projecte/contracte: Estudio 3D de los datos magnetotelúricos de la zona de estudio en el Proyecto Riotinto para obtención de un modelo final de distribución de resistividades 3D del subsuelo
Empresa/Administració finançadora: Atalaya Riotinto Minera, S.L.U.
Import (despeses indirectes incloses): 21.647,06 **Durada: des de** 2016 **Fins:** 2016
Investigador/a Principal: Juan Jose Ledo Fernandez

Títol del projecte/contracte: Estudio de CSEM empleando el cable minero del proyecto Mina las Cruces
Empresa/Administració finançadora: Geognosia, S.L.
Import (despeses indirectes incloses): 17.500,00 **Durada: des de** 2016 **Fins:** 2016
Investigador/a Principal: Juan José Ledo Fernández

Títol del projecte/contracte: Estudio de tomografía eléctrica y CSEM empleando electrodos largos (LEERT) del proyecto Mina las Cruces
Empresa/Administració finançadora: Geognosia, S.L.
Import (despeses indirectes incloses): 12.500,00 **Durada: des de** 2016 **Fins:** 2016
Investigador/a Principal: Juan Jose Ledo Fernandez

Títol del projecte/contracte: Modelo 3D a partir de base de datos magnetotelúricos del proyecto Mina las Cruces
Empresa/Administració finançadora: Geognosia, S.L.
Import (despeses indirectes incloses): 28.000,00 **Durada: des de** 2016 **Fins:** 2016
Investigador/a Principal: Juan Jose Ledo Fernandez

Títol del projecte/contracte: Realització de treballs de camp per a l'adquisició de dades magnetotel·lúriques i treballs de modelització i interpretació geofísica 3d (inversió 3d de les dades) per l'estudi d'estructures geològiques profundes en dues àrees de Catalunya: La Garriga (Vallès Oriental) i el Baridà (Alt Urgell, Cerdanya)
Empresa/Administració finançadora: Institut Cartogràfic i Geològic de Catalunya
Import (despeses indirectes incloses): 119.625,00 **Durada: des de** 2016 **Fins:** 2016
Investigador/a Principal: Juan José Ledo Fernández

Títol: Course on flood risk management. Haití.
Entitat Finançadora: Federal Department of Foreing Affairs, Switzerland Confederation.
Import Concedit: 25.130,08 **Durada**: 2016

Projectes participants:

Títol: Avalanchas en Biofísica, geofísica, materiales y plasmas.
Entitat Finançadora: Ministerio de Economia y Competitividad.
Nº de Projecte: MAT2015-69777-REDT **Durada**: 2015 - 2017
Import Concedit: 30.000 €
Investigador Principal: Eduard Vives Santa-Eulalia

Títol: El papel de la insularidad y posterior aislamiento geográfico de Iberia en grandes crisis bióticas del Cretácico-Paleógeno. Aplicaciones bioestratigráficas y paleoambientales.
Entitat Finançadora: DGICT **Nº de Projecte:** CGL2015-69805-P (MINECO, FEDER, EU). **Durada**: 2016-2018
Import Concedit:
Investigador Principal: Carles Martín-Closas.

Títol: Exploración y Valoración de Nuevos Recursos de Aguas Subterráneas en la Depresión Central de la Región de Antofagasta
Entitat Finançadora: Ministerio de Educación. Chile.
Import Concedit: 300.000,00 $ **Nº de Projecte:** ACT1203 **Durada:** 2013**-**2016
Investigador Principal: Christian Herrera Lameli

Títol: Análisis ecológico de la culturización del paisaje de alta montaña desde el Neolítico: los Parques Nacionales de montaña como modelo (CUL-PA)
Entitat Finançadora: MINISTERIO DE AGRICULTURA, ALIMENTACION Y MEDIO AMBIENTE. Programa de Investigación de Parques Nacionales **Nº de Projecte:** 998/2013
Import Concedit: 64.837,00 **Durada:** 2014**-**2016
Investigador Principal: Jordi Catalan Aguila

Títol: Variaciones rápidas de la intensidad del campo geomagnético en el Mediterraneo: Caracterización a partir de yacimientos del bronce final y de cerámicas finas tardoromanas. (GEOMED)
Entitat Finançadora: MINECO **Nº de Projecte:** CGL2015-63888-R. **Durada**: 2016-2020
Import Concedit: 50.000 €
Investigador Principal: Miriam Gómez Paccard (CSIC)

Títol: Análisis del Potencial Sísmico de las Zonas Intersegmento de Fallas de Desgarre mediante Análisis y Monitoreo Geológico, Geodésico y Geofísico.
Entitat Finançadora: MCOC - Ministerio de Economia y Competitividad
Nº de Projecte: CGL2013-47412-C2-1-P **Durada**: 2014-2016
Import Concedit: 162.000,00 €
Investigador Principal: José J Martínez Díaz

Títol: RedPyrMove. Ajuts per a accions de cooperación en el marc de la Comunitat de Treball dels Pirineus CTP 2014. Generalitat de Catalunya-AGAUR
Nº de Projecte: 2014 CTP 00051 **Durada**: 2015 to 2016
Import Concedit: 5000 €
Investigador Principal: José Moya Sànchez (Univ. Politècnica de Catalunya, UPC)

Title: Caracterizacion de fallas activas en el Centro del Cinturon Volcanico Transmexicano: Geomorfologia cuantitativa, Paleosismología y Sondeos geofisicos.
Program: Programa de apoyo a proyectos de investigación e innovación tecnológica- PAPIIT
Funding from: Universidad Autónoma Nacional de México.
Nº project: IN-112110
Budget: 152,400 pesos mexicanos
Duration: 2015 hasta: 2016 (2 years).
Responsible: Pierre Gilles Lacan (UNAM, Mexico)

TESIS

Thesis

6

geomodels

institut de recerca

Títol: Facies y secuencias deposicionales mixtas carbonático-siliciclásticas del Miocene Inferior de la Cuenca de Falcón (noroeste de Venezuela) como modelo exploratorio en el Caribe.
Doctorand: Eduard Albert-Villanueva
Directors: Ramon Salas and Telm Bover-Arnal
Universitat: Universitat de Barcelona. Facultat de Geologia
Any defensa: 2016
Qualificació: Excellent

Títol: Implementación del lidar terrestre en la caracterización y modelización de análogos de análogos de reservorios fluviales: desarrollo y aplicación de nuevas metodologías en afloramientos del Abanico Fluvial de Huesca (Mioceno de la Cuenca del Ebro)
Doctorand: Rubén Calvo Tortajada
Directors: Emilio Ramos Guerrero
Universitat: Universitat de Barcelona. Facultat de Geologia
Any defensa: 2016
Qualificació: Excellent

Títol: Architecture, dynamique et modélisation sismique synthétique d'un système fluvio-deltaïque syntectonique. Le complexe deltaïque éocène moyen du Sobrarbe, bassin d'avant-pays sud-pyrénéen (Aragon, Espagne)
Doctorand: Nicolas Grasseau
Director: Miguel López Blanco / Philippe Razin
Universitat: Universitat de Barcelona / Université Bordeaux Montaigne
Any defensa: 2016
Qualificació: Tres Honorable

Títol: Mesozoic extension and Cenozoic contraction in the Eastern Iberian Chain (Maestrat Basin).
Doctorand: Marina Nebot Miralles
Director: Joan Guimerà
Universitat: Universitat de Barcelona. Facultat de Ciències de la Terra
Any defensa: 2016
Qualificació: Excl·lent *cum laude*

Títol: CSEM monitoring at the Hontomín CO_2 storage site: modeling, experimental design and baseline results
Doctorand: Eloi Vilamajó Llobera
Director: Pilar Queralt Capdevila
Universitat: Universitat de Barcelona. Facultat de Ciències de la Terra
Any defensa: 2016
Qualificació: Excel·lent cum laude

Títol: Combining Discrete Element and Process-based Sedimentary Models: A New Tool to Model Syntectonic Sedimentation
Doctorand: Ana Carmona Bardella
Director: Òscar Gratacós / Stuart Hardy
Universitat: Universitat de Barcelona. Facultat de Ciències de la Terra
Any defensa: 2016
Qualificació: Excel·lent

Títol: Forward Numerical Modelling of Carbonate Basins: an Ecological Approach
Doctorand: Roger Clavera-Gispert
Director: Òscar Gratacós / Helmut Schaeben
Universitat: Department of Geophysics and Geoinformatics. Technische Universität Bergakademie Freiberg
Any defensa: 2016
Qualificació: Good - cum laude

PhD student: Manuel Jesús Royán Cordero
Title: Caracterización y predicción de desprendimientos de rocas mediante LiDAR Terrestre
Supervisor: Joan Manuel Vilaplana Fernández y Antonio Abellán Fernández
Universitat: Universitat de Barcelona. Facultat de Geologia
Any defensa: 2015
Qualificació: Excel.lent

PhD student: Francesc Xavier Roig
Title: Blocs de tempesta i tsunami a les costes rocoses de les Illes Balears. Anàlisi geomorfològica i morfomètrica.
Supervisor: Joan Manuel Vilaplana Fernández
Universitat: Universitat de Barcelona. Facultat de Geologia
Any defensa: 2016
Qualificació: Excel.lent cum Laude

Títol: Velocitat de desplaçament de la falla d'Alhama de Murcia (Bètiques Orientals); implicacions en el seu potencial sísmic
Doctorand: Marta Ferrater Gómez
Director: Eulàlia Masana Closa i Maria Ortuña Candela
Universitat: Universitat de Barcelona. Facultat de Geologia
Any defensa: 2016
Qualificació: Excel·lent cum laude

Títol: Advanced seismic methods applied to the study of snow avalanche dynamics and avalanche formation
Doctorand: Cristina Pérez Guillén
Director: Emma Suriñach Cornet
Universitat: Universitat de Barcelona. Facultat de Geologia
Any defensa: 2016
Qualificació: Excel·lent cum Laude

Títol: Late Holocene climate variability in the North Atlantic based on biomarker reconstruction. The Lake Azul (São Miguel island, Azores archipelago) case
Doctorand: María Jesus Rubio de Inglés
Director: Santiago Giralt i Alberto Saez
Universitat: Universitat de Barcelona. Facultat de Geologia
Any defensa: 2016
Qualificació: Excel·lent cum laude

MEMBRES Institut de Recerca

Geomodels Personnel

7

geomodels

institut de recerca

Fins a desembre del 2016, un total de 82 persones pertanyen a l'Institut de Recerca, distribuides segons:

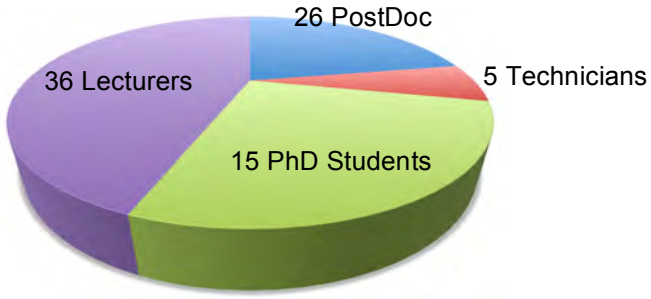

De les quals:

22 Geòlegs estructurals

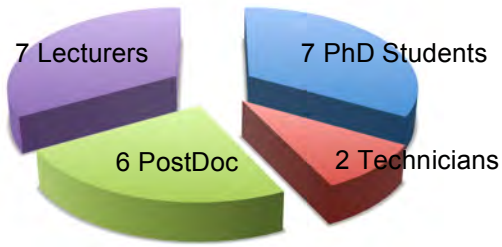

27 Sedimentòlegs - Petròlegs

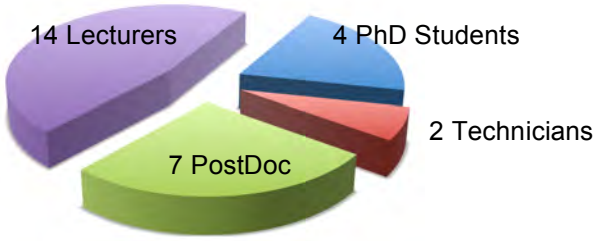

15 Geofísics

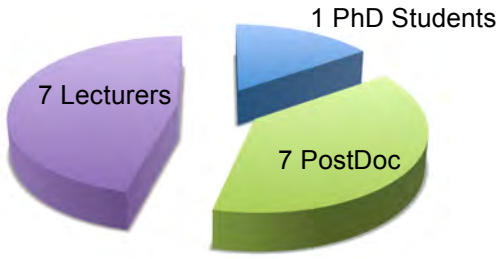

17 Geomorfòlegs - Neotectònics

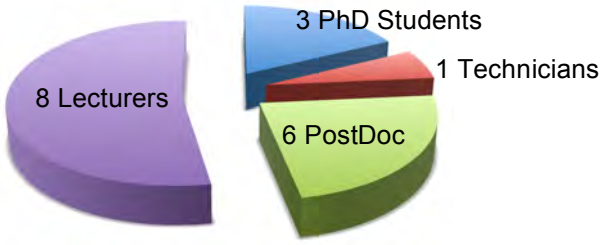

ALBERT VILLANUEVA, EDUARD
ARBUES CAZO, PAU
ASENSIO FERREIRA, EVA
BAQUES ALMIRALL, VINYET
BEAMUD AMOROS, ISABEL
BEAMUD AMOROS, TERESA MARIA
BELLMUNT TRAVER, FABIAN
BORDONAU IBERN, JAUME
BOSCH ROS, DAVID
BOVER ARNAL, TELM
BUSQUETS BUEZO, PEDRO
BUTILLE MASSAGUE, MIREIA
CABELLO LOPEZ, PATRICIA
CABRERA PEREZ, LUIS
CALVET PORTA, JAUME
CAMPANYA I LLOVET, JOAN
CANTARERO ABAD, IRENE
CARMONA BARDELLA, ANA
CAROLA MOLAS, ELOI
CARRERA GARCIA DE CORTAZAR, NURIA
CASAS TUSET, JOSEP MARIA
CLIMENT DOMENECH, HASDRUBAL
COLOMBO PIÑOL, FERNANDO
COSTA GISBERT, ELISENDA
CUEVAS MARTINEZ, JOSE LUIS
DE MATTEIS , MARCO
ECHEVERRIA MORENO, ANNA
ESCALAS OLIVER, MAGDALENA
ESCOSA BERNAL, FREDERIC
FERRER GARCIA, JOSE ORIOL
FERRATER GÓMEZ, MARTA
FONTQUERNI GORCHS, SARA
FURDADA BELLAVISTA, GLORIA
GARCES CRESPO, MIGUEL
GARCIA SELLES, DAVID
GORRIZ IBAÑEZ, ESTEFANIA
GRATACOS TORRA, OSCAR
GUIMERA ROSO, JOAN JOSEP
GUINAU SELLES, MARTA
HARDY , STUART
IZQUIERDO LLAVALL, ESTHER
KHAZARADZE TSILOSANI, GIORGI
LEDO FERNANDEZ, JUAN JOSE
LOPEZ BLANCO, MIGUEL
MARCUELLO PASCUAL, ALEJANDRO
MARQUES ROCA, MA. ANGELES
MARTI CASTELLS, ANNA
MARTIN MARTIN, JUAN DIEGO
MARTINEZ GRANADO, PABLO
MARZO CARPIO, MARIANO
MASANA CLOSA, EULALIA
MENCOS BELLPUIG, JOANA
MERCEDES MARTIN, RAMON
MORENO BEDMAR, JOSEP ANTON
MUÑOZ DE LA FUENTE, JOSEP ANTONI
NEBOT MIRALLES, MARINA
OGAYA GARCIA, XÈNIA
ORTUÑO, MARIA
PALLAS SERRA, RAIMON
PERMANYER BASTARDAS, ALBERT
PEREZ GUILLÉN CRISTINA
PLA DE CASACUBERTA, ORIOL
POUS FABREGAS, JAUME
QUERALT CAPDEVILA, PILAR NEUS
RAMOS GUERRERO, EMILIO
RAMOS ORDOÑO, ADRIA
ROCA ABELLA, EDUARD
ROMA NUÑEZ, MARIA
ROYAN CORDERO, MANUEL JESUS
SABAT MONTSERRAT, FRANCESC
SAEZ RUIZ, ALBERTO
SALAS ROIG, RAMON
SERRA KIEL, JOSE
SNIDERO , MARCO
SURIÑACH CORNET, EMMA
TRAVE HERRERO, ANNA MARIA
VALCARCEL RODRÍGUEZ, MANOEL
VALERO MONTESA, LUIS
VICTORIANO LAMARIANO, ANE
VILAMAJO LLOBERA, ELOI
VILAPLANA FERNANDEZ, JOAN MANUEL
VINYOLES BUSQUETS, ANDREU